

MEASUREMENT AND MODELING OF WATER
QUALITY FROM A SMALL FORESTED
WATERSHED IN SOUTHEASTERN
OKLAHOMA

By

DONALD JAMES JURTON

Bachelor of Science
SUNY College of Environmental
Science and Forestry
Syracuse, New York
1977

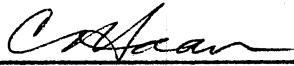
Master of Science
University of Washington
Seattle, Washington
1982

Submitted to the Faculty of the
Graduate College of the
Oklahoma State University
in partial fulfillment of
the requirements for
the Degree of
DOCTOR OF PHILOSOPHY
May, 1989

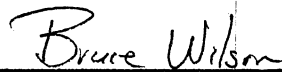
Thesis
1989D
1962m
Cup. 2

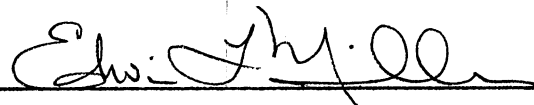
MEASUREMENT AND MODELING OF WATER
QUALITY FROM A SMALL FORESTED
WATERSHED IN SOUTHEASTERN
OKLAHOMA

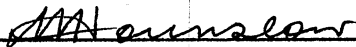
Thesis Approved:

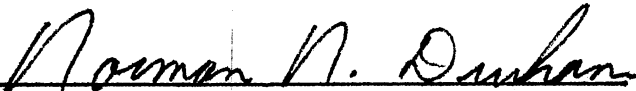


Thesis Adviser









Dean of the Graduate College

ACKNOWLEDGEMENTS

Good research is seldom the result of one person's effort. Such is the case here. This project is the result of a team effort, both in the field, office, and behind the scenes.

I would especially like to thank my major advisor, Dr. Tom Haan for his support and suggestions. I hope that I may live up to his expectations and standards in the future. Thanks also go out to Dr. Ed Miller, for suggestions, facilities, and many runs. Thanks also go out to the remaining members of my graduate committee, Drs. Bruce Wilson and Arthur Hounslow.

I would also like to thank the Department of Agricultural Engineering for their support, the Department of Forestry, especially Micheal Kress and Jill Boggs, and Weyerhauaer Company for use of the backhoe. Special thanks go out to the USDA National Needs Fellowship Program, who's support made my degree program possible.

Extra special thanks go to Jacque, for her love, patience and support. Many warm hugs kept me going through difficult and tense times. Thank you all.

TABLE OF CONTENTS

Chapter	Page
I. INTRODUCTION.....	1
Problem.....	1
Needs.....	2
Objectives.....	3
II. STREAMFLOW AND CHEMISTRY GENERATING PROCESSES ON FORESTED WATERSHEDS.....	6
Streamflow Generating Processes.....	6
Flow Processes and Water Chemistry.....	10
III. WATERSHED HYDROLOGY AND WATER QUALITY MODELING.....	13
Watershed Hydrology Models.....	13
Kentucky Daily Watershed Model.....	14
BROOK Model.....	19
Stanford Watershed Model.....	26
USGS Precipitation-Runoff Modeling System.....	31
CREAMS.....	39
TOPMODEL.....	44
USDAHL.....	49
FESHM.....	54
ANSWERS.....	58
VSAS I and II.....	69
Watershed Water Quality Models.....	74
Introduction.....	74
Agricultural Runoff Management Model... Nonpoint Source Pollutant Loading Model.....	75
Agricultural Chemical Transport Model.....	79
CREAMS.....	81
Shenandoah Watershed Study Model.....	86
Birkenes, Norway Model.....	92
Birkenes, Norway Model.....	94

Chapter	Page
Some Considerations in Hydrologic Modeling	
Modeling.....	96
Conclusions.....	98
Some Considerations in Water Quality	
Modeling.....	99
Introduction.....	99
Hydrologic Processes.....	99
The Watershed System.....	100
Streamflow Generating Processes.....	100
Macropore Flow.....	101
Old vs. New Water.....	101
Source Area.....	101
Chemical Transport Processes.....	102
Conclusions.....	104
IV. METHODS.....	106
Study Site.....	106
Climate.....	109
Topography.....	109
Geology.....	110
Soils.....	110
Vegetation.....	112
Field Methods.....	112
Precipitation.....	113
Bulk Precipitation and Throughfall.....	113
Soil Solution.....	120
Subsurface Flow.....	123
Streamflow.....	128
Chemical Analysis.....	130
Analysis and Storage.....	130
pH.....	131
Conductivity.....	131
Nitrate Nitrogen.....	131
Dissolved Organic Carbon.....	132
Cations.....	133
Other Analysis.....	134
V. RESULTS AND DISCUSSION OF FIELD STUDY.....	135
Introduction.....	135
Study Site Description.....	135

Chapter	Page
Extrapolation of Results.....	141
Hydrologic Processes.....	142
Precipitation and Throughfall.....	143
Canopy Storage.....	147
Subsurface Flow Volumes.....	150
SSF Hydrographs, Rates, and Timing.....	162
SSF Volume Contributions to Streamflow.....	181
Chemical Processes.....	188
Chemical Transformations.....	188
Chemical Loads in Streamflow.....	199
 VI. WATERSHED MODEL DEVELOPMENT AND DESCRIPTION.....	 177
Rationale for Development.....	207
Modeling Concept.....	208
Model Structure.....	212
Data Input Requirements.....	216
Hydrologic Processes.....	219
Evapotranspiration.....	219
Throughfall.....	222
Litter Layer.....	224
Soil Storages.....	225
Quick Release Zone.....	232
Riparian Zone.....	236
Water Chemistry Processes.....	239
 VII. RESULTS AND DISCUSSION OF WATERSHED MODELING STUDY.....	 241
Introduction.....	241
Modeling With Standard Parameter Set.....	241
Standard Parameters.....	241
Annual Runoff and Water Balance.....	247
Annual Chemical Loads.....	249
Daily Runoff.....	251
Individual Storm Predictions.....	251
Modeling With Different Sets of Parameters..	266

Chapter	Page
VIII. CONCLUSIONS.....	273
Field Study Conclusions.....	273
Watershed Modeling Conclusions.....	274
Suggestions for Future Field Research.....	276
Suggestions for Future Model Improvements...	277
LITERATURE CITED.....	280
APPENDIX A - HYDROLOGIC PROCESSES SUMMARY TABLES.....	290
APPENDIX B - SOURCE CHEMISTRY SUMMARIES BY STORM.....	348
APPENDIX C - SUMMARY OF THROUGHFALL DATA.....	375
APPENDIX D - WATERSHED MODEL PROGRAM.....	381

LIST OF TABLES

Table	Page
1. Hillslope Study Site Characteristics.....	137
2. Hillslope Study Site Soil Depths at Subsurface Flow Collection Troughs.....	137
3. Watershed Stream Channel Characteristics.....	140
4. Precipitation and Mean Throughfall for the Study Period.....	144
5. Precipitation (mm) - Throughfall (mm) Relationships for All Data and the Dormant and Growing Seasons.....	145
6. Precipitation - Throughfall (mm) Relationships for Mixed Hardwood-Pine Cover Types.....	147
7. Canopy Storages for Various Mixed Pine-Hardwood Cover Types.....	149
8. Total Hillslope Segment SSF for Eight Streamflow Producing Storms.....	150
9. SSF Volumes by Site, Soil Horizon, and Storm....	154
10. Statistics and ANOVA for Storm SSF Classified by Site.....	155
11. Estimates of the Hillslope Contributing Length for Eight Streamflow Producing Storms.....	160
12. Maximum Shallow Subsurface Flow Rates in Liters per Second.....	173
13. Comparison of SSF Peak Rates to Streamflow Peak Rates.....	174
14. Comparison of SSF Volumes and Streamflow Volumes for Eight Streamflow Producing Storms.....	187
15. Source Mean Chemistry Summary Precipitation and Throughfall.....	189

Table	Page
16. Source Mean Chemistry Summary Soil and Subsurface Flow Collectors.....	190
17. Concentrations of NO ₃ -N for A Horizon Soil Samplers.....	193
18. Concentrations of NO ₃ -N for B Horizon Soil Samplers.....	194
19. Changes in Mean Concentrations Between Sources, Clayton Watershed #3 1/87-6/87.....	196
20. Ratios of Mean Chemical Concentrations Between Sources for Various Forested Watersheds.....	197
21. Subsurface Flow Chemical Transport Loads Storm of 3/01/87.....	201
22. Subsurface Flow Chemical Transport Loads Storm of 3/17/87.....	202
23. Subsurface Flow Chemical Transport Loads Storm of 6/30/87.....	203
24. Listing of Model Input Parameters.....	217
25. Estimated Quick Release Zone Contributing Areas and Soil Water Contents.....	233
26. Standard Input Parameters and Their Expected Ranges in Value.....	243
27. Chemical Transport Input Parameters.....	245
28. Soil Storage Properties Obtained From the Model Using Standard Parameters.....	248
29. Predicted Annual Water Balance From Clayton Watershed #3 for the 1986 and 1987 Water Years.....	248
30. A Comparison of Predicted and Measured Chemical Loads.....	250
31. Simulated and Actual Daily Runoff, Water Year 1987.....	253
32. Comparison of Actual and Predicted Stormflow Volumes and Peak Flow Rates.....	261

Table	Page
33. Sensitivity of Predicted Annual Water Balance to Changes in Pan Coefficients and the Percolation Function.....	269
34. Hydrologic Processes Data for the Storm of 1/15/87.....	291
35. Hydrologic Processes Data for the Storm of 2/1/87.....	294
36. Hydrologic Processes Data for the Storm of 2/15/87.....	297
37. Hydrologic Processes Data for the Storm of 2/24/87.....	302
38. Hydrologic Processes Data for the Storm of 2/28/87.....	304
39. Hydrologic Processes Data for the Storm of 3/17/87.....	310
40. Hydrologic Processes Data for the Storm of 3/23/87.....	317
41. Hydrologic Processes Data for the Storm of 3/26/87.....	318
42. Hydrologic Processes Data for the Storm of 4/13/87.....	319
43. Hydrologic Processes Data for the Storm of 5/4/87.....	320
44. Hydrologic Processes Data for the Storm of 5/16/87.....	321
45. Hydrologic Processes Data for the Storm of 5/21/87.....	322
46. Hydrologic Processes Data for the Storm of 5/25/87.....	323
47. Hydrologic Processes Data for the Storm of 5/28/87.....	327
48. Hydrologic Processes Data for the Storm of 5/31/87.....	338
49. Hydrologic Processes Data for the Storm of 6/19/87.....	342

Table	Page
50. Hydrologic Processes Data for the Storm of 6/30/87.....	343
51. Watershed Processes Chemistry Data for the Storm of 1/15/87.....	349
52. Watershed Processes Chemistry Data for the Storm of 2/11/87.....	351
53. Watershed Processes Chemistry Data for the Storm of 2/16/87.....	352
54. Watershed Processes Chemistry Data for the Storm of 2/21/87.....	354
55. Watershed Processes Chemistry Data for the Storm of 2/24/87.....	355
56. Watershed Processes Chemistry Data for the Storm of 2/28/87.....	356
57. Watershed Processes Chemistry Data for the Storm of 3/17/87.....	358
58. Watershed Processes Chemistry Data for the Storm of 3/23/87.....	360
59. Watershed Processes Chemistry Data for the Storm of 3/26/87.....	361
60. Watershed Processes Chemistry Data for the Storm of 4/13/87.....	362
61. Watershed Processes Chemistry Data for the Storm of 5/4/87.....	363
62. Watershed Processes Chemistry Data for the Storm of 5/19/87.....	364
63. Watershed Processes Chemistry Data for the Storm of 5/22/87.....	365
64. Watershed Processes Chemistry Data for the Storm of 5/25/87.....	367
65. Watershed Processes Chemistry Data for the Storm of 5/28/87.....	369
66. Watershed Processes Chemistry Data for the Storm of 5/31/87.....	371

Table	Page
67. Watershed Processes Chemistry Data for the Storm of 6/30/87.....	373
68. Summary of Throughfall Data.....	376

LIST OF FIGURES

Figure	Page
1. Structure of the Kentucky Daily Watershed Model (from: Sloan et al., 1983).....	15
2. Structure of the BROOK Hydrologic Model (from: Federer and Lash, 1978).....	20
3. Division of a Watershed Into Elements and Division of Area Drained per Element for ANSWERS (from Beasley and Huggins, 1981).....	61
4. Location Map of the Research Watershed.....	107
5. Topographic and Soils Map of Clayton Watershed #3..	108
6. 3-D View of a Typical Hillslope Study Site and the Equipment Installed at Each Site.....	114
7. Throughfall Collection System.....	119
8. Tension-free Soil Lysimeter.....	122
9. Cut-away View of Subsurface Flow Interceptor Troughs.....	126
10. Cross Sectional View of the Subsurface Flow Collection Troughs.....	127
11. Collection Drum and Water Level Recording System Used in the Subsurface Flow Collection System....	129
12. Watershed Map Showing Stream Channels and Research Sites.....	138
13. Profiles of Hillslope Study Segments.....	139
14. Plot of Total Storm SSF vs. Precipitation.....	152
15. Shallow Subsurface Flow Hydrographs for Site 1, the Storm of 3/17/87.....	163
16. Shallow Subsurface Flow Hydrographs for Site 2, the Storm of 3/17/87.....	164

Figure	Page
17. Shallow Subsurface Flow Hydrographs for Site 3, the Storm of 1/17/87.....	165
18. Shallow Subsurface Flow Hydrographs for Site 1, the Storm of 5/28/87.....	166
19. Shallow Subsurface Flow Hydrographs for Site 2, the Storm of 5/28/87.....	167
20. Shallow Subsurface Flow Hydrographs for Site 3, the Storm of 5/28/87.....	168
21. Shallow Subsurface Flow Hydrographs for Site 1, the Storm of 6/30/87.....	169
22. Shallow Subsurface Flow Hydrographs for Site 2, the Storm of 6/30/87.....	170
23. Shallow Subsurface Flow Hydrographs for Site 3, the Storm of 6/30/87.....	171
24. Shallow Subsurface Flow Hydrograph from Site 1, B Horizon, the Storm of 3/17/87.....	178
25. Shallow Subsurface Flow Hydrograph from Site 3, B Horizon, the Storm of 5/28/87.....	179
26. Shallow Subsurface Flow Hydrograph from Site 2, B Horizon, the Storm of 6/30/87.....	180
27. Semi-Log Plot of a Shallow Subsurface Flow Hydrograph, Site 1, B Horizon, 3/17/87.....	182
28. Semi-Log Plot of a Shallow Subsurface Flow Hydrograph, Site 2, B Horizon, 6/30/87.....	183
29. Plot of the Total SSF and Streamflow Hydrographs for the Storm of 3/17/87.....	184
30. Plot of the Total SSF and Streamflow Hydrographs for the Storm of 6/30/87.....	185
31. Simultaneous Plot of NO ₃ -N Concentration and Streamflow for the Storm of 3/17/87.....	205
32. Flow Diagram of the Watershed Model.....	209
33. Division of the Watershed Into Zones.....	211
34. Flow Chart of the Watershed Model Program.....	213
35. Flow Chart of Time Increment Control Subroutine....	215

Figure	Page
36. AET/PET Relationships for Soil Storage Tanks.....	223
37. An Example of the Hydrograph Separation Technique Used to Estimate the Soil Tank Storage Release Coefficients.....	229
38. The Relationship Between Soil Water Content in <i>LOSOIL</i> (as <i>LOSTAR/LOMAX</i>) and the ln of the Estimated SSF Contributing Area.....	235
39. Comparison of Actual and Predicted Streamflow for the Storm of 11/17-11/19/85.....	257
40. Comparison of Actual and Predicted Streamflows for the Storm of 3/17/87.....	258
41. Comparison of Actual and Predicted Streamflows for the Storm of 5/28/87.....	259
42. Comparison of Actual and Predicted Streamflows for the Storm of 6/30/87.....	260
43. Comparison of Actual and Predicted NO ₃ -N Concentrations for Storm of 3/17/87.....	264
44. Comparison of Actual and Predicted NO ₃ -N Concentrations for the Storm of 3/17/87.....	267
45. Parameter Sensitivity of <i>LOAWC</i> on the Predicted Streamflow of the Storm of 3/17/87.....	271
46. Watershed Model Program.....	381

CHAPTER I

INTRODUCTION

Problem

Interest in the effects of land use on water quality and the passage of non-point source pollution control legislation in the 1970's, such as P.L. 92-500 Sec. 208, spawned numerous watershed water chemistry modeling and research efforts. Information was needed immediately, so early water chemistry models were developed around existing hydrologic models such as the well known Stanford Watershed Model (Donigian and Crawford, 1976b). Research took a monitoring approach to obtain measures of pollutant concentrations and loads produced between various land uses.

Unfortunately, many of the early water chemistry models used simplifying assumptions that did not represent the physical processes taking place on the watershed (Bevin et al., 1984). Watershed research efforts did not quantify the physical processes controlling water quantity and chemistry, thereby failing to establish a direct physical link between changes in land use and water chemistry.

Needs

Streamflow water chemistry is a function of the chemistry of the incoming precipitation, flow paths taken by the water, the types of materials encountered along the flow path, and the length of time water remains in contact with a particular substrate (Dowd and Nutter, 1985). In order to improve hydrologic and water chemistry models, the flow paths taken and the physical and chemical processes encountered by water as it travels through the watershed system to become streamflow must be described and quantified (Dowd and Nutter, 1985 and Nix, 1985). Additionally, the spatial and temporal variation of the dominant processes must also be described and quantified (Bevin et al., 1984). Regional differences between dominant flow generating processes must also be understood (Nix, 1985).

The need to improve the physical basis of water chemistry models and our overall understanding of watershed water chemistry generating processes has become greater with recent concerns over the effects of acid precipitation and the use and disposal of chemicals (pesticides and wastes) on the environment. In a review of the directions of modern hydrologic research, Burges (1986) pointed out that additional research is needed to adequately describe hydrologic interactions of vegetal cover, topography, soil chemistry and land use at the small watershed scale.

The physical and chemical processes that generate streamflow and water chemistry in streams draining small forested watersheds of the Ouachita Highlands of southeastern Oklahoma are not fully understood. Recent research by Miller (1984) quantified differences in water and sediment yield between clearcut and undisturbed forested watersheds in the region. Rochelle and Wigington (1986) investigated the role of surface flow as a streamflow generating process on three small forested watersheds in the Ouachita Highlands. The above mentioned research has contributed to the understanding of how streamflow and water chemistry is generated on small forested watersheds of the region. However, if the effects of forestry activities on streamflow and water chemistry of the region are to be fully understood and modeled, additional research to describe and quantify the physical and chemical processes that generate streamflow and water chemistry must be performed.

Objectives

In order to gain an understanding of the effects, and later model the effects of silvicultural practices on hydrologic processes and water quality, a good understanding of the hydrologic and chemical processes on an undisturbed forested watershed is required. This study represents a first attempt at measuring and modeling relationships between streamflow and chemistry generating

processes on a small, undisturbed, forested watershed typical of the Ouachita Mountain region of Oklahoma and Arkansas. It consists of two components, a field component and a modeling component. The field component attempts to establish basic relationships between the source of streamflow and water chemistry, by answering the following questions:

1. What are the discharge rates, timing, and volume contributions to total streamflow of shallow subsurface flow?
2. How does the chemistry of water entering a watershed change as it moves through the canopy and soil to become streamflow?
3. Can basic relationships, that can later be used in modeling efforts, between shallow subsurface flow and streamflow and water chemistry and flow source be developed using the data collected?

The objectives of modeling efforts often determine, in part, the design of a model used in a particular application. For this study model requirements and goals are:

1. To produce continuous simulation of streamflow and water chemistry on a water year basis.
2. To represent the hydrologic and chemical processes on the study watershed.
3. To use physically-based parameters and algorithms whenever possible.
4. To keep the model structure as simple as possible to minimize the number of parameters required.

Initially an attempt to meet the objectives by adapting an existing models was made. As work progressed, it became apparent that it would be more desirable to develop a new model, borrowing various components and concepts from existing models.

CHAPTER II

STREAMFLOW AND CHEMISTRY GENERATING PROCESSES ON FORESTED WATERSHEDS

Streamflow Generating Processes

Total streamflow at a watershed outlet may be viewed as the sum of streamflow generated from individual source areas within the watershed. Streamflow from a source area is controlled by five general streamflow generating processes: channel interception, overland flow, subsurface flow, saturation overland flow, and percolation to the groundwater table (Dunne, 1978). The proportion of streamflow produced by each process is a function of watershed characteristics including soils, geology, vegetation, climate and topography. The watershed characteristics mentioned above vary spatially over a watershed. Therefore, the dominant runoff generating processes also vary spatially over a watershed (Betson and Marius, 1969 and Dunne, 1978). The proportions of runoff produced by different runoff generating processes also varies with time and time and space concurrently (ie: as in the variable source concept, Hewlett and Nutter, 1970).

Undisturbed forested watersheds generally have highly permeable soils that have infiltration capacities much greater than the rainfall rates of the most intense storms. Therefore, overland flow is non-existent except on rock outcrops or zones of saturated soils (Hewlett and Nutter, 1970 and Dunne, 1978). A protective covering of litter that accumulates on the forest floor also aids precipitation to infiltrate into the soil. Channel interception generally contributes little to the total streamflow. Therefore, the major streamflow generating processes on undisturbed forested watersheds include subsurface flow through highly permeable surface soil horizons (Hewlett and Hibbert, 1967; Betson and Marius, 1969; Whipkey, 1965; Freeze, 1972; and Dunne, 1978), and saturation overland flow from saturated soils in topographically low concave areas (Dunne and Black, 1970 and Hewlett and Nutter, 1970). Deep percolation to the groundwater table and the subsequent release of groundwater to the stream may also contribute significantly to total streamflow on watersheds that contain deep permeable soils.

Subsurface flow, also called throughflow or interflow, is defined as infiltrated precipitation that travels through the soil to the stream without entering the groundwater table (Whipkey, 1965 and Dunne and Black, 1970). Subsurface flow takes place in sloping surfaces composed of highly permeable soils underlain by less permeable layers such as fragipans, claypans, or partially weathered shallow bedrock (Dunne, 1978). Flow in the subsurface environment takes

place through pores in the soil matrix, and through macropores (Bevin and German, 1981). Macropores are formed by old root channels, animal burrows and soil cracks. Macropore flow is a significantly different process capable of delivering subsurface flow at velocities much greater than velocities that occur in the saturated soil matrix (Pilgrim et al., 1979; Devries and Chow, 1978; Mosley, 1979). In fact, Mosley (1979), found flow velocities through a soil containing macropores up to 300 times as great as the saturated hydraulic conductivity of the soil. The partitioning of subsurface flow between soil matrix and macropore flow is not well understood. However, conceptual models of the partitioning process do exist (Bevin and German, 1981; Thomas and Beasley, 1986a).

The extent to which subsurface flow contributes to total streamflow is a function of the vegetation, topography, soils and geology of a watershed. Examples of the percent of storm precipitation that leaves a watershed as subsurface runoff range from 18 to 53% for large storms on deep sandy loams in Ohio (Whipkey, 1965), to 2 to 20% on deep sandy loams in North Carolina. Beasley (1976) showed that 5.1 to 49.2% of the annual runoff from two Mississippi coastal plain watersheds containing deep permeable soils was subsurface runoff.

Saturation overland flow may be divided further into return flow, subsurface flow that emerges and flows to a channel along the surface, and direct precipitation on

saturated areas (Dunne, 1978). The presence of saturated areas or areas where subsurface flow can emerge as return flow is largely a function of topography. Saturated zones tend to form in concave areas of low relief where water flowing downslope may collect (Dunne et al., 1975; O'Loughlin, 1981; Anderson and Kneale, 1982; O'Loughlin, 1986). The area of saturation increases and decreases in response to precipitation inputs (Hewlett and Nutter, 1970 and Dunne and Black, 1970). Therefore, the area contributing to streamflow by saturation overland flow is variable over time. Since precipitation falling on saturated zones is transported to a stream channel rapidly as surface flow, saturation overland flow can account for very rapid rises and falls in streamflow (Dunne and Black, 1970).

Watershed physical characteristics determine the proportion of flow generated by subsurface runoff and saturation overland flow. Dunne (1978) provides an excellent summary based on a continuum of watershed characteristics. On watersheds with thin soils, concave footslopes, wide valley bottoms, and soils of high to low permeability, direct precipitation and return flow control streamflow generation. Subsurface flow controls streamflow generation on watersheds having straight steep hillslopes, deep permeable soils, and narrow valley bottoms.

Flow Processes and Water Chemistry

The flow path water takes through a watershed controls water chemistry by determining what materials the water comes in contact with, the time of contact or residence on the watershed, and the rates and quantity of water through each path (Dowd and Nutter, 1985). As water enters a watershed as precipitation, it undergoes numerous chemical transformations as it comes in contact with vegetation, soil and rock. Water flowing from a source with unique chemical properties should as a result, also have unique chemical properties.

The concept that water has chemical properties representative of the source has been used extensively to chemically separate groundwater flow from overland flow (Pinder and Jones, 1969). Ebise (1984) used nitrate-nitrogen loading to distinguish between surface, prompt subsurface flow, and base flow. Reid, et al. (1981) used the concentrations of dissolved organic carbon to determine the percentage of total streamflow produced from peat bog source areas. The concentrations of naturally occurring isotopes have been used more recently by Sklash and Farvolden (1979); Pearce, et al. (1986); and Hooper and Shoemaker (1986), to separate groundwater flow from total storm flow.

Direct measurements of the volumes, rates, and timing of flow from different sources have been made in numerous studies (Whipkey, 1965; Dunne and Black, 1970; Beasley,

1976; Weyman, 1973; and Mosely, 1979). Measurements of the water chemistry from different sources have been limited to the analysis of bulk samples (Jackson, et al., 1973; Kachonski and DeJong, 1982; and DeOliveira Liete, 1985) collected from each source. These studies did not investigate the changes in concentration of chemical constituents concurrently with the changes in flow over time during storm events.

Recent research has investigated the concept that streamflow is composed of a mixture of old and new water (Pilgrim, et al., 1979). Old water is water stored in the watershed prior to an event. New water is added to the watershed during an event. Old water is displaced from the subsurface matrix by newly added water. As a result, streamflow is a mixture of old water and new water. The concept seems to support the concept of translatory flow (Hewlett and Hibbert, 1967), where existing water in the soil matrix is displaced downhill through the subsurface to a stream. Old water has been shown to form a large proportion of stormflow. Sklash and Farvolden (1979) used naturally occurring isotopes to show stormflow from a watershed with deep permeable sands was primarily generated from pre-event groundwater. Employing similar natural isotope techniques, old water was also found to be a major component of stormflow from small forested watersheds with steep slopes and shallow soils (Pearce, et al., 1986 and Hooper and Shoemaker, 1986). Thomas and Phillips (1979)

theorized that actual flow through soil is most likely a combination of displacement of old water and flow through macropores of new water. Although the process is not totally understood, the implications for water chemistry modeling are great.

CHAPTER III

WATERSHED HYDROLOGY AND WATER QUALITY MODELING

Watershed Hydrology Models

Watershed hydrology models are simply mathematical algorithms that attempt to solve the hydrologic processes responsible for streamflow or water yield from a watershed. The approach used to model hydrologic processes varies from model to model. Numerous watershed models, representing a range of modeling approaches from simple to highly complex, have been devised. Renard et al. (1982), offer summaries of 75 watershed models currently in use by government agencies and research institutions. The purpose of this review, is to look at a few of the watershed models that have been used, or have potential, with modification, to be used for modeling forested watersheds. Hydrologic processes important on forested watersheds are emphasized. Processes emphasized include precipitation, interception and through-fall, infiltration, surface runoff, channel interception, variable source area, subsurface flow, evapotranspiration, soil water balance, groundwater flow, and channel streamflow routing.

The review is not all-encompassing. Rather, it reviews models representing a range of modeling approaches, from lumped to distributed, conceptual to physical, and from simple to complex. The watershed model review consists of two parts. The first part contains a general review of each modeling approach used. The second part looks at how the individual processes of the hydrologic cycle are modeled. The models are arranged in increasing order of complexity of representation of the hydrologic processes.

Kentucky Daily Watershed Model

Modeling Approach

The Kentucky Daily Watershed Model (KDW) was designed to simulate daily streamflows from small forested watersheds in eastern Kentucky continuously throughout a water year (Sloan et al., 1983). The KDW model is a lumped-parameter, deterministic model. The model consists of a series of connected stores (Figure 1). Inputs and outputs represent physical processes. The model is somewhat physically based because some of the process parameters are measurable in the field. Other parameters must be obtained from calibration with known streamflows. Therefore, the KDW model is not well suited for application to ungaged watersheds. The KDW model contains thirteen parameters.

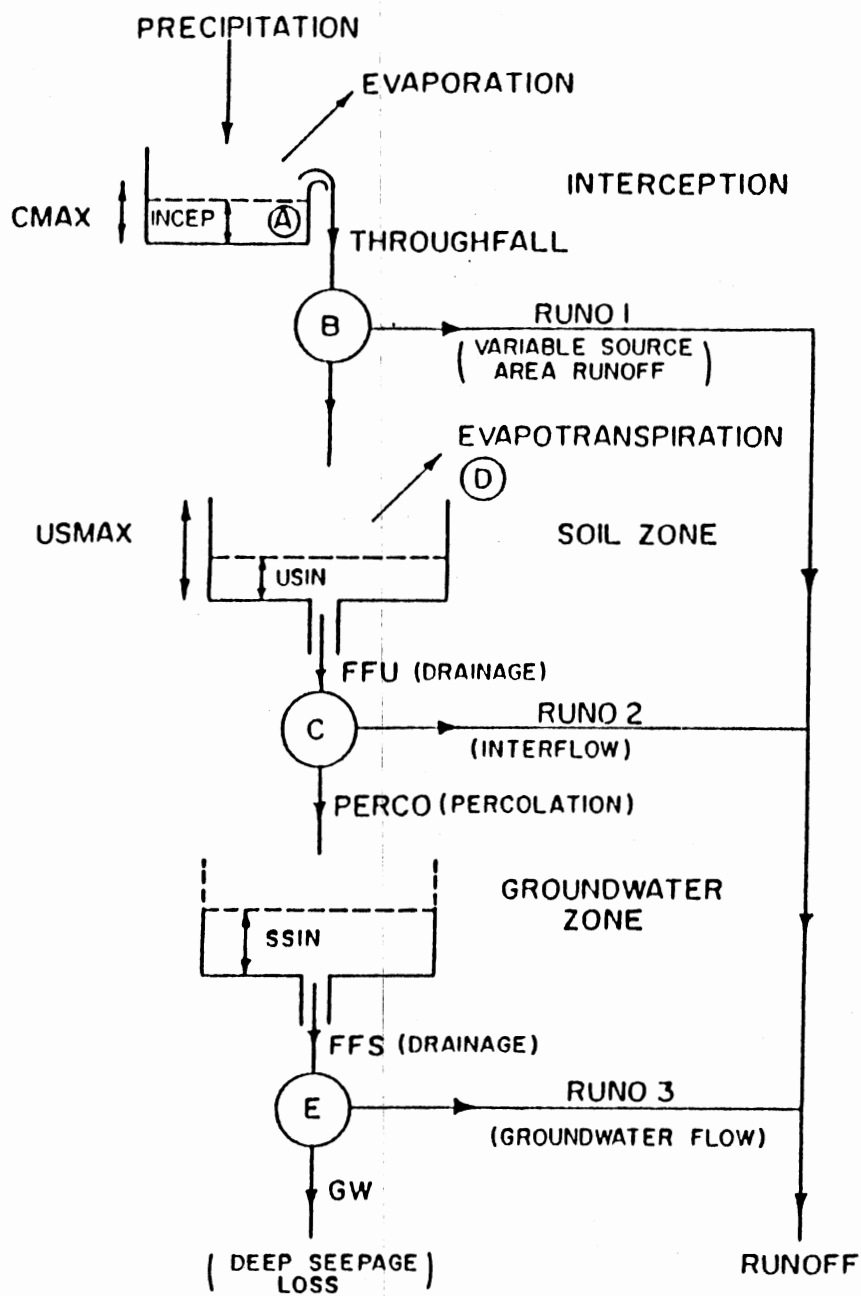


Figure 1. Structure of the Kentucky Daily Watershed Model (from: Sloan et al., 1983).

Hydrologic Processes

Precipitation. Daily precipitation provides the input to the model.

Interception. Interception is represented by a store having a maximum capacity of CMAX. CMAX is a function of a maximum interception storage capacity (CEPMAX) and the degree of canopy development (FCAN).

$$CMAX = CEPMAX * FCAN$$

FCAN is a function of the seasonal changes in leaf area index and canopy cover. FCAN is at a minimum during the winter, and at a maximum of 1 during the summer. Evaporation is removed from the store for each time step. When the store is filled, throughfall is available.

Infiltration. All water is assumed to infiltrate, except on the saturated source area. Total infiltration (INFIL) , is equal to the fraction of the watershed area not in the saturated source area (1-PB) times the net throughfall (RAIN - CMAX)

$$INFIL = (1-PB)*(RAIN - CMAX)$$

Surface Runoff. Surface runoff is assumed to occur only on saturated areas.

Variable Source Area. The function used to calculate the fraction of the watershed occupied by the variable

source area (PB) was taken from the BROOK model (Federer and Lash, 1978).

$$PB = FSTP + PC * \exp[PAC * (USIN/USMAX)]$$

where PAC and PC are variable source area constants, FSTP is the fraction of the watershed area in stream channels, USIN is the water content of the soil zone, and USMAX is the maximum soil zone water content.

Channel Interception. Channel interception is included in the variable source area routine. The area occupied by stream channels (FSTP) is considered to be a fixed percentage of the watershed area.

Evapotranspiration. Actual evapotranspiration is limited by either the potential evapotranspiration (PET), or the plant-available water (USIN - USWP). Plant available water is equal to the actual soil water content (USIN) less the water content at the -15 bar soil water potential (USWP). Potential evapotranspiration was estimated by evaporation pan data. However, Sloan et al.(1983) point out equations using mean daily temperature to calculate PET could be added to the KDWM.

Soil Water Balance. The daily soil water balance is calculated by accounting for daily inputs of infiltration (INFIL), and outputs, percolation (FFU) and evapotranspiration (EVAP)

$$USIN = INFIL - EVAP - FFU.$$

As in the BROOK model (Federer and Lash, 1978), drainage from the soil zone (FFU) is assumed to be equal to the hydraulic conductivity. Hydraulic conductivity is calculated as a function of soil water content.

$$FFU = FU * \theta^{2b+3}$$

where FU is a constant, θ is the soil water content, and $2b+3$ is a constant obtained from the soil moisture release curve. The soil moisture release constant ($2b+3$) is calculated from the following pressure head (h) soil moisture (θ) relationship

$$h = a\theta^{-b}$$

where a and b are constants obtained by measurement.

Subsurface Flow. Subsurface flow (RUNO2) is released from the soil zone store as a fixed fraction (K1) of the drainage from the soil zone

$$RUNO2 = K1 * FFU$$

The interflow constant (K1) must be obtained from calibration with known streamflow.

Groundwater. Input to the groundwater store (SSIN) is percolation (PERCO) from the soil water store.

$$PERCO = (1-K1) * FFU .$$

Release of flow from the non-linear groundwater store (FFS) is calculated by

$$FFS = FS * (SSIN)^{KS}$$

where SSIN is the quantity of water in storage, and KS and FS are groundwater constants obtained from calibration, or from recession curve analysis.

Channel Flow Routing. All releases from storages are summed at the outlet for each daily time step.

BROOK Model

Modeling Approach

BROOK (Federer and Lash, 1978) is a deterministic, lumped parameter, continuous simulation, daily streamflow model. The model was originally designed to simulate water yield differences from forested watersheds under different hardwood cover types in New Hampshire. The model is composed of a series of storages, each representing a component of the hydrologic cycle (Figure 2). Interception, evapotranspiration, and soil water balance are tree species dependent. Both processes are related to the leaf area index (LAI), stem area index (SAI), and rooting depth of a tree species. BROOK also contains a variable source area component.

Snow interception, accumulation, melt, and evaporation routines, were omitted from the discussion provided by Fed

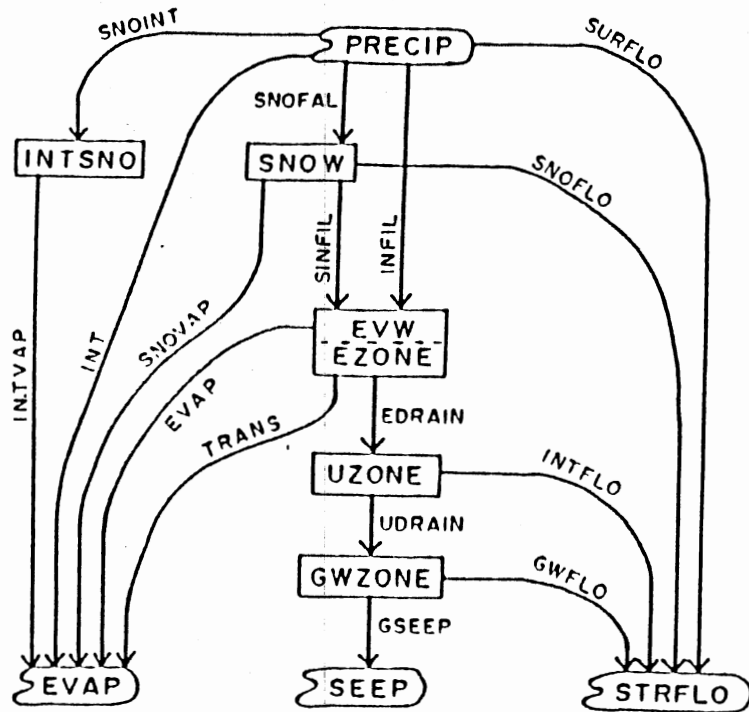


Figure 2. Structure of the BROOK Hydrologic Model (from: Federer and Lash, 1978)

erer and Lash (1978), because the research was carried out for watersheds dominated by rain. Since watersheds in southeastern Oklahoma are also dominated by rain, the snow routines are not considered important. The daily time step is divided into smaller intervals during intense storms for calculating rapid changes in soil water content, moisture dependent hydraulic conductivities, and flows from the variable source area. The number of intervals increases with rainfall and initial soil water content.

Hydrologic Processes

Precipitation. Daily precipitation provides input for the model. BROOK arbitrarily assumes the precipitation is snow for average daily temperatures below -2.8°C .

Interception. The interception store is divided into rain and snow components. Rainfall interception (INT) is limited by the lesser of potential evapotranspiration (PET) and daily rainfall (RAIN). Interception is given by

$$\text{INT} = 0.75(0.67\text{LAI}/4 + 0.33\text{SAI}/2) * \text{minimum of}(\text{PET or RAIN})$$

where LAI is the leaf area index and SAI is the stem area index. A portion of the rain is allowed to penetrate the canopy before the interception store is filled.

Infiltration. All water is assumed to infiltrate into the soil. Infiltration (INFIL) is equal to the throughfall

(RAIN - INT) times the fraction of the watershed area not occupied by the saturated variable source area.

$$\text{INFIL} = (1 - \text{PRT})(\text{RAIN} - \text{INT})$$

where PRT is the fraction of watershed area covered by a saturated contributing area.

Surface Runoff. Surface runoff was assumed to not occur, except on the saturated areas.

Channel Interception. A fixed impervious area for channel interception of 1% of the total watershed area was assumed.

Variable Source Area. The variable source area (PRT), or saturated contributing area, is defined as an exponential function of the available water in the root zone plus the 1% channel area.

$$\text{PRT} = 0.01 + \text{PC} * \exp[\text{PAC}(\text{EZONE}/\text{EZDEP} - \text{EZ15})]$$

where EZONE is water storage in the root zone, EZDEP is the maximum root zone water storage, EZ15 is the water content at the 15 bar wilting point, PC is a variable source parameter, and PAC is a variable source parameter. The two variable source parameters, PC and PAC, must be calibrated. Surface runoff generated in the variable source area is assumed to enter the channel in one time step.

Evapotranspiration. Potential evapotranspiration (PET) was calculated from the mean daily temperature using the Hamon procedure. Evaporation from the interception store is equal to the potential rate. Soil evaporation (SEVAP) and soil transpiration (TRANS) are calculated individually using a rate equal to the lesser of the potential evapotranspiration (PET) times the ratio of the daily potential insolation on the watershed to that of a horizontal surface (RS), or a soil water supply function.

$$SEVAP = [(LAI-4)^2/16.84+0.05]*\min\{EVWA/CE \text{ or } PET*RS(1-0.3SAI)\}$$

where EVWA is the evaporation water available in top 50mm of soil, is equal to $EVW - 50 * EZ15$, EZ15 is the relative soil water storage at -15 bar potential, EVW is the maximum water storage in the top 50 mm of soil, and CE is an evaporation constant. Transpiration is given by

$$TRANS = [1-(LAI/4-1)^2] * \min \{EZA/CT \text{ or } PE * RS\}$$

where EZA is the available water in the entire root zone. EZA is equal to $EZONE - EZDEP * EZ15$. EZONE is the current water storage in the root zone, EZDEP is the root zone depth, and CT is a constant for transpiration. The evaporation constant, CE, and the transpiration constant, CT, must be obtained from calibration.

Soil Water Balance. The soil water balance for the root zone (EZONE) is simply an accounting of the inflows and outflows

$$EZONE = INFIL - SEVAP - TRANS - EDRAIN$$

where EDRAIN is the outflow (percolation) from the root zone. EDRAIN is assumed to equal the hydraulic conductivity at the mean water content of the root zone. A power law relationship between hydraulic conductivity and water content is assumed.

$$EDRAIN = KEINT * (EZONE / EZDEP)^{KESLP}$$

where KEINT and KESLP are soil parameters obtained from moisture release curves of the soils.

Subsurface Flow. Subsurface flow, or interflow, is released from an unsaturated store directly below the root zone. Input to the store is EDRAIN. Output from the store is interflow (INTFLO) and deep percolation to the groundwater storage (UDRAIN). Total drainage (TD) from the unsaturated zone is calculated in a manner analogous to drainage from the root zone, as a power law function of the ratio of water in the storage (UZONE) to the total zone depth (UZDEP).

$$TD = UAEINT * (UZONE / UZDEP)^{UKESLP}$$

where UAEINT and UKESLP are soil parameters obtained from moisture release curves. Losses to evapotranspiration are

not removed from the unsaturated zone. The total drainage is arbitrarily divided into deep percolation to the groundwater store (UDRAIN) and interflow (INTFLO). The fraction of drainage going to interflow may also be calculated by model calibration.

Groundwater Flow. Groundwater flow is released from the groundwater store. Federer and Lash assumed groundwater flow (GWFLOW) was equal to a constant fraction (0.005) times the amount of water in the store (GWZONE):

$$GWFLOW = 0.005 * GWZONE.$$

Evapotranspiration from the groundwater store is assumed to not occur.

Channel Flow Routing. All storage releases are summed at the outlet for each time step.

Stanford Watershed Model

Modeling Approach

No discussion of watershed models can be complete without mentioning the Stanford Watershed Model (SWM) (Crawford and Linsley, 1966). SWM was one of the first general purpose watershed models developed and applied with success (Fleming, 1975). The model has been used world-wide and has undergone numerous revisions. The model is mentioned here, not because of its suitability or non-suitability for modeling forested watersheds, but because it has been used as

the hydrologic component in two water quality models, the Non-Point Source Model (Donigian and Crawford, 1976b) and the Agricultural Runoff Model (Donigian et al., 1977) discussed in a later section.

SWM is essentially a lumped-parameter deterministic model of watershed hydrology (Fleming, 1975). SWM produces continuous simulations of streamflow at increments as small as 15 minutes. Small watersheds that comprise a larger basin may be modeled as lumped basins and linked via channel routing. Functions that model the various hydrologic processes have changed in the different versions of SWM. Functions and parameters of the Stanford Model IV, as summarized by Fleming (1975), are discussed here. SWM IV, contains 34 parameters, 4 of which must be optimized through calibration with known streamflows. Therefore, the model has limited applicability to ungaged watersheds.

Hydrologic Processes

Precipitation. Time increments as small as 15 minutes may be used. SWM also accepts snow as precipitation input to the watershed.

Interception. Interception is modeled using the simple storage equation

$$S_i = (P * D_c) - E_{in}$$

where S_i is the change in interception storage, P is the precipitation per unit area, D_c is the canopy density, or

fraction of total area covered, and E_{1n} is the evaporation from storage. Throughfall occurs from the fraction of the area not covered by the canopy and when the interception store is full.

Infiltration. Infiltration is treated as a function of soil moisture storage and time.

$$f_t = (INF)/(LZS_{t-1}/LZSN)^b$$

where f_t is the mean infiltration capacity at time t (in), INF is a parameter related to soil characteristics (in), LZS_{t-1} is the actual soil moisture at $t-1$ in the lower soil zone (in), LZSN is the field capacity of lower soil zone (in), and b is an exponent, normally equal to 2. Spatial variability in infiltration capacity is accounted for by fitting infiltration capacity to a linear frequency distribution. From the distribution, one may calculate the percent of the watershed area having a particular infiltration capacity.

Surface Runoff. A surface storage, or detention storage, technique is used to solve the continuity equation of overland flow. The surface storage consists of a plane having an average slope (SS) and average length (L). The depth of storage-discharge relationship uses a modified form of Manning's equation.

$$q = 1.486/n \text{ SS}^{1/2} * (D/L)^{5/3} * [1.0 + 0.6(D/D_m)^3]^{5/3}$$

where q is the discharge from the overland flow plane, n is Manning's coefficient of surface roughness, D is the current level of surface detention storage, and D_e is the surface detention storage at equilibrium.

During receding flows, D/D_e is assumed to be 1.0. The current depth of surface detention storage (D) is calculated by solving the continuity equation.

$$D_2 = D_1 + D - q \Delta t$$

where D_2 is the detention storage in present time interval, D_1 is the detention storage in previous time interval, D is the rainfall excess added during time interval, q is the outflow from the overland flow equation above, and Δt is the modeling time increment.

Variable Source Area. None per se. However, the infiltration distribution does account for impervious, or presumably saturated areas.

Channel Interception. Channel interception is accounted for by assuming the stream channel is a permanently saturated area.

Evapotranspiration. Actual evapotranspiration (E_a) is calculated as a function of the potential rate (PET) and the soil moisture deficit (LZS/LZSN).

$$E_a = PET * (LZS/LZSN) * B$$

where B is the portion of residual PET applied to soil storage. The potential evapotranspiration may be calculated from daily evaporation pan data, or from an evapotranspiration equation.

Actual evapotranspiration from the lower soil zone (root zone) is represented by the evapotranspiration opportunity (r).

$$r = [0.25/(1.0-K3)]*[LZS/LZSN]$$

where r is the evapotranspiration opportunity (in or mm), and K3 is a vegetation areal cover index. The evapotranspiration opportunity represents the change in evapotranspiration over time as soil and vegetative characteristics change. Evapotranspiration is removed from all soil zones and the groundwater storage.

Soil Water Balance. Two soil water storages, an upper zone and a lower zone are modeled. The upper soil zone is an infiltration control zone that is immediately responsive to rainfall. The lower soil zone represents storage from near the surface down to the capillary fringe. The lower soil zone is assumed to contain the majority of plant roots. Input to the lower soil zone includes gross infiltration and drainage from the upper soil zone. Drainage from the upper soil zone (D_r) is given by

$$D_r = 0.1 * INF * UZSN * [(UZS/UZSN) - (LZS/LZSN)]$$

where INF is the gross infiltration, UZSN is the nominal upper soil zone storage, LZSN is the nominal lower soil zone storage, UZS is the actual upper soil zone storage, and LZS is the actual lower soil zone storage. Outflow consists of evapotranspiration, drainage, and subsurface flow.

Subsurface Flow. The quantity of water allocated to subsurface flow, or interflow, is calculated using an empirical function of the local infiltration rate.

$$f_t = f + f * (c-1)$$

where f_t is the total mean infiltration capacity, f is the mean infiltration capacity of an area, and c is an interflow component that is a function of the soil water deficit.

The volume of interflow storage (SRGX) is calculated using the linear frequency distribution for infiltration and $f(c-1)$ from above. Interflow (q_i) is calculated as a function of the quantity of water in interflow storage (SRGX) and the daily interflow recession rates (IRC) obtained from observed hydrographs.

$$q_i = [1.0 - (IRC)^{1/96}] * SGRX$$

The term $1/96$ converts the daily rate to a 15 minute time interval.

Groundwater Flow. The quantity of water in the groundwater storage is given by

$$\{S_{gw}\}_t = \{S_{gw}\}_{t-1} + p\Delta t - q_g\Delta t - c\Delta t - q_{dg}\Delta t$$

where S_{gw} is the groundwater storage at times t and $t-1$, p is the seepage rate to the groundwater store, q_g is the groundwater flow rate, c is the upward flow rate due to capillary rise, q_{dg} is the deep percolation to an inactive groundwater store, and Δt is the simulation time increment.

The ground water flow rate is a function of the storage (S_{gw}) and observed recession rates.

$$q_g = [1.0 - (KK24)^{1/96}] [1.0 + KV * S] * S_{gw}$$

where $KK24$ is the observed daily groundwater recession, $1/96$ is a conversion factor that converts daily time to 15 min increment, KV is a variable groundwater recession parameter, and S is the groundwater slope (fixed value, GWS , + incremental slope based on inflow).

Channel Flow Routing. Time delay histograms of flow from each watershed are lagged and summed.

USGS Precipitation-Runoff Modeling System

Modeling Approach

The USGS Precipitation-Runoff Modeling System (PRMS) (Leavesley et al., 1983) was developed to provide continuous daily or storm event predictions of streamflow and sediment transport from watersheds under various land uses and climatic regimes. PRMS is a distributed parameter, deterministic, physical process model. All hydrologic processes are described using known relationships, or empirical relation-

ships that have physical meaning. The modeling system is modular in structure to allow for the linking of the hydrologic core model to a library containing subroutines. The library contains individual subroutines for snowmelt, sediment transport, parameter optimization, and other hydrologic process routines.

Hydrologic processes are modeled as a series of linked storage reservoirs. Surface runoff and channel flow are modeled using kinematic wave routing procedures. Watershed hydrology may be simulated in a daily or storm mode. The storm mode has a 1 minute minimum simulation time interval.

All parameters may be lumped for a watershed. To run PRMS in the distributed parameter mode, the watershed is broken down into hydrologic response units (HRU's). Hydrologic processes are considered to be homogeneous in each HRU. Water balance and energy balance are computed daily for each HRU. Partitioning of a watershed into HRU's may be done on the basis of vegetation, land use, slope, aspect, and soil type. Soil zone reservoirs and groundwater reservoirs may be defined for the whole watershed or the individual HRU's.

A second, more detailed level, of partitioning is available for storm hydrograph simulation. A watershed can be broken into flow planes for surface runoff routing and channel segments for channel routing. An HRU can be considered a flow plane, or be divided into a number of flow

planes. Up to 50 overland flow planes and 50 channel segments may be designated.

Hydrologic Processes

Precipitation. Break point or daily precipitation values may be used. The model contains an algorithm to calculate whether the precipitation is rain, snow, or a mixture of rain and snow, based on maximum and minimum daily temperatures.

Interception. Interception is calculated as a function of the seasonal cover density (COVDN, COVDNS and COVDNW for summer and winter, respectively) and the available storage of the predominant vegetation (STOR). The net precipitation (direct precipitation + canopy wash) is

$$PTN = [PPT * (1 - COVDN)] + (PTF + COVDN)$$

where PPT is the incoming precipitation, and PTF is the precipitation falling through the canopy. PTF is calculated as a function of maximum storage (STOR) and the current level of canopy storage (XIN). For PPT greater than the quantity (STOR-XIN), PTF is equal to PPT - (STOR - XIN). For cases where PPT is less than the quantity (STOR-XIN), PTF is equal to zero.

STOR is defined for season and precipitation form. Evaporation from the canopy is assumed to occur at the free-water surface rate (EVCAN). EVCAN is equal to the pan

evaporation rate, or calculated from the potential evapotranspiration rate (PET).

$$EVCAN = PET/EVC(MO)$$

where EVC = the evaporation pan coefficient for month MO.

Infiltration. Infiltration for storm mode calculations is calculated using a modified form of the Green-Ampt equation.

$$FR = KSAT * (1.0 + PS/SMS)$$

where FR is the point infiltration capacity (in/hr), KSAT is the hydraulic conductivity of the transmission zone (in/hr), PS is the product of capillary drive and moisture deficit (in), and SMS is the current accumulated infiltration (in). PS is calculated as a linear function of the ratio of the current moisture (RECHR) to the maximum moisture storage in the recharge zone (REMX) over the range of PS.

$$PS = PSP * [RGF - (RGF - 1) * (RECHR/REMX)]$$

where PSP is the value of PS at field capacity, and RGF is the maximum value of PS. Net infiltration (FIN) is equal to $PTN - PTN^2/2FR$, for cases when PTN is less than FR.

Surface Runoff. Rainfall excess is routed over the flow planes by a kinematic wave approximation. All flow planes must discharge to a channel flow segment.

Variable Source Area. The daily runoff mode calculates the contributing area using either a simple linear or nonlinear function of soil moisture. The percent of HRU area contributing to runoff (CAP) at a particular time is calculated using the linear relationship

$$CAP = SCN + [(SCX - SCN) * (RECHR/REMX)]$$

where SCN is the minimum possible contributing area, SCX is the maximum possible contributing area, RECHR is the current available water in recharge zone, and REMX is the maximum storage capacity of the recharge zone.

The nonlinear method uses a soil moisture index (SMIDX) equal to the sum of the current available soil water plus one-half of the daily net precipitation.

$$CAP = SCN * 10^{(SC1 * SMIDX)}$$

where SCN and SC1 are coefficients calculated from direct measurements of soil moisture and streamflow.

The coefficients may also be calculated from initial runs of the model using a regression technique of the form

$$\log CAP = a + b * SMIDX$$

where SCN is equal to 10^a and SC1 is equal to b. Surface runoff is equal to CAP multiplied by the net precipitation. The variable source area concept is not used in the storm mode calculations.

Channel Interception. Channel interception is not specifically mentioned in the model. However, channel interception may be regarded as the minimum contributing area (SCN).

Evapotranspiration. Evapotranspiration is computed on a daily basis. Three methods of calculating potential evapotranspiration, based on pan evaporation, mean daily air temperature and possible hours of sunshine, and daily solar radiation, respectively, are available. The mean daily temperature method is used in the BROOK model, discussed below. Potential evapotranspiration (PET) from pan data is computed by

$$PET = EPAN * EVC(MO)$$

where EPAN is the daily pan-evaporation loss (in) and EVC is the monthly pan coefficient for month MO. PET using the daily solar radiation option is

$$PET = CTS(MO) * (TAVF - CTX) * RIN$$

where TAVF is the mean daily air temperature (°F), CTS is a coefficient for month MO, CTX is a coefficient, and RIN is the daily solar radiation expressed in inches of evaporation potential. The monthly correction coefficient CTS corrects for under estimation of PET by the method during winter months.

$$CTS = [C1 + (13.0 * CH)]^{-1}$$

where C_1 is an elevation correction factor equal to $68.0 - [3.6 * (\text{median elevation in feet}/1000)]$, and CH is a humidity index equal to: $50/(e_2 - e_1)$. The constants e_2 and e_1 are equal to the saturation vapor pressure (mb) for the mean maximum air temperature for the warmest month of the year, and the saturation vapor pressure (mb) for the mean minimum air temperature for the warmest month of the year, respectively.

The coefficient CTX , calculated for each HRU, is

$$CTX = 27.5 - 0.25 * (e_2 - e_1) - (\text{median HRU elevation in feet}/1000)$$

Actual evapotranspiration (AET) is computed as a function of the ratio of the actual moisture storage to the maximum moisture storage in the soil zone. AET is assumed to equal PET when moisture is not limiting. PET is satisfied from the interception, detention, and snow pack storages first. The remaining PET demand is divided between the recharge and lower soil zones. The ratio of AET to PET for different percentages of maximum water storages and soil textures are presented by Leavesley et al. (1983).

Soil Water Balance. The soil zone is divided into a recharge zone and a lower zone (Figure 4). The depth of the soil zone is defined as the rooting depth of the predominant vegetative cover. Water losses from the recharge zone are from evaporation and transpiration. Losses from the lower zone are from transpiration only. When the maximum storage

capacity of the recharge zone (SMAX) is filled, water flows to the lower zone. Water in excess of the lower zone maximum storage (LZMX) enters the subsurface flow reservoir.

Subsurface Flow. A nonlinear subsurface reservoir is used to simulate subsurface flow. Inflow to the reservoir is provided by water in excess of the maximum moisture storage content of the soil reservoir. Outflow from the subsurface flow reservoir (RAS) is given by

$$RAS = RCF * RES + RCP * RES^2$$

where RCF and RCP are coefficients, and RES is equal to the reservoir storage. The equation above is combined with the continuity equation ($dS/dt = \text{inflow} - \text{outflow}$) and solved for the initial condition where $RES = 0$. For a given time increment, RAS is given by

$$RAS * t = INFLOW * t + SOS * (1 + (RCP/XK3) * SOS) * (1 - e^{-XK3 * t})$$

$$1 + (RCP/XK3) * SOS * (1 - e^{-XK3 * t}),$$

where $SOS = RES_0 - (XK3 - RCF) / (2 * RCP)$, $XK3 = (RCF^2 + 4 * RCP * INFLOW)^{1/2}$, and t is the simulation time increment.

Estimates of the routing coefficients may be obtained from analysis of hydrograph recession curves. RES and RAS may be calculated using

$$RES = -RAS / \log_e K_r$$

where K_r is the subsurface recession constant for $t=1\text{day}$.

Each HRU may have its own subsurface reservoir, or IN-FLOW may be combined into one reservoir from several HRU's. Outflow from the subsurface reservoir to the groundwater reservoir (GAD) is given by

$$GAD = RSEP * (RES/RESMX)^{REXP}$$

where RSEP is a daily recharge coefficient, RES is the current storage in subsurface reservoir, and RESMX and REXP are coefficients.

Groundwater Flow. Groundwater flow is modeled as a linear reservoir. Input to the groundwater reservoir is provided by direct seepage from the soil zone (SEP) and outflow from the subsurface flow reservoir (GAD). Outflow from the groundwater reservoir is given by

$$BAS = RCB * GW$$

where BAS is the base flow in acre-inches, RCB is a reservoir routing coefficient, and GW is the groundwater storage (acre-in).

The groundwater reservoir routing coefficients may be calculated using the same procedure described above for calculating the subsurface flow reservoir routing coefficients. Recession curve analysis may be used to estimate the groundwater recession constant. The model also allows for deep seepage losses to areas outside the watershed.

CREAMS

Modeling Approach

The field scale model for Chemicals, Runoff, and Erosion from Agricultural Management Systems (CREAMS), is a lumped parameter deterministic model designed to predict streamflow and sediment and chemical transport from small agricultural watersheds (Knisel, 1980). The hydrology component contains two options, daily runoff, using the SCS runoff Curve Number method, and individual storm analysis, using breakpoint precipitation data (Smith and Williams, 1980). The model is capable of supplying continuous predictions for a time period of interest. Soil water storage and evapotranspiration are calculated on a daily basis in both hydrology options. The model is designed for use on small (<40 ha.), or field scale, agricultural watersheds.

The model is essentially physically-based, in that parameters may be obtained directly from field measurements. The ten parameters required for the breakpoint hydrology option are effective hydraulic slope, effective slope length, Manning's n for the field surface, effective hydraulic conductivity of the soil, effective capillary tension, soil evaporation, soil porosity, the percent of available water storage at field capacity, soil water content at 15 bar tension, and leaf area index.

Hydrologic Processes

Precipitation. Break point or daily inputs are used.

Interception. SCS Curve Number method is used to calculate initial abstractions.

Infiltration. Infiltration is calculated using a modified form of the Green and Ampt equation.

$$K_s t = F - \phi H_c (S_0 - S_1) \ln [1 + F / \phi H_c (S_0 - S_1)]$$

where K_s is the effective saturated conductivity, t is the time from start of ponding, H_c is the effective capillary tension, F is the cumulative depth of infiltration, S_0 is the beginning saturation, S_1 is the interval saturation, and ϕ is the soil porosity.

The infiltration rate for a time interval ($f = dF/dt$) is estimated by a finite difference technique and a series approximation for the natural logarithm, so that

$$F = 4A[GD + F] + (F-A)^2 + A - F$$

where $A = K_s t/s$, $G = H_c$, $D = \phi(S_0 - S_1)$, and ϕ is the soil porosity. Rainfall excess is calculated by subtracting the average infiltration for the time interval from the interval precipitation.

Surface Runoff. Rainfall excess is routed over the land surface using a kinematic wave approximation. An equivalent single plane with an effective hydraulic slope

and an effective slope length is used to represent the watershed surface. Chezy's equation of open channel flow is used as the storage-discharge equation.

Channel Interception. No channel interception is provided.

Evapotranspiration. The evapotranspiration term includes direct soil evaporation and losses due to plant use. Potential evapotranspiration (E_o) is calculated daily using the Ritchie equation.

$$E_o = 1.28 H_o / (\Delta + \eta)$$

where $\Delta = (5304/T^2) * e^{(21.255 - 5304/T)}$, T is the mean daily temperature in degrees K, $H_o = (1-L)R/58.2$, R is the mean daily solar radiation, L is the albedo for solar radiation, and η is a psychrometric constant.

Soil and plant evaporation are computed separately. Soil potential evapotranspiration is computed as an exponential function of E_o and leaf area index. Actual soil evaporation is limited by a soil water transmission coefficient. Plant use evaporation (transpiration) is a function of the crop type and leaf area index, and is limited by available soil moisture at the 15 bar wilting point.

Soil Water Balance. The soil water balance is calculated on a daily interval. The soil is divided into a surface zone and a root zone. The surface zone controls infiltration. The surface zone is subject to soil evaporation

and evapotranspiration from plants. The root zone extends to the maximum rooting depth. It is subject to evapotranspiration losses during the growing season. The soil water budget equation is given by

$$SM_i = SM_{i-1} + Fi - ET_i - O_i + M_i$$

where F_i is the infiltration on day i , ET_i is the plant and soil evapotranspiration, O_i is the seepage below the root zone, M_i is the snow melt, and SM_i is the soil water storage in the root zone.

Soil Water Flow. The model contains no lateral subsurface flow component. Water leaving the root zone (O_i in the equation above) is accounted for, but not included in runoff calculations. Percolation from the upper soil zone to the root zone (q_u) is a function of the positive difference in saturation between the two zones.

$$q_u = C_u S_u (S_u - S_p) \phi D_u$$

where q_u is the flow from upper to lower zone, S_u is the saturation by volume in surface zone, S_p is the saturation by volume in root zone, C_u is a coefficient, normally 0.1, ϕ is the soil porosity, and D_u is the depth of surface zone (2-5 cm). Percolation from the root zone occurs when the water content exceeds field capacity.

TOPMODEL

Modeling Approach

TOPMODEL is a deterministic, distributed model of watershed hydrology (Bevin and Kirkby, 1979). TOPMODEL is capable of providing a continuous simulation of streamflow at small time increments over a desired time interval. The model is composed of five linear and non-linear reservoirs, each of which represent hydrologic processes. A major feature of the model is the inclusion of a variable contributing area routine. The area and dynamics of the variable contributing area are controlled by topographic features and the rate of subsurface inflow from the hillslope above.

The watershed is divided into sub-basins, based on whether convergence or divergence of flow occurs as a result of topography. The sub-basins are further divided into segments along contour lines. Calculations of soil water balance, surface runoff, and subsurface flow are made on a time, hillslope segment, and sub-basin basis. Sub-basins are linked to the channel systems by a routing function.

TOPMODEL was improved (Bevin and Wood, 1983) and tested on three United Kingdom watersheds (Beven et al., 1984). TOPMODEL was later adapted to model a forested watershed in Virginia (Hornberger et al., 1985). The Virginia model, which represents the latest version of TOPMODEL, will be discussed here. All of the parameters may be measured in

the field, or from topographic maps. Therefore, TOPMODEL may be used to model ungaged watersheds.

Hydrologic Processes

Precipitation. Any break point time increment may be used in the model. The model was designed only for rainfall.

Interception. The interception store contains two stores, an interception store (SINT), and a litter layer store (SL). The inputs, outputs, and changes in storage are calculated on a basin wide scale. Water is routed through the litter layer to account for changes in water chemistry as it passes through the litter. Direct throughfall (DTF) is allowed to occur before the interception store is filled. Evaporation from both stores occurs at a decreasing rate proportional to the quantity of water in storage and the maximum storage.

Infiltration. All rainfall is assumed to infiltrate on unsaturated hillslopes.

Surface Runoff. Surface runoff is assumed to occur only from the saturated variable contributing area. No hillslope surface routing function is used. Surface runoff is assumed to reach the channel system during the same time interval in which it is generated.

Variable Source Area. The calculation of subsurface flow and the variable source area are both related to a topographic shape variable given by

$$\ln(a/\tan B)$$

where a is the upslope area drained through a point, per unit width of contour length, and $\tan B$ is the gradient of the slope, assumed to be constant for each sub-basin.

Values of $\ln(a/\tan B)$ are large for convergent topography, and small for divergent topography. From numerous point measurements of $a/\tan B$ over the sub-basin, an overall distribution, or an average value for $\ln(a/\tan B)$ may be obtained. Watershed sub-basins are divided into topographic increments, based on average $\ln(a/\tan B)$. All variable contributing area and subsurface flow calculations are performed for each time and $\ln(a/\tan B)$ increment in each sub-basin.

The saturated storage deficit (SD) for any value of $\ln(a/\tan B)$ is related to an average sub-basin storage deficit (S) by

$$SD = S + (m/A) \int_A \ln(a/\tan B) dA - m \ln(a/\tan B)$$

where m is the recession constant of the subsurface reservoir. Saturated topographic increments have an $SD \leq 0$, whereas for unsaturated increments, $SD > 0$. The water balance for each topographic increment is calculated for each time step. The area included in a $\ln(a/\tan B)$ increment is

added to the contributing area when the incremental storage becomes saturated ($SD=0$), or is deleted when the incremental storage becomes unsaturated ($SD > 0$). The contributing area may be obtained from an Ac/A vs. $\ln(a/\tan B)$ distribution calculated from watershed topography.

Channel Interception. The area of the watershed containing the stream channels and the surrounding riparian areas are assumed to be saturated. Throughfall falling into the channels and riparian areas is assumed to be immediately available to streamflow.

Soil Water Balance. Two storage elements are used to account for water in the soil and vertical percolation. Calculations for both stores are made by topographic segment $\ln(a/\tan B)$. One store (SRZ) represents the quantity of water below field capacity of the soil. The other store (SUZ) represents the quantity of water in the soil above field capacity that is available for vertical percolation to the delayed flow reservoir. Additions to SRZ includes all water infiltrated. Evaporation is removed from the SRZ store at a rate proportional to the potential rate and the fraction of the maximum storage filled. Evaporation is given by

$$\text{evaporation} = \text{PET} * (\text{SRZ} / \text{SRZMAX})^{\text{EPWR}}$$

where PET is the potential evaporation, SRZMAX is the maximum storage in the zone, and EPWR is an evaporation parameter.

The percolation storage, SUZ, is assumed to behave as a linear reservoir. Vertical drainage (QV) is given by

$$QV = SUZ * UO/SD$$

where UO is a constant parameter and SD is the saturation deficit. Under normal conditions, water does not reach the SUZ until evaporation in the SRZ store is satisfied. However, a fraction of the infiltrated water may be assumed to travel directly to the SRZ store if desired. Evaporation is not removed from the SUZ store.

Subsurface Flow. Subsurface flow is calculated from each topographic segment in a sub-basin as release from a non-linear delayed flow reservoir (S_3). Input to the reservoir is provided by release from the SUZ store. Subsurface flow (QB) is an exponential function of the ratio of the saturated zone deficit to the maximum saturated zone storage (SZMAX).

$$QB = SZQ * e^{(-s/sz)} * e^{(-s/szm)}$$

Groundwater Flow. Groundwater flow is assumed to emanate from the delayed flow reservoir. Since evaporation is not removed from the delayed flow reservoir, the model is not suitable for prediction of flows from watersheds with prolonged groundwater components.

Channel Flow Routing. Runoff produced during each time step (and for each sub-basin) is uniformly distributed over a number of time steps, as a function of maximum channel flow distance (DTW) and a constant channel kinematic wave velocity parameter (SUBV).

USDAHL

Modeling Approach

USDAHL is a deterministic, semi-empirical, semi-distributed model of watershed hydrology (Holtan and Lopez, 1971). The model was designed primarily for small agricultural watershed engineering planning. USDAHL can predict streamflow on an annual, monthly, daily, or event basis.

The model is semi-distributed because the watershed is divided into several (minimum of 1) hydrologic response zones. Soil moisture storage, infiltration, actual evapotranspiration, land use, and surface and subsurface flows are calculated for each response zone. Other processes and their parameters are lumped for the entire watershed. Surface and subsurface flow generated in a response zone is cascaded to the next downslope zone, until the flow reaches a stream channel. The hydrologic response zones are delineated on the basis of soil properties, cropping system, and land use. The zones also represent the natural elevational sequence of uplands, hillslopes, and bottom lands. Bottom lands near streams frequently become saturated source areas. Soils within each response zone are divided into

layers, representing soil horizons. Flow separation of percolation and subsurface flow from each soil layer is calculated by the model.

USDAHL has a large input requirement of 72 parameters. Parameters are arranged in four groups, watershed characteristics, soils, land use, and hydraulic properties. However, many of the parameters are required to represent the agricultural cropping system. Many of the parameter values are obtainable from soil surveys, maps, or direct measurement. Other parameters may require evaluation by calibration. Therefore, the model may not be suitable for ungaged watersheds.

Although USDAHL was not designed specifically for small forested watersheds, it does have potential for use, after some modification, on forested watersheds. USDAHL is, however, structured to supply flow information for water quality modeling (Campbell et al., 1983). Water quality parameters from respective zones and sources are stored in a subroutine called POLLUT. USDAHL has also been used as the hydrologic component in the Agricultural Chemical Transport Model (ACTMO)(Frere, et. al, 1975). ACTMO is discussed herein, in the water quality modeling section.

Hydrologic Processes

Precipitation. Breakpoint precipitation data is required for individual storm simulation. Daily rainfall data may be used for daily or longer simulation periods.

Interception. No forest canopy interception model is included in the model.

Infiltration. USDAHL uses the Holtan model of infiltration.

$$f = GI * a * (SA)^{1.4} + f_e$$

where f is the infiltration rate, GI is a crop growth index, SA is the available storage in the surface layer, a is an index of surface-connected porosity, and f_e is the constant rate of infiltration after prolonged wetting (equal to the saturated hydraulic conductivity).

Drainage from the surface layer, or infiltration control zone, occurs when gravitational detention storage is exceeded. The infiltration parameters are measurable soil properties. A routine to account for surface depression storage is also included.

Surface Runoff. Rainfall excess is routed as surface runoff across each response zone and cascaded through subsequent down slope zones. Infiltration of surface runoff in subsequent zones is accounted for. Surface runoff depth is calculated using a form of the continuity equation given by

$$Pe - Q = dD$$

where Pe is the rainfall excess rate (in/unit time) including input from the neighboring upslope zone, Q is the out-

flow rate (in/unit time), and dD is the change in depth (in).

The average depth of flow (D) is routed over the surface using the kinematic wave approximation

$$q_o = aD^n$$

where q_o is the surface runoff rate (in/unit time), a is a coefficient of roughness, slope gradient, and slope length, and $n = 3.0$ for laminar flow and 1.67 for turbulent flow. Surface roughness and slope characteristics are measurable parameters.

Variable Source Area. No variable source area routine is included. However, saturated source areas tend to occupy bottom land areas near stream channels. A hydrologic response zone can be delineated to represent such an area. Additionally, soil characteristics often follow drainage patterns. The slope, contributions of flow from upslope zones, and soil properties in the streamside zone, may cause the zone to behave as a saturated source area.

Channel Interception. No accounting of channel interception is made in the model.

Evapotranspiration. Potential evapotranspiration (PET) is calculated from weekly pan evaporation data times evaporation coefficients for crop growth

$$PET = GI * k * E_p * [(S-SA)/AWC]x$$

where GI is the growth index of crop in % of maturity, k is the ratio of GI to pan evaporation (usually 1.0-1.2 for grasses and 1.6-2.0 for forests), E_p is the pan evaporation in inches per day, S is total soil porosity, SA is the available soil porosity, AWC is the porosity drainable only by evapotranspiration, and x is set equal to AWC/gravity water. Evapotranspiration losses are calculated on a daily time basis. Evapotranspiration is removed only from the upper two soil zones that comprise the root zone.

Soil Water Balance. The soil zone may be divided into a number of layers to represent different soil horizons. The water balance of each zone for each time step is equal to the inputs minus the outputs. Input to a layer store is seepage from the layer above. Output is the sum of seepage to the layer below and subsurface flow.

Subsurface Flow. USDAHL allows for the modeling of subsurface flow from any or all of up to four soil layers. Subsurface flow regimes are considered to be sequential. The change in storage from a soil layer store is calculated using

$$S = m' \Delta q$$

where m' is the slope of a straight line section of the hydrograph recession curve, and Δq is the flow rate at the point where straight line segments of the recession curve intersect.

Values of m are assumed to represent the release from successive flow regimes, including the channel (m_c) and the soil layers (m_1, \dots, m_4). Outflow from each soil layer storage is calculated sequentially, using the outflow from the previous soil layer storage as input. Outflow from a storage unit is calculated using

$$q_i = (2 \Delta I)/(2m + \Delta t) + q_{i-1} * (2m - \Delta t)/(2m + \Delta t)$$

where q_i is the flow from the i th storage, q_{i-1} is the flow from the preceding storage, m is the recession slope for respective storages, and Δt is the time step. The calculation of the subsurface flow recession constants requires a streamflow record from a period of little or no evapotranspiration.

Groundwater Flow. Seepage from the preceding soil storage provides input to the groundwater storage. Flow from the groundwater storage is calculated using the equations for subsurface flow discussed above, with the appropriate recession constants.

Channel Flow Routing. A linear reservoir function is used to route channel flow.

FESHM

Modeling Approach

The Finite Element Storm Hydrograph Model (FESHM) is a single event, deterministic, distributed parameter model of

watershed hydrology (Smolen et al., 1983). The model adopted the distributed approach to model varying rates of erosion and water yield resulting from different land uses and agricultural practices. (Ross et al., 1980). FESHM was specifically designed for use on ungaged watersheds. The model parameters may be evaluated by direct measurement or from soil surveys and topographic maps.

In order to account for the distributed nature of soil properties, land use, and topography, FESHM uses two discretization schemes to break the watershed into homogeneous components. The first discretization scheme breaks the watershed into Hydrologic Response Units (HRU's) based on infiltration properties of the soils. The second scheme breaks the watershed into a number of topographic units. Subsheds are created by delineating areas draining into major tributaries. Subsheds are divided into overland flow strips, based on slope and average overland flow direction. Overland flow strips are further divided into overland flow elements to account for spatial variability in overland flow direction. The equations of motion are solved, using a finite element numerical method, for each flow element. The sequence of operations in FESHM is as follows. Rainfall excess is first calculated for each element. Later, overland flow for each flow strip is calculated and stored in an array. Finally overland flows are routed through the channels.

The watershed discretization scheme and the solution to the flow equations taken in FESHM is similar to the approach taken in ANSWERS (Huggins and Monke, 1968). However, whereas ANSWERS uses a grid of square elements, FESHM uses a variable shaped grid to better represent watershed topography. To date, FESHM contains no interception or subsurface flow routines. FESHM was also designed to be used to predict erosion and sedimentation from watersheds. The erosion and sedimentation scheme will not be discussed here.

Hydrologic Processes

Precipitation. Break point rainfall data is required for storm simulation.

Interception. FESHM contains no interception component. The lack of an interception component was assumed to be not limiting for large, high intensity storms, but may limit the use of FESHM for simulating flows resulting from low intensity storms (Smolen et al., 1983).

Infiltration. Infiltration is calculated using the Holtan equation. the infiltration rate (in/hr) is given by

$$F = GI * a * S^n + F_e$$

where GI is a monthly vegetation growth index, a is an index of cover density, S is the available pore space (in), n is the ratio of gravitational water (GW) to plant available water (PAW), and F_e is the final infiltration rate (in/hr).

Total infiltrated and rainfall excess volumes are calculated by numerically integrating the equation above over each time step.

Surface Runoff. Rainfall excess is routed across each flow element as overland flow. The flow direction is calculated from topographic maps. Each element is considered to be a flow plane. An average flow length and plane slope are calculated for each element. Overland flow length is taken as the longest flow path in the element, adjusted by a factor of two thirds. The area-weighted average rainfall excess is treated as a lateral input to the plane. The continuity equation is solved for each element and time step. Manning's n is used to estimate the surface roughness.

Variable Source Area. No variable source routine is provided.

Channel Interception. Channel interception is not included.

Evapotranspiration. Evapotranspiration was considered to be inconsequential during a large storm event.

Soil Water Balance. Only rainfall excess as overland flow is modeled by FESHM. However, an algorithm is provided to calculate the antecedent moisture condition. The algorithm requires a thirty day sequence of precipitation values, and an estimate of monthly evapotranspiration.

Subsurface/Groundwater Flow. Neither flow is modeled in FESHM.

Channel Flow Routing. Channel flow routing is computed analogously to overland flow. The channel is broken into elements. Input to a channel element includes flow from the upstream element and lateral inflow. Lateral inflow from overland flow strips is divided equally between overlapping channel elements when channel elements boundaries do not match strip boundaries. Routing is accomplished by solving the equations of motion for each channel element and time step.

ANSWERS

Modeling Approach

ANSWERS (Areal Nonpoint Source Watershed Environment Response Simulation) is a deterministic, distributed model of watershed hydrology and water quality (Beasley et al., 1980). The model was designed for use on agricultural lands to predict transport of water and sediment under different agricultural management practices. The parameters and calculations are distributed over a watershed, by breaking the watershed into a number of square elements. Each element has its own set of slope, soil, and land use conditions. Therefore, as land use and agricultural practices change, parameters in individual elements may be updated. The size of the elements must be small enough to adequately represent

a process or change, but not so large, that one element exerts too much influence on the simulation. The model is currently only capable of producing event based simulations in small time increments. Parameters for the model may be obtained from maps, soil surveys and field measurements, Therefore, the model is suitable for use on ungaged watersheds. The distributed nature of the model also makes it suitable for modeling variable source areas.

The original concept behind the ANSWERS model was developed by Huggins and Monke (1968). Flows are calculated for each element by solving the continuity equation

$$I - O = dS/dt$$

where I is the inflow rate, O is the outflow rate, S is the storage within an element, and t is the time increment, for each element.

The continuity equation is solved in the model using a finite element approach.

$$I_1 + I_2 - Q_1 + 2S_1/\Delta t = Q_2 + 2S_2/\Delta t$$

where the subscripts represent the time increment number. Inflow (I) to an element is the sum of rainfall and all flows from adjacent elements for each time increment. The direction of outflow from an element is determined by calculating an area weighted average slope direction (Figure 3). The program actually uses the angle of the average element slope to make the flow separation calculation. Angles are

measured from the horizontal axis in a counter-clockwise direction. The fraction of outflow going to an adjacent row element (RFL) is given by

$$\text{RFL} = \tan(\text{ANG})/2 \quad \text{when } \text{ANG} \leq 45^\circ, \text{ and}$$

$$\text{RFL} = 1 - (\tan(90-\text{ANG}))/2 \quad \text{when } 45^\circ < \text{ANG} < 90^\circ,$$

where ANG is the angle of the average slope from the vertical axis.

The remaining fraction of outflow goes to the adjacent column element. Subsurface flows are assumed to follow the same average slope direction. Simulation starts at a time when all of the parameter values for all of the elements are known. The continuity equation is applied sequentially to all elements until all conditions are known at one time step later. The process is repeated at time increments until the entire storm is simulated.

ANSWERS has been applied successfully in modeling alternative management practices as part of Sec. 208 planning in the midwestern U.S. (Beasley et al., 1982). Recently, Thomas and Beasley (1986, a and b) adapted ANSWERS to forested watershed applications. The forestry version of ANSWERS retains the same basic structure of the original version of ANSWERS. However, routines to model subsurface

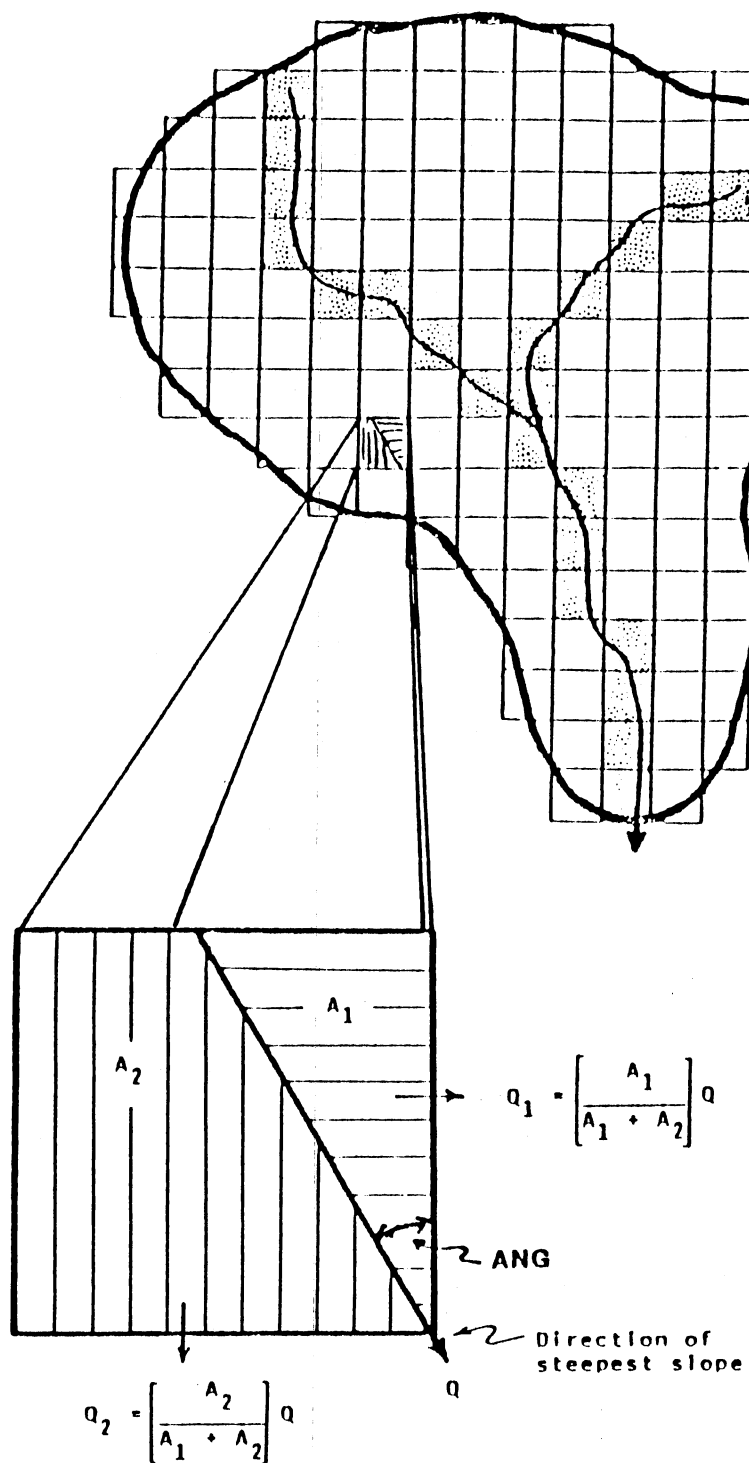


Figure 3. Division of a Watershed Into Elements and Division of Area Drained per Element for ANSWERS (from Beasley and Huggins, 1981).

flow as matrix flow and pipe flow in macropores, were added to more closely represent the physical processes controlling runoff on forested watersheds. The accounting procedure of soil water in each element allows for the calculation of saturated source areas. The forestry version of ANSWERS is discussed in detail in the following sections. Major departures from the original ANSWERS model will be noted.

Hydrologic Processes

Precipitation. Break point data is required for individual storm simulation. The distributed nature of the model allows for spatially variable rainfall rates.

Interception. The interception volume for a time increment (INT) is calculated as an exponential function of the ratio of incremental rainfall (RAIN) to maximum canopy coverage interception storage (PIT).

$$\text{INT} = \text{PIT} * (1 - \exp(-\text{RAIN}/\text{PIT})) * \text{PER}$$

where PER is the percentage of maximum canopy coverage.

Surface Detention Storage. Water that is detained on the surface may be infiltrated, aid infiltration, or be evaporated. Surface detention (STOR) is estimated using

$$\text{STOR} = \text{HU} * \text{ROUGH} * (\text{H}/\text{HU})^{1/\text{ROUGH}}$$

where STOR is the depth of stored water, ROUGH is a surface variability parameter, H is the height above a datum, and

HU is the height of maximum micro-relief. Methods used to estimate the surface detention parameters are given in the ANSWERS User's Manual (Beasley and Huggins, 1982).

Infiltration. Infiltration is calculated using a modified form of the Holtan-Overton equation.

$$F = FC + A * (PIV)^P / TP$$

where F is the infiltration rate, FC is the steady state, or final infiltration rate, A is the maximum rate in excess of FC, TP is the total pore space within a control volume, PIV is the maximum control volume storage before saturation, and P is a dimensionless coefficient relating the decrease in infiltration rate with increasing soil moisture.

The control volume for infiltration is defined as the total soil volume down to an impeding layer. In the original version of ANSWERS, the control zone was taken as one-half of the A-Horizon depth. Even though infiltration capacity usually exceeds rainfall rates on undisturbed forested watersheds, the control volume concept was retained so the model could be used on disturbed or mixed-use watersheds.

Surface Runoff. Surface runoff on forested watersheds usually does not occur, except on impermeable areas or on saturated source areas. The distributed nature of ANSWERS does allow for the modeling of impermeable and saturated areas. Overland flow produced on an element is divided be-

tween adjacent elements based on the angle of the average slope direction, as described previously. Surface flow generated on an element is routed to an adjacent element in the next time step.

As in the original version of ANSWERS, the continuity equation of overland flow is solved by applying Manning's equation as the depth-discharge relationship.

Variable Source Area. In order to model the dynamic nature of saturated runoff producing areas throughout a storm, a model must be capable of accounting for the distributed nature of the soil water budget. By modeling the soil water budget for each element through time, ANSWERS accounts for the expansion and contraction of saturated elements throughout the event. Precipitation falling on saturated areas, saturation overland flow, is rapidly routed through the element by the surface flow procedure described above. ANSWERS is also capable of modeling the surfacing of subsurface flow to become saturation return flow.

Channel Interception. No term for channel interception is included.

Soil Water Balance/Evapotranspiration. Solving the continuity equation for each time step effectively calculates the soil water balance during a storm. Since the model is an event model, a continuous accounting of soil water storage between storms is not made. Evapotranspiration is assumed to be insignificant during the event. However,

soil water storage at the beginning of a storm is important. Beasley and Huggins (1982) suggest that the antecedent soil water storage (ASM) may be calculated from

$$ASM = ASML + RAIN - ET - RO - PERC$$

where ASML is the last known soil moisture, RAIN is the daily rainfall, ET is the daily evapotranspiration, RO is the daily runoff, and PERC is the deep percolation.

ET is calculated using a coefficient that relates the reduction in available soil water as moisture content decreases.

$$ET = CF * SF * PET$$

where CF is a crop factor or percent of canopy cover, SF is coefficient of available soil moisture, and PET is the potential daily evapotranspiration. Calculation of potential evapotranspiration (PET) uses the empirical relationship

$$PET = 0.40 * T * [(RS+50)/(T+15)]$$

where T is the average daily temperature in °C, and RS is the net daily solar radiation in Langley's.

Subsurface Flow. Two processes of subsurface flow generation are incorporated in the model, seepage through the soil matrix and flow through macropores. Both processes are described separately below.

Seepage Component. The infiltration control zone of the original version of ANSWERS was extended to include all soil down to an impermeable layer and renamed the seepage element. The assumption is that in an undisturbed forested watershed all rainfall is able to penetrate the soil until an impermeable layer is reached. Horizontal flow through the seepage element is calculated using a form of Darcy's Law.

$$Q_s = K * I * D$$

where Q_s is the volume rate of seepage flow from the element, K is the hydraulic conductivity (assumed to equal the steady state infiltration rate, FC), I is the hydraulic gradient, assumed to be equal to the element surface slope (SC), and D is depth of flow.

Vertical percolation through the seepage element to the impermeable layer is calculated as a function of the steady state infiltration rate and the ratio of maximum storage before saturation to the gravitational water storage capacity. The equation is analogous to the equation of percolation through the infiltration control zone of the original version of ANSWERS.

$$DR = FC * (1 - PIV/SWC)^2$$

where DR is the drainage rate from the upper section of the seepage zone, FC is the steady state infiltration capacity of seepage element, PIV is the maximum volume of water that

can be stored in the control zone before saturation, and SWC is the gravitational water capacity of the control zone (total porosity minus field capacity).

Deep percolation through the impermeable layer is assumed to not contribute significantly to stormflow. The outflow from the seepage element through the impermeable layer (FCIL) is calculated using

$$FCIL = FCIL * [(DIMP - DIP) / (DMAX - DIP)]$$

where DIMP is the actual depth to an impervious layer, DIP is the actual depth to an impeding layer, and DMAX is the maximum allowable depth to an impervious layer. Values for the soil depth parameters may be obtained from soil surveys or field investigations.

Pipe Flow Component. Flow through macropore networks or "pipes" (Q_p) is calculated using an extension of the Darcy - Weisbach equation.

$$Q_p = CON2 * SL^{0.5} * g^{0.5} * (PI) * DIAP^{2.5} * (FFM)^{-0.5} * PORES * STOR$$

where Q_p is the volume flow rate, CON2 is a constant and units conversion factor, SL is the average slope of the element in percent, g is gravitational acceleration constant, $PI = 3.14159$, DIAP is the average effective diameter of the pipes, FFM is the pipe friction factor, PORES is the number of horizontal pipes per unit depth of storage for the width of the flow surface, and STOR is the depth of water available for pipe flow.

Evaluation of the parameters DIAP, FFM, and PORES is a difficult task. Little information exists on macropore characterization. Thomas and Beasley (1986a) used a representative pipe diameter obtained from the literature to estimate DIAP. Values for FFM were obtained from calibration with known streamflows. PORES was calculated using an algorithm in the model called CALPO. The average flow width is the same as for the partitioning of surface flow. Macropores must be slope oriented to contribute significantly to flow. The number of macropores is based a relationship between macropore space and soil depth obtained from the literature. The macropore space that is horizontally oriented is calculated using

$$\text{Macropore Space} = 1.0 - \text{FCIL}/\text{FC}$$

where FCIL is the permeability of the impeding layer and FC is the permeability of the seepage layer. Assumed upper and lower boundaries for slope-oriented, horizontal macropore space are 50 and 20 percent, respectively.

Groundwater. Groundwater contributions to streamflow are considered insignificant because the model is event-based.

Channel Flow/Routing. Each surface element that contains a stream channel also contains a channel "shadow" element. In elements containing a stream channel, overland and subsurface flow are routed directly into the channel, in-

stead of the direction of the average slope. Channel flow routing is accomplished by solving the continuity equation between channel shadow elements. Manning's equation is used to represent the depth-discharge relationship of the channel.

VSAS I and II

Modeling Approach

VSAS I and II (Variable Source Area Simulator) are deterministic, distributed parameter, event simulation models of forest watershed hydrology. VSAS I, developed by Troendle (1985), was later improved and renamed VSAS II by Bernier (1985). VSAS models a variable source area by dividing the watershed into topographic segments, increments, and cells. Increasing or decreasing soil water content in each cell is accounted for during the storm. By doing so, the area and distribution of saturated runoff producing zones are modeled. VSAS solves hillslope soil moisture and flow equations using measurable parameters. Therefore, the model is suitable for use on ungaged watersheds. At this time, the model is considered to be in the development phase.

Hydrologic Processes

Precipitation. Break point precipitation data is used.

Interception. A simple interception store is used in VSAS. Throughfall occurs when the store is filled.

Infiltration. All throughfall is assumed to infiltrate, except on impervious or saturated surfaces.

Surface Runoff. Surface runoff occurs only on impermeable surfaces and saturated cells. Water in excess of storage is considered to be surface flow. Surface flow is assumed to reach the stream channel in one (15 min.) time step.

Channel Interception. The channel is considered to be part of the saturated area.

Variable Source Area. A major assumption of the model is that since the variable source area is responsible for generating stormflow, detailed modeling of the variable source area is more important than crude estimates of soil water content. To accomplish this task, the watershed is delineated into hillslope segments having converging and diverging flows. Each segment is divided into increments that run parallel to the stream. The width of the increments is narrow near the stream and wider near the divide to allow better delineation of the variable source area. The incrementing rule is given by

$$d_n = D(n/N)$$

where d_n is the horizontal distance from the stream to the upslope boundary of increment n , D is the horizontal distance from the stream to the ridge top, n is the increment number, starting with 1 at the stream, and N is the total number of increments.

The increments are further divided into 3-5 soil layers above an impeding layer, to form volumetric cells. Flow is routed through the center of mass of each cell. Flow may enter or leave a cell through one or all of four faces of the cell, the upslope, downslope, top, or bottom faces. Flow is not allowed to pass laterally across the right or left cell faces. The soil water budget of each cell is solved using an explicit finite difference scheme.

Subsurface flow is calculated by using Darcy's law with a moisture content dependent hydraulic conductivity. Convergence and divergence of flow is expressed by the unequal width of the increments. Each time a downstream element becomes saturated, the hillslope is re-incremented, with the first increment located next to the saturated element. In this way, increments near saturated areas are kept as small as possible to provide more detail to the expanding and contracting source area.

Soil Water Storage. Initial soil water content values are chosen from antecedent conditions. The continuity equation is solved explicitly for soil water content in each cell for each time increment using

$$\theta_{t+\Delta t} = \theta_t + [\Delta t/V] * (Q_1 + Q_2 - Q_3 - Q_4)$$

where θ_t is the volumetric soil water content for a time step, t is the simulation time step, Q_i is the flow through one of 4 cell faces (x and z dimensions only), and V is the volume of the soil element. The calculation of the soil water content and soil water flow are interrelated. The subsurface flow equation is discussed in the next section.

Subsurface/Soil Water Flow. Saturated and unsaturated flows through the subsurface are represented by a three dimensional form of Darcy's law.

$$q = -K(\theta) \nabla H$$

where q is the apparent water velocity (cm h^{-1}), $-K$ is the hydraulic conductivity (cm h^{-1}), θ is the volumetric soil water content ($\text{cm}^3 \text{cm}^{-3}$), and ∇H is the hydraulic gradient (cm cm^{-1}).

The Darcy's law equation is combined with a two dimensional form of the continuity equation to solve for the change in soil water content over time (t)

$$\frac{\partial \theta}{\partial t} = \frac{\partial}{\partial x} \left[K(\theta)_x \frac{\partial H}{\partial z} \right] + \frac{\partial}{\partial z} \left[K(\theta)_z \frac{\partial H}{\partial z} \right] + 1$$

where H is the total hydraulic gradient, matrix potential plus hydraulic head.

Flow is allowed to occur in only two dimensions. Analogous to the stream tube concept, flow is not allowed to

travel laterally across cell (tube) boundaries. In order to solve for flow moving parallel to the segment slope, the x-axis is transposed by

$$x^* = x \cos a$$

where x^* is the transposed axis and a is the slope angle.

The resulting continuity equation is solved for each time step by applying a block-centered, finite difference, explicit solution scheme. The newly calculated soil water content is used to calculate the hydraulic conductivity of the soil for flow calculations in the following time step. Convergence and divergence of flow resulted from the respective decrease and increase of cell volume.

Hysteresis effects were ignored in soil water content calculations. Values of the hydraulic conductivity ($K(\theta)$) for unsaturated conditions were obtained from moisture release curves:

$$Y(\theta) = \alpha \theta^\beta$$

and:

$$K(\theta) = ae^{b\theta}$$

where α , β , a , and b are constants for a particular soil. Values of K for saturated conditions were obtained by measurement with a constant head permeameter.

Groundwater Flow. Groundwater flow was considered to be unimportant for a storm event simulator. Bernier (1985)

pointed out that errors can result if VSAS is used on watersheds that have prolonged groundwater components.

Channel Flow Routing. Outflows from each hillslope segment were lagged, according to average channel velocities, and summed at the watershed outlet. The routing procedure was assumed to work well for short travel distances on steep channels that have little storage.

Watershed Water Quality Models

Introduction

Water quality models encompass a wide range of modeled constituents, such as sediment, nutrients, dissolved oxygen, temperature, heavy metals, and pesticides. The range of modeled situations is equally wide, ranging from a receiving water quality model of a short reach of a stream, to basin-wide models of chemical and sediment transport. Watershed water quality models simulate the rates and quantities of chemicals and pollutants transported from diffused, or non-point sources, on watersheds (Novotny and Chesters, 1981). Chemicals and pollutants may be naturally occurring, or applied by man.

Several watershed water quality models are discussed below. They represent a range of detail of description of the chemical processes, application, and chemicals modeled. The discussion of each model consists of a description of the modeling approach and a detailed description of the

chemical or nutrient submodel. Sediment and pesticide transport are beyond the scope of this project. Therefore, sediment and pesticide transport are mentioned briefly, but not discussed in detail.

The first four models presented model sediment, nitrogen, phosphorus, and pesticide runoff from watersheds. The last two models are concerned with the transport of cations and associated anions resulting from acidic atmospheric deposition.

Agricultural Runoff Management Model

Modeling Approach

The Agricultural Runoff Management (ARM) Model was developed to enable the user to make event-based and continuous predictions of streamflow and sediment, pesticide, and nutrient transport from small agricultural watersheds under various management practices (Donigian and Crawford, 1976a). ARM was subsequently refined and improved in Version 2 (Donigian et al., 1977 and Donigian and Davis, 1978). Two plant macro nutrients, nitrogen and phosphorous are simulated. A continuous accounting of all nutrient and chemical transformations is made. The model requires records of precipitation, daily potential evapotranspiration, and daily maximum and minimum temperatures. Many of the hydrologic, chemical, and nutrient parameters require calibration. Therefore, a record of streamflow and stream water chemistry is also required.

ARM consists of six major components. The MAIN component controls the execution of the other components. The LANDS component contains the hydrologic submodel and information on the specific cropping practice. The hydrologic submodel contained in LANDS is an adaptation of the Stanford Watershed Model (SWM)(Crawford and Linsley, 1966). A major adaptation of SWM is the way in which the soil profile is divided. The soil profile is divided into a surface zone (depth = SZDEPTH), an upper zone (depth = UZDPTH), a lower zone (set at 1.83 meters thick), and a groundwater zone. The division of the soil profile into zones allows the model to calculate the mass of soil within each zone for chemical transport calculations. The depth of the surface zone is assumed to be the depth of mixing of soil-incorporated chemicals.

The SEDT component models erosion and sediment transport and supplies values of sediment size distributions and enrichment ratios. The ADSRB component simulates the absorption and desorption of pesticides in the soil profile. Standard Freundlich isotherms are used to predict the adsorption/desorption of pesticides on soil particles. The DEGRAD component simulates the changes in pesticide storage within the soil profile, resulting from volatilization, microbial decomposition, and other attenuation mechanisms.

Of particular interest in this discussion is the nutrient (NUTRNT) component. NUTRNT simulates the transport of nitrogen and phosphorous in runoff. Both adsorbed and dis-

solved phases are simulated. Transformation processes, such as immobilization, mineralization, nitrification/denitrification, plant uptake, and adsorption/desorption are used to account for changes in the available store of the different forms of nitrogen and phosphorous. ARM assumes first-order reaction rates for all transformations except plant uptake.

Chemical Transport

The LANDS, SEDT, ADSRB, and NUTRNT components operate on a 5 or 15 minute increment for days when storms occur. The DEGRAD component operates on a daily basis. For days on which storms do not occur, LANDS operates on a 5 or 15 minute basis, while the remaining components operate on a daily basis. Chemical contributions to streamflow may occur from the surface zone, the upper soil zone, or the groundwater zone. Chemicals applied to the ground surface or incorporated within the surface zone are available for transport. The nutrient transport process is reduced to a simple budgeting process. The mass of chemical available for transport (storage) in each time increment is equal to the algebraic sum of the initial mass, the input from other zones or chemical applications, transformations, degradation, and outputs. Rate constants and extraction and adsorption/desorption coefficients are obtained empirically and optimized through model calibration.

Surface runoff is assumed to mix in the soil to a depth equal to the surface zone depth. The surface zone depth is equal to the infiltration control zone depth in the SWM hydrologic model. Surface zone depths range from 0.2 to 0.6 cm. The mass of chemical removed by surface runoff is equal to the incremental volume of surface runoff times the mass of chemical in the surface zone soil times an empirical extraction coefficient. The extracted chemicals may be transported in a dissolved or adsorbed state. Partitioning between the dissolved and adsorbed state is calculated from the amount and type of sediment (SEDT component) and empirically derived adsorption coefficients. Surface applied chemicals washed off by surface runoff may be dissolved or adsorbed to sediment.

Dissolved chemicals leached from the surface zone supply input to the upper soil zone storage. Chemicals entering and leaving the upper and lower soil zones are assumed to be completely mixed with the volumes of water entering and leaving the zones. Volumes of water entering and leaving the soil zones are calculated by the LANDS component. The upper soil zone depth is set as an input parameter. Upper zone depths range from 5 to 20 centimeters. The lower zone depth is arbitrarily fixed at 1.83 meters.

Storage losses of a particular chemical occur as a result of degradation, transformation, or plant uptake. Chemicals may be adsorbed or desorbed as water passes through the soil zones. The mass of chemical lost to leaching or

subsurface flow is equal to the amount of available chemical times the quantity of water percolating or leaving as subsurface flow times empirical extraction constants for interflow and percolation. Further plant uptake, transformations, and degradation may occur in the lower soil zone. However, the lower soil zone does not contribute to subsurface flow. Percolation from the lower soil zone enters the groundwater reservoir.

The groundwater reservoir is considered to be a sink for chemicals. Chemicals are not lost from the groundwater reservoir by plant uptake. Chemical transformations and adsorption/desorption are allowed to occur. The mass of chemical lost from the groundwater reservoir is equal to the volume of groundwater flow times the concentration of chemical in solution. The groundwater component of ARM is not highly developed, because it was assumed groundwater flow from small agricultural watersheds was not significant.

Nonpoint Source Pollutant Loading Model

Modeling Approach

The Nonpoint Source Pollutant Loading (NPS) model was developed to provide continuous simulations of pollutant transport from watersheds under various land uses (Donigan and Crawford, 1976b). Like the ARM model, the NPS hydrologic component is based on an adaptation of the Stanford Watershed Model (Crawford and Linsley, 1966). The basic structure of the NPS model is also similar to the ARM model.

The model consists of three components, MAIN, LANDS and QUAL. The MAIN component controls the operation of the entire program. The LANDS component contains the hydrologic submodel. The QUAL component simulates erosion and sediment transport, and the transport of pollutants. The NPS model is capable of providing simulations at 5 or 15 minute time increments. Many of the hydrologic and chemistry parameters require calibration with a record of streamflow and stream water sediment and chemistry.

Chemical Transport

The QUAL component simulates the transport of chemicals under the assumption that sediment transport is a good indicator of chemical transport. Chemical transport is calculated by multiplying the sediment mass produced in a time interval times a potency factor. The simulation is performed separately for pervious and impervious areas.

For pervious areas,

$$POLP(t)_{p,1} = ERSN(t) * PMP_{p,1,m}$$

whereas for impervious areas,

$$POLI(t)_{p,1} = EIM(t) * PMP_{p,1,m} ,$$

where $POLP(t)_{p,1}$ is the mass of pollutant p transported from pervious areas in land use 1 during time interval t, $POLI(t)_{p,1}$ is the mass of pollutant p transported from impervious areas in land use 1 during time interval t,

$ERSN(t)_1$ is the sediment loss from pervious areas in land use 1 during time interval t , $EIM(t)_1$ is the sediment loss from impervious areas in land use 1 during time interval t , $PMP_{p,1,m}$ is the potency factor for pollutant p on pervious areas in land use 1 for month m , and $PMI_{p,1,m}$ is the potency factor for pollutant p on impervious areas in land use 1 for month m .

Pollutant concentrations for each time interval are calculated by dividing the pollutant mass from the equations above by the volume of flow for the increment. Potency factors are obtained empirically and optimized by calibration. Dissolved forms of the pollutant are accounted for by the potency factor. However, in applying the model, large errors were found in the prediction of highly soluble chemicals such as nitrate (Donigian and Crawford, 1977).

Since all chemical transport simulations are associated with sediment transport, dissolved pollutants from interflow and groundwater sources are not simulated. The model assumes that a majority of the quantity of pollutants on a watershed will be transported as a result of surface runoff and erosion.

Agricultural Chemical Transport Model

Modeling Approach

The Agricultural Chemical Transport Model (ACTMO) was designed to simulate the movement of agricultural chemicals following their application to croplands (Frere, et al,

1975). The model was originally designed for watersheds and cropping practices found in the Corn Belt of the United States. The model is composed of three sections, hydrology, erosion, and chemical. The hydrology section is designed around the USDAHL-74 model (Holtan et al., 1975). The erosion section uses a modified form of the Universal Soil Loss Equation to simulate interrill and rill erosion. ACTMO is capable of providing continuous simulations of streamflow and chemical transport at break point time increments. ACTMO is capable of simulating both the dissolved and sediment adsorbed phases of chemical transport. Based on temperature and soil moisture conditions provided by the hydrologic component, ACTMO continuously accounts for the transformation, degradation and quantity of a chemical in the soil.

The soil profile is divided vertically into four layers for the simulation of chemical transport. The surface layer is equal to the depth of the plow layer. The second layer is defined as the depth of the potential rooting zone. Only the first two layers are physically defined. The third and fourth layers are empirically defined as subsurface flow zones.

Chemical Transport

Chemical transport may occur when chemicals are dissolved in runoff, or adsorbed to sediment particles. The chemical submodel traces the movement of a single applica-

tion of a chemical over and through the watershed. Cultivation is the only management practice accounted for because it rearranges the soil, and hence the distribution of chemicals. The movement of nitrate is performed in a separate option.

The movement of a chemical into a soil by leaching, and the calculation of surface concentrations for surface runoff and erosion are simulated by simple chromatographic theory. The myriad of chemical reactions occurring in the soil was reduced to three significant processes, adsorption, degradation or loss, and dispersion. Adsorption (S), in pounds adsorbed per pound of soil, is simulated using a linear adsorption isotherm.

$$S = AC * C$$

where AC is the adsorption coefficient, and C is the pounds of chemical per pound of solution. Adsorption coefficients are available for many soils of varying textures and organic carbon contents.

A simple first order rate equation is used to simulate the degradation of a chemical between storms (Frere, 1975). The amount of chemical remaining (A) is given by

$$A = A_0 * \text{EXP}(-BC * T)$$

where A_0 is the initial amount, BC is the breakdown rate coefficient, and T is the time increment. The breakdown rate coefficient (BC) is a function of temperature and soil

moisture conditions. BC is recalculated for changes in soil temperature and soil moisture.

The factors controlling the depth of movement of a chemical are combined in one equation. The average depth of chemical movement (D) is calculated by

$$D = IN/FC * [FC/(AM + BD * AC)]$$

where IN is the amount of water infiltration in depth units, FC is volumetric moisture content at field capacity, AM is the volumetric water content of the soil where and when the chemical passes through, BD is the soil bulk density, and AC is the adsorption coefficient.

A bell-shaped chromatographic distribution of the chemical is assumed. The distribution of the chemical about the peak concentration at depth D is given by

$$C(X) = [(A*U)/(4t*DF*D)^{1/2}] * EXP -[(D-X)/(4*DF*D)^{1/2}]^2$$

where C(X) is the concentration of the chemical in solution at X cm from the surface, A is the amount of chemical in the soil at time T, DF is a dispersion distribution factor, and U is a units conversion factor. U is equivalent to $10/(SM+BD*AC)$, where SM is the volumetric soil moisture content at depth X.

At X = D, the peak concentration is calculated. At X = 0, the concentration at the surface is calculated. The surface concentration is assumed to equal the concentration of the chemical dissolved in surface runoff. The bell-shaped

chromatographic distribution is assumed to hold for all non-adsorbed chemicals (nitrates) and linearly adsorbed chemicals (phosphate). The distribution does not apply to cation movement.

The total quantity of chemical lost in surface runoff is calculated as the product of the mean concentration during a time increment and the volume of runoff. Estimates of lateral outflow, or subsurface flow, are provided by the hydrology model. The quantity of chemical transported with subsurface flow is equal to the average chemical concentration in the layer times the quantity of subsurface flow. The average concentration of chemical in a soil layer is obtained from the chemical distribution curve.

ACTMO accounts for between-storm transformations of nitrogen separately. Mineralization of organic nitrogen to nitrate is calculated by a first-order rate equation.

$$\ln NT = \ln NO - MR * T$$

where NT is the amount of mineralizable N left after time T, NO is the initial amount, MR is the mineralization rate coefficient, and T is the time in days.

The mineralization rate coefficient is the same for most soils, but is a function of soil moisture and the absolute temperature. The mineralization rate coefficient is given by

$$\ln MR = 15.807 - 6350/TM$$

where TM is the absolute temperature in degrees K. The relative mineralization is given by

$$-0.97 + 1.1 (SM/FC)$$

where SM is the average volumetric soil moisture content and FC is the field capacity soil moisture content.

Total mineralization uses the three relationships described above. The amount of nitrate taken up by plants (UP) is estimated as the concentration of nitrate times the volume of water transpired adjusted by the soil water content. Plant uptake (UP) is calculated from the relationship

$$UP = AU * ET / (SW * WD)$$

where AU is the pounds of nitrate per acre available, and $SW * WD$ gives the inches of water in the soil.

CREAMS

Modeling Approach

The Chemicals, Runoff, and Erosion from Agricultural Management Systems model (CREAMS) was developed to simulate the transport of nutrients and pesticides from field scale agricultural watersheds (Kniesel, 1980). The model is used mainly to evaluate the effects of different agronomic practices on non-point source pollution. CREAMS consists of four submodels that simulate hydrology (previously discussed), erosion and sediment yields, nutrient yields, and pesticide yields. Only the nutrient submodel will be dis-

cussed in detail here. Methods for estimating the hydrologic and chemical parameters are available. Therefore, calibration is not required.

Chemical Transport

The nutrient submodel of CREAMS simulates the loads of adsorbed and dissolved nitrogen and phosphorous produced during each storm (Frere et al., 1980). A graph of the change in nutrient concentrations over time is not produced. The submodel predicts the average concentration of each nutrient present in surface runoff. The total yield is calculated by multiplying the average concentration times the volume of runoff. The hydrology and erosion submodels provide the necessary runoff volumes and sediment data inputs to the nutrient submodel.

The transport of adsorbed and insoluble nutrients are simulated by multiplying the sediment yield times an enrichment ratio.

$$\text{SED}_- = \text{SOIL}_- * \text{SED} * \text{ER}_-$$

where SED_- is quantity of adsorbed nitrogen or phosphorous (kg/ha), SOIL_- is the content of N or P in the soil (kg/kg), SED is the quantity of sediment produced (kg/ha) in the erosion model, and ER_- is an enrichment ratio for N or P. The parameters in the equations above are specific to N and P. The enrichment ratio is calculated separately for N and P by

$$\text{ER}_- = \text{A}_- * \text{SED}^{\text{P}}_-$$

where $A_$ is a coefficient and $B_$ is an exponent, based on the size fractions and organic matter content of the soil.

The algorithm for calculating nutrient yields accounts for nutrient inputs from precipitation, plant residues, and fertilizer and solid waste applications, and losses from runoff, leaching, plant uptake, and transformations. The transport of soluble nitrogen and phosphorus is simulated by assuming surface runoff interacts with the top 1 cm of the soil. The change in concentration over time of soluble nutrient in the soil water in the top 1 cm of soil (dC/dt) is assumed to be proportional to the difference between the existing concentration (C_o) and the concentration of nutrient in the rainfall (C_r).

$$dC/dt = K_1 * f(t) * (C_r - C_o)$$

where K_1 is a rate constant for downward movement and $f(t)$ is the infiltration rate. The dissolved phosphorus input from rainfall is assumed to be zero. However, because of the buffering effect of the soil mass on dissolved phosphorus, the concentration of phosphorus in the soil is not allowed to fall below a characteristic value.

Average concentrations of nutrients in the surface soil zone during (\bar{C}_1) and after (\bar{C}_2) infiltration are

$$\bar{C}_1 = ((C_o - C_r) / K_1 F) (1 - \exp(-K_1 F)) + C_r$$

where F is the total infiltration, and

$$\bar{C}_2 = ((C_1 - C_r) / K_2 Q) (1 - \exp(-K_2 Q)) + C_r$$

where K_2 is a rate constant for movement into runoff, and Q is the total runoff.

The amount of soluble nutrient in surface runoff (RO) is calculated by multiplying the average nutrient concentration in the surface 1 cm during runoff (\bar{C}_2) by the total runoff and an extraction coefficient (EXK).

$$RO = \bar{C}_2 * EXK * Q * 0.01$$

The 0.01 term corrects the equation for the depth of the surface layer. Extraction coefficients must be calculated for each nutrient. The extraction coefficient is equal to the surface layer depth times the porosity, times the movement rate constant for the particular nutrient. The total amount of nitrate leached during infiltration (DWN) is given by

$$DWN = \bar{C}_1 * EXN_1 * FI * 0.01$$

where EXN_1 is the extraction coefficient of the downward movement of nitrate and FI is the total infiltration minus an initial abstraction equal to the pore space in the surface layer.

CREAMS also simulates the cycling and leaching of nitrogen during and between storms. Plant uptake and denitrification are two losses of nitrate simulated. Mineralization, residue decay, and fertilizer and waste application are simulated as inputs to the nitrate pool. Mineral-

ized nitrogen (MN) during a period DAYS between storms is given by

$$MN = POTM * WK * (1 - \exp(-TK * DAYS))$$

where POTM is the potential mineralizable nitrogen in the soil (kg/ha), WK is a water coefficient calculated by dividing the average water content for the period by the field capacity, and $TK = \exp(15.807 - 6350/TA)$. TA is the average absolute temperature in °K for the period.

Two options are available for the simulation of plant uptake of nitrogen. One option is based on the total accumulated dry matter produced during an interval (DM_i).

$$UN_i = c_i DM_i$$

where UN_i is the accumulated nitrogen uptake for day i and c_i is the concentration of nitrogen in the plant on day i.

The second option assumes nitrogen uptake follows a normal probability (S-shaped) curve, reduced for moisture stress.

$$PUN = 1 - 1/2 (S)^{-4}$$

where PUN is the fraction of potential N uptake used in T days.

$$S = 1.0 + 0.196854X + 0.115194X^2 + 0.000344X^3 + 0.01957X^4$$

and

$$X = (T - M) / SD$$

where M is the days of growth required to uptake 50% of available N, and SD is the number of days between 50% and 84% uptake; equivalent to one standard deviation.

The total nitrogen uptake is given by

$$UN = (PUN - PPUN) * PU * TR$$

where PPUN is previous uptake at the last storm, PU is the potential annual nitrogen uptake for a crop (kg/ha), and TR is the ratio of actual to potential evapotranspiration for the period. The CREAMS manual (Knissel, ed. 1980) provides methods for estimating the various crop and uptake parameters required in the equations above.

Denitrification can occur under anaerobic conditions. For well drained agricultural soils, loss to denitrification is insignificant. CREAMS uses a first-order rate equation that is a function of soil organic carbon, temperature, and moisture, to simulate denitrification. The quantity of soil carbon (SC) is equal to the percent of soil organic matter divided by 0.1724. The denitrification rate constant (DK) is

$$DK = 24 * (0.011 * SC + 0.0025)$$

The denitrification rate corrected for temperature (DKT) is given by

$$DKT = \exp(0.0693 * ATP + DB)$$

where ATP is the average temperature in °C and $DB = \ln DK - 2.4255$. The quantity of denitrification between storms (DNI) is given by

$$DNI = NO_3 * (1 - \exp(-DKT*(DT-0.5)))$$

where NO_3 is the quantity (kg/ha) of nitrate in the root zone and DT is the number of days of drainage since the last storm.

Nitrate leaching from the root zone (TOTNL) is simply calculated as a function of the fraction of the root zone water leached (FL) times the available root zone nitrate (NO_3) during the storm.

$$TOTNL = FL * NO_3$$

The fraction of root zone water leached (FL) is given by

$$FL = PERC / (PERC + RZC)$$

The nitrate leaching algorithm assumes complete mixing of nitrate within the root zone.

Shenandoah Watershed Study Model

Modeling Approach

The Shenandoah Watershed Study Model (SWSM) is a lumped parameter model developed to predict the long-term response of soil and stream water to acid deposition (Cosby et al., 1985). Two assumptions are used to simplify the chemical processes occurring on a watershed. The first assumption,

is that if a knowledge of the chemistry at the watershed outlet is all that is required, then the spatial distribution of chemical processes occurring on a watershed may be lumped. Soil processes were assumed to be described by using average soil properties. The second assumption, is that for the watershed modeled, soil water processes control the chemistry of the streamflow. It was assumed the soil chemical processes could be described by a small number of processes including cation exchange. SWSM is used with a known record of stream chemistry to back calculate unknown soil properties. The authors suggest that once the unknown properties are calculated, the model can be coupled with a hydrology model to predict stream water chemistry.

The model uses thermodynamic principles of equilibrium to calculate the concentrations of base cations, anions, and inorganic aluminum and inorganic carbon in soil and stream water. All equations are solved simultaneously by assuming the ionic charges must balance (sum of positive and negative charges = 0). The model contains 33 variables and 21 parameters. Sixteen of the parameters are thermodynamic equilibrium constants that may be obtained from the literature. The remaining 5 parameters are soil properties calculated by the model.

Birkenes, Norway Model

Modeling Approach

The Birkenes Model is a lumped parameter continuous daily simulation model of streamflow and water chemistry (Christophersen et al., 1982). The model was developed for predicting cation transport (H^+ , Al, Ca, and Mg) from watersheds receiving acidic atmospheric deposition. The model uses a small number of physically realistic processes to represent the complex chemical processes on the watershed. The Birkenes Model was the first model developed to simulate daily concentrations of cations in streamflow from small watersheds (Christophersen et al., 1982).

Hydrologic Component

The hydrologic component is a simple lumped parameter two reservoir model. The model produces daily simulations of streamflow. Daily evapotranspiration is calculated from mean daily temperature. Evapotranspiration occurs from the upper reservoir until it is empty. After that, evapotranspiration occurs from the lower reservoir. The upper reservoir supplies quick flow. The upper reservoir is considered to represent flow and storage in the upper soil horizons. The lower reservoir provides baseflow. Drainage half-times, or release constants, from the reservoirs are calculated from streamflow recession constants. Drainage

half-times for the upper and lower reservoirs were set as 0.9 and 15.4 days, respectively.

Chemical Transport

The transport of four cations, H^+ , Al, Ca, and Mg, is simulated by the model. All aluminum is assumed to be trivalent (Al^{+3}). Several simplifying assumptions are made in the chemistry transport model. The first assumption is that concentrations of Na are linked directly to Cl. Na and Cl are assumed to not affect the concentrations of the other cations. The second assumption, is that ions such as NH_4 , NO_3 , and HCO_3 are ignored because they form a small percent of the ionic sum. The third assumption is that the concentration of sulfate determines the sum of the concentrations of the four cations. Three equations are solved simultaneously for each reservoir.

$$[H^+] + 2[M^{2+}] + 3[Al^{+3}] = 2[SO_4^{2-}]$$

$$[Al^{+3}][H^+]^{-3} = K_{so}$$

and

$$[H^+]/[M^{2+}]^{1/2} = K_c$$

where M^{2+} = the sum of Ca and Mg, $K_{so} = 10^{8.1}$, aluminum solubility constant, and $K_c = 10^{-2.2}$, Ca/Mg solubility constant.

The chemical concentrations of all constituents in the streams the model was applied to were low. Therefore ionic

activities were assumed to be equal to the concentrations. Due to the simplifying assumptions, the model may not be applicable in other regions.

Some Considerations in Hydrologic Modeling

The hydrologic models reviewed previously represent only a fraction of the currently available models. No one "master" model that fits all situations currently exists. Betson and Ardis (1978) addressed the question: "Why are there so many models?". Working formulations for describing hydrologic processes were available in the 1950's, yet new models are continually being developed (Betson and Ardis, 1978).

Three reasons for the plethora of models are cited by Betson and Ardis (1978), advancing technology, numerous nature-imitating approaches, and application oriented design. Advances in computing capabilities have led to the ability to solve complex equations numerically and rapidly. New research has also increased our understanding of basic hydrologic processes, such as the concept of old vs. new water (Pearce et al., 1986). Hydrologic modeling is essentially nature-imitating. Numerous approaches, from simple to complex, can simulate a streamflow response to precipitation, without truly representing all of the natural processes. However, the degree of precision of the simulation varies from approach to approach (Betson and Ardis, 1978). Finally, many hydrologic models were developed with one spe-

cific application in mind. Therefore, many models have been developed to fit many specific applications.

The intended use of a model puts constraints on the selection or development of a model (James and Burges, 1982). For example, if a model is to be used on ungaged watersheds, the model should have physically based parameters that can be estimated without calibration. The intended use also determines the level of detail required in a model. If peak flows for structural design are the topic of interest, a simple stochastic model may suffice. Watershed models used for the prediction of water quality must include more detail on the flow paths and points of chemical change (discussed below).

James and Burges (1982) point out that the degree of detail used in representing the physical processes of a watershed is one of the most basic issues in model development. An increase in detail does not guarantee better results. Loague and Freeze (1985) compared efficiencies of simulations produced by three models of varying complexity, a regression model, a unit hydrograph model, and a quasi-physically based model, to field data during the verification phase. The simulations produced by the data intensive quasi-physically based approach were found to be no better than the simulations produced by the simpler models. Loague and Freeze (1985) felt that the unmeasurable spatial variability of parameters limited the precision of simulations produced by the quasi-physically based model.

The degree of precision required by complex physically based models can be greater than the degree of precision provided by the input data (James and Burges, 1982). Often, only one raingage located away from the watershed is available as input. In such a case, the use or development of a complex physically based model may not be warranted (Betson and Ardis, 1978). One suggested "rule-of-thumb" in hydrologic modeling is to use the most simple model that provides the desired results (Dawdy, 1969).

Conclusions

Freeze (1978) concluded that quality of predictions from hydrologic models are constrained by five basic limitations due to, assumptions of the theoretical developments, a lack of correspondence between reality and theory, a scarcity of and uncertainty in the input data, inadequacy of computer capacity, and inadequacies of calibration techniques. Many of the limitations, such as computing capacity, can be overcome. Other limitations, such as the degree of uncertainty in the input data, may place an upper limit on the precision of predictions from even the most complex physically based models (Anderson and Burt, 1985).

In general, a hydrologic model should provide the kind of information required (James and Burges, 1982), be structured to describe the watershed system being modeled (Anderson and Burt, 1985), have parameters sensitive to the significant flow producing processes (James and Burges,

1982), but not more complex than the input data available (Anderson and Burt, 1985), and provide results suitable for the intended use (James and Burges, 1982).

Some Considerations in Water Quality Modeling

Introduction

Water is considered to be the transport medium for solutes leaving a watershed (O'Loughlin, 1981). The quality of water reaching a watershed outlet is determined by path of flow, the materials and chemical environment encountered, and time of residence on the watershed (O'Loughlin, 1981; Dowd and Nutter, 1985). The hydrologic processes characteristic of a watershed determine the flow path and residence times. Chemical and biological processes determine what reactions and transformations may take place (Donigian, 1981). All of the processes are interdependent to some degree. Therefore, watershed water quality models must link together, the hydrologic, chemical, and biologic processes responsible for the composition of stream water at the outlet (Donigian, 1981).

Hydrologic Processes

The hydrologic component forms the base of a watershed water quality model (Donigian and Crawford, 1976b). The hydrology component must be capable of modeling the processes responsible for producing both streamflow and chemical transformations. In some cases, an insignificant flow pro-

cess may produce a highly significant chemical change (Chapman et al., 1982). Some hydrologic processes significant to water quality are discussed below.

The Watershed System

Chapman et al. (1982) present an outline of significant processes comprising the hydrologic cycle of a forested watershed from a water quality modeling perspective. The vegetative canopy and litter layer are shown to be significant sources of chemical change. On undisturbed forested watersheds, almost all of the rainfall entering the system flows through the canopy and litter.

Streamflow Generating Processes

The streamflow generating runoff processes determine, in part, the flow path, timing, and substrate the water contacts. Subsurface flow dominates on forested watersheds. The physics of subsurface flow is a necessary consideration in determining the flow paths of subsurface flows on hillslopes (Ahuja, 1986). For layered soils on hillslopes underlain by an completely impermeable layer, flow lines tend to run parallel to the slope. However, if the impeding layer has as little as 1/100 the permeability of the topsoil, flow lines run at an angle to the slope.

Macropore Flow

The flow path of subsurface flow in a forested watershed is also affected by the presence of macropores in the soil. Macropore channels may rapidly transport water through the soil with little or no contact with the surrounding soil. On the other hand, turbulent mixing and diffusion into or out of the macropore, may cause chemical changes (Dowd and Nutter, 1985). The effect of macropore transport on water quality is not well understood.

Old vs. New Water

The manner in which the water travels through the soil matrix may also be important. Streamflow has been found to be a mixture of "new water" added during the storm event, and "old water" that existed in the soil matrix before the storm (Pearce et al., 1986). Old water is displaced from the soil matrix by new water. New water reaches the stream through the soil matrix or macropores. Old water, presumably is different in chemical composition, due to a greater contact time with the soil. The process is not well understood at this time. Thomas and Phillips (1979) suggest that soil water flow is a combination of both displacement and macropore flow mechanisms.

Source Area

Finally, the source area of streamflow must also be considered. Streamflow is not generated evenly over a wa-

tershed (O'Loughlin, 1981). Variable source areas may exist in topographic lows and in riparian areas. Overland flow from saturated source areas may enter a stream rapidly, having undergone little or no chemical change (Dowd and Nutter, 1985). Such water would have nearly the same chemical characteristics as the incoming precipitation. Chemicals deposited in the riparian area may also enter the stream rapidly and with little change.

Chemical Transport Processes

Transport processes responsible for the movement of chemicals through a watershed may be broken into physical, chemical, and biological processes (Frere et al., 1982). The transport processes acting on water along its flow path are numerous. Chemical processes may be reversible or irreversible (Hem, 1985). Rates of reactions are often controlled by temperature, moisture, and biological activity (Frere et al., 1982). Physical processes are a function of soil texture, substrate composition, and environmental factors. Many of the chemical, physical, and biological transport processes are interdependent.

Physical processes include convection, suspension and deposition, dispersion, diffusion, and tillage or land use activities. Chemical processes include sorption, ion exchange, crystallization, hydrolysis, oxidation-reduction, and photochemical reactions (Frere et al., 1982). Biological processes include nitrification by bacteria, the produc-

tion of enzymes and other biochemicals, addition of compounds by decay, and removal by plant uptake. The transport processes, like hydrologic processes, are highly spatially and temporally variable (Frere et al., 1982).

Certain chemicals are affected to a greater or lesser degree by each process. For example, phosphorus is highly adsorbed, whereas nitrate is very weakly adsorbed. Chemicals may be transformed chemically or biologically into more or less mobile compounds. Transformations between forms are especially important for nitrogen. Other compounds, especially organic compounds, may degrade over time. The rates and amounts of transformation and degradation must be considered in water quality modeling (Donigian, 1981). The interaction between processes may be significant for particular chemicals. For example, dispersion tends to reduce the concentration of a chemical in solution. The resulting dilution may cause the desorption of chemicals from the soil. Changes in pH can cause subsequent changes in the oxidation-reduction state of some compounds (Hem, 1985).

Early watershed water quality models were concerned mainly with predicting the transport of sediment, nutrients, and pesticides from a watershed (Donigian, 1981). More recently, concern over the effect of acidic atmospheric deposition on water quality has spawned the development of cation/anion transport models (Cosby et al., 1985). Field scale models of salt movement on agricultural land have also been developed (Frere et al., 1982). Cation/anion transport

is controlled by the processes of cation exchange, diffusion, crystallization, and chemical equilibria. The processes involved in cation/anion transport are highly complex and interdependent. Hence, cation/anion transport models use broad assumptions to model the transport process.

A water quality model that models all of the chemicals and chemical transport processes that occur on a watershed does not exist (Frere et al., 1982). As in hydrologic modeling, simplifying assumptions are made in chemical transport modeling. A number of approaches, varying in detail, have been taken. One approach is to model only the most significant transport processes (Donigian, 1981). Adsorption/desorption is often assumed to follow linear Freundlich isotherms (Frere et al., 1982). Rates of degradation, decay, biological activity, and transformations are normally assumed to be first order rate processes (Donigian, 1981). Rates of reactions are adjusted for environmental conditions. Broad assumptions are normally made in modeling biological processes, such as plant uptake. Plant uptake may be assumed to be equal to the volume of water transpired multiplied by an average concentration of a chemical.

Conclusions

In general, a water quality model should be representative of the system to be modeled. The model should not direct the description of the system (Ford and McGhee, 1979). The degree of detail in water quality models reflects the

modeling goals, the ability to measure or estimate parameters, current understanding of the processes involved, and a trade off between costs, detail and the quality of the predictions.

CHAPTER IV

METHODS

Study Site

Three small forested watersheds in southeastern Oklahoma, located near Clayton, Oklahoma, have been the sites of an ongoing research project investigating the effects of silvicultural activities and acid deposition on water resources since late 1979 (Figure 4). The Clayton Watersheds are located in Pushmataha County in the Ouachita Mountain region of southeastern Oklahoma. The watershed topography, soils, vegetation and land use history are "typical" of small forested watersheds in the Ouachita Mountains of southeastern Oklahoma and southwestern Arkansas. A continuous record of precipitation and streamflow were available from the Clayton Watersheds. Additionally, a continuous record of water chemistry, beginning in early 1982, was also available. This research was conducted on Clayton Watershed #3, a 7.73 ha. watershed which has served as an undisturbed control in the three watershed study (Figure 5).

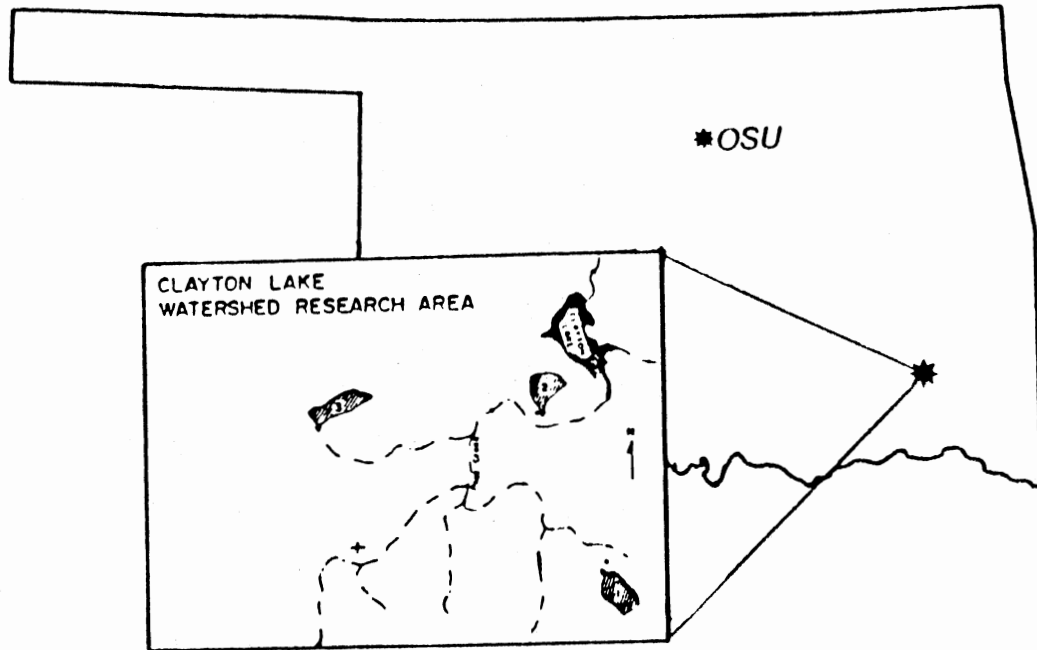


Figure 4. Location Map of the Research Watershed.

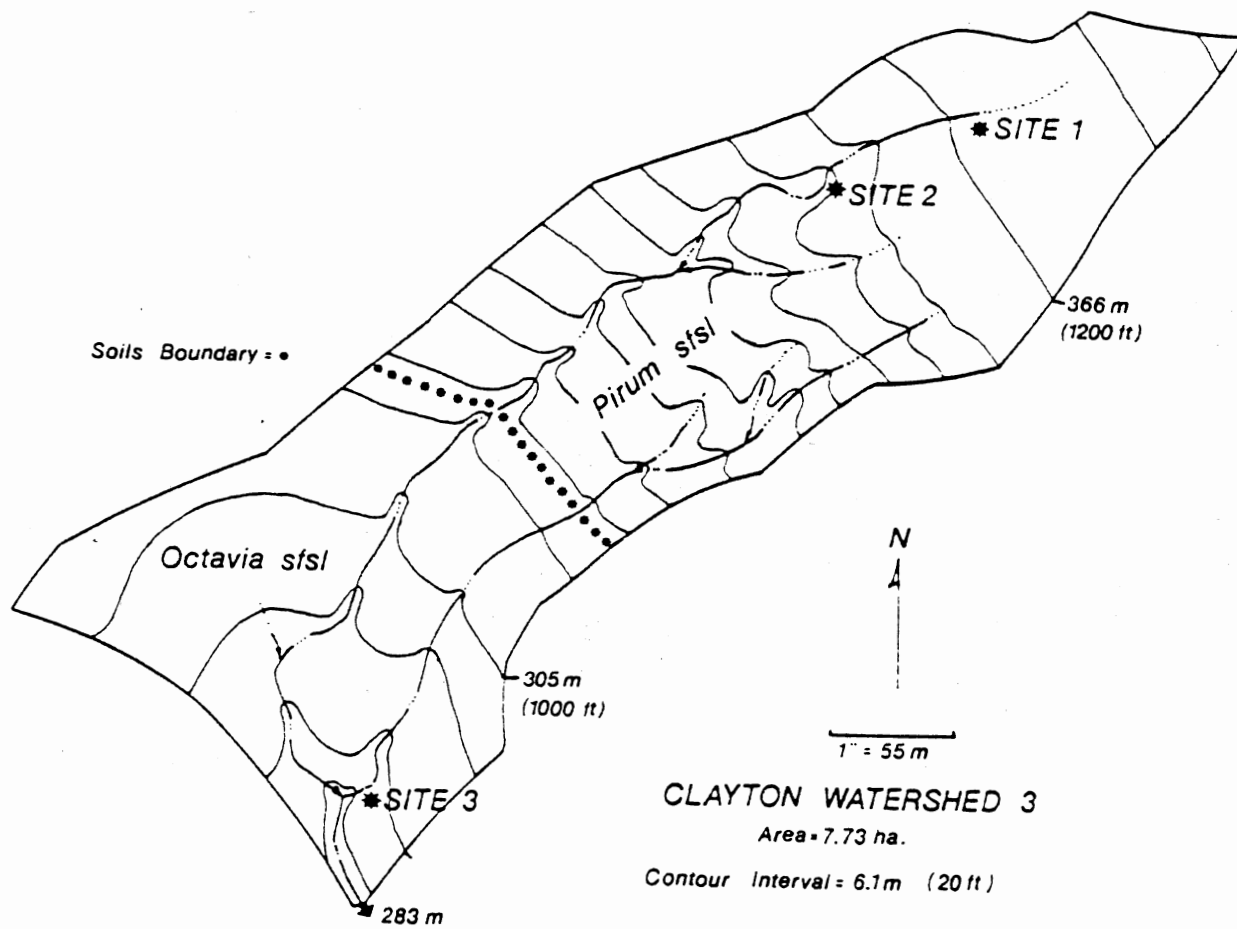


Figure 5. Topographic and Soils Map of Clayton Watershed #3

Climate

The Clayton watersheds are in a temperate climate regime (Bain and Watterson, 1979). Mean annual precipitation is 1194 mm. Of the total annual precipitation, about 60 percent falls between April and September as a result of convectional thunderstorm activity. About 6 percent of the total annual precipitation (76 mm) occurs as snow. However, accumulations are generally 25 mm or less. The mean annual actual evapotranspiration for the region, calculated by subtracting annual runoff from precipitation on large basins, is 813 mm. Actual evapotranspiration from the Clayton watersheds may or may not fit the regional pattern. Mean annual runoff for streams in the region is 381 mm (Pettyjohn, et al., 1983).

The mean daily temperature is 7 and 26 °C in the winter and summer respectively. The mean daily minimum temperature during the winter is -0.6 °C. The mean daily maximum temperature during the summer is 34 °C. Relative humidities average 50 and 82 percent in the mid-afternoon and early mornings respectively.

Topography

Clayton Watershed #3 ranges in elevation from 283 meters at the outlet to 381 meters at the upper divide. Slopes range from 10 to 25 percent. Stream channels tend to be incised below the surrounding land surface. Slopes near the stream channels formed by the stream incision range

from 40 to 50 percent. Approximately 2 percent of the watershed is occupied by stream channels. Flat alluvial areas near the stream channels occupy an additional 2 percent of the watershed area. An Additional 8.5 percent of the watershed area is occupied by steep slopes formed by channel incision into the surrounding topography. Total stream channel length is 1100 meters. Stream channel slopes range from 0 percent in pools to 25 percent in steep sections. The overall average channel slope is 12 percent.

Geology

The Ouachita Mountains at the Clayton Watersheds are composed of rock of the Atoka and Jackfork units (Hartronft and Hayes, 1966). Both units consist of interbedded, highly fractured, gray sandstones and shales. The Atoka consists of about 75 percent shale, whereas the Jackfork unit is predominantly sandstone. The shales in both units are silty and micaceous. Sandstones tend to form ridges, while the more erodible shales form sideslopes. Both units are highly spatially variable in the percentages and thicknesses of the alternating beds of shale and sandstone contained in each.

Soils

The soils on the watershed are formed from highly weathered, interbedded sandstones and shales of the Jackfork Unit. As a result of the inter-bedding, soil properties are

highly spatially variable over short distances. The soils are classified within the Carnasaw-Pirum-Clebit soil association and the Octavia soil series (Bain and Waterson, 1979). The upper half of the watershed is occupied primarily by the Pirum soil series, with inclusions of the Carnasaw (10%) and Clebit (15%) soil series. The lower half is occupied by the Octavia soil series.

The Pirum stony fine sandy loam series (fine-loamy, siliceous, thermic Typic Hapludult) consists of moderately deep, well drained, moderately permeable soils. The stony fine sandy loam A horizons average 25 cm in depth. The sandy clay loam B horizons (B21t and B22t) average 61 cm in thickness. Bedrock is found at an average depth of 94 cm. Permeabilities range from 15 - 51 mm/hr in the A and B horizons. Soils on the lower half of the watershed are composed of the Octavia series. The Octavia stony fine sandy loam series (fine-loamy, siliceous, thermic Typic Paleudults) consists of deep, well drained, moderately slowly permeable soils that formed in loamy colluvium over clay. The stony fine sandy loam A horizons (A1 and A2) average 15 cm in depth. The A horizons are underlain by 30 cm thick gravelly loam B1 horizons, followed by 30 cm thick gravelly clay loam B21t horizons. Below the B21t horizons are 89 cm thick clay IIB23t horizons. The permeabilities of the A, B1 and B21t horizons range from 15 - 51 mm/hr. Permeability in the IIB23t horizons are sharply lower, ranging only from 5 - 15

mm/hr. The reaction of the watershed soils ranges from medium to strongly acid.

Vegetation

Clayton Watershed #3 is covered by a pine-hardwood complex composed mainly of shortleaf pine (*Pinus echinata*), hickory (*Carya* sp.) and oaks (*Quercus* sp.). The understory contains smaller trees, such as elms (*Ulmus* sp.) and flowering dogwood (*Cornus florida*), and lower ground cover composed of blueberry (*Vaccinium* sp.), poison ivy (*Rhus radicans*), and bluestem grasses (*Andropogon* sp.).

Field Methods

Three study sites were located on the watershed (Figure 5). The locations of the sites were chosen to reflect changes in soil, topographic and vegetative characteristics. It was realized that three sites would probably not account for the true variation in subsurface flow processes and chemistry on the watershed. However, it was felt an intensive study at three locations would provide better information than more sites studied less intensively. Additionally, cost of construction, equipment and sample analysis, as well as increased disturbance to the watershed, made more sites unfeasible.

Each study site contained one subsurface flow collection system, four throughfall collectors and nine tension free soil lysimeters (Figure 6). Throughfall collectors and

soil solution collectors were located randomly about the area drained by the subsurface flow collectors, as opposed to locating the collectors randomly about the entire watershed area, to better describe the chemical transformations on the hillslope segment. In this way, differences in streamflow and chemistry generating processes on different parts of the watershed could be compared. Each piece of equipment is described in detail below.

Precipitation

Precipitation was measured with a continuous recording weighing bucket rain gage. Precipitation depths were recorded to the nearest 0.25 mm. Incremental times were measured to the nearest 5 minutes. A standard 4 inch rain can was also located near the weighing bucket gage.

Bulk Precipitation and Throughfall

Bulk precipitation and throughfall represent inputs of water and chemicals to a forest watershed system. Bulk precipitation consists of the precipitation itself (wetfall), dry deposition (dryfall) that accumulates between events and all water-soluble and water-insoluble components contained in the wetfall and dryfall (Likens, et al., 1977 and Lewis and Grant, 1978).

The number of samples required to obtain representative samples of bulk precipitation and throughfall for nutrient cycling and mass balance studies has been the subject of

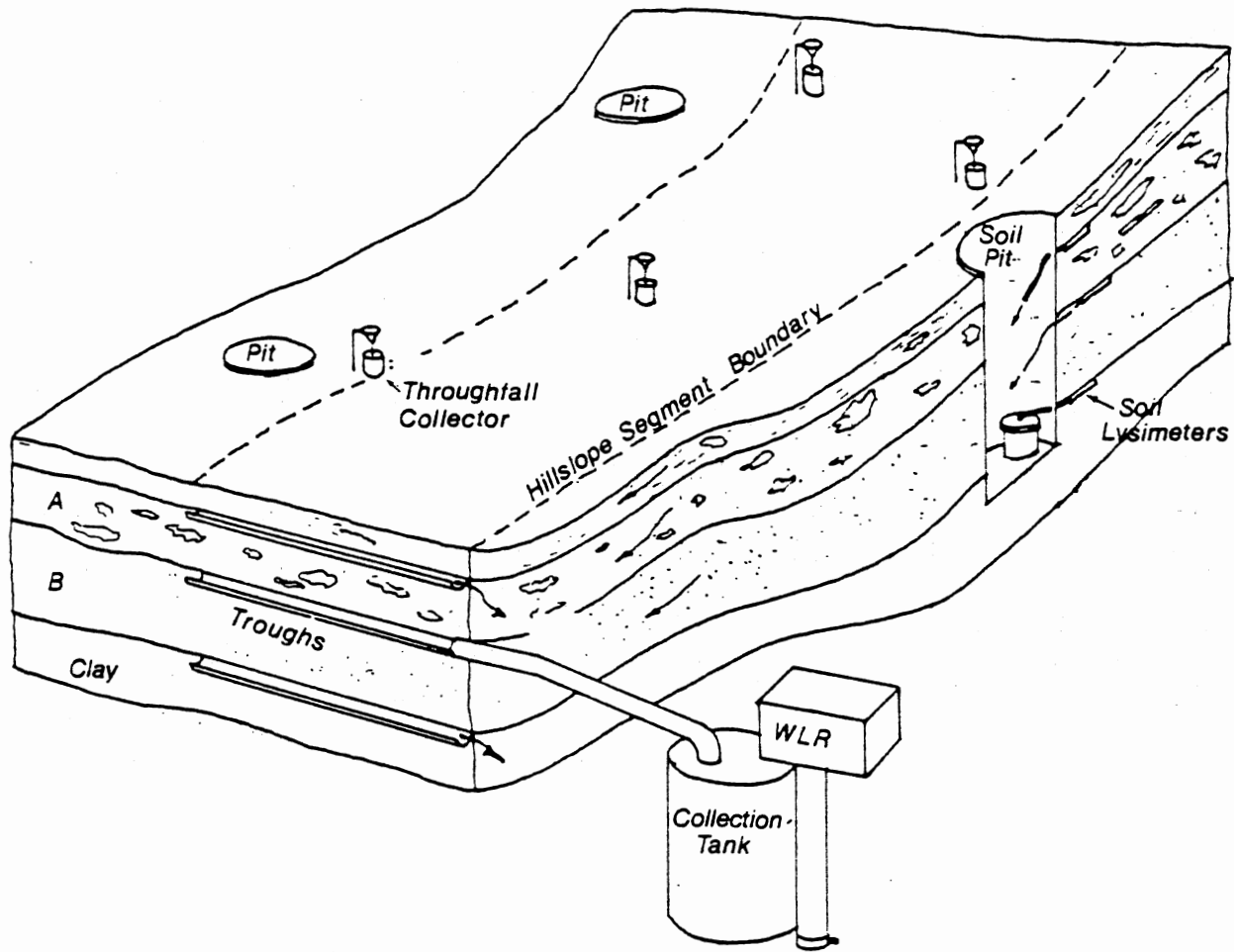


Figure 6. 3-D View of a Typical Hillslope Study Site and the Equipment Installed at Each Site

considerable study. The spatial variation of bulk precipitation chemistry is a function of the chemical constituent under study (Richter et al., 1983, Reynolds, 1984, and Lewis and Grant, 1978), proximity to bodies of water or chemical sources (Richter et al., 1983 Reynolds, 1984 and Sober and Bates, 1979) and spatial variation in rainfall amounts (Reynolds, 1984 and Lewis and Grant, 1978). Further variation between bulk precipitation samples may be a result of the type of sampler used, size of the sampler opening and the method of chemical analysis (Lewis and Grant, 1978).

The spatial variation of throughfall chemistry and quantity is further complicated by the type of vegetation (Kimmins, 1973, Likens et al., 1977, Raison and Khanna, 1982 and Lawrence, 1985) and density of vegetative crown cover (Kimmins, 1973 and Raison and Khanna, 1982).

In a study of the spatial variation of the chemical composition of bulk precipitation in South Carolina, Richter et al. (1983) found 19 collectors would be required to provide annual bulk precipitation inputs within 10% (at $P < 0.05$) of the true mean for sulfate, nitrate, calcium, magnesium, chloride, hydrogen and sodium. For phosphate, ammonium and potassium, 35 collectors were found to be required. The study was conducted on a 500 ha coastal plain watershed. Reynolds (1984), however, found only one collector was required to provide annual bulk precipitation inputs within 10% of the true mean (at $P < 0.05$) for sodium, calcium, magnesium, nitrate, sulfate, hydrogen and chloride. For potas-

sium, only two collectors were found to be required.

Reynold's study was conducted on a 600 ha coastal watershed in Wales.

Kimmins (1973) conducted an exhaustive investigation of the spatial variability and vegetative effects on throughfall quantity and chemical composition in a coastal watershed in British Columbia. Kimmins found over 500 collectors would be required to provide individual storm bulk throughfall inputs within 10% of the true mean (at $P < 0.05$) for potassium on a 900 m² plot. Potassium was, however, the constituent with the highest spatial variability in the study. In order to provide annual bulk throughfall inputs within 10% of the true mean (at $P < 0.05$), Kimmins found an average of 30 collectors would be required to account for spatial and vegetative variations in throughfall quantity and chemistry on a 900 m² area.

Obviously, bulk precipitation and throughfall are highly variable quantities to attempt to measure. Lewis and Grant (1978) suggested increasing the collector area to reduce spatial variability in bulk precipitation measurements. They suggested a minimum opening area of 1200 cm² for regions of average precipitation chemistry. Kimmins (1973) and Richter et al. (1983) used collector funnel openings of 121 and 201 cm², respectively. The collector funnels used in this study had an opening of 507 cm².

Lawrence (1985) measured throughfall for a three month period on Clayton Watershed #1 using 10 randomly located

collectors similar to the type used in this study. The area of the study was 7.86 ha. Using the mean and coefficient of variation of phosphate and nitrate concentrations of the ten collectors for individual storms, the number of samplers required to provide bulk throughfall inputs of phosphate and nitrate within 10% of the true mean (at $P < 0.05$) was calculated using the method given by Richter et al. (1983)

$$n = \frac{t^2 * CV^2}{r^2}$$

where n = the number of samples required, t = Student's t value (2 at 95% level) CV = coefficient of variation, and r = relative error desired (here $r = 0.10$).

For individual storms the number of collectors ranged from 1 to 268 and 1 to 104 for phosphate and nitrate respectively. The number of collectors required using average values for the three month study period were 62 and 14 for phosphate and nitrate respectively.

Based on the information presented above, it can be seen a large number of collectors are required to account for all of the spatial variability of throughfall from individual storms on the 7.73 ha proposed study area. A trade-off must be reached between level of accuracy, the number of samplers and the number of samples that can be reasonably analyzed in the lab. The number of samples for analysis may be reduced by lumping or combining individual collector samples as suggested by Lewis and Grant (1978). Based on the discussion above, it was decided that a total of twelve

collectors, four at each of the three study sites, would be adequate.

The bulk precipitation and throughfall collectors used were similar in design to those used by Likens, et al. (1977) at the Hubbard Brook Experimental Forest, New Hampshire. Lawrence and Wigington (1987) successfully used a similar design to gather bulk precipitation and throughfall samples on Clayton Watershed #1. The collectors consisted of a 254 mm diameter polyethylene funnel supported by a 25.4 mm wide ring cut from a 203.2 mm (8 in) diameter PVC pipe (Figure 7). The funnel drained through 9.525 mm (3/8 in) inside diameter plastic tubing into a polyethylene collection bucket. The collection bucket was sealed by use of a breather bottle. A glass wool plug in the funnel outlet served as a filter to keep debris out of the bucket. A plastic screen was suspended over the funnel opening to keep out large particles. The funnel and tubing was suspended by a frame made from 38.1 mm (1 1/2 in) diameter PVC pipe. A 4 inch acrylic can rain gage was also attached to the frame to obtain accurate measurements of throughfall depths.

Bulk precipitation and throughfall samples were collected as soon after storm events as was possible. A 500 ml aliquot of the sample was saved for later analysis. Throughfall collected in the cans was measured to the nearest 0.25 mm. Following sample collection, the funnels, tubing, and buckets were thoroughly washed with de-ionized distilled water.

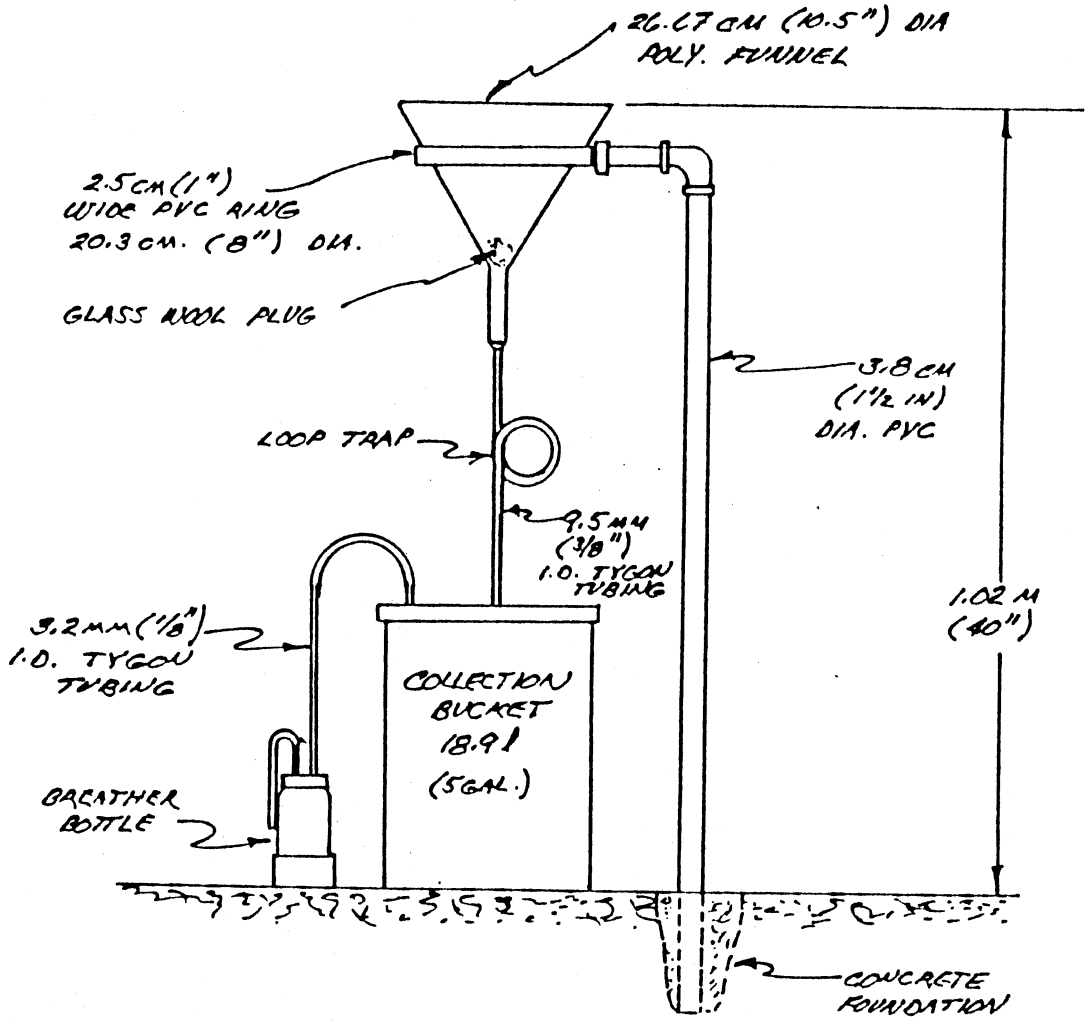


Figure 7. Throughfall Collection System

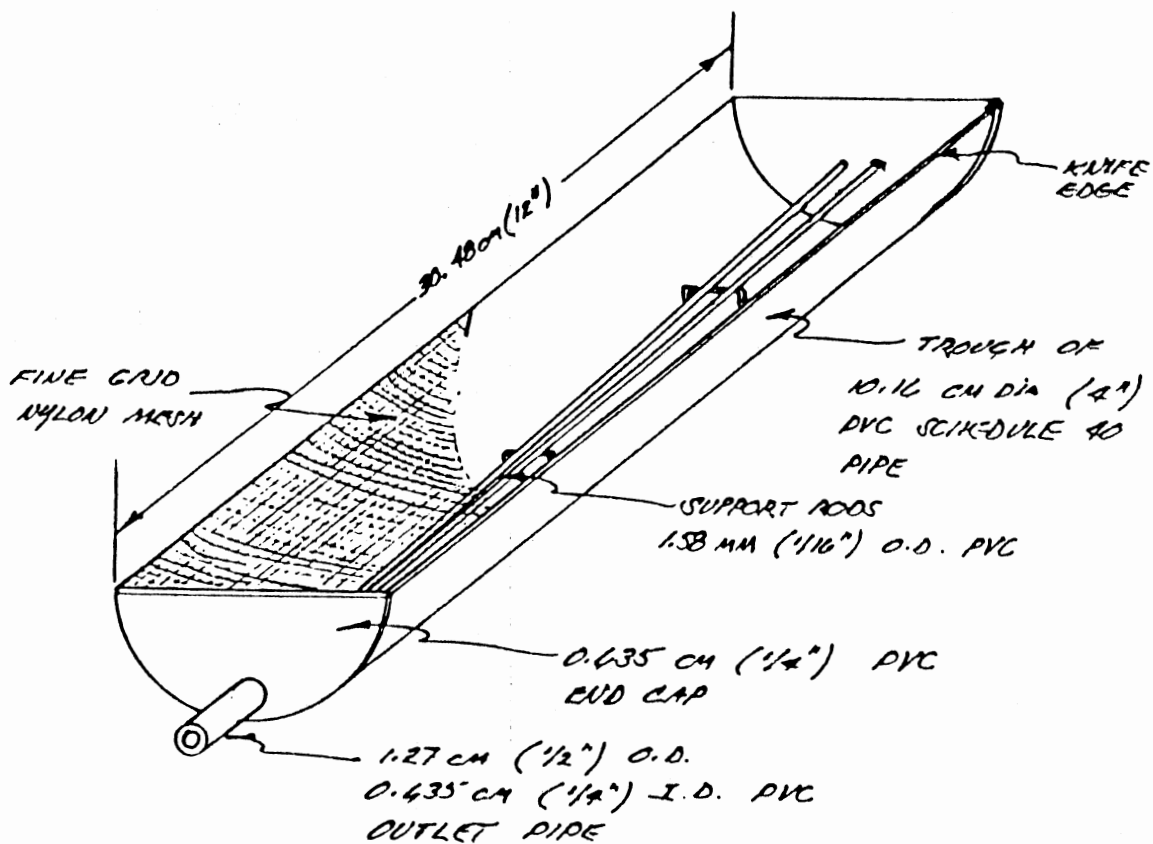
Soil Solution

Litaor (1988) investigated the variability associated with sampling soil solution and found that similarly large numbers of collectors as those required for sampling throughfall are required to obtain mean soil solution concentrations within specified limits about the true mean. For example it was found that 246 samples would be required to obtain an estimate of the mean soil solution nitrate concentration that was within 5 percent of the true mean. Such large estimates of replications required are in part the result of assuming the samples are normally distributed. Litaor (1988) suggests they are not normally distributed. Therefore, mean values should be calculated based on the frequency distribution of individual replicates.

Since the number of samplers required to obtain reasonable estimates of soil solution mean concentrations is prohibitively large, a compromise must be met. Three banks of collectors were located at each of the hillslope study sites. Each bank of collectors consisted of three lysimeters (Figure 6). A lysimeter was placed below the litter layer, below the A horizons (A1 and A2), and below the B1 horizon. The lysimeters were staggered so a lysimeter above would not interfere with the flow into a lysimeter below. The soil pit used to provide access to the soil was lined with a 208 liter (55 gal) oil drum to provide a housing for the collection buckets.

The collectors used were tension-free lysimeters (Figure 8) based on the design of Jordan (1968). The lysimeters consisted of a trough cut from a 101.6 mm (4 inch) diameter PVC pipe. End caps made of 6.35 mm (1/4 inch) thick PVC sheeting were glued to both ends. A fine mesh fiberglass screen was glued across the trough to prevent the entry of soil particles. Two PVC rods were glued inside of the trough to provide support for the screen and to break surface tension and allow soil water to drip into the collector. Tygon plastic tubing carried the sample from the trough to a 7.57 liter (2 gallon) polyethylene plastic collection bucket. Samples were collected as soon after a storm as possible. Following sample collection, the collection bucket was replaced with a clean bucket. A 500 ml aliquot was saved for chemical analysis.

The tension-free lysimeters of Jordan's (1968) design were chosen for this study because they were inexpensive to make and designed for soils with many rocks and roots, such as those in the Clayton Watersheds. Porous ceramic plates, such as those used by Cole (1968) and Wooldridge and Larson (1980), require a smooth contact with the soil. The tension-free lysimeters also do not require an expensive vacuum apparatus to maintain suction on the sampler, as the ceramic plates do. Tension-free lysimeters do, however, have some inherent disadvantages. The disadvantages of the soil solution sampling methods used are discussed in the Results chapter.



DETAIL
(SIDE CUTAWAY VIEW)

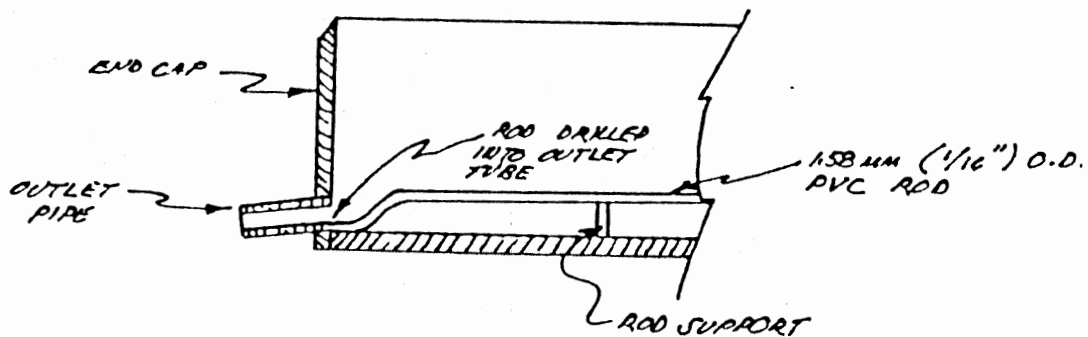


Figure 8. Tension-free Soil Lysimeter

Subsurface Flow

Atkinson (1978) has summarized a number of methods used to study hillslope water movement. For this study, a system of trough type collectors similar to those described by Atkinson (1978) were installed. Trough type collectors have been used in a number of other studies of subsurface flow. Whipkey (1965) used troughs to measure subsurface contributions to stormflow on a small forested watershed. Weyman (1970) also used troughs to study subsurface flow processes on a small catchment in Great Britian. Beasley (1976) used gravel filled troughs 12.2 m long to study subsurface flow processes on two small forested coastal plain watersheds in northern Mississippi. Flow from the troughs was routed through 0.305 m HS flumes. Chow (1976) used metal troughs to measure shallow subsurface flows (5 cm below the surface) on a 30 m long 30 percent forested hillslope in Newfoundland, Canada. The flow was measured with a tipping bucket gage designed specifically for the project. Later, Kachanoski and DeJong (1982) used Chow's system to measure surface and subsurface storm runoff on plots located on a small forested watershed in Saskatchewan, Canada. Kachanoski and DeJong studied the flow processes before and following clearcut timber harvesting on the plots. De Oliveira Leite (1985) also reported successfully using troughs to measure subsurface flow on an 85 year old cacao plantation in Brazil. Subsurface flow was collected in

tanks. Samples were also analyzed for their chemical characteristics.

It is recognized that the installation of the subsurface flow plots may change the natural pattern of flow at the site. The creation of a free surface along the soil profile face acts as a drain that may direct saturated flow towards the collector system. The unsaturated flow net may be changed in two ways (Atkinson, 1978). The formation of a saturated wedge above the troughs will reduce pressure potentials near the troughs and cause the flow to move away from the troughs. Drying at the soil profile face increases pressure potentials at the troughs, causing flow to be directed in towards the troughs. The effects of the former and latter conditions are to decrease and increase the size of the contributing area respectively. In order to reduce the effects of the troughs on the existing flow net, Atkinson (1978) suggests locating subsurface flow collection systems at natural seepage faces such as streambanks and the base of slopes. Therefore, the subsurface flow collection systems were located along the streambanks at natural seepage faces.

Numerous variations of the trough and the method of sample collection have been applied, based on the goals of the particular study. Each subsurface study plot used in this study consisted of three troughs and the collection system (Figure 6). Troughs were placed where changes in soil chemical and hydraulic properties were anticipated to

occur. One trough was located just below the litter layer to trap flow travelling over or through the litter. A second trough was located at the interface between the A and B soil horizons. The third trough was placed above the dense clay layer (between B21t and IIB23t horizons), where a sharp reduction in hydraulic conductivity was expected to occur. The placement of the troughs coincided with the placement of the soil solution samplers. The depth of placement of the troughs from the surface varied according to soil conditions.

Each trough was cut from a 101.6 mm (4 in) diameter PVC drain pipe, approximately 1.83 m (6 ft) in length, cut in half lengthwise to form a trough. Polyethylene sheeting was inserted in the soil between soil horizons to a reasonable depth to direct flow into the troughs (Figure 9). The sheeting also prevented downward seepage from upper horizons to lower ones. A combination of galvanized wire screen (6.35 mm (1/4 inch mesh)) and a fine plastic mesh screen was used to hold the soil face in place (Figure 10). Given that the soil face was stable, screen was a good alternative for backfilling the troughs with gravel. Gravel could change the chemical characteristics of the soil water, unless it was of an inert mineralogy. Polyethylene sheeting was draped over the outside edge of the trough to serve as a cover for the trough and the soil face.

Flow captured by the troughs was stored in 208 liter (55 gal) oil drums lined with a polyethylene liner. The

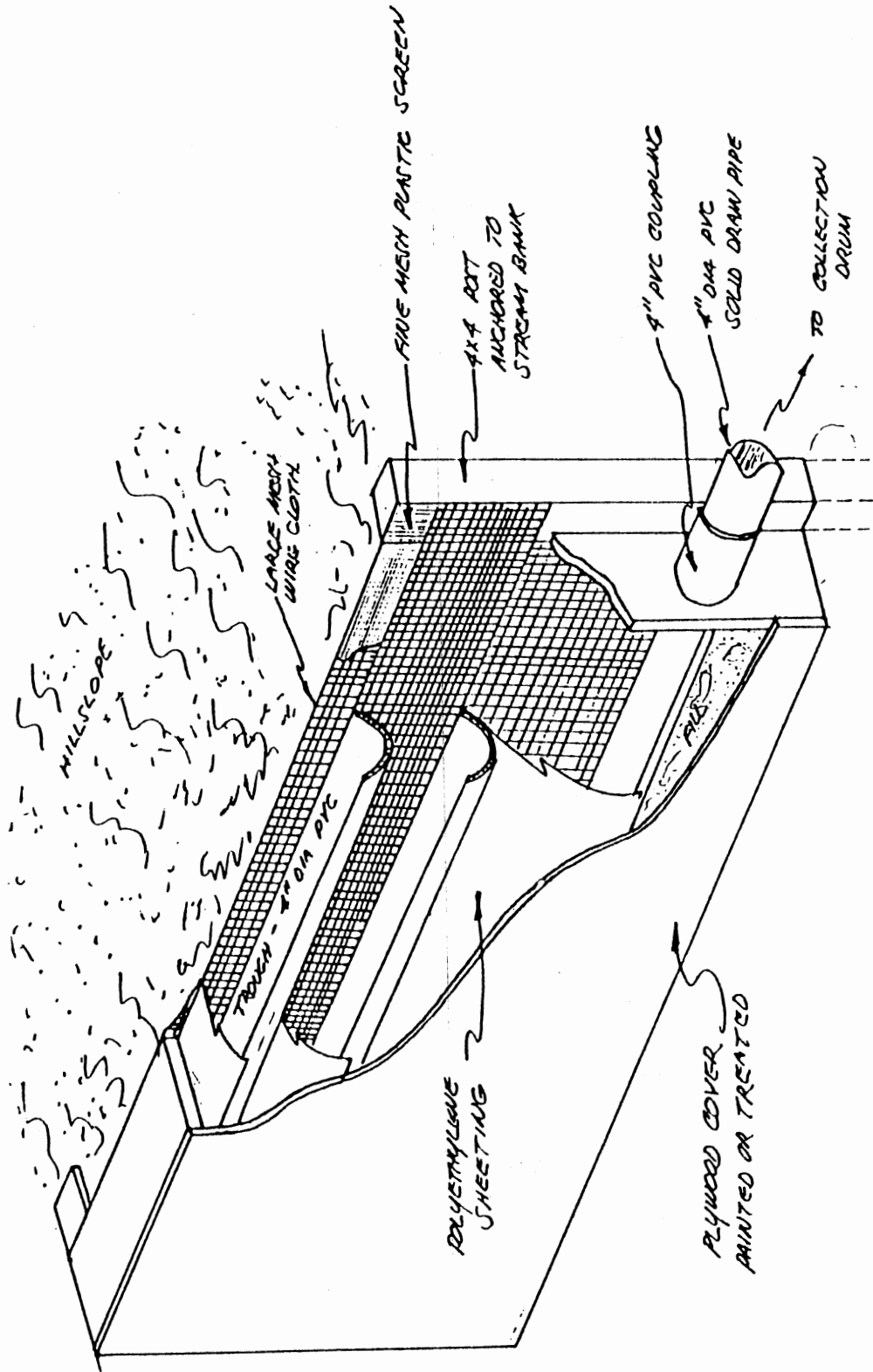


Figure 9. Cut-away View of Subsurface Flow Interceptor Troughs

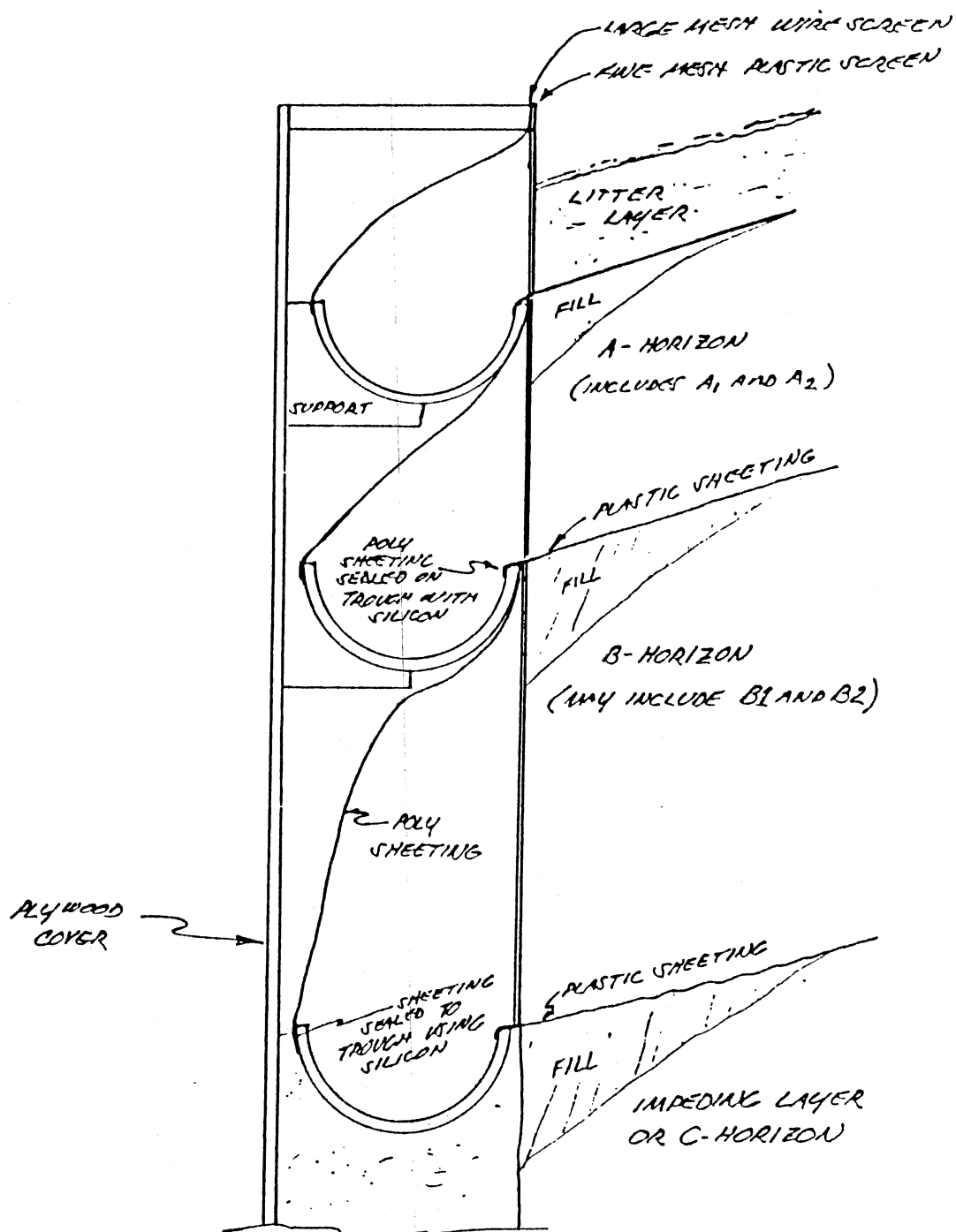


Figure 10. Cross Sectional View of the Subsurface Flow Collection Troughs.

accumulated depth of flow gathered in the collection tanks was recorded over time with FW-1 water level recorders. The water level recorders were connected to stilling wells attached to the side of the drums (Figure 11). The stilling wells were

constructed from 152.4 mm (6 in) diameter PVC pipes. The water level recorders provided records of cumulative volume of subsurface flow over time. From these records, the subsurface flow hydrographs for each soil horizon and study site was constructed.

Samples for chemical analysis of the subsurface flow were also collected. A 500 ml composite sample from each collection tank was gathered. Discrete samples during storm events were obtained from automatic pumping samplers connected to a sump (Figure 11) in the tank inlet pipe. The pumping samplers were set to operate as soon as water began to flow into the collection tank. A sampling interval of 10 minutes was used. Three pumping samplers were used in the study. The samplers were connected to the litter layer troughs at each study site.

Streamflow

Streamflow was measured at the watershed outlet by a 1.22 m (4 ft) H-Flume. Streamflow chemistry was sampled with an automatic pumping sampler. The sampler was activated at discrete levels of stage by a magnetic switch col

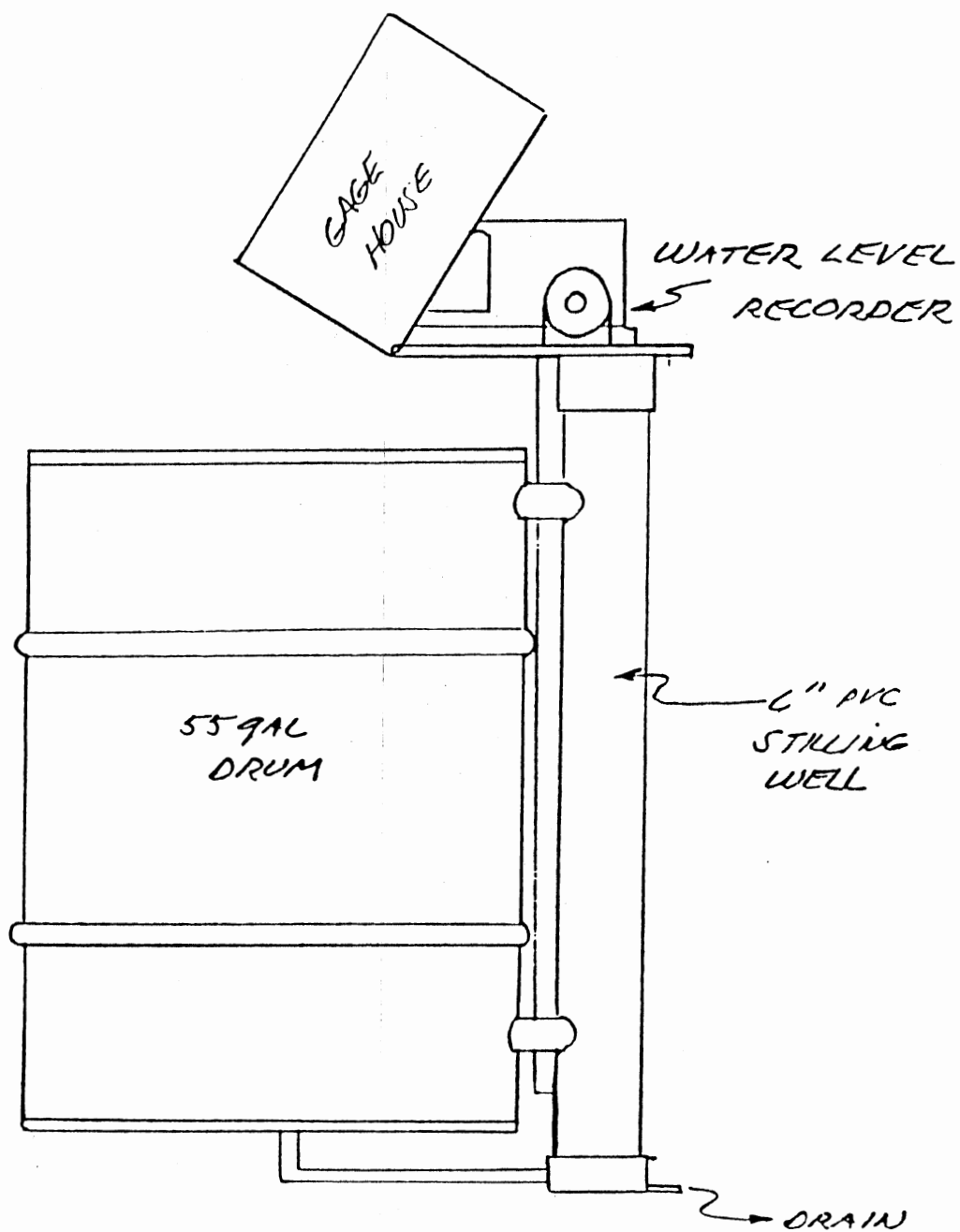


Figure 11. Collection Drum and Water Level Recording System Used in the Subsurface Flow Collection System

umn (Turton and Wigington, 1983), providing sampling throughout a storm event. Sample chemical analysis and streamflow data file management was provided as part as the ongoing Clayton Watersheds research project.

Chemical Analysis

Analysis and Storage

All bulk precipitation, throughfall, soil water, sub-surface water and streamwater samples were analyzed for pH, conductivity, NO₃-N, dissolved organic carbon, calcium, magnesium, potassium and sodium. Additional analysis, such as sulfate, chloride, total dissolved solids, and alkalinity were performed on some samples.

All samples were retrieved as soon as possible following a storm event. After collection the samples were immediately frozen in a freezer located near the field site. Samples were kept frozen until the day they were analyzed in the lab. All chemical analysis were performed according to procedures outlined in Standard Methods for the Examination of Water and Wastewater (APHA, 1980) and Methods for Chemical Analysis of Water and Wastes (EPA, 1983). One duplicate sample was analyzed for every ten samples. One spiked sample for every 20 samples was run to test the percent recovery of the methods. Reagent blanks were also analyzed. Additionally, quality control samples provided by the US Environmental Protection Agency were also included in the analysis each day a batch of samples was analyzed.

pH

Sample pH was measured electrometrically with a research grade combination electrode and a pH meter. A two buffer calibration procedure was followed. Performance of the combination electrode was checked before each sample run against a poorly buffered pH 4.30 quality control standard. All pH readings were recorded to the nearest 0.01 pH units.

Conductivity

The conductivity of each sample was measured using a conductivity meter equipped with a platinum glass electrode. A correction factor used to convert all conductivity readings to equivalent conductivities at 25°C, was calculated by comparing the measured conductivity of a standard solution with the standard's known conductivity at 25°C. All readings were recorded to the nearest 0.1 micromho.

Nitrate-Nitrogen

Nitrogen as nitrate and nitrite (NO₃ and NO₂ - N) was measured using the cadmium reduction procedure (EPA, 1983). Since nitrite is readily converted to nitrate in natural waters, almost all of the nitrogen measured was assumed to have been in the nitrate form. The detection limit of the procedure is 0.01 mg/l.

Dissolved Organic Carbon

A quick spectrophotometric method was used to obtain measurements of the total dissolved organic carbon content of the water samples (Moore, 1985). For watersheds not contaminated by man-made organic compounds, total dissolved organic carbon is a good indicator of the quantities of naturally occurring organic compounds in streamflow (Ried, et al., 1981). Naturally occurring organic compounds include a large number of various compounds. No attempt was made to identify the individual organic compounds present. As long as watershed conditions remain the same, the organic substances present and the relative proportions of each substance should remain the same (Moore, 1985). Some seasonal changes may occur. If this assumption is met, then the method is valid as an indicator of the differences in concentration of total dissolved organic carbon of water between sources.

In forested watersheds the majority of the dissolved organic compounds will be organic acids such as fulvic and tannic acid. Organic acids are of particular interest because they contribute weak acids to the overall acidity of water and are important in the transport of metal ions by complexation and chelation (Ried, et al. 1981). Total dissolved organic carbon was also chosen for analysis because it was felt that it would be a good chemical constituent to use to separate flow emanating from shallow soil

horizons (high in organic matter) from flow emanation from deeper horizons (lower in organic matter).

The method of analysis consisted simply of reading the absorbance of a filtered (45 μ m) water sample at a wavelength of 330 nm. For comparison, a standard curve of tannic acid standards was developed. The absorbance of the water samples was converted to "total dissolved organic carbon as tannic acid in mg/l" using the standard curve equation. The relationship between absorbance and the concentration of tannic acid in the standards was linear from 0 to 500 mg/l. Samples above 500 mg/l were diluted so they would read in the linear portion of the curve. Since it is not actually a quantitative measurement of TDOC, the results obtained by the method are intended only to be used to compare relative amounts of dissolved organics in water from different sources.

Cations

Water samples were analyzed for the cations calcium, magnesium, potassium, and sodium on a Varian SpectrAA-40 atomic adsorption spectrophotometer. Flame emission techniques were used. AA procedures and guidelines given by Methods for Chemical Analysis of Water and Wastes (EPA, 1983) were followed. The detection limits for calcium, magnesium, potassium and sodium were respectively 0.01, 0.001, 0.01 and 0.002 mg/l.

Other Analysis

The analysis discussed above were performed on all samples. Additional analysis were performed on a small number of selected samples. Alkalinity was measured as total alkalinity (mg/l CaCO_3) by titrating the sample with N/50 HCl to an end point pH of 4.3. Sulfate (SO_4) and chloride (Cl^-) were measured by ion chromatography using a Dionex Ion Chromatograph.

CHAPTER V
RESULTS AND DISCUSSION OF
FIELD STUDY

Introduction

All of the field equipment previously described was installed and operational on January 11, 1987. The study was terminated on July 3, 1987. During the period of study, hydrologic and chemistry data were collected for twenty two storm events. More than 1200 water samples were collected and analyzed for chemical characteristics. Due to the volume of hydrologic and chemistry data collected, only summary tables of those data required to meet the research objectives will be presented. However, the complete set of raw data is presented in various appendicies. Appendix A contains tables of precipitation and subsurface flow for each storm event. Chemistry data is summarized in Appendix B on a storm by storm basis.

Study Site Description

Measurements of watershed characteristics important to the generation of streamflow from the watershed were made at various times during the course of the study. The results

of the measurements are presented here to provide easier reference for the discussions following in this chapter. The lengths of the hillslope study segments (Table 1) were obtained from the topographic map of the watershed. Flow was assumed to occur in a direction perpendicular to the contour lines until a divide was reached (Figure 12). It is doubtful that surface or subsurface flow actually travels this distance or direction. However, in lieu of actual measurements of flow paths, the assumption that water flows perpendicular to the contours was used as a first approximation. The areas of the hillslope study segments (Table 1) were calculated by multiplying the estimated length times the width of the subsurface flow collection troughs (1.83 m). Mean slopes of the hillslope study segments (Table 1) were obtained by field measurements. Hillslope slope profiles were also measured and mapped (Figure 13).

The depths of the soil horizons sampled by the subsurface flow collection troughs varied between sites and within hillslope study segments themselves. The depths from the surface and thickness of each soil horizon at the streambank face where the subsurface flow collection troughs were located are presented in Table 2. The total depth sampled by the subsurface collection system for sites 1, 2, and 3 were 40, 35, and 46 cm respectively. As can be seen, the maximum depth sampled was relatively shallow. The subsurface flow collection system did not sample flow from the deeper soil

TABLE 1
HILLSLOPE STUDY SITE CHARACTERISTICS

Site	Hillslope Length (m)	Hillslope Segment Area (m ²)	Mean Slope (%)
1	58	106	11
2	50	92	24
3	61	112	14
Total	na	310	na

TABLE 2
HILLSLOPE STUDY SITE SOIL DEPTHS AT
SUBSURFACE FLOW COLLECTION TROUGHS

Site	Litter Depth* (cm)	A Horizon Depth* (cm)	B Horizon Depth* (cm)
1	0-5	5-22	22-40
2	0-8	8-18	18-35
3	0-10	10-22	22-46

*range of depths as measured from the surface

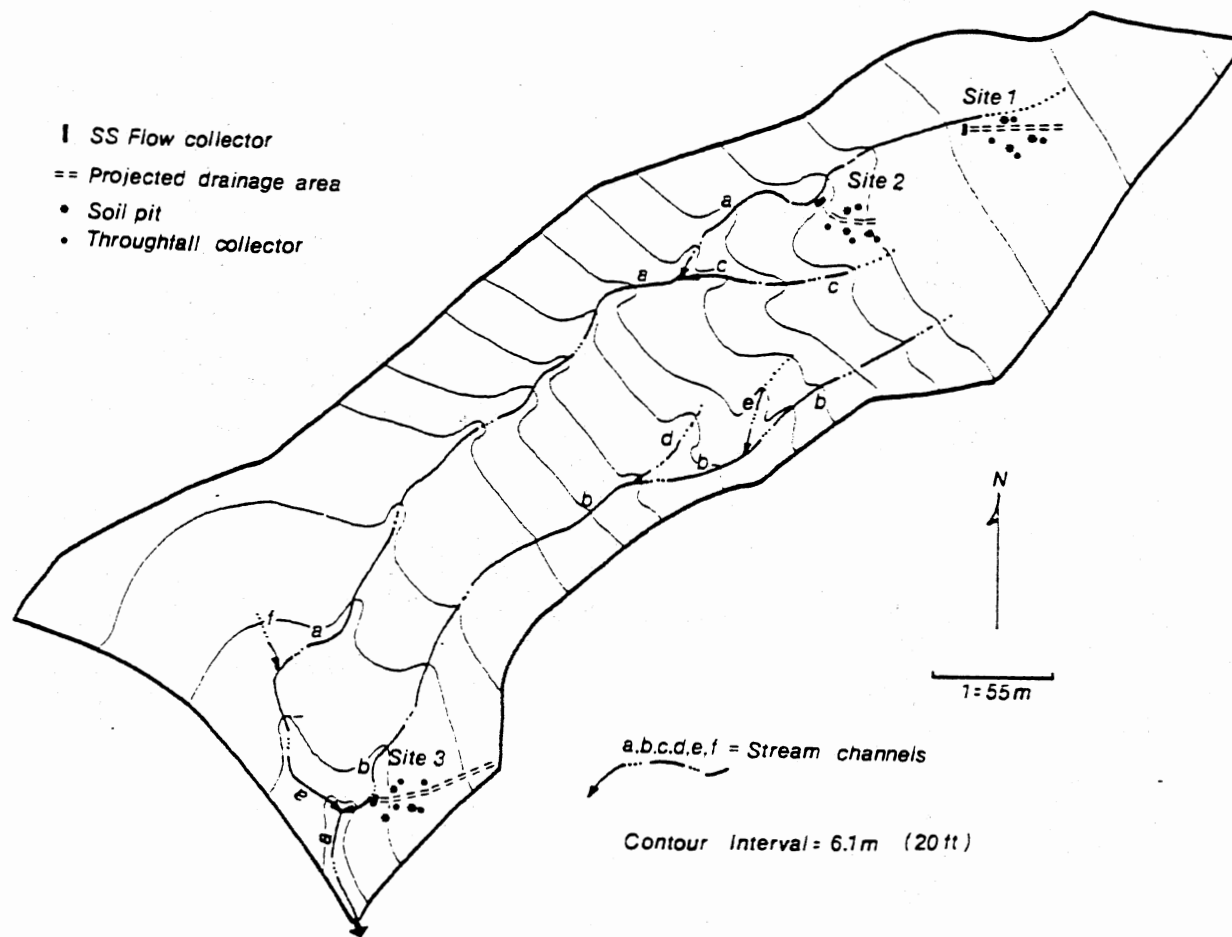


Figure 12. Watershed Map Showing Stream Channels and Research Sites

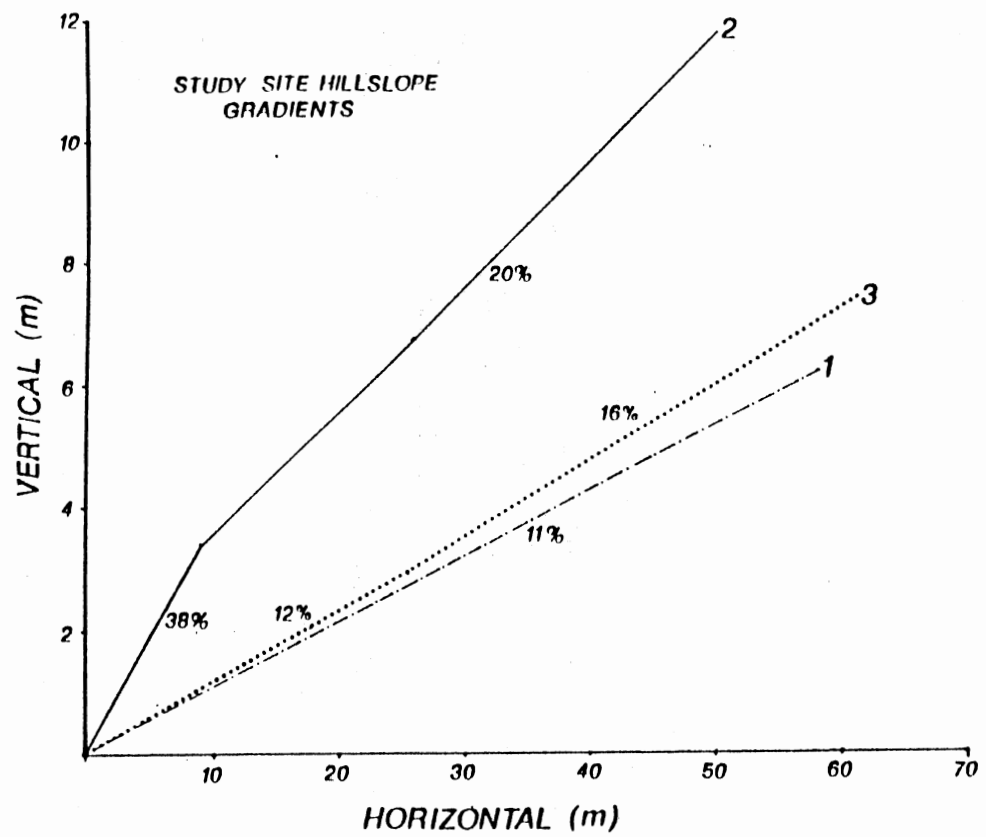


Figure 13. Profiles of Hillslope Study Segments

horizons. Total soil depth on the watershed varied considerably, but clays extended to depths of 125 cm in places. To distinguish the subsurface flow measured in this study from deeper subsurface flows, the subsurface flow is hereafter defined as shallow subsurface flow (SSF).

Stream channel lengths, the areas occupied by stream channels, and the slopes of the channels (Table 3) were obtained by field measurement. The total length of all of the stream channels was 1117 meters. A stream channel was defined as any channel that was capable of conveying flow.

TABLE 3
WATERSHED STREAM CHANNEL CHARACTERISTICS

Channel	Length (m)	Area (m ²)	Mean Slope (%)
a	610	881	14
b	318	533	14
c	92	91	18
d	46	78	20
e	23	35	20
f	28	17	18
Total	1117	1635	na

The definition included well-defined alluvial channels and shallow vegetated depressions, or swales.

The stream channels were broken into 30 meter segments. The slope was measured for each segment. Twenty measurements of the channel width were obtained for each segment to obtain an average width for each segment. For alluvial channels, the width included the width of the alluvial material that appeared to convey water at normal high water. Widths for less well-defined channels were more subjectively determined. A best estimate of where water flowed was made based on field evidence. The segment area was calculated by multiplying the average width by the segment length.

Extrapolation of Results

Data obtained in this study includes volumes and rates of SSF. In order to extend the results obtained at the hillslope study segments to explain the behavior of the entire watershed, some assumptions had to be made. One logical assumption would be to determine what percentage of the total watershed area is included in the hillslope study segments. The total area of the three study sites, as estimated above, is 310 m². This area represents 0.40 percent of the total watershed area, 77300 m².

As discussed previously, it is doubtful that surface and subsurface flow followed the path as shown by the contour map. It was very difficult to obtain accurate measurements of the flow path lengths and directions of the 1.8 m wide hillslope segments. Therefore, a different approach was taken. Accurate measurements of the stream channel lengths

were obtained. It was assumed that the three hillslope study segments adequately sampled the range of hillslope characteristics found on the watershed. This assumption was probably statistically incorrect, but there was also no practical way of obtaining more samples (more SSF collectors) in this type of a study. The three SSF collection systems sampled a total of 5.488 m, or 0.25 % of the 2234 m of streambank (total stream channel length of 1117 m times 2) found on the watershed. This percentage is equivalent to 1/400 of the total watershed streambank length. Therefore, a watershed scale factor (WSF) of 400 was defined for extrapolating SSF volumes to the entire watershed. The WSF is referred to frequently in further discussions of the results.

Hydrologic Processes

Of the 22 storm events monitored, 5 storms produced no measurable streamflow. Of the 17 remaining storms, only 9 storms were large enough to produce measurable streamflow greater than the level of base flow that existed prior to the storm. Sampling for the first storm (1/16/87) was incomplete due to equipment failures. Therefore, the presentation of the hydrologic processes results will concentrate on the eight events that produced significant streamflow.

Precipitation and Throughfall

Measurements of precipitation were available for all storms. The total depth of precipitation measured over the study period was 620 mm (Table 1). Event precipitation ranged from 1.8 mm (6/2/87) to a maximum of 102 mm (5/28/87). Only four storms during the study period were greater than 50 mm, four storms were between 50 and 25 mm in depth, and the remaining storms accumulated less than 25 mm of depth. During the winter months, storms tended to be of low intensity and long duration. During the spring and summer months, convective thunderstorms produced events of short duration and high intensity (Appendix A). The maximum rainfall intensity recorded during the study period was 122 mm/hr. The duration of this intense burst was, however, only 5 min.

Throughfall was measured at each of the twelve throughfall bulk chemistry collectors using 101.6 mm (4 in) plastic rain cans. The use of rain cans, instead of volumes collected by the bulk collectors, insured that an accurate measurement of throughfall depth was obtained. The arithmetic mean and standard deviation of throughfall depths were calculated for each storm (Table 4). As expected, throughfall depths were less than incoming precipitation, due to interception loss. The mean interception loss for the study period (precipitation - throughfall) was 9 percent of the incoming precipitation. A table of all of the

TABLE 4
 PRECIPITATION AND MEAN THROUGHFALL
 FOR THE STUDY PERIOD 1/13 - 7/3/87

Storm Date	PCPN (mm)	Mean Throughfall (mm)	Std. Dev. (mm)	# of samples
1/16*	46	45	2	6
2/1	22	19	1	10
2/15*	32	31	2	10
2/21	6	6	1	11
2/24*	14	13	2	12
3/1*	54	49	4	12
3/17*	62	61	4	12
3/25	10	10	2	11
4/1	12	11	1	11
4/13	20	19	2	12
4/30	20	15	2	12
5/24	37	30	6	12
5/25*	37	34	5	12
5/28*	102	92	12	12
5/31*	13	11	2	12
6/2	2	1	1	12
6/9	11	9	2	12
6/10	10	8	2	12
6/23	50	44	6	12
6/30*	60	57	9	11

*signifies streamflow producing events

precipitation and throughfall data from individual storms and collectors is presented in Appendix C.

Linear regression analysis was applied to the precipitation-throughfall data to determine the relationship between precipitation (PCPN) and throughfall (TFALL). The precipitation-throughfall data was divided into two parts, a growing season and a dormant season, to represent different canopy conditions. The dormant season included data from

January to March 31. The growing season included data from May 1 to July 3. The leaf-out transition period, April 1 to April 30, was not analyzed due to the small number of storms during the period. Three regression analyses were performed, using storm precipitation vs. individual throughfall collector depths for each storm, for the entire data set, dormant season data, and growing season data (Table 5).

TABLE 5
PRECIPITATION (MM) - THROUGHFALL (MM) RELATIONSHIPS
FOR ALL DATA AND THE DORMANT AND GROWING SEASONS

Type P**	Regression Equation	r ²	F*
All Data <0.005	TFALL = -0.26 + 0.92(PCPN)	0.96	4410
Dormant <0.005	TFALL = -0.27 + 0.97(PCPN)	0.98	4204
Growing <0.005	TFALL = -1.7 + 0.93(PCPN)	0.95	1642

*F = analysis of variance F-ratio
**P = significance level of F

An analysis of variance showed that all of the regression equations were significant at a significance level of < 0.005 (Table 5). All slope coefficients tested to be not equal to zero at a significance level of < 0.005 (two-tailed test). However, all of the constants were found to be

not significantly different than zero at a significance level of 0.10 (two-tailed test).

The relationships obtained agree closely with precipitation-throughfall relationships for similar pine-hardwood cover types obtained by other researchers (Table 6). The slope terms for this and the studies cited are similar. The major differences between the studies are in the constant term. Differences exist because throughfall and interception are in part a function of the stand density and tree species mix present (Helvey, 1965 and Rogerson, 1965). There was a great deal of difference in stand density and species mix between this study and the studies cited. For example, the basal area in Lawson's (1967) study was about 1.5 times the basal area of the trees on Clayton Watershed 3. As a result, the constant terms in Lawson's (1967) equation are almost twice as large (Table 6) as those obtained in this study (Table 5), even though the slopes are nearly equivalent. Lawson's watersheds also had a greater percentage of pines. In general, conifers have a greater canopy storage and interception loss due to a greater leaf area index and because they do not lose their foliage in the winter. The results obtained in this study agreed more closely with those obtained by Clingenpeel (1978) and Lawrence (1985) on Clayton Watershed 1. Clayton Watershed 1

TABLE 6
 PRECIPITATION-THROUGHFALL (MM) RELATIONSHIPS FOR
 MIXED HARDWOOD-PINE COVER TYPES

Summary of all eastern hardwoods (Helvey and Patric, 1965):

Dormant Season	TFALL = $-0.38 + 0.94(\text{PCPN})$
Growing Season	TFALL = $-0.79 + 0.90(\text{PCPN})$

Arkansas, Ouachita Mountains, mixed oak, hickory, shortleaf pine (Lawson, 1967):

Annual	TFALL = $-2.4 + 0.94(\text{PCPN})$
Dormant Season	TFALL = $-1.8 + 0.96(\text{PCPN})$
Growing Season	TFALL = $-3.1 + 0.93(\text{PCPN})$

Oklahoma, Ouachita Mountains, mixed oak, hickory, shortleaf pine, Clayton Watershed 1 (Clingenpeel, 1978):

Growing Season	TFALL = $-0.7 + 0.91(\text{PCPN})$
----------------	------------------------------------

Oklahoma, Ouachita Mountains, mixed oak, hickory, shortleaf pine, Clayton Watershed 1 (Lawrence, 1985):

Annual	TFALL = $-1.2 + 0.94(\text{PCPN})$
--------	------------------------------------

did, however, contain a greater percentage of pines in its species mix. The number, location, type and size of the collector used may also have contributed to differences in throughfall measurements between studies.

Canopy Storage

Total canopy storage on a watershed is a function of the leaf area, stand density and the areal distribution of vegetation (Leonard, 1965). Leaf area, in turn, is a function of tree species and season. The quantities

previously mentioned are highly spatially variable and difficult to measure. An estimate of canopy storage may be obtained from throughfall regression equations such as those discussed above (Leonard, 1965). Throughfall is set to zero, and the equation is solved for the maximum depth of precipitation that produces no throughfall. This depth is assumed to be equivalent to the maximum canopy storage. Canopy storage values were calculated for the precipitation-throughfall relationships developed in this study using the procedure described above (Table 7). For comparison, canopy storages were also calculated for the precipitation-throughfall relationships cited in Table 6. The differences in canopy storage estimates reflect differences in tree species and stand density. The watershed in Lawson's (1967) study had a greater percentage of pines and 1.5 times the basal area on Clayton Watershed 3. As a result, the estimated canopy storages for Lawson's study are greater than those estimated for Clayton Watershed 3. As with throughfall, the estimate of canopy storage is also effected by the size, location and number of collectors used in the particular study. Despite the differences in the estimates of maximum canopy storage, it should be noted that all of the storage values are less than 5 mm. This value may be less than the areal variability in precipitation depth. Such a small depth of storage may be insignificant in modeling large storm events. On the other hand, it may be a significant

TABLE 7
CANOPY STORAGES FOR VARIOUS
MIXED PINE-HARDWOOD COVER TYPES

Season	Canopy Storage (mm)
<hr/>	
This study, Clayton Watershed 3, mixed oak, hickory, shortleaf pine:	
Annual	0.3
Dormant	0.3
Growing	1.8
<hr/>	
Summary of all eastern hardwoods (Helvey and Patric, 1965):	
Dormant	0.4
Growing	0.9
<hr/>	
Arkansas, Ouachita Mountains, mixed oak, hickory, shortleaf pine (Lawson, 1967):	
Annual	2.6
Dormant	1.9
Growing	3.3
<hr/>	
Oklahoma, Clayton Watershed 1, mixed oak, hickory, shortleaf pine (Clingenpeel, 1978):	
Growing	0.8
<hr/>	
Oklahoma, Clayton Watershed 1, mixed oak, hickory, shortleaf pine (Lawrence, 1985):	
Annual	1.3
<hr/>	

quantity in modeling small storm events, in the accounting of the annual water balance, and for modeling chemical changes as water passes through the canopy.

Subsurface Flow Volumes

SSF Volume vs. Precipitation

The volumes of shallow subsurface flow intercepted by the trough collection system varied greatly between sites, soil horizons, and precipitation quantities (Table 8). Even though only eight storms were available for analysis, some trends between precipitation and subsurface flow volume were detected. Total subsurface flow, the sum of subsurface flow from each horizon and each site, was calculated for each storm (Table 8). A plot of total subsurface flow vs. precipitation (Figure 14) indicates that total subsurface

TABLE 8

TOTAL HILLSLOPE SEGMENT SSF FOR EIGHT STREAMFLOW PRODUCING STORMS

Date	Precipitation (mm)	Shallow Subsurface Flow (l)
2/15	32	51
2/24	14	7
3/1	54	214
3/17	62	603
5/25	37	94
5/28	102	2568
5/31	13	40
6/30	60	123

flow increased exponentially with, or as a power function of precipitation. Subsurface flow was log transformed and regressed on precipitation. Not unexpectedly, the analysis indicated that the log of subsurface flow volume was highly correlated with precipitation. The regression explained 88 percent of the variation in the logarithms of subsurface flow ($r^2 = 0.88$). The regression was found to be significant ($F=41.80$) at a significance level of 0.001, and the slope ($t = 6.465$) and intercept ($t = 4.553$) were found to be significantly different than zero at significant levels (two tailed test) of 0.004 and 0.001 respectively. The largest storm of the research study period (5/28/87) may have exerted undue influence on the shape of the relationship. The resulting relationship was

$$\text{LogSSF} = 0.941 + 0.025\text{PCPN}$$

where PCPN is the storm precipitation in millimeters and SSF is the shallow subsurface flow in liters.

Even though a good statistical relationship between precipitation and the log of subsurface volume exists, the use of the relationship to predict subsurface flow from a given amount of precipitation can lead to considerable error. A direct statistical comparison between precipitation and subsurface flow ignores other variables, such as storage and contributing area, that control flow generation. A certain initial quantity of soil moisture storage may have to be met before subsurface flow can be generated. For example, a

SSF vs. Precipitation

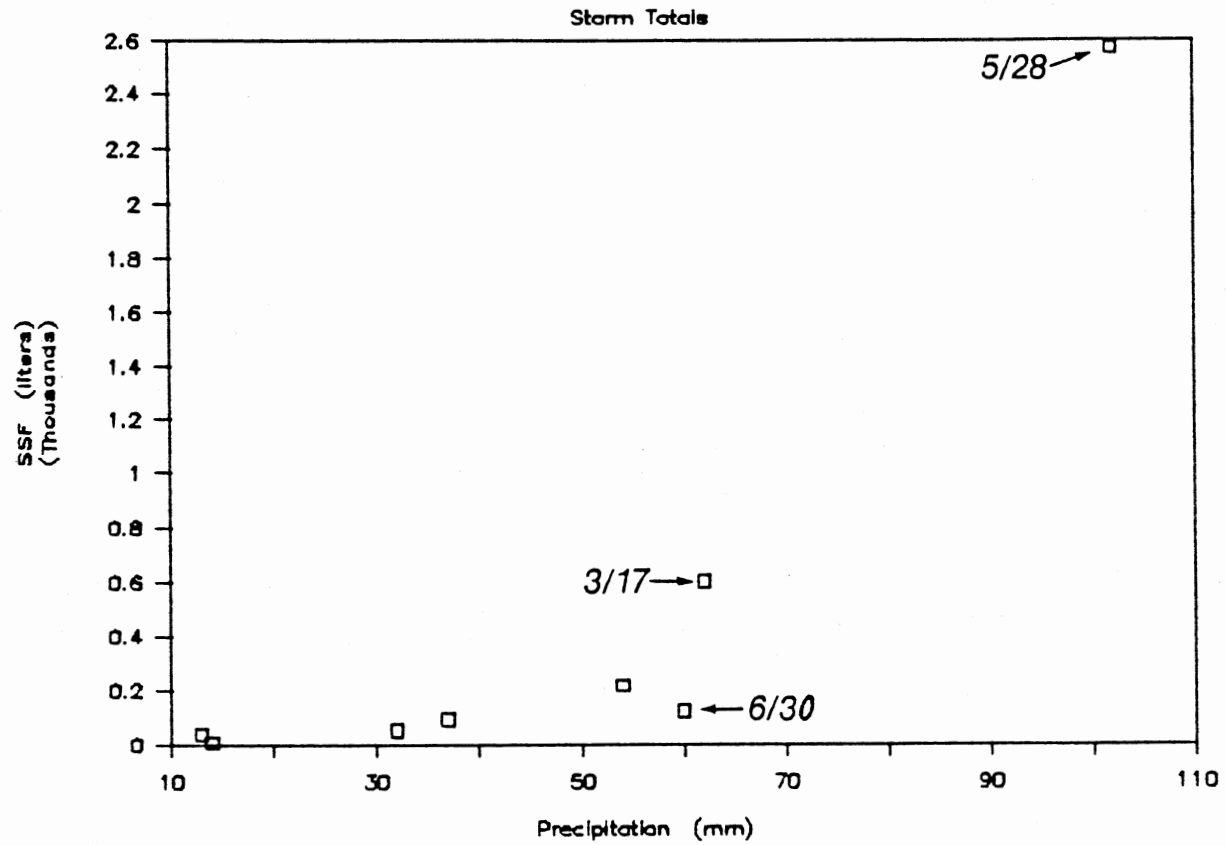


Figure 14. Plot of Total Storm SSF vs. Precipitation

storm of 62 mm (3/17) and a storm of 60 mm (6/30) produced 603 and 123 liters of subsurface flow respectively. The 62 mm storm occurred in March when soil moisture was high. The 60 m storm occurred in late June, following a long period of low precipitation and high evapotranspiration. The predicted value of subsurface flow for 61 mm of precipitation is 292 liters.

Site and Soil Horizon Differences

Each hillslope study segment had different characteristics (slope, soils, vegetation, etc) that could have affected the quantity of SSF produced from each site for a given quantity of precipitation. By observation (Table 9), it can be seen that for all storms, the total volume of SSF from Site 2 was greater than SSF from the other sites. Site 2 had the steepest average slope (24%), but the smallest projected drainage area (92 m²). Within storms, Site 2 produced a greater percentage of the total SSF from the three sites during small storms preceded by dry conditions. For large storms (>60 mm), Site 1 produced more SSF than Site 3. By observation, it appears that the three sites do not produce the same amount of SSF for a given quantity of precipitation. Statistical tests were made to confirm the observations.

The means and variances of site SSF quantity for each storm were calculated (Table 10). The three site means were found to be not significantly different ($H_0: x_1 - x_2 = 0$; H_a

TABLE 9
 SSF VOLUMES BY SITE, SOIL HORIZON,
 AND STORM

Date	PCPN (mm)	Site #	Soil Horizon			Total (1)
			Litter (1)	A (1)	B (1)	
2/15	32	1	1	1	2	4
		2	9	26	1	36
		3	11	1	0	12
		Horizon Totals	21	28	3	52
2/24	14	1	0	0	0	0
		2	3	1	0	4
		3	2	1	0	3
		Horizon Totals	5	2	0	7
3/1	54	1	5	1	2	7
		2	14	110	32	156
		3	10	10	31	51
		Horizon Totals	29	121	65	214
3/17	62	1	22	4	86	112
		2	34	340	75	449
		3	25	17	0	42
		Horizon Totals	81	361	161	603
5/25	37	1	10	3	6	19
		2	20	27	10	57
		3	18	0	0	18
		Horizon Totals	48	30	16	94
5/28	102	1	320	5	533	858
		2	558	520	201	1279
		3	36	109	286	431
		Horizon Totals	914	634	1020	2568
5/31	13	1	3	0	2	5
		2	8	15	3	26
		3	4	0	5	9
		Horizon Totals	15	15	10	40
6/30	60	1	4	6	4	14
		2	17	72	13	102
		3	5	0	2	7
		Horizon Totals	26	78	19	123

TABLE 10
 STATISTICS AND ANOVA FOR STORM
 SSF CLASSIFIED BY SITE

Statistic	SITE 1	SITE 2	SITE 3		
n of cases	8	8	8		
minimum	0.50	3.5	3.2		
maximum	858	1279	431		
mean	127.38	263.56	71.48		
standard dev.	297.50	434.53	146.31		
variance	88508	188814	21405		
Pooled variance for t-test of means	Sites 1-2: 161771 Sites 2-3: 122627 Sites 1-3: 64115				
ANOVA - SSF for all storms, classified by site (treatment)					
Source	Sum-of-Squares	DF	Mean-Square	F-Ratio	P
Site	156185.208	2	78092.604	0.784	0.469
Error	2091089.669	21	99575.699		

$x_1 - x_2 <> 0$) from each other at the 0.05 confidence level. A one way ANOVA was also run to determine whether or not there were significant differences between sites (treatments). The error variance was large compared to the treatment variance ($F=0.784$). Therefore, there was no significant difference between sites (treatments) at a significance level < 0.469 . Further tests were not run. It was recognized that the data set was small, thereby not providing a good sampling of storm sizes and conditions. Other factors not included in the statistical tests, such as antecedent moisture, the intensity and duration of precipitation may control the release of SSF

from the sites as much or more than differences in site characteristics such as slope and drainage area.

Horizon SSF totals were calculated for each storm (Table 9). By observation, it can be seen that for most storms more SSF was produced from the A horizon for a given quantity of precipitation. The majority of the A horizon SSF was produced on Site 2. Conditions conducive to SSF include steep slopes and highly porous soils. Site 2 had the steepest slopes of the three sites in the study. The A horizons of the soils on the sites are highly porous fine sandy loams. The A horizons are also riddled with roots and macropore channels.

For small storms and small storms preceded by dry conditions, the litter layer produced the next largest quantity of SSF for a given quantity of precipitation. For large storms and wet initial conditions, the B horizon produced more SSF than the litter layer. For the largest storm of the study period (5/28), the B horizons collectively produced more SSF than either the litter layer or the A horizon. An especially noteworthy observation is that significant quantities of SSF are produced from the shallower litter layers and A horizons when the B horizon produces little or none (Table 9; storms of 2/24, 5/25, and 6/30). Under dry antecedent conditions, the shallow soil layers would be wetted to a moisture content at which flow can be released (ie: field capacity) earlier than the deeper B-horizons. The B-horizons are composed of deep clay loams,

and thereby retain a greater quantity of water before it is released.

Differences in the generation of SSF between soil horizons and storms within sites was also observed (Table 9). On the steepest site, Site 2, the A horizon produced more SSF than the litter layer or the B horizon for all storms. This was not the observed trend on Sites 1 and 3, however. More SSF was produced from the litter layer than the B horizon from small storms and storms preceded by dry conditions. The opposite was true for large storms and wet antecedent conditions, more flow was produced by the B horizon than the litter layer. For most conditions on Sites 1 and 3, little SSF was produced by the A horizon (Table 9). This is the opposite situation that exists on Site 2. Both Sites 1 and 3 have gentle slopes, 11 % and 7% respectively. As a result, the lateral flow component may be small. Water would tend to move vertically into the soil through the highly permeable A horizon instead of being directed laterally. An exception to this observation occurred on Site 3 during the largest storm of the study period (5/28). SSF from the A horizon was 109 liters. In this case, the saturated zone may have extended up into the A horizon.

Estimated SSF Contributing Area

If the watershed hillslopes were covered by an impervious surface, one would expect that the surface flow volume collected at the base of the hillslope would be

linearly related to precipitation depth. The area contributing to runoff would remain constant throughout the storm. In reality, the hillslopes are pervious, and water is partitioned between soil horizons, storage, soil matrix flow and soil macropore flow. Water may travel laterally through macropores over long or short distances. The actual length of the flow paths may vary greatly. The physical factors determining this partitioning are currently not well understood and were not an objective of this study.

Even though direct measurements of flow paths and soil physical conditions were not made during the study, it was felt that a rough estimate of the SSF contributing area was desirable to obtain. A conceptual minimum hillslope contributing length was calculated by assuming the total hillslope segment SSF (Table 8) was produced from a single impervious conceptual plane or hillslope. The minimum hillslope contributing length was calculated by dividing the SSF volume by the segment width (5.488) times the throughfall depth. This calculation assumes that the entire width of the hillslope segment contributes SSF. In reality, a smaller width having a much longer length upslope, such as preferential flow through a macropore network, may be contributing flow. Calculations of the conceptual minimum hillslope contributing length were carried out for the eight streamflow-producing storms (Table 11).

Shallow subsurface flow was considered to be a unique and separable flow generating processes. An estimate of the

area of the hillslope segment that contributed SSF was desired for use in the modeling effort. The hillslope segment area that contributed SSF was calculated by dividing the SSF volume by the throughfall depth. The hillslope segment contributing area was extrapolated to the entire watershed by multiplying the estimated hillslope segment contributing area times the watershed scale factor (Table 11).

Hillslope contributing lengths ranged from 0.3 m to 5.1 m for the largest storm in the study period (5/28). The total watershed contributing areas ranged from 222 m² to 11192 m². The maximum and minimum areas represent 0.3 to 14.5 percent of the total watershed area respectively. Since SSF volume was found to be an exponential function of precipitation, and the hillslope contributing length was calculated from SSF volume, it is not surprising to observe that hillslope contributing length is also an exponential function of precipitation.

It is recognized that the estimates of hillslope contributing area are crude. The estimates of contributing hillslope length could be improved if field measurements of the physical conditions within the hillslope soil body were available. Such measurements were beyond the scope of this study. Despite the lack of in-soil physical process information some interesting observations on hillslope SSF

TABLE 11
ESTIMATES OF THE HILLSLOPE CONTRIBUTING LENGTH
FOR EIGHT STREAMFLOW PRODUCING STORMS

Date	Throughfall (mm)	Conceptual Minimum Hillslope Contributing Length (m)	Estimated SSF Contributing Area (m ²)
2/15	31	0.3	658
2/24	13	0.1	222
3/1	49	0.8	1747
3/17	61	1.8	3954
5/25	34	0.5	1106
5/28	92	5.1	11192
5/31	11	0.7	1454
6/30	57	0.4	863

can be made. Hillslope contributing lengths ranged from 0.1 to 5.1 meters. The short contributing slope lengths indicate that shallow subsurface flow is generated in a small zone near the stream channels. Hillslopes in the near stream zone, formed by channel incision, tend to be much steeper than the surrounding land slopes. Steep slopes are more conducive to lateral subsurface flow than flat slopes. Therefore, rapid subsurface flow through highly permeable upper soil horizons on the steep slopes is likely to occur. Flow paths are short, as indicated by the short contributing slope lengths. The rapid response of hillslope SSF to precipitation, discussed in detail in the next section, is also indicative of short flow paths.

The physical characteristics of the soil on the hillslope study segments are also conducive to lateral SSF

with short flow paths. In research on sloping soils with horizons of varying permeabilities underlain by impervious materials, Ahuja (1986) found that the flow path length is a function of the relative hydraulic conductivities and depths of each soil layer and the soil slope. If the hydraulic conductivity of the surface layer is very high compared to the underlying layers, as was the case on the hillslope study sites, appreciable interflow can occur. Shallow interflow rates, flow paths and contributing area were found to increase with increased slope (Ahuja, 1986). However, if a highly permeable surface horizon was underlain by a horizon that had a hydraulic conductivity of only 1/100 of the surface horizon, percolation into the lower horizon occurred and reduced the quantity of interflow in the upper horizon (Ahuja, 1986). Permeabilities of the soils on the study sites vary with soil horizon. Permeabilities of the fine sandy loam A horizon(s) and clay loam upper B horizon(s) range from 15 - 51 mm/hr. The lower B horizons have a greater clay content and lower permeabilities, 5 - 15 mm/hr. Given these soil physical conditions, flow paths of SSF through the upper horizons should be short except where slopes are very steep.

SSF Hydrographs, Rates and Timing

Charts from the nine SSF collection tanks were reduced to obtain the date, time and accumulated volume of SSF (Appendix A). The continuous traces of accumulated volumes over time were broken into increments of equal discharge. From the data file of discharge, date and time, hydrographs of SSF were plotted. Data from only three storms, representing the largest storm of the study period (5/28), the second largest storm (3/17), and one storm preceded by dry conditions (6/30) have been plotted for discussion here (Figures 15 through 23). The small winter storms produced very little flow. Chart clock operation and synchronization between the nine clocks and the chart clock at the watershed outlet was a problem in the winter storms. Some clock operation and synchronization problems were also encountered in later storms. As a result the comparative times between recorders is questionable. However, the time changes within storms was felt to be accurate. Therefore, the calculated discharge rates are considered to be true. The three storms chosen for simultaneous plotting of SSF, precipitation and streamflow were also chosen because they represent the three storms with the fewest timing problems.

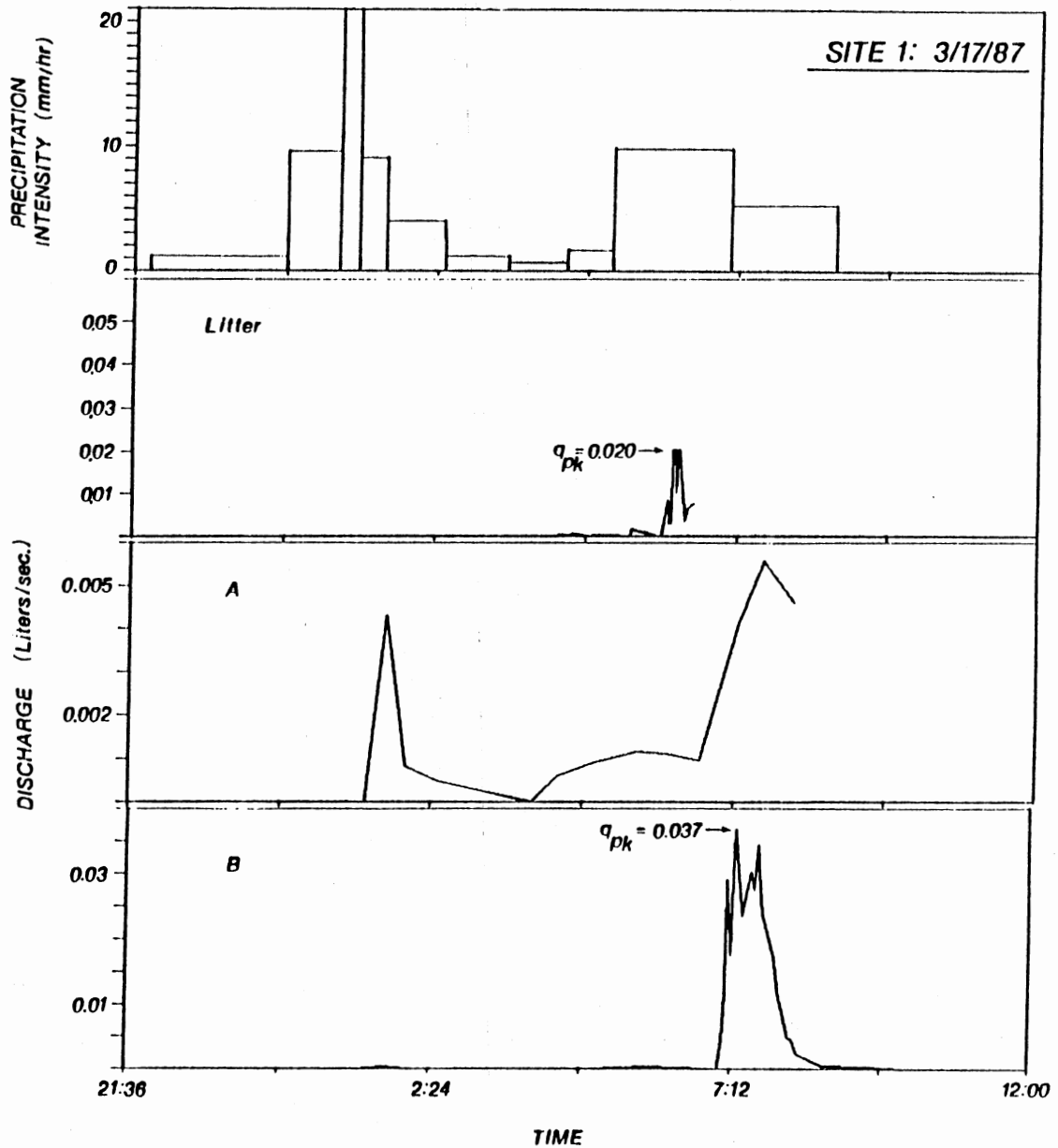


Figure 15. Shallow Subsurface Flow Hydrographs for Site 1, the Storm of 3/17/87

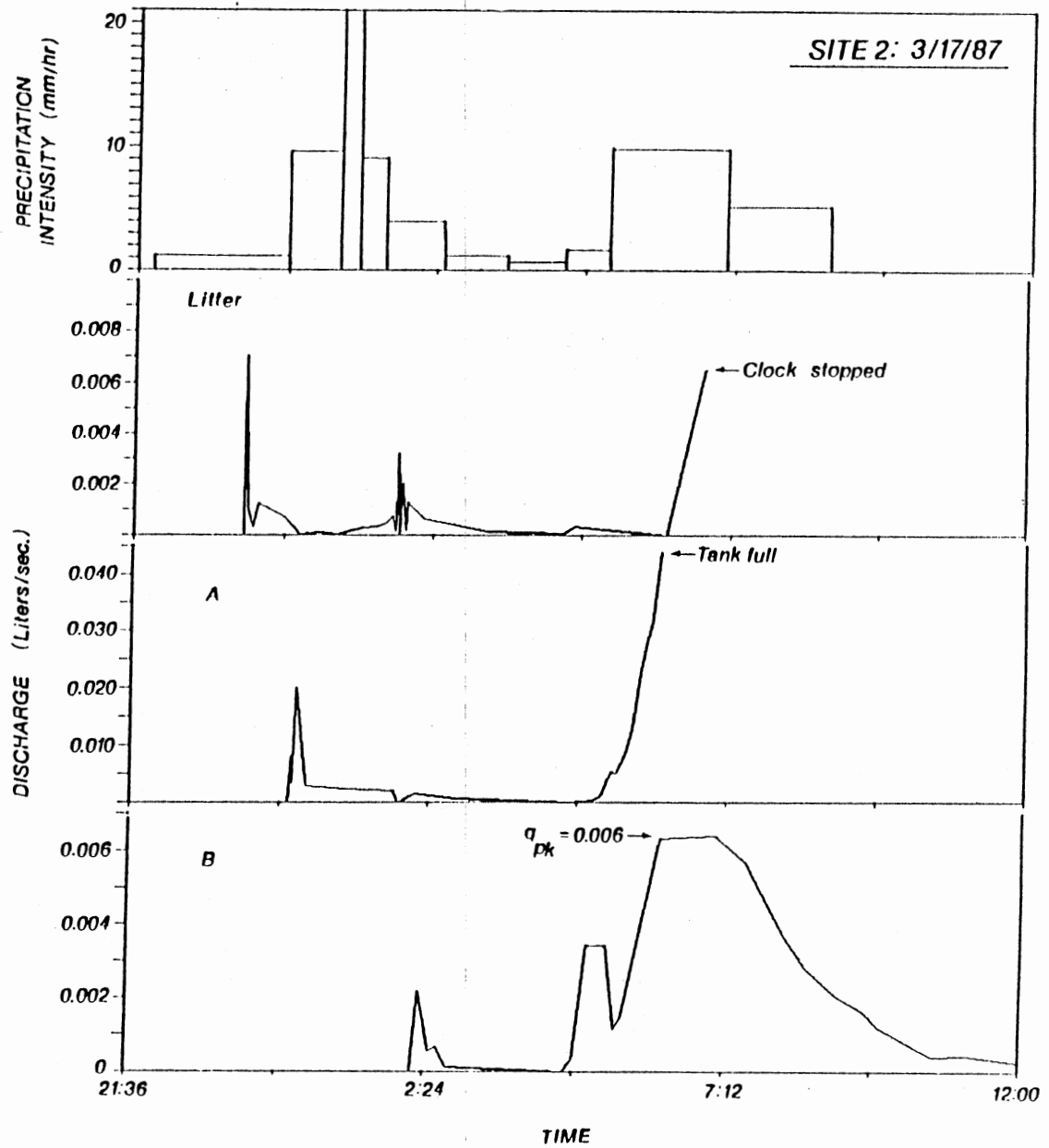


Figure 16. Shallow Subsurface Flow Hydrographs for Site 2, the Storm of 3/17/87

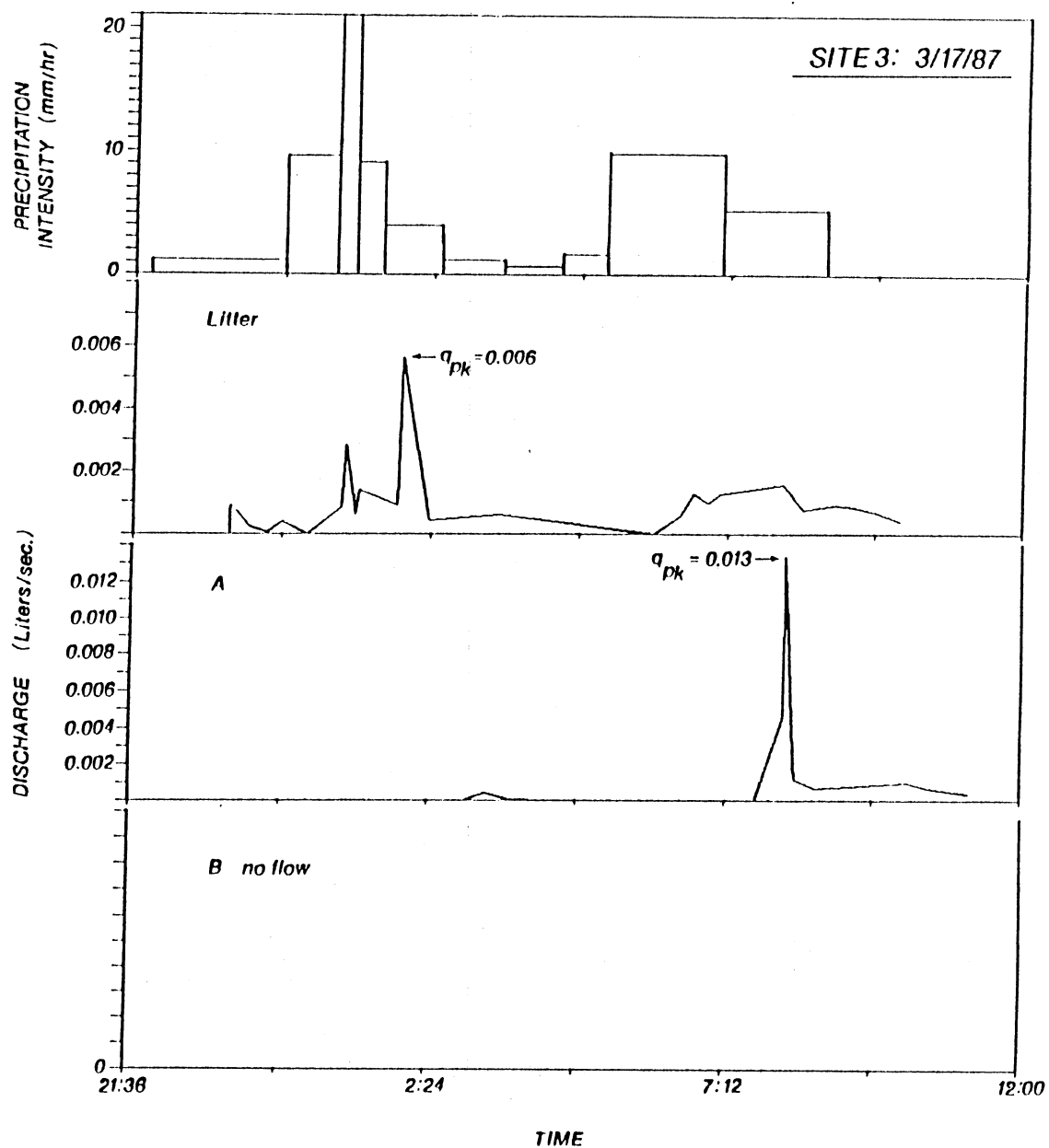


Figure 17. Shallow Subsurface Flow Hydrographs for Site 3, the Storm of 3/17/87

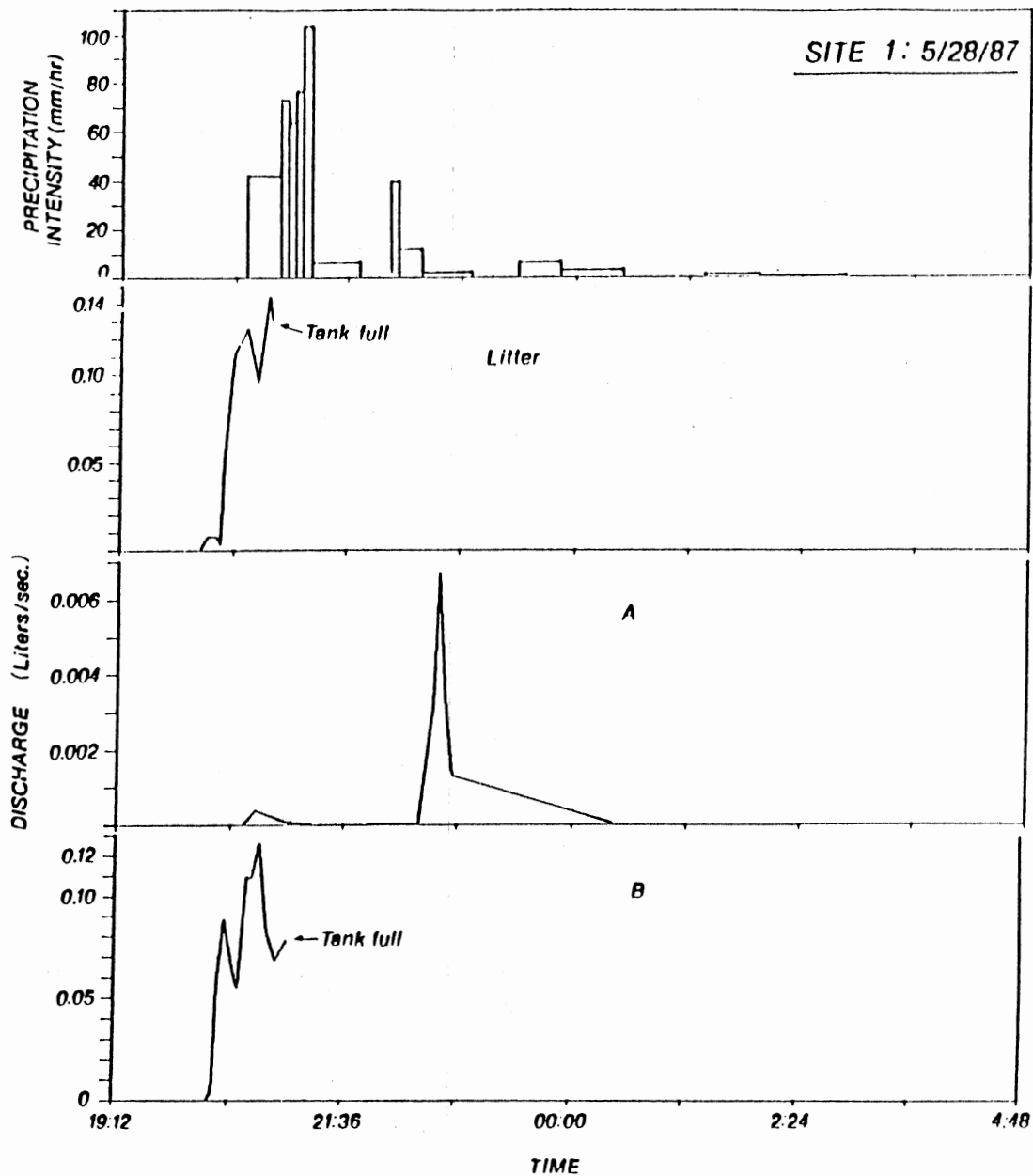


Figure 18. Shallow Subsurface Flow Hydrographs for Site 1, the Storm of 5/28/873

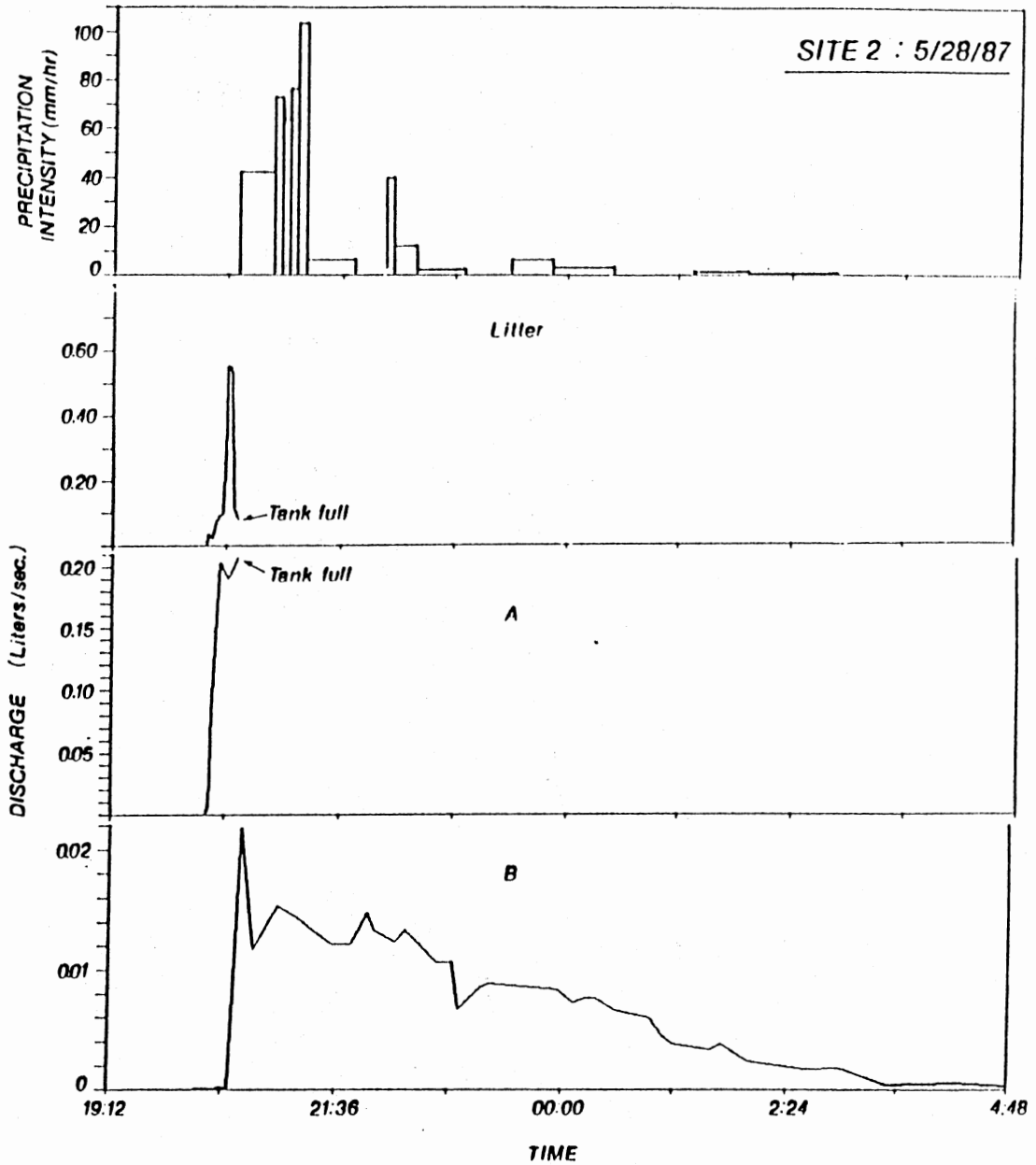


Figure 19. Shallow Subsurface Flow Hydrographs for Site 2, the Storm of 5/28/87

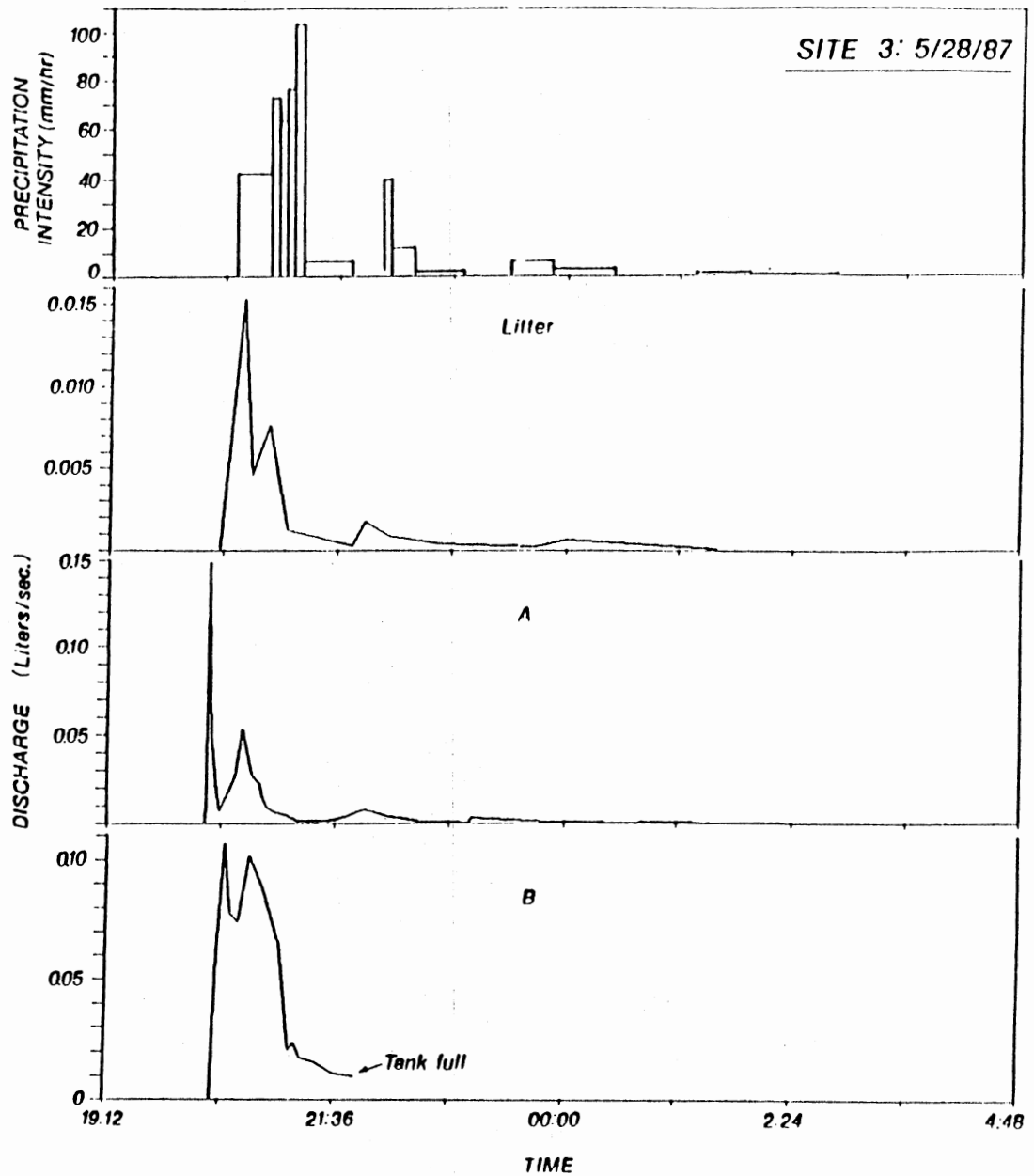


Figure 20. Shallow Subsurface Flow Hydrographs for Site 3, the Storm of 5/28/87

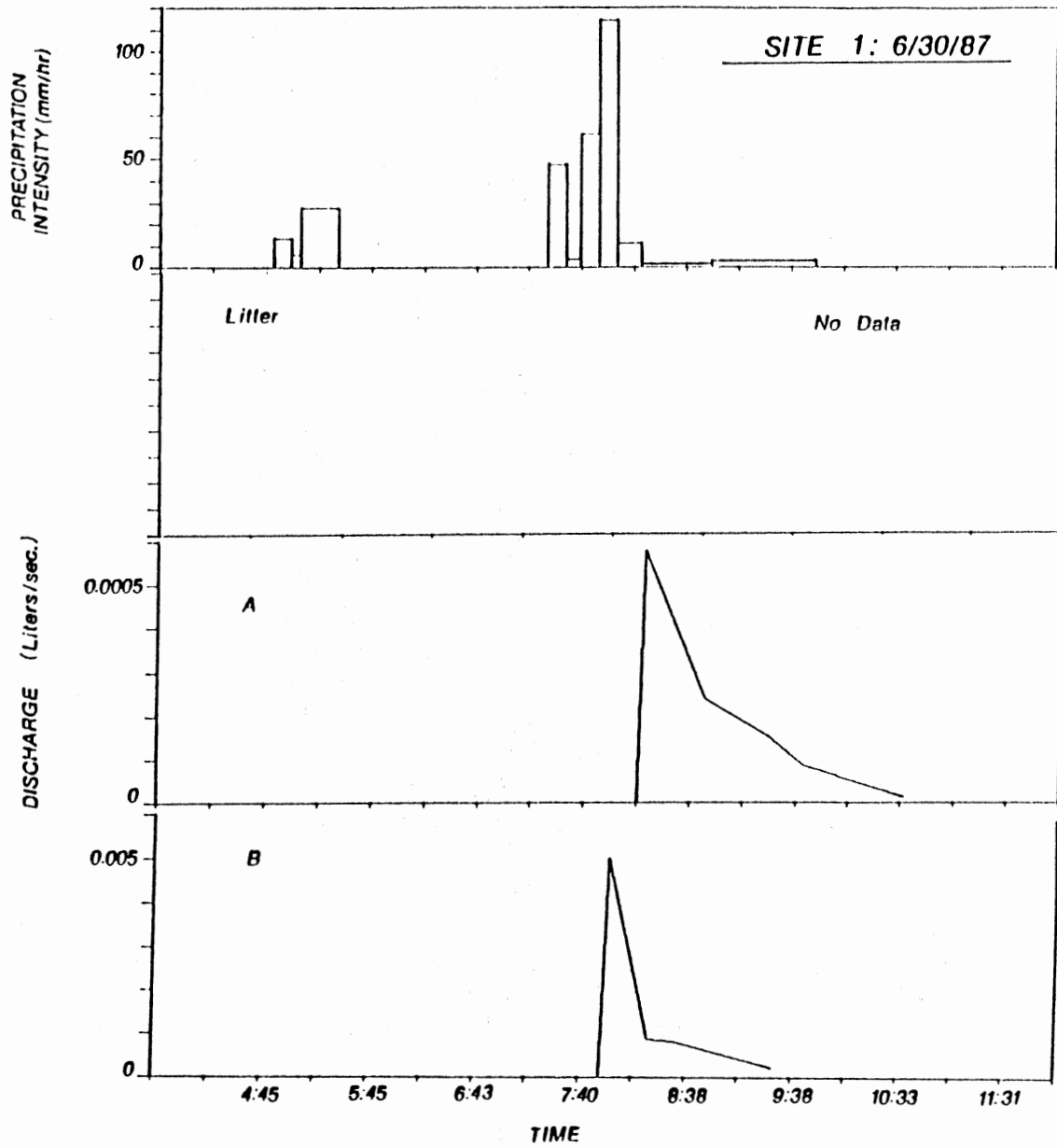


Figure 21. Shallow Subsurface Flow Hydrographs for Site 1, the Storm of 6/30/87

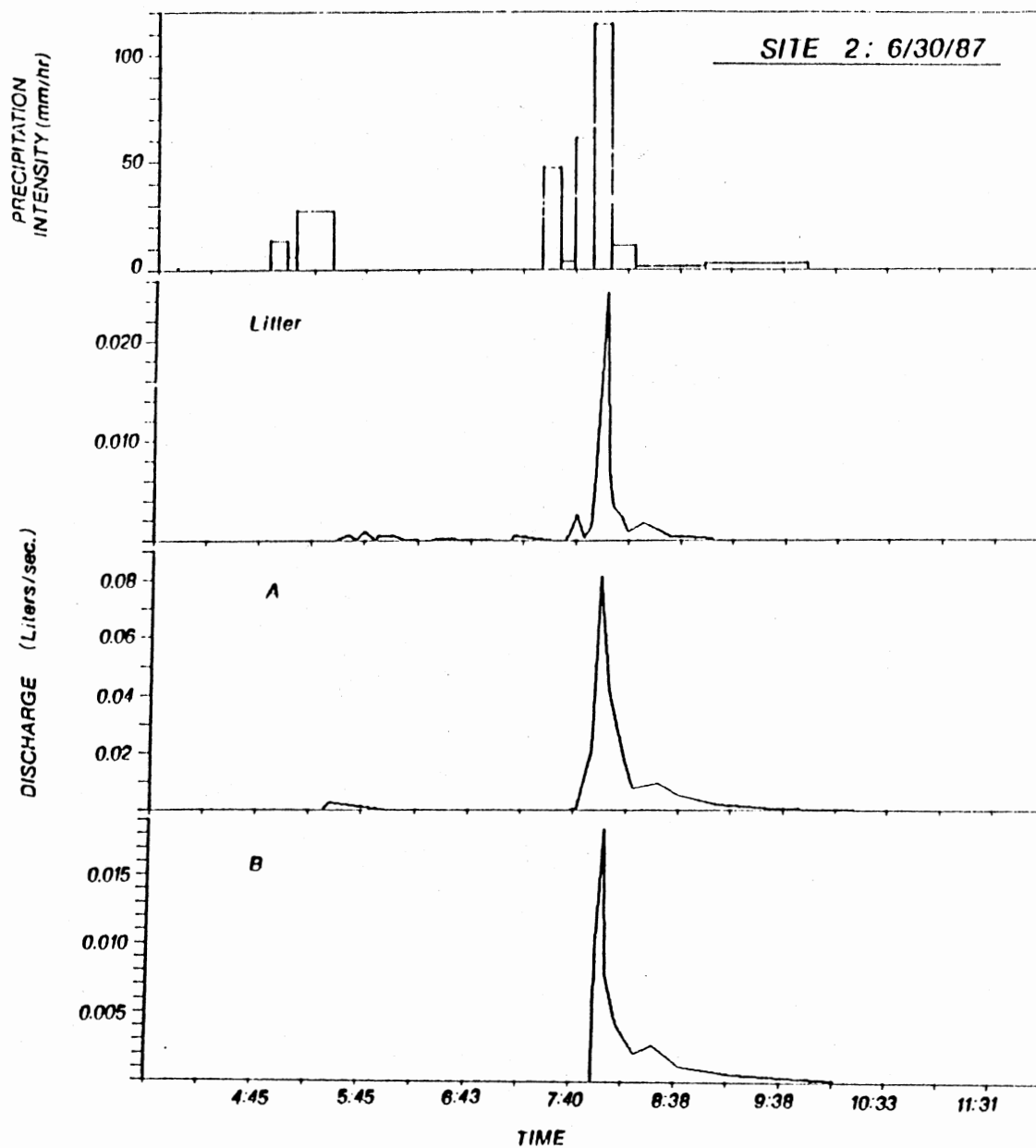


Figure 22. Shallow Subsurface Flow Hydrographs for Site 2, the Storm of 6/30/87

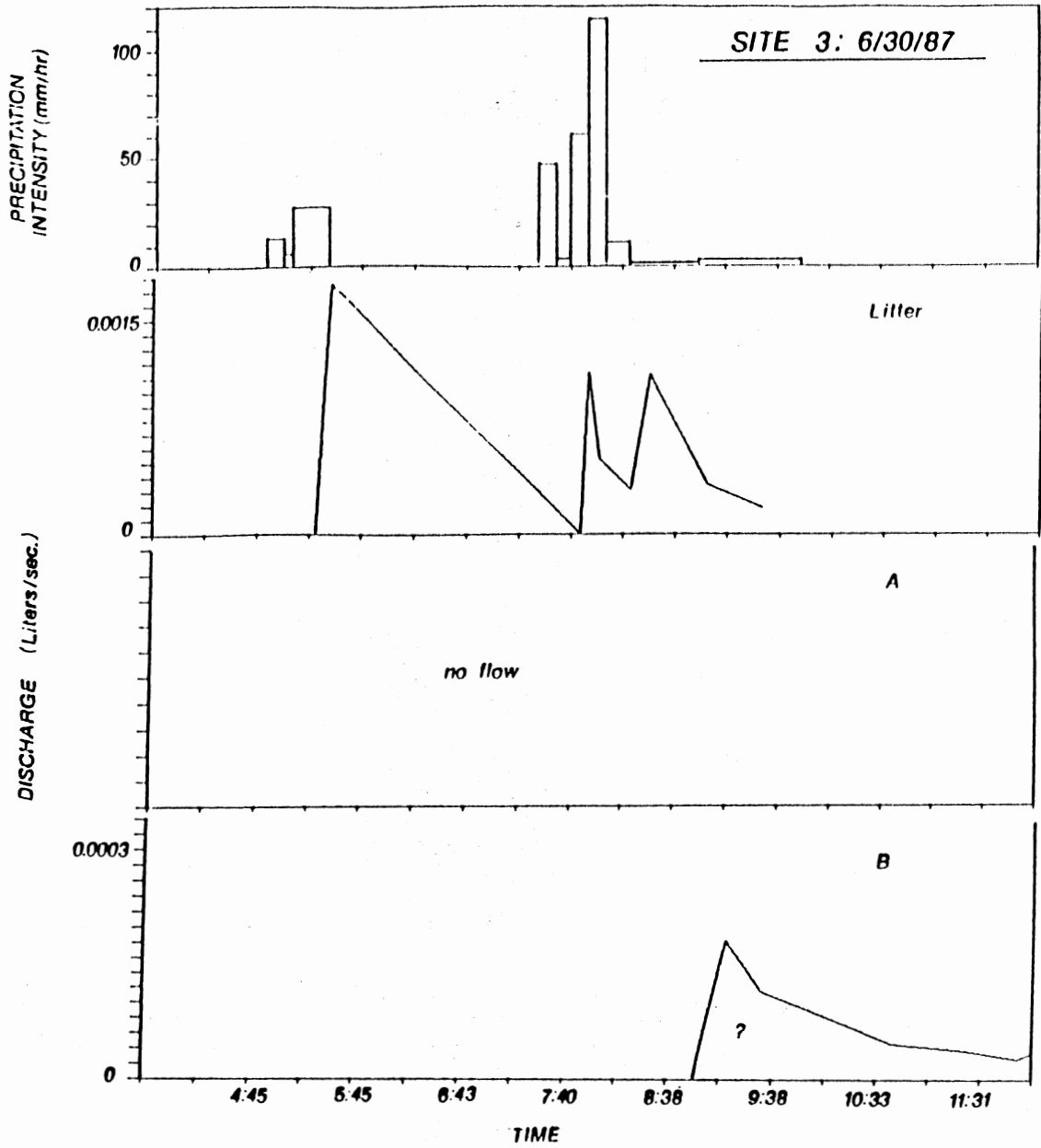


Figure 23. Shallow Subsurface Flow Hydrographs for Site 3, the Storm of 6/30/87

Peak SSF Rates

Peak discharge rates of SSF ranged from <0.001 to 0.711 l/s (Table 12). The peak SSF discharge rates varied between storms and between sites and soil horizons within storms. The largest storm of the study period (5/28) generated the greatest peak discharge rates. The second largest storm (3/17) generated the second largest set of peak discharge rates. Storms with intense precipitation rates (5/28, 3/17, 5/31 and 6/30) also produced higher SSF peak discharge rates. Within storms, site 2, the steepest site, generally generated the greatest peak SSF discharge rates. On site 2, the litter and A horizons produced the largest peaks. On sites 1 and 3, the A horizon generated very low peak SSF discharge rates (except Site 3, 5/28). During the largest storm of the study (5/28) the peak SSF discharge rate from the B horizons of sites 1 and 3 were relatively large, 0.125 and 0.106 l/s respectively. The large quantity of precipitation (102 mm) deposited during the storm probably produced saturated flow in the B horizons. The result was high rates of discharge through the B horizons. The existence of a perched water table in the B horizon was confirmed by field observation of water levels in the soil lysimeter soil pits. The measured peak discharge rates of SSF may seem relatively small. However, the hillslope study segments represented only $1/400$ of the streambank length on the watershed. For comparison, the total and mean peak SSF discharge rates of horizons and sites within individual storms were calculated,

TABLE 12
 MAXIMUM SHALLOW SUBSURFACE FLOW RATES
 IN LITERS PER SECOND

Storm Date	Source	Site 1	Site 2	Site 3
2/15	L	0.001	0.006	0.006
	A	*	0.013	*
	B	*	*	0.000
2/24	L	0	0.002	0.001
	A	0	*	0
	B	0	0	0
3/1	L	0.009	0.019	0.008
	A	*	nd	0.002
	B	*	0.008	0.001
3/17	L	0.020	0.007	0.006
	A	0.001	0.039	0.013
	B	0.037	0.006	0
5/25	L	0.006	0.010	nd
	A	0.001	0.020	0
	B	0.003	*	0
5/28	L	0.143	0.532	0.015
	A	0.007	0.208	0.149
	B	0.125	0.022	0.106
5/31	L	0.006	0.016	0.007
	A	0	0.029	0
	B	*	0.005	0.001
6/30	L	nd	0.024	0.002
	A	0.001	0.081	0
	B	0.005	0.018	*

multiplied by the watershed scale factor, and compared to the peak streamflow discharge rates (Table 13).

TABLE 13
COMPARISON OF SSF PEAK RATES TO
STREAMFLOW PEAK RATES IN L/S

Storm Date	Total SSF Peak Flow	Total SSF * WSF	Mean SSF Peak Flow	Mean SSF * WSF	Peak Stream-flow
2/15	0.034	14	0.011	5	11
2/24	0.003	1	0.003	1	3
3/1	0.047	19	0.016	6	29
3/17	0.129	52	0.043	17	68
5/25	0.040	16	0.013	5	16
5/28	0.690	276	0.495	198	393
5/31	0.064	26	0.021	8	12
6/30	0.131	52	0.044	17	18

On the watershed scale, the SSF peak discharge rates appear to form a significant part of the peak stream discharge. This comparison ignores storage effects and assumes that all of the SSF is immediately translated to the outlet. In pry reality, SSF peaks are probably attenuated by channel storage or differences in the timing of release.

Timing of Flow

Two timing effects are significant to the generation of streamflow, how quickly the hillslope SSF responds to precipitation and when during a storm the SSF is produced. Precipitation and SSF were plotted by site on the same time scale, for three storms (Figures 15 through 23). In all cases, the response of SSF to precipitation was rapid. Fluctuations in SSF coincided closely with fluctuations in precipitation intensity.

The litter layers appeared to respond the quickest to precipitation and changes in precipitation intensity. Whipkey (1965), Weyman (1970) and Dunne and Black (1970) found that the response to precipitation was slower and attenuated with increasing depth in the soil. Similar trends were observed in this study. However, for some events, clock synchronization problems made this type of comparison questionable.

The clocks were synchronized and running on time on Site 2 during the storm of 6/30 (Figure 22). The litter layer responded rapidly to changes in precipitation intensity. The A horizon responded very little to the first burst of rainfall, but responded rapidly to the second burst. The B horizon responded only to the second burst of rainfall. The B horizon response was rapid, but occurred slightly after the A horizon response. The storm was preceded by a long period of no precipitation and high temperatures. Therefore the antecedent soil moisture was low. The time lag of response

may have been due to the filling the soil moisture deficit that must be filled before SSF can occur. Time lags between horizons existed, but were less pronounced during the storm of 5/28 (Sites 2 and 3). The storm consisted of a small burst of precipitation (26 mm) early in the day (0400 hrs) followed by an intense second burst (76 mm) later in the day (2000 hrs.). The plotted hydrographs (Figures 18,19 and 20) are the result of the second burst of precipitation. In this case, the antecedent soil moisture was high. The observed time lags may also have been due to the longer flow paths associated with the deeper soil horizons.

The hillslope SSF response to precipitation was not attenuated greatly by depth. Once the initial moisture deficit was satisfied, SSF from all horizons increased rapidly (Figures 15-23). This response indicates that either the soil horizons are highly permeable, flow paths are very short, a rapid mode of transport such as piping through macropores, or some combination of all of the factors listed previously is responsible for the rapid transmission of water through the soil. This rapid transmission probably took place in unsaturated conditions. Even during the largest storm (5/28), it is doubtful that the shallow soil horizons ever reached saturation early in the storm when the flow occurred. No measurements of the piezometric surface were taken, so this assumption can not be confirmed. Some shallow temporary saturated zones may have built up during intense bursts of rainfall.

The recession of SSF in response to a decrease or end of precipitation was noticeably different between soil horizons (Figures 15-23). Litter layer flows declined very rapidly following the end of precipitation. Flows from the A horizon also decreased rapidly, but more slowly than litter layer flows. SSF from the B Horizon exhibited a rapid decline following the end of precipitation, followed by a slower recession. This trend was more pronounced during the two largest storms of the study period (3/17 and 5/28) when the soil profile was more thoroughly wetted. Hydrographs of SSF from Site 1, B Horizon, the storm of 3/17, from Site 3, B Horizon, the storm of 5/28, and from Site 2, B Horizon, the storm of 6/30, show the trend of rapid drainage followed by a slower recession period (Figures 24, 25, and 26). This dual drainage pattern has been observed in lab studies of undisturbed, forest soil columns (Kneale, 1985) and in the field on undisturbed forest soils using tension infiltrometry (Watson and Luxmoore, 1986).

Semi-log plots of the natural log of SSF discharge vs. time were made for Site 1, B Horizon, the storm of 3/17 and for Site 2, B Horizon, the storm of 6/30 (Figures 27 and 28). Data from the storm of 5/28 was not used because continuing precipitation affected the shape of the recession curve. The semi-log plots further exemplify the change in drainage rate during the recession. Recession constants were estimated for the two distinct slopes in each recession curve using proce-

SSF Site 1 B Horizon

Storm of 3/17

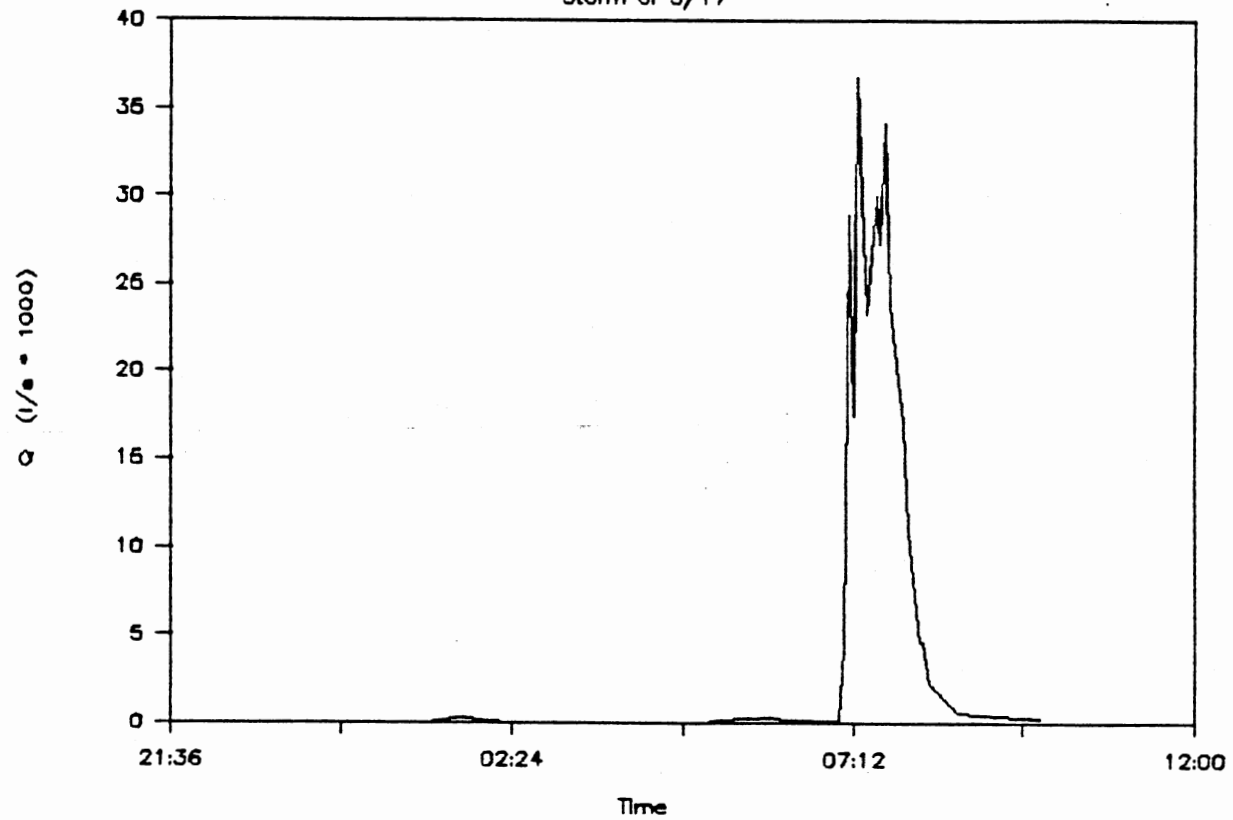


Figure 24. Shallow Subsurface Flow Hydrograph from Site 1, B Horizon, the Storm of 3/17/87

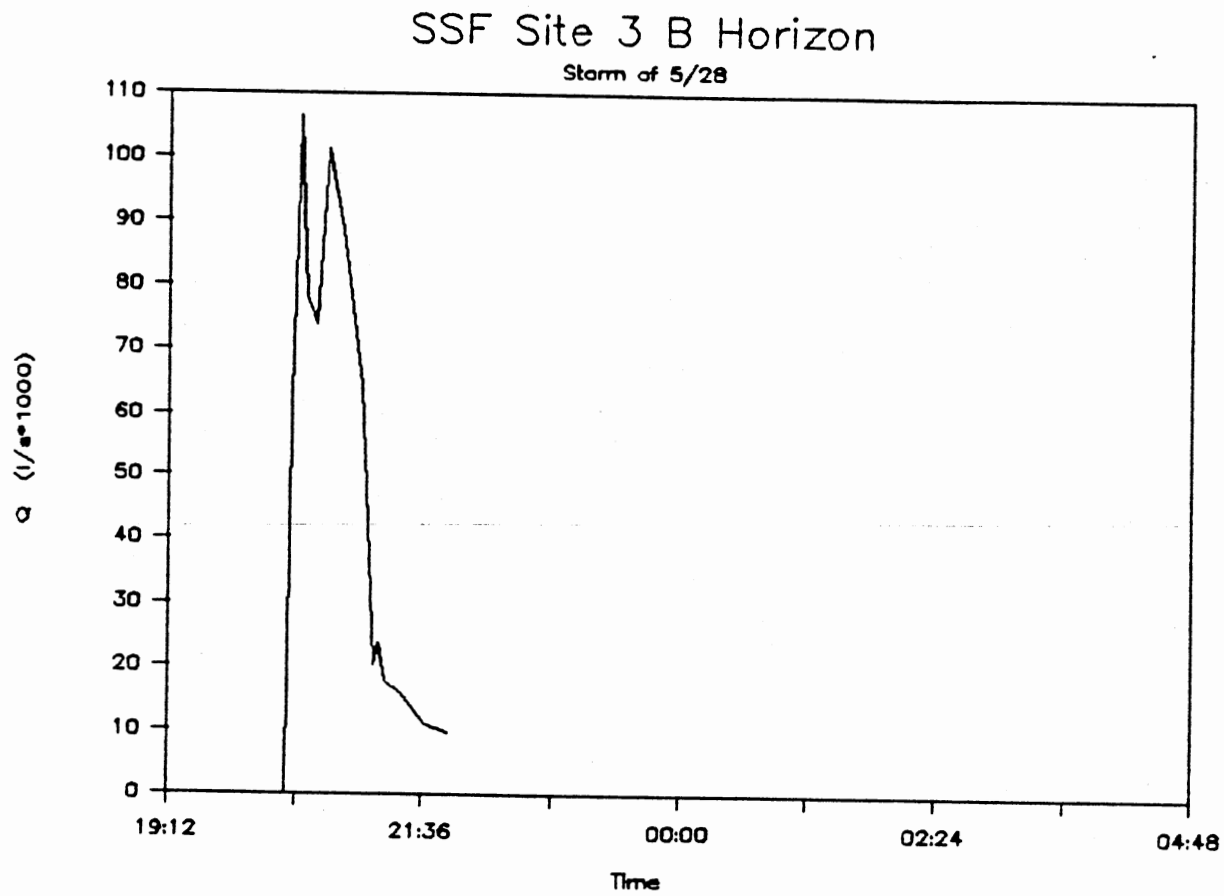


Figure 25. Shallow Subsurface Flow Hydrograph from Site 3, B Horizon, the Storm of 5/28/87

SSF Site 2 B Horizon

Storm of 6/30

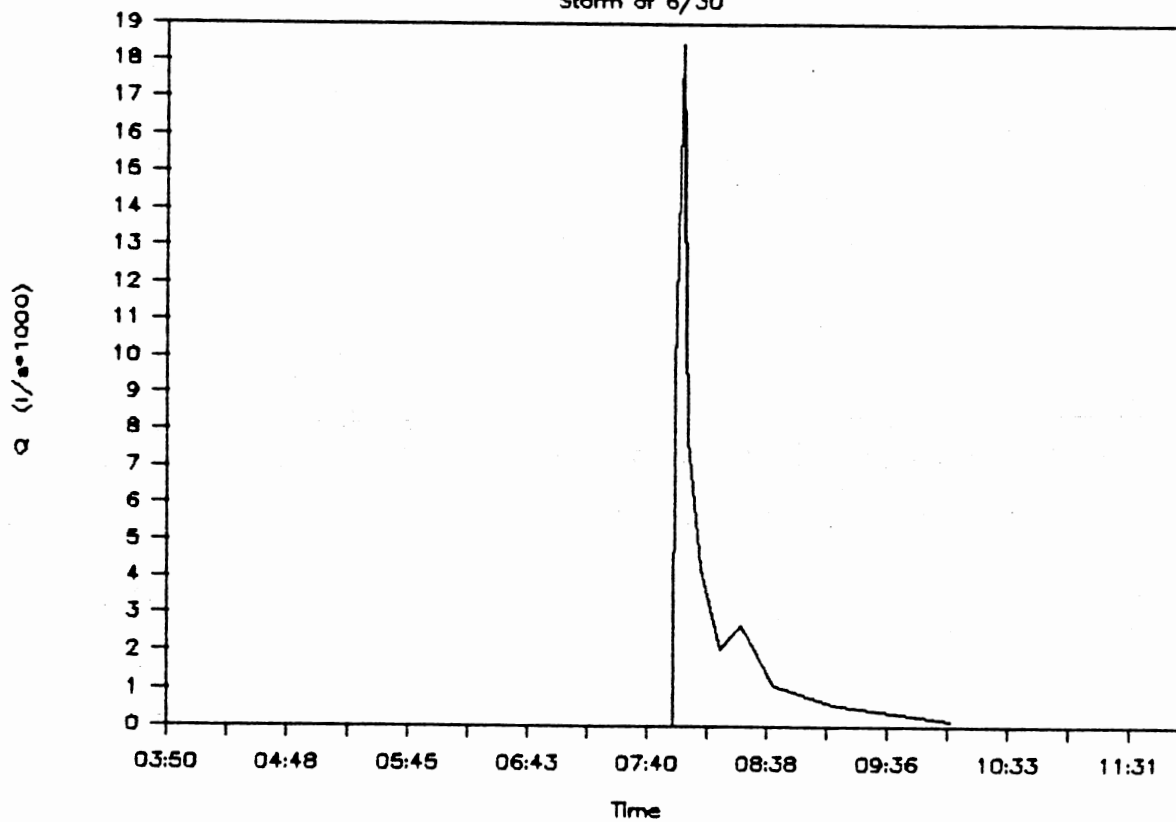


Figure 26. Shallow Subsurface Flow Hydrograph from Site 2, B Horizon, the Storm of 6/30/87

dures described for calculating streamflow recession constants (Linsley, Kohler, and Paulhus, 1975). The absolute values of the recession constants may be doubtful due to a lack of better data from more storms. However, it is interesting to note that in both cases, there is a change of an order of magnitude or more between the rapid and slow recession. This result indicates that a dual mechanism of drainage, rapid drainage through large pores and slow drainage through smaller pores, is in operation on the hillslope study segments.

Shallow subsurface flow responded rapidly to precipitation. As a result, the majority of subsurface flow occurred early in the storm. Precipitation, streamflow, and the combined SSF response from the three hillslope segments (the sum of the individual hydrographs) were plotted concurrently for the storms of 3/17 and 6/30 (Figures 29 and 30). The total response was multiplied by the watershed scale factor so the two hydrographs could be viewed at the same scale. For both storms, the precipitation ended before peak streamflow occurred. The majority of the SSF also occurred before peak flow.

SSF Volume Contributions to Streamflow

The total storm SSF from the three hillslope study segments for the eight streamflow producing storms were compared to streamflow volumes at the watershed outlet.

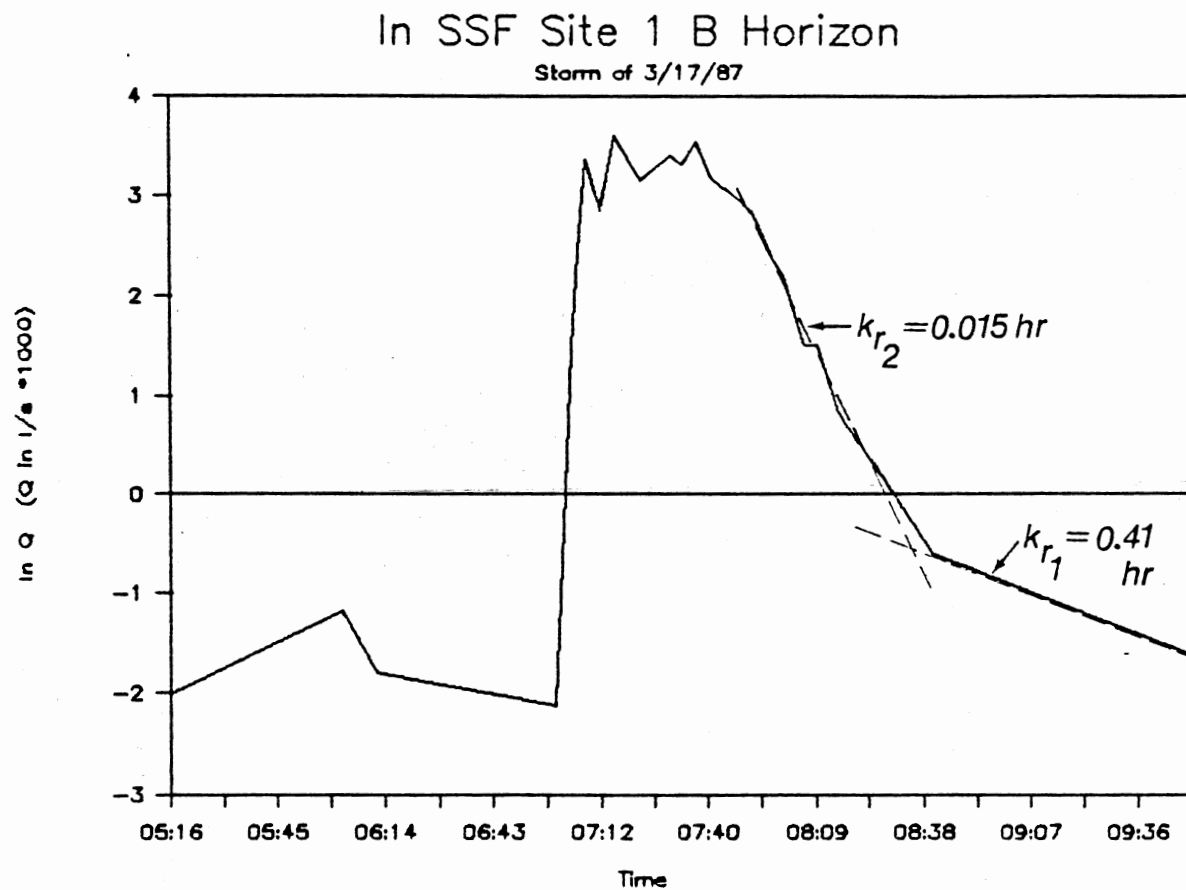


Figure 27. Semi-Log Plot of a Shallow Subsurface Flow Hydrograph, Site 1, B Horizon, 3/17/87

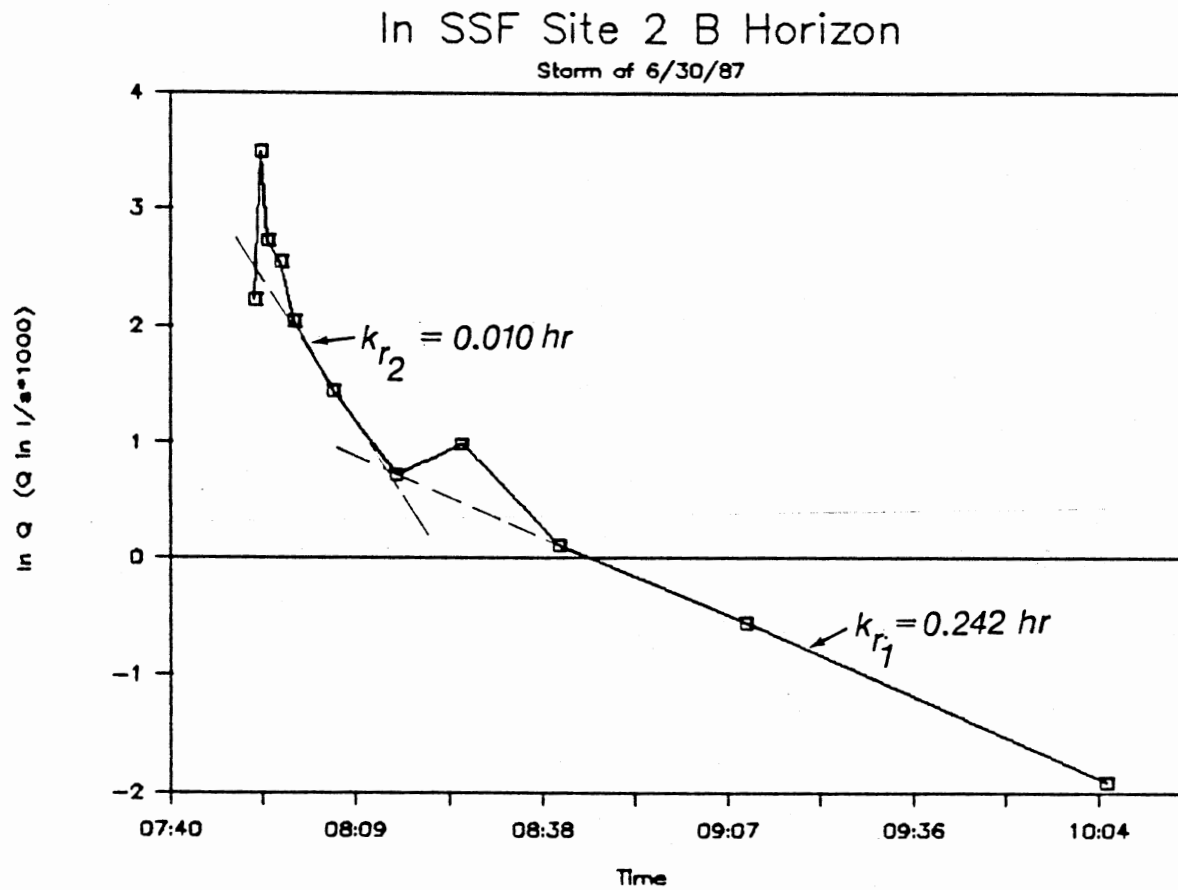


Figure 28. Semi-Log Plot of a Shallow Subsurface Flow Hydrograph, Site 2, B Horizon, 6/30/87

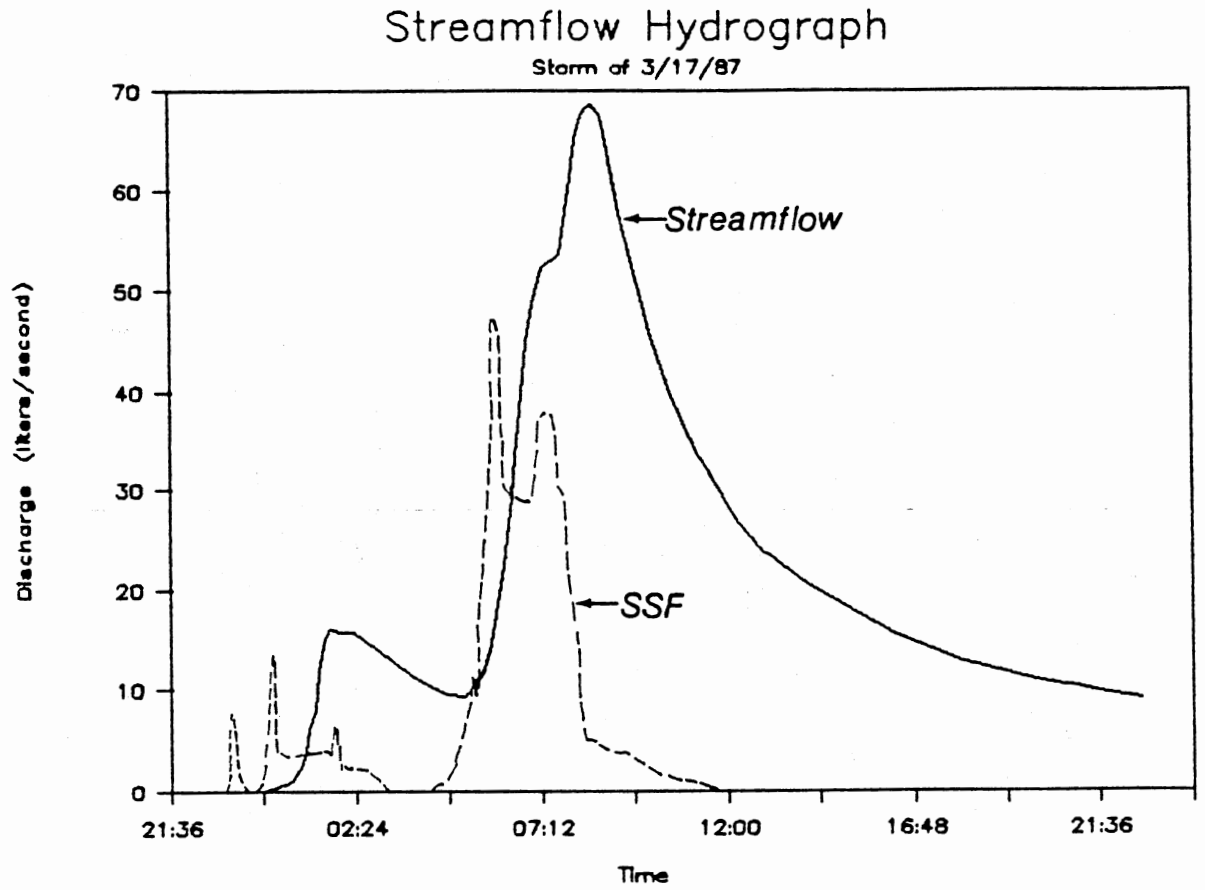


Figure 29. Plot of the Total SSF and Streamflow Hydrographs for the Storm of 3/17/87

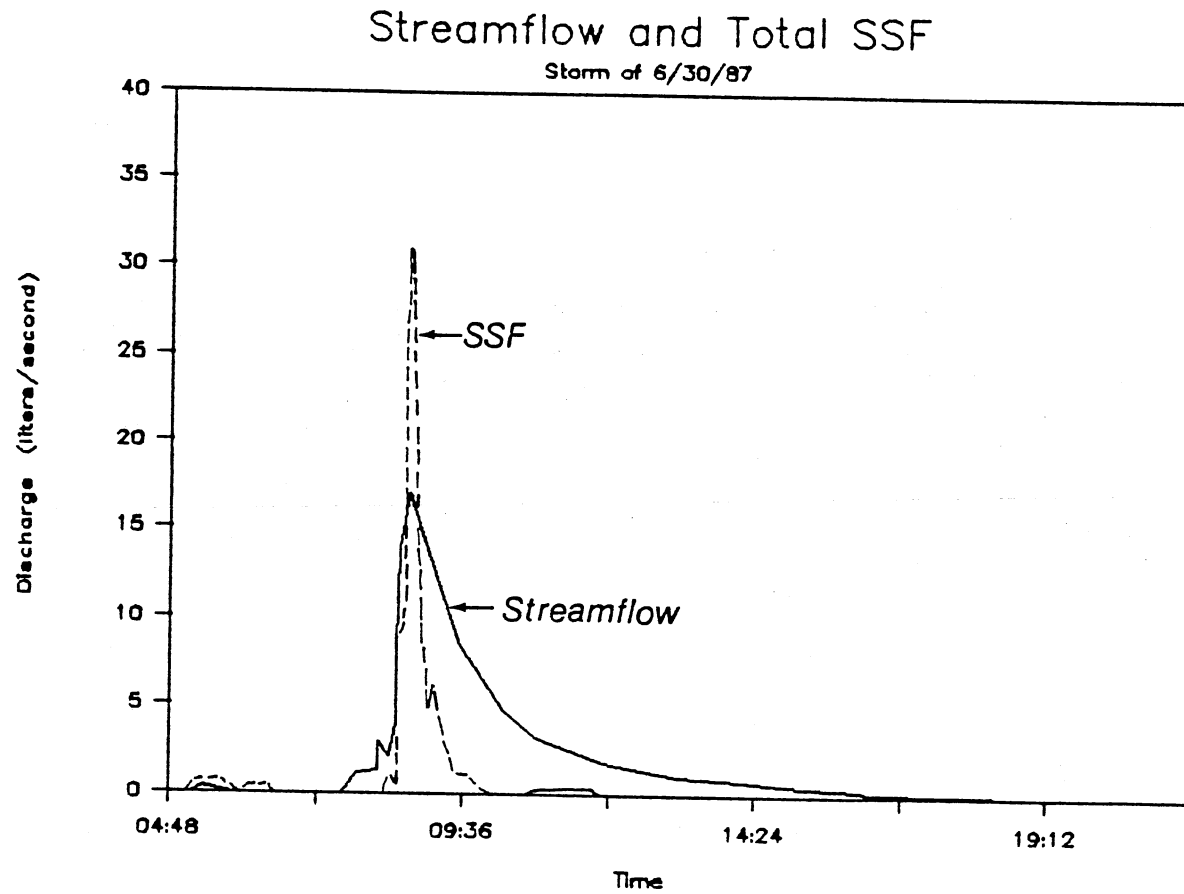


Figure 30. Plot of the Total SSF and Streamflow Hydrographs for the Storm of 6/30/87

The total storm SSF was multiplied by the watershed scale factor for the comparisons (Table 14). Streamflow volume was broken into the volume before and the volume after peak discharge. The percent of streamflow generated by SSF ranged from 1 to 48 percent, depending on storm size and antecedent conditions. The percent of streamflow generated by SSF before peak discharge ranged from 5 to 318 percent. Percentages greater than 100 percent are probably due to the assumptions used in this comparison. Channel storage was not considered, the SSF from the sites was assumed to translate to the outlet before peak flow. In some cases precipitation and additional SSF occurred following peak flow. The comparisons may be slightly erroneous. However, the point of comparing SSF to streamflow volume before peak discharge was simply to show that SSF may be responsible for generating a large percentage of streamflow early in an event, and not to account accurately for all of the flow. Trends between the percentage of streamflow volume generated by SSF and the volume of SSF do not seem to exist. The largest storm of the study period (5/28) produced 2568 liters of SSF and generated 23 percent of the streamflow volume. The storm of 5/25 also generated 23 percent of the streamflow volume, but produced only 95 liters of SSF. The storm of 6/30 produced only 123 liters of SSF, but generated 48 percent of the total streamflow volume. The storm of 6/30 was preceded by a long dry period. Streamflow rose and fell rapidly without a prolonged recession. The storm of 5/28 was large enough to

TABLE 14
 COMPARISON OF SSF VOLUMES AND STREAMFLOW VOLUMES
 FOR EIGHT STREAMFLOW PRODUCING STORMS

Storm Date	Total SSF x WSF (1)	Streamflow Volumes			% of Streamflow Generated by SSF	
		Before Peak (1)	After Peak (1)	Total (1)	Before Peak	Total
2/11	5640	10270	57020	67290	55	8
2/16	20400	56000	224000	280000	36	7
2/24	2880	57440	200000	257440	5	1
3/1	85600	656300	2339000	2995300	13	3
3/17	241600	666400	2050000	2716400	36	9
5/25	38000	16590	151400	167990	229	23
5/28	1027200	597700	3814000	4411700	172	23
5/31	16000	16340	396900	413240	98	4
6/30	49200	15450	87250	102700	318	48

more thoroughly wet the entire depth of the soil profile. A considerable amount of the streamflow volume was generated during the recession period, long after SSF subsided. More than likely, as soil moisture conditions change during storms events, the streamflow generating processes also change. Seepage from deeper soil profiles becomes more important to streamflow generation as the soil becomes wetter.

Chemical Processes

As previously mentioned, over 1200 water samples were collected and analyzed for 8 chemical constituents and properties. All of the raw data is presented in Appendix B on a storm by storm basis. Various analyses were performed using the entire data set. Only those topics important to the stated objectives are discussed in detail here.

Chemical Transformations

Source Means

The mean concentrations of chemical constituents or properties were calculated for each source monitored, bulk precipitation, throughfall, litter layer, A Horizon, B Horizon and the three subsurface collection troughs intercepting flow from the litter layer and the A and B horizons (Tables 15 and 16). The bulk precipitation concentrations were weighted against precipitation depth. Throughfall concentrations were weighted against throughfall.

TABLE 15
 SOURCE MEAN CHEMISTRY SUMMARY
 PRECIPITATION AND THROUGHFALL

	pH	H+ (mg/l)	Cond. (umhos)	NO3-N (mg/l)	DOC (mg/l)	Ca++ (mg/l)	Mg++ (mg/l)	K+ (mg/l)	Na+ (mg/l)
Bulk Precipitation All Data									
mean	4.63	0.023677	18.6	0.3	2.5	0.31	0.03	0.08	0.15
s		0.0267	22.8	0.22	3.2	0.34	0.04	0.11	0.14
Bulk Precipitation - Dormant Season									
mean	4.64	0.02	15.1	0.34	0.8	0.33	0.02	0.04	0.11
s		0.02732	18	0.21	2	0.34	0.03	0.03	0.09
Bulk Precipitation - Growing Season									
mean	4.56	0.027364	22.6	0.25	2.8	0.16	0.04	0.12	0.18
s		0.020755	0.16	0.16	3.4	0.23	0.04	0.13	0.17
Throughfall - All Data									
mean	4.63	0.023529	18.9	0.28	55	0.65	0.13	2.89	0.2
s		0.026046	15.1	0.3	94	0.56	0.13	31.6	0.2
Throughfall - Dormant Season									
mean	4.62	0.023988	17.6	0.39	17	0.69	0.09	0.4	0.17
s		0.026456	15.4	0.38	20	0.56	0.09	0.47	0.14
Throughfall - Growing Season									
mean	4.61	0.024542	19.5	0.17	88	0.48	0.14	0.89	0.23
s		0.022894	13.5	0.16	116	0.49	0.15	1.31	0.26

TABLE 16
 SOURCE MEAN CHEMISTRY SUMMARY
 SOIL AND SUBSURFACE FLOW COLLECTORS

	pH	H+ (mg/l)	Cond. (umhos)	NO3-N (mg/l)	DOC (mg/l)	Ca++ (mg/l)	Mg++ (mg/l)	K+ (mg/l)	Na+ (mg/l)
Litter Layer									
mean	5.73	0.001851	32.7	0.22	314	2.78	1	3.13	0.35
s		0.00149	13.5	0.21	185	1.7	0.58	2.51	0.2
A Horizon									
mean	5.39	0.004056	27.7	0.24	99	1.39	0.91	1.24	0.87
s		0.0030902	7.3	0.37	49	0.65	0.29	0.39	0.5
B Horizon									
mean	5.48	0.003311	28	0.09	50	0.86	0.92	1	1.43
s		0.002587	9	0.18	44	0.44	0.33	0.66	1.9
Subsurface Flow Collectors									
Litter Layer									
mean	5.75	0.001792	49.1	0.25	315	3.4	0.88	3.68	1.05
s		0.001554	35.7	0.36	125	1.45	0.21	2.97	1.29
A Horizon									
mean	5.67	0.002154	34.2	0.14	152	2.4	0.65	2.37	0.56
s		0.00185	25.9	0.14	78	1.45	0.34	2.5	0.27
B Horizon									
mean	5.73	0.001878	30	0.12	188	1.94	0.83	2.29	0.68
s		0.0001544	5.2	0.14	47	0.52	0.13	1.78	0.29

depth. The degree of transformation of the chemical composition of water as it moves through the compartments of the watershed ecosystem varies between constituents.

One of the objectives of this research is to see whether or not significant differences in source chemistry exist. The relationships between sources will be used later in the modeling effort. Differences in the average concentrations of chemical constituents between precipitation, throughfall and the soil horizons are evident (Tables 15 and 16), however, the variations about the estimated mean values as expressed by the standard deviations are very large. In many cases, the standard deviation from the mean was as large as, or larger than, the mean itself. The source means were obtained by averaging each of the individual collector concentrations for all storms throughout the study period. The data suggest that the source concentrations may not be normally distributed. The wide variations of concentrations about the estimated means are probably due to chemical differences between storms and spatial variation of precipitation, throughfall, soil chemical processes, and laboratory error. An estimate of the precision of the laboratory analysis was made for each constituent. The estimate is equal to the standard deviation of the differences between random pairs of samples and duplicate samples that were analyzed. The estimates of the laboratory precision for NO_3^- -N, Ca^{++} , Mg^{++} , K^+ , Na^+ and DOC are 0.01, 0.10, 0.04, 0.10, 0.05, and 2.3 mg/l. As can be seen, the

laboratory error is much smaller than the standard deviations of the overall source means for all constituents. Therefore, laboratory error is negligible compared to the other sources of variation.

An attempt to remove the effect of spatial variation was made by calculating mean chemical concentrations for individual collectors within sources. Nitrate-Nitrogen concentrations were the most variable of all of the constituents. Mean study period concentrations of $\text{NO}_3\text{-N}$ were calculated for each of the soil solution collectors in the Litter, A and B horizons. Due to the large volume of data, only the results of the A and B horizons are shown (Tables 17 and 18). By observation, it can be seen there are considerable differences in the mean $\text{NO}_3\text{-N}$ concentrations between soil pits. However, the variation about the estimated collector mean is generally much lower than variation about the overall source mean, now that the effect of spatial variability across the watershed has been eliminated. Similar results were observed for the litter layer collectors. Mean concentrations between individual throughfall collectors were also considerably different. Variation about the estimated throughfall collector means was lower than the variation about the overall throughfall means.

One way to observe the degree of transformation between sources is to calculate the ratio of the change in concentration between sources. The ratios of change between sources for this study were calculated and tabulated (Table

TABLE 17
 CONCENTRATIONS OF NO₃-N FOR A HORIZON SOIL SAMPLERS
 (NO₃-N in mg/l)

Storm Date	Site 1			Site 2			Site 3		
	1	2	3	1	2	3	1	2	3
2/15	-	-	-	-	0.02	-	0.09	-	-
2/24	-	-	-	-	-	-	0.06	-	-
3/1	0.06	-	0.78	0.14	0.03	0.03	0.02	0.02	0.03
3/17	0.23	0.44	1.26	0.12	0.05	0.04	0.06	0.01	0.47
5/25	0.34	-	-	-	-	-	0.33	0.07	0.85
5/28	0.07	0.34	0.21	0.13	0	0.07	0.05	0.01	0.16
5/31	0.04	0.36	-	-	0.03	0.05	0.135	0.02	-
6/30	0.19	-	0.16	-	0.04	0.05	0.16	0.05	0.13
n	6	3	4	3	6	5	8	6	5
mean	0.16	0.38	0.6	0.13	0.03	0.05	0.11	0.03	0.33
s	0.12	0.05	0.52	0.01	0.02	0.02	0.1	0.02	0.34

TABLE 18
 CONCENTRATIONS OF NO₃-N FOR B HORIZON SOIL SAMPLERS
 (concentrations in mg/l)

Storm Date	Site 1			Site 2			Site 3		
	1	2	3	1	2	3	1	2	3
1/16	0	0.05	0	0.013	0.013	-	0	-	-
2/15	-	-	-	-	-	-	0	-	-
2/21	0.023	-	-	-	-	0.011	-	-	0.009
2/24	0.006	0.086	0.015	0.034	0.03	0.016	-	-	-
3/01	0.015	0.079	0.009	0.026	0.034	0.019	0.016	0.015	0.013
3/17	0.06	0.29	0.05	0.08	0.18	0.014	0.06	0.03	0.013
3/25	0.026	-	0.026	-	0.02	0	-	0.009	0.006
4/01	0.008	-	-	-	-	0.013	-	-	-
5/21	-	-	-	0.234	-	-	0.039	0.024	-
5/25	0.073	1.121	0.05	0.128	0.073	0.041	0.054	0.062	-
5/28	0.298	0.647	0.028	0.064	0.013	0.093	0.018	0.048	0.376
5/31	0.075	0.457	0.035	0.035	0.028	0.031	0	0.03	0.102
6/30	0.053	0.703	0.023	0.097	-	0.239	0.146	0.007	0.174
n	11	8	9	9	8	10	9	8	7
mean	0.06	0.429	0.025	0.079	0.049	0.06	0.049	0.028	0.053
s	0.08	0.354	0.016	0.065	0.053	0.072	0.054	0.018	0.106

19). One advantage of calculating the ratios of change is that it allows comparisons between watersheds of different regions that have different concentration levels. As mentioned previously, the estimated mean constituent concentrations have a large degree of variation associated with them. The use of ratios of change allows for a relative comparison between sources independent of the magnitude of the concentration. However, it should be kept in mind that the ratios were calculated from concentrations having a large degree of variability. The ratio of change in constituent concentrations between sources for various studies were also calculated and tabulated (Table 20).

The degree of transformation between sources depended on the constituent under study. The greatest degrees of chemical change (increases or decreases) occurred as water passed through the canopy and litter layer. All constituents in soil water solution, except H^+ and NO_3-N , decreased in concentration as water passed through the A Horizon. H^+ increased (pH decreased) as water passed through the A Horizon, while NO_3-N increased slightly. As soil water passed through the B horizon, H^+ , NO_3-N , DOC, Ca, and K decreased. Conductivity and the concentration of Mg showed no change. Only the concentration of Na in soil solution increased. Concentrations of constituents in SSF were generally greater than those in soil solution for most constituents (Table 16). Some exceptions did exist. The degrees of transformation between throughfall and the litter

TABLE 19
 CHANGES IN MEAN CONCENTRATIONS
 BETWEEN SOURCES, CLAYTON WATERSHED #3 1/87-6/87*

Source	H+ (mg/l)	Cond. (umhos)	NO3-N (mg/l)	DOC (mg/l)	Ca++ (mg/l)	Mg++ (mg/l)	K+ (mg/l)	Na+ (mg/l)
<u>Throughfall</u>	0.99	1.02	0.93	22	2.1	4.3	36	1.3
Dormant	1.19	1.16	1.15	21	2.1	0.2	10	1.5
Growing	0.9	0.86	0.68	31	3	3.5	7.4	1.3
<u>Soil Solution Collectors - compared to all throughfall data</u>								
Litter Layer	0.08	1.7	0.79	5.7	4.3	7.7	1.1	1.8
A Horizon	2.2	0.85	1.1	0.31	0.5	0.91	0.4	2.5
B Horizon	0.82	1	0.38	0.51	0.62	1	0.81	1.6
<u>Subsurface Flow Collectors - compared to all throughfall data</u>								
Litter Layer	0.08	2.6	0.89	5.7	5.2	6.8	1.3	5.2
A Horizon	1.2	0.7	0.56	0.48	0.71	0.73	0.64	0.53
B Horizon	0.87	0.88	0.86	1.2	0.8	1.3	0.97	1.2

*change expressed as a ration between source above/source below

TABLE 20

RATIOS OF MEAN CHEMICAL CONCENTRATIONS BETWEEN SOURCES
FOR VARIOUS FORESTED WATERSHEDS

Location	Source	H+	Cond.	NO ₃ -N	Ca ⁺⁺	Mg ⁺⁺	K+	Na+
Oklahoma, Clayton WS 3 (Kress, 1988)	Throughfall	0.59	1.4	1.7	2.5	6	5.7	1.6
	Litter	0.05	1.8	0.85	2	3.6	2	1.1
	A Horizon	0.8	1.3	0.65	1.2	1.2	0.85	1.2
Arkansas, Alum Creek WS 11 (Kress, 1988)	Throughfall	1.1	1.7	1.9	1.2	2.8	13	1.5
	Litter	0.12	1.8	0.47	3.9	7.4	1	2.4
	A Horizon	2.1	1.3	1	0.55	0.49	0.78	0.62
Hubbard Brook, New Hampshire (Likens, et al. 1977)	Throughfall	0.11		3	9.9	15	91	2.3
Tower Creek, Washington (Wooldridge and Larson, 1980)	Throughfall		1.9	0.75	2.1	2.5	14	1.3
	Litter		0.9	1.3	1.6	1.2	0.27	0.93
	A Horizon		0.96	0.95	0.83	0.93	0.62	1
	B Horizon		0.85	1.1	1	0.89	0.83	0.92

layer were roughly alike between SSF and soil solution (Table 19). A notable exception was sodium. For most constituents, the degree of transformation was less for A horizon SSF and greater for B horizon SSF than for A horizon and B horizon soil solutions respectively.

The ratios of change in constituent concentration between sources for other sites are presented for rough comparison with the results obtained in this study (Table 20). Some agreements and disagreements between data sets are evident. However, differences are generally within the same order of magnitude. Differences in the degrees of transformation are due to different climates, cover types, and cover densities. Some differences may be due simply to the type of collector used, or the locations of the collectors. For example, Kress (1988) located throughfall collectors directly under tree canopies. In this study, throughfall collectors were located at random, with some directly under canopies, and some in more open areas. This may explain in part why Kress's (1988) studies (Oklahoma and Arkansas) showed a greater degree of transformation (1.7 and 1.9 respectively) in the concentration of $\text{NO}_3\text{-N}$ between precipitation and throughfall (Table 20) than did this study (0.93). Although some trends can be observed, the large degree of variation of constituent concentrations about the estimated means makes it difficult to make definitive statements about chemical transformations of water within small forested watersheds.

Chemical Loads in Streamflow

Shallow subsurface flow has already been shown to generate significant quantities of streamflow before or shortly after peak flow. The load of chemicals associated with SSF may also significantly influence the streamwater chemistry before or shortly after peak flow. To determine the effect of SSF chemistry on the total watershed streamflow chemistry, the SSF chemical loads were calculated for selected storms. The storm SSF load was calculated by multiplying the SSF volume from each collector times the mean concentration. The total storm load was calculated by adding together the individual collector loads from the three study sites. The SSF collector loads were multiplied by the watershed scale factor (WSF) to extrapolate the results to the entire watershed. This procedure was carried out for three storms (3/1, 3/17, and 6/30) for which streamflow chemistry data was available. The storm of 3/1 represents a winter storm produced by long duration, low intensity precipitation. The storm of 3/17, was produced by relatively high, short duration precipitation, and was the second largest storm of the study period. The storm of 6/30 represents the only summer season storm for which streamflow chemistry information was available. Unfortunately, no streamflow chemistry data was available for the largest storm of the study period (5/28), due to equipment failure.

As expected, the chemical load varies with each chemical constituent. All SSF and streamflow loads are relatively low

(Tables 21, 22, and 23). Dilute chemistry is characteristic of small watersheds in the Ouachita Mountains region that drain shallow, highly leached soils. The ratios of the chemical loads of each constituent supplied by SSF to the total streamflow load for each of the three storms was also calculated (Tables 21, 22, and 23). For storms with a distinguishable peak, the ratios of the chemical loads of each constituent supplied by SSF to the streamflow load before peak flow was also calculated (Tables 22 and 23). The ratios of SSF to streamflow load varied according to constituent. The ratios of SSF to streamflow load ranged from 0.03 to 2.14. The ratios of SSF to the streamflow load before peak ranged from 0.3 to 11.4.

For the storm of 3/1, SSF accounted for about 3 and 13 percent of the total streamflow and the streamflow before peak respectively (Table 14). SSF accounted for 65 percent of the total $\text{NO}_3\text{-N}$ load, but only 8, 3, and 12 percent of the total loads of Ca, Mg, and K, respectively (Table 21). For the storm of 3/17, SSF accounted for 9 and 36 percent of the total streamflow and the streamflow before peak respectively. SSF accounted for 72 percent of the total streamflow $\text{NO}_3\text{-N}$ load, but only 17, 7, and 17 percent of the total loads of Ca, Mg, and K, respectively (Table 22). For the period of time before peak flow, SSF accounted for 186 percent of the streamflow $\text{NO}_3\text{-N}$ load and 68, 30, and 75 percent of the Ca, Mg, and K loads respectively. The high percentage of the $\text{NO}_3\text{-N}$ load transported before peak is probably due to the

TABLE 21
 SUBSURFACE FLOW CHEMICAL TRANSPORT LOADS
 Storm of 3/01/87

Site/ Source	Storm SSF (1)	Site SSF * WSF	SSF Chemical Loads						
			H+ (gm)	NO3-N (gm)	DOC (gm)	Ca (gm)	Mg (gm)	K (gm)	Na (gm)
1L	5	2000	0.00107	0.3	342	6.3	2.1	2.9	1.9
1A	1	400	0.00073	0.1	10	0.2	.0	0.1	.0
1B	2	800	0.00037	0.4	254	2.2	0.7	4.3	0.2
2L	14	5600	0.00755	0.5	2044	12.9	3.6	12.3	2.0
2A	110	44000	0.09192	2.1	6160	79.6	35.2	43.1	33.0
2B	32	12800	0.03777	1.8	1933	21.2	11.1	19.2	5.4
3L	10	4000	0.01746	0.6	1760	12.8	2.8	13.7	1.2
3A	10	4000	0.01452	1.7	240	6.6	0.6	4.0	0.7
3B	31	12400	0.00985	5.7	2678	16.5	6.9	93.5	18.8
Totals	214		0.18125	13	15422	158	63	193	63
Total Storm Stream Load:			1.6883	20		1868	2256	1678	
SSF/Stream Load:			0.11	0.65		0.08	0.03	0.12	

Storm consisted of multiple peaks, before peak flow comparisons could not be performed

TABLE 22
 SUBSURFACE FLOW CHEMICAL TRANSPORT LOADS
 Storm of 3/17/87

Site/ Source	Storm SSF (1)	Site SSF * WSF	SSF Chemical Loads						
			H+ (gm)	NO3-N (gm)	DOC (gm)	Ca (gm)	Mg (gm)	K (gm)	Na (gm)
1L	22	8800	0.02314	0.7	1593	20.0	4.8	21.1	6.6
1A	4.1	1640	0.00248	0.3	36	0.9	0.1	0.7	0.3
1B	86	34400	0.08253	4.1	5882	51.9	24.4	46.1	19.6
2L	34	13600	0.05171	1.9	1673	15.9	7.6	16.7	8.2
2A	340	136000	0.46077	2.7	16048	156.4	81.6	161.8	107.4
2B	75	30000	0.10164	0.9	3990	36.0	20.4	31.2	22.5
3L	25	10000	0.02512	15.0	2320	35.9	8.4	41.3	5.7
3A	17	6800	0.00258	0.4	1095	24.8	6.6	19.3	4.6
3B	0	0							
Totals	214	241240	0.74997	26	32637	342	154	338	175
Total Storm Stream Load:			2.3426	36		1979	2068	1962	
SSF/Stream Load:			0.32	0.72		0.17	0.07	0.17	
Stream Load Before Peak:			0.6136	14		502	510	448	
SSF/Load Before Peak:			1.22	1.86		0.68	0.3	0.75	

TABLE 23
 SUBSURFACE FLOW CHEMICAL TRANSPORT LOADS
 Storm of 6/30/87

Site/ Source	Storm SSF (1)	Site SSF * WSF	SSF Chemical Loads						
			H+ (gm)	NO3-N (gm)	DOC (gm)	Ca (gm)	Mg (gm)	K (gm)	Na (gm)
1L	4	1600	0.00003	.0	709	6.7	1.7	3.8	10.2
1A	6	2400	0.00007	0.1	533	9.2	1.4	22.6	2.4
1B	4	1600	0.00075	0.7	509	4.4	1.4	8.6	0.4
2L	17	6800	0.00460	1.4	1850	15.6	5.9	19.2	2.4
2A	72	28800	0.15114	2.0	4694	40.0	21.3	40.0	11.2
2B	13	5200	0.01535	0.7	785	8.6	4.5	7.8	2.2
3L	5	2000	0.00025	0.6	1372	15.5	2.8	29.6	4.9
3A	0.5	200	0.00001	0.1	48	0.7	0.2	1.6	0.2
3B	2	800	0.00064	0.4	173	1.1	0.4	6.0	1.2
Totals	214		0.17283	6	10673	102	40	139	35
Total Storm Stream Load:			0.1102	2.8		89	74	240	
SSF/Stream Load:			1.57	2.14		1.14	0.54	0.58	
Stream Load Before Peak:			0.0152	0.9		11	10	14	
SSF/Load Before Peak:			11.4	6.7		9.3	4	9.9	

fact that some of the SSF occurred after peak flow was reached. For the storm of 6/30, SSF accounted for about 48 and 318 percent of the total streamflow and the streamflow before peak respectively. SSF accounted for more $\text{NO}_3\text{-N}$ than was measured at the watershed outlet for the total stormflow and stormflow before peak, 214 and 670 percent respectively. SSF also accounted for more, or very high percentages of the cation transport both for the total storm and the streamflow before peak (Table 23). The storm of 6/30 was the result of a short duration high intensity precipitation event. Due to dry antecedent conditions, there was little flow from the deeper soil horizons, and a very short recession period. Most of the flow occurred as a result of SSF and an unmeasured source. The high percentages of chemical loads accounted for by SSF may be due to errors or variation in the chemical concentrations from the SSF collectors. The still higher percentages of chemical loads before peak accounted for by SSF are probably due to a large portion of the SSF occurring after peak flow.

Even though the data are limited, the trends indicated by the results are consistent with other observations of streamflow chemical transport on the Clayton Experimental Watersheds. For example, during storm events, $\text{NO}_3\text{-N}$ concentrations reach peak levels before peak streamflow, and decline to low levels later in the event (Lawrence, 1985). A concurrent plot of streamflow and $\text{NO}_3\text{-N}$ concentration for the storm of 3/17/87 demonstrates this trend clearly (Figure 31).

Streamflow and NO₃-N Concentration

Storm of 3/17/87

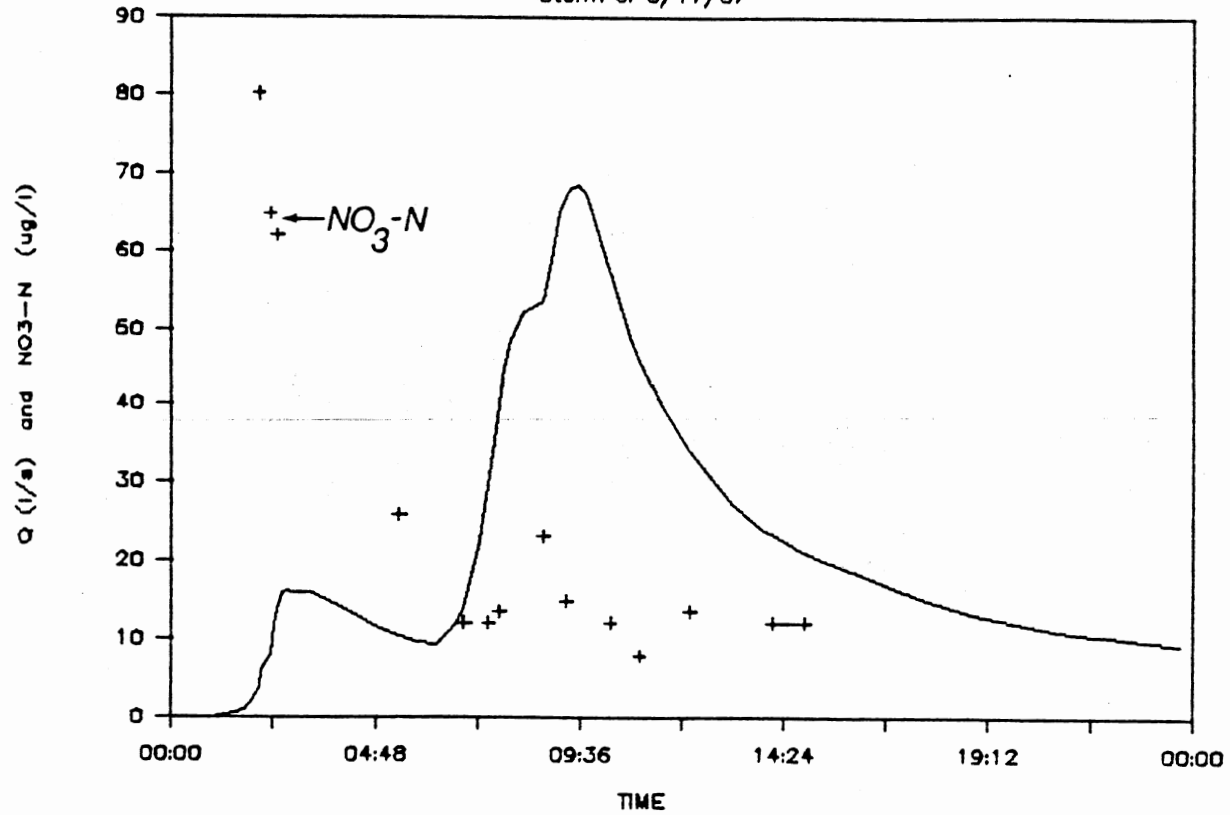


Figure 31. Simultaneous Plot of NO₃-N Concentration and Streamflow for the Storm of 3/17/87

As can be seen, high concentrations of $\text{NO}_3\text{-N}$ also coincide with the generation of SSF. Therefore, it appears that SSF is responsible for generating a large portion of the total $\text{NO}_3\text{-N}$ load, especially early on in a storm event. For storms during wet periods when soil moisture is at a higher level (3/1 and 3/17), SSF accounts for a small percentage of the total cation load and the total streamflow. A source of flow not measured in this study, subsurface flow from the deeper soil horizons, is most likely responsible for generating the largest portion of the streamflow. This observation is consistent with the long recession periods observed from storms during wet periods. Long recessions are not observed from small storms that are preceded by dry conditions. Cation concentrations tend to vary little during storm events, and do not show the hysteresis in concentration that $\text{NO}_3\text{-N}$ does. The concentrations of cations in soil solution and streamwater are mainly a function of soil cation exchange processes. Therefore, streamwater produced from deeper soil layers should have a relatively high load of cations. As a result, SSF accounts for the streamflow cation load for storms that have a large percentage of their streamflow generated from deeper soil sources.

CHAPTER VI

WATERSHED MODEL DEVELOPMENT AND DESCRIPTION

Rationale for Development

Numerous watershed models with potential for use on small forested watersheds already exist. The modeling approach and data input requirements vary from model to model. Modeling objectives included finding or adapting a simple model to minimize execution time and the number of parameters required, with a structure that allowed for the addition of chemical transport routines, with physically based parameters that could be measured or obtained from the literature, and with routines that represent hydrologic processes unique to forested watersheds. Following an extensive review of existing watershed models (Chapter 3), it was decided to develop a new model to meet the study objectives, rather than adapting an existing model to the conditions on Clayton Watershed #3.

The model developed is not intended to be universally applied to all watershed. Parts of the model are specific to the study watershed (Clayton, OK Watershed #3). The model represents a first attempt at modeling streamflow,

water yield, and chemical transport from a small forested watershed typical of those in the Ouachita Mountains. It was hoped that by developing a model, a better understanding of the hydrologic and chemical processes in operation, the variability of the processes, and the identification of needs for future modeling and research work would be gained.

Modeling Concept

The model is conceptual in nature. It uses a simple storage tank or reservoir concept to represent hydrologic and chemical processes (Figure 32). The continuity equation is solved for each simulation time increment for each tank in the order indicated (Figure 32). The maximum storages and rates of transfer within and between tanks vary. The model is also somewhat physically based because each storage tank represents a hydrologic process important to the generation of streamflow or streamflow chemistry, and physically based parameters are used to calculate the rates of transfer in and between storage tanks. The hydrologic component of the model contains 36 parameters, most of which can be estimated from field measurements or data in the literature. The water quality component adds six additional parameters. The water quality parameters may be estimated from soil solution chemical concentration measurements. In the following discussion, model names including, variables, zones, subroutines and parameter names are italicized

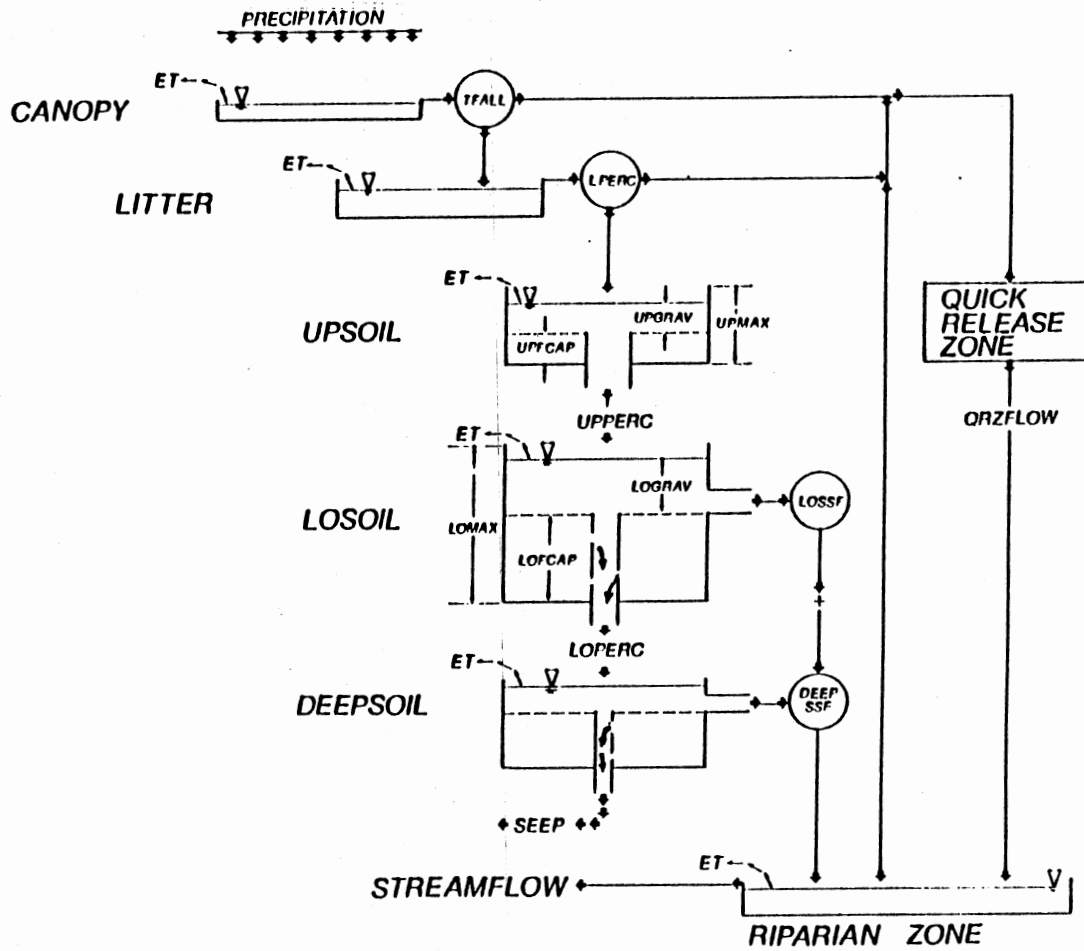


Figure 32. Flow Diagram of the Watershed Model

(ie: *NAMES*) to distinguish them from acronyms used to describe processes such as evapotranspiration (ET).

The model is semi-distributed in nature. A lumped approach was originally desired to maintain simplicity. However, while developing the model, it became evident that a completely lumped approach would not adequately describe the different streamflow generating mechanisms operating on the watershed. Two zones, a riparian zone and a variable area quick release zone (*QRZ*) were designated to represent the flow generating processes unique to each area (Figure 33). The remaining watershed area was lumped into a third zone. The riparian zone encompasses the stream channels and the readily saturated topographically low alluvial areas near the stream channels. The quick release zone (*QRZ*) represents the contributing area of quickly released shallow subsurface flow from steep hillslopes that surround the stream channels. The area of *QRZ* is a function of the lower soil zone water content. Throughfall is calculated for the entire watershed area. Litter interception is assumed to occur everywhere except in the stream channels. The remaining hydrologic and chemical processes are simulated separately in each zone.

The model provides continuous simulations of streamflow and chemical constituent concentrations. The maximum simulation increment (*MAXINC*) within a one day period is specified by the user. A maximum increment of 15 minutes for within day calculations was used in this study. All

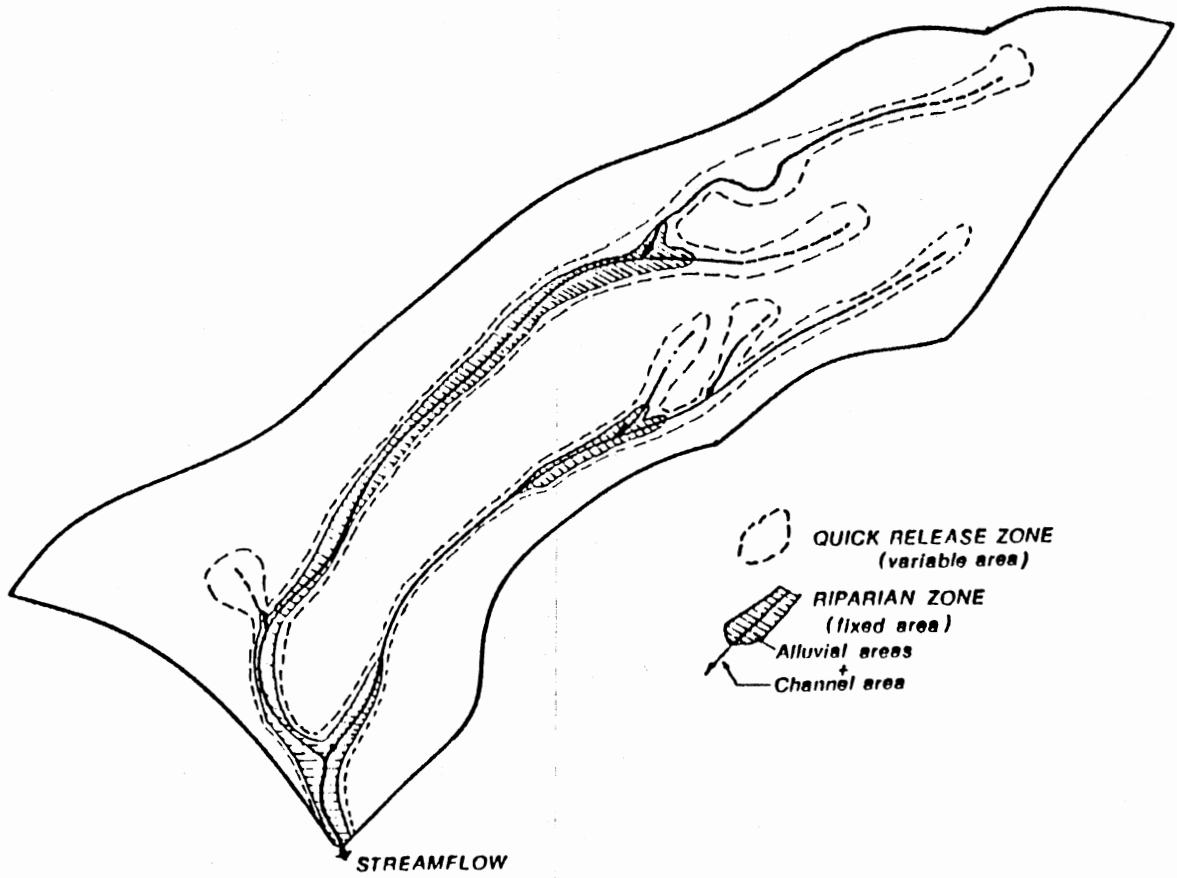


Figure 33. Division of the Watershed Into Zones

calculations are carried out on a time incremental basis.

Model Structure

The watershed model is modular in structure and has two main loops. A control module asks for the appropriate input files and other information, calculates soil water parameters, and controls data input and output. The year loop repeats calculations until the last line in the annual data input file is read (Figure 34). Within the main control loop is a loop that operates on a daily time increment. The day loop repeats calculations for each day until a new day is reached. At the end of one day, daily runoff and chemical transport summaries are calculated and printed to the output device or file. Within the day loop, the break point data is tested to determine whether or not the change in time between two lines of input data is greater than or less than *MAXINC*.

After the time increment test is made, the program branches to one of three time control subroutines, *NoTimeSplit*, *TimeSplit1*, and *TimeSplit2*. The appropriate time control subroutine divides the time increment read from the data input file (*DELTAT*) into increments that are less than the maximum simulation increment (Figure 35).

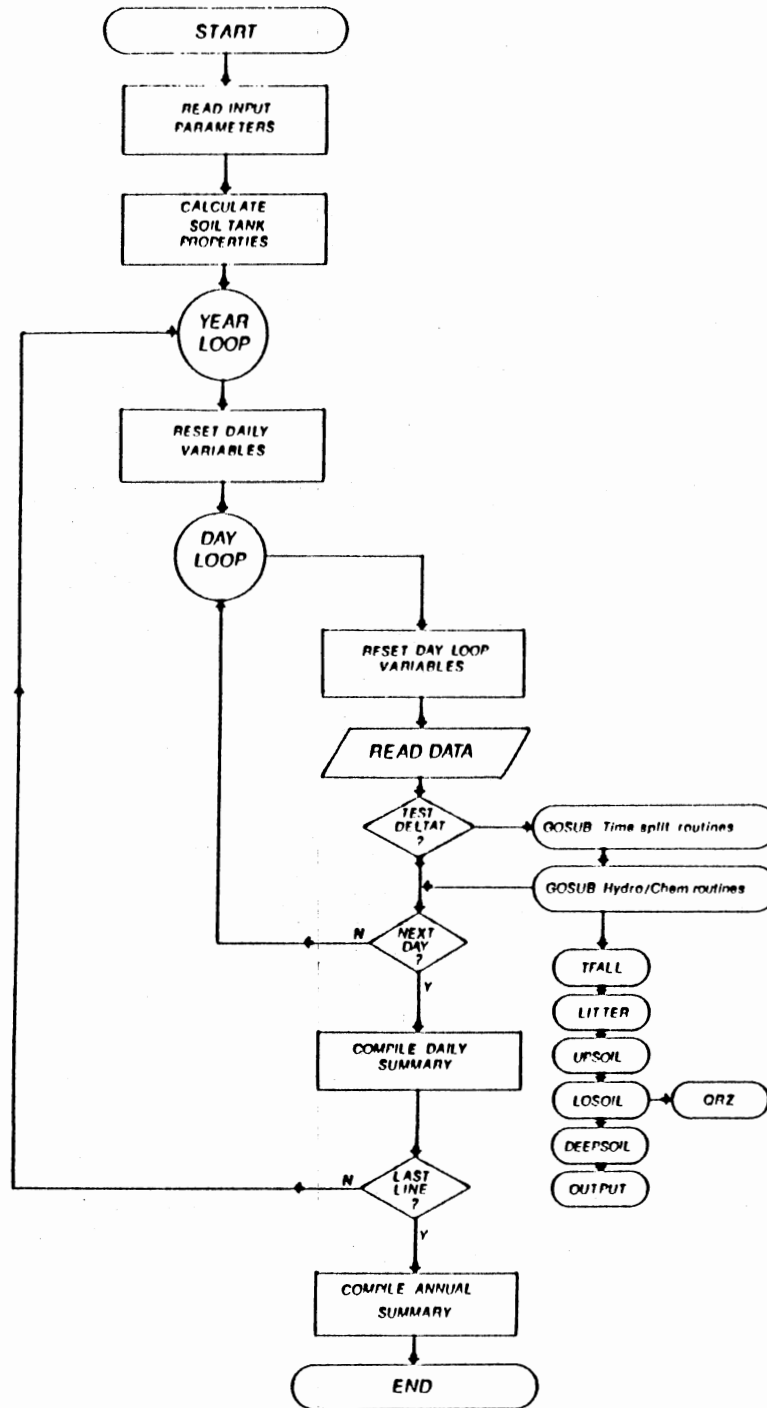


Figure 34. Flow Chart of the Watershed Model Program

A maximum increment of one day is used during periods of no precipitation and no streamflow.

The hydrologic and chemical process subroutines are accessed by the time control subroutines. The hydrologic and chemical process subroutines carry out calculations in each of the conceptual storage tanks. The order of operation follows the naturally occurring vertical transport of water through the watershed system (Figure 34), from *Throughfall*, *Litter*, *Upper Soil Storage*, *Lower Soil Storage*, to the *Deep Soil Storage*. The *QRZ* subroutine is accessed from within the *Lower Soil Storage* subroutine so the current value of the lower soil storage moisture content can be used. Flow from the *Riparian Storage* is accounted for separately. Flow generated from all other sources is combined in the riparian zone storage tank (*RIPSTOR*) to produce streamflow. Complete mixing of chemical constituents is assumed to occur within one time increment.

Detailed descriptions of each of the hydrologic and chemical processes are presented in the following sections. Since outputs from one tank are required inputs for the next tank, computations of inputs, outputs and internal transfers are made for each tank within a time increment. The modular structure of the hydrologic and chemical process subroutines allows users to substitute other routines without changing the basic model structure. The model program is written in the BASIC language (Microsoft Quick

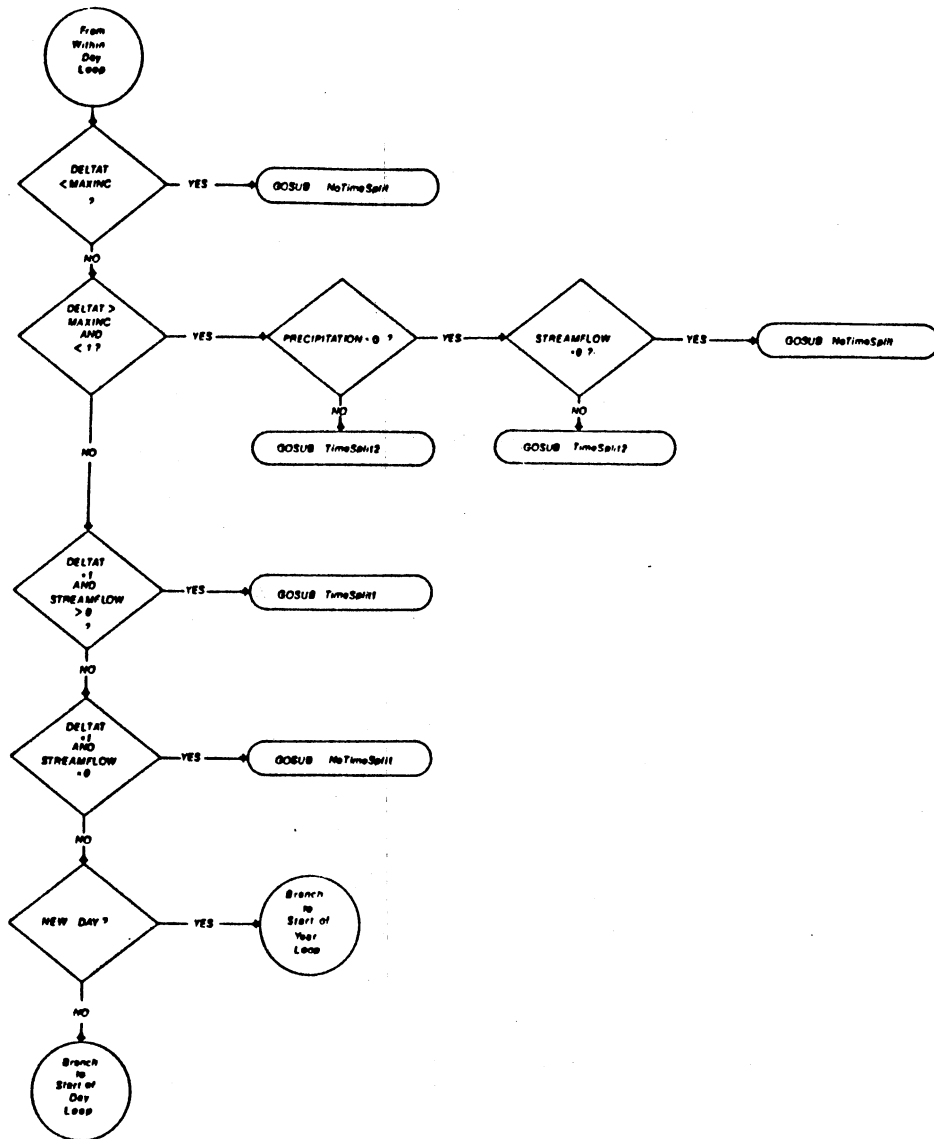


Figure 35. Flow Chart of Time Increment Control Subroutines

Basic Version 4). A complete listing of the program is presented in Appendix D.

Data Input Requirements

The model is designed to simulate on a water year basis. Each data input file line must contain, in the following order, the number of the month, the calendar day, the day number (Julian Date), the time in a decimal fraction of a day, the accumulated storm precipitation, and the daily, unadjusted pan evaporation. A storm must be defined with a precipitation value of 0 ($PCP=0$) at the start of the event. Thereafter the accumulated storm precipitation is recorded on each data file line. The program subtracts precipitation values from two lines to calculate the incremental precipitation ($IPCP$). The program also tests two data lines to determine whether or not precipitation has ceased.

Soil, vegetative, and other parameters necessary to operate the model are also required. These parameters are discussed in detail in the appropriate hydrologic and chemical subroutine description. A listing of parameters is presented in Table 24. Initial soil storage tank values are obtained by a "best estimate" based on antecedent climatic conditions, or from simulating the previous year with the model.

TABLE 24
LISTING OF MODEL INPUT PARAMETERS

Parameter	Definition
<u>Program Control</u>	
MAXINC (days)	Maximum storm simulation time increment
<u>Geomorphologic Characteristics</u>	
TOTAREA	Total watershed area (m ²)
CHANAREA	Stream channel area (m ²)
ALLUVAREA	Area of topographically low areas (m ²)
<u>Soil Hydrologic Properties</u>	
UPSOILDEP	Upper soil storage depth (mm)
UPPOR	" " soil porosity (mm/mm)
UPROCK	" " rock content (mm/mm)
UPAWC	" " available water (mm/mm)
UPWILTP	" " wilting point (mm/mm)
LOSOILDEP	Lower soil storage depth (mm)
LOPOR	" " soil porosity (mm/mm)
LOROCK	" " rock content (mm/mm)
LOAWC	" " available water (mm/mm)
LOWILTP	" " wilting point (mm/mm)
DEEPSOILDEP	Deep soil storage depth (mm)
DEEPPOR	" " soil porosity (mm/mm)
DEEPROCK	" " rock content (mm/mm)
DEEPAWC	" " available water (mm/mm)
DEEPWILTP	" " wilting point (mm/mm)
HSATLO (mm/day)	Lower soil saturated hydraulic conductivity
BLOSOIL	Lower soil percolation constant
HSATDEEP (mm/day)	Deep soil saturated hydraulic conductivity
BDEEP	Deep soil percolation constant
UPSTOR	Upper soil initial storage (mm)
LOSTOR	Lower " "
DEEPSTOR	Deep " "
RIPSTOR	Riparian zone initial storage value

TABLE 24 (continued)

Parameter	Definition
<u>Potential Evapotranspiration</u>	
PANCOEFF	Monthly evaporation pan coefficient
<u>Vegetative Characteristics</u>	
GROWSTOR	Maximum growing season canopy storage (mm)
DORMSTOR	Maximum dormant season canopy storage (mm)
LITMAX	Maximum litter layer storage (mm)
UPWEIGHT	Upper soil root density weighting factor
LOWEIGHT	Lower soil " "
DEEPWEIGHT	Deep soil " "
<u>Subsurface Flow Tank Release Coefficients</u>	
KLO	Lower soil flow release coefficient (days ⁻¹)
KDEEP	Deep soil " "
<u>Quick Release Zone</u>	
ZSLOPE	Quick release zone parameter
<u>Water Quality</u>	
TFCHEM	Throughfall mean concentration (mg/l)
LITCHEM	Litter layer " "
UPCHEM	Upper soil " "
LOCHEM	Lower soil " "
DEEPCHEM	Deep soil " "
QRZCHEM	Quick release " "

Hydrologic Processes

Evapotranspiration

Since evaporative loss is a component of all of the storage tanks, the methods used to estimate evapotranspiration (ET) are presented first. Potential evapotranspiration (PET) is estimated from daily pan evaporation data. Pan evaporation was chosen to estimate PET because it is a good integrator of climatic variables such as humidity and radiation that were not available for the watersheds. A reliable record of pan evaporation was available. Unadjusted daily pan evaporation, read from the data input file, is adjusted by a pan coefficient. A suitable set of pan coefficients, in lieu of actual ET measurements, is difficult to obtain. An evaporation pan is essentially a two dimensional surface. The forest canopy is a multi-layered three dimensional surface capable of absorbing greater energy than an evaporation pan. The results of some investigations indicate that PET from forests can exceed the unadjusted pan evaporation by up to 1.5 times (Federer and Lash, 1978, Swift, et al., 1975, and England, 1977). Some of these results have been obtained from water balance calculations using models and may be subject to some question. However, the evidence seems to indicate that pan coefficients for forest watersheds should be greater than pan coefficients for field crops and grasses.

The daily pan evaporation is adjusted by a suitable pan

coefficient in the model subroutine called *PanCoefficients*. The resulting daily PET demand (*DAYPET*) is divided by the simulation time increment to provide a maximum incremental PET (*IPET*). The priority of water loss to ET follows the order of execution the hydrologic processes subroutines. Actual evapotranspiration (AET) during a simulation time increment is limited by the lesser of the remaining incremental demand (*IREMPET*) and the available water in any of the storages. AET within a daily period is also limited by the daily demand (*DAYPET*). ET from the canopy and litter storage tanks occurs at the potential rate as long as water is available. ET from the soil storage tanks is a function of the soil water content, the rooting density and a seasonal transpiration factor. The PET demand remaining after the canopy and litter storages have been satisfied is applied to the three soil storage tanks as a whole.

The fraction of the remaining PET demand applied to each soil storage tank is determined by a root density weighting factor. The root density weighting factor for the soil storage tanks was assumed to be equal to the percentage of fine roots (< 5mm diameter) found in the depth of the soil represented by the soil storage tank. The sum of the root density weighting factors must equal 1. Estimates of the root density weighting factors were made from field observations in combination with data from the literature (Kochenderfer, 1973). The root density weighting

factors estimated for Clayton Watershed #3 were 0.5, 0.4 and 0.1 for the upper soil, lower soil, and deep soil storage tanks respectively.

The incremental PET applied to the soil storage tanks is further adjusted by a seasonal transpiration factor (*SEATRANS*). During the growing season, *SEATRANS* is assumed to equal 1. During the dormant season., the seasonal transpiration factor is reduced by the reduction in the leaf area index (LAI) resulting from the loss of leaves from deciduous trees. Using an average LAI of 8 for conifers and 4 for hardwoods, it was estimated that the leaf area index of Clayton Watershed #3 decreased by 85%, from 5.6 to 0.84 between the growing and dormant seasons respectively. Therefore, *SEATRANS* was estimated to be 0.15 for the dormant season. During the transition months of November and April, *SEATRANS* was assumed to decrease and increase linearly to represent the respective loss and gain of leaves. *SEATRANS* is applied only to the lower and deep soil storage tanks. Evaporation is assumed to occur from the upper soil storage tank throughout the year at the potential rate.

AET from the soil storage tanks is also limited by the available soil moisture. Above field capacity, ET is allowed to occur at the potential rate. Below field capacity, the ability of the soil to provide water for ET is a function of soil texture and water content. Simple relationships between soil water content and the ratio of

AET to PET were developed for each soil storage tank. Many forms of the AET/PET ratio, from linear to exponential, have been suggested. A consensus does not seem to exist. S-curve functions, similar to those developed by Holmes (1961), were chosen to estimate the relationship between AET and PET for the three textural classes of soil found in the soil storage tanks (Figure 36). AET for a simulation increment is equal to the lesser of $IREMPET \times$ the root density weighting factor \times the AET/PET ratio, or the available soil water content.

Throughfall

Throughfall (*TFALL*) is modeled as a simple storage tank (Figure 21). Precipitation (*IPCP*) provides input to the canopy storage tank. Outflow, or throughfall, occurs when the current level of canopy storage (*CANSTOR*) exceeds the maximum canopy storage (*CANMAX*). Canopy storage may also be lost to evaporation. The amount of evaporation (*CANLOSS*) is limited by the lesser of the incremental potential evapotranspiration (*IPET*) or the available storage.

Estimates for the maximum canopy storages for the dormant and growing seasons were obtained from data obtained in the field component of the study (Table 7). *CANMAX* was estimated to be 0.43 and 1.8 mm for the dormant and growing seasons, respectively. Based on field observations, the growing season was estimated to operate from May 1 to October 31, and the dormant season from December 1 to March

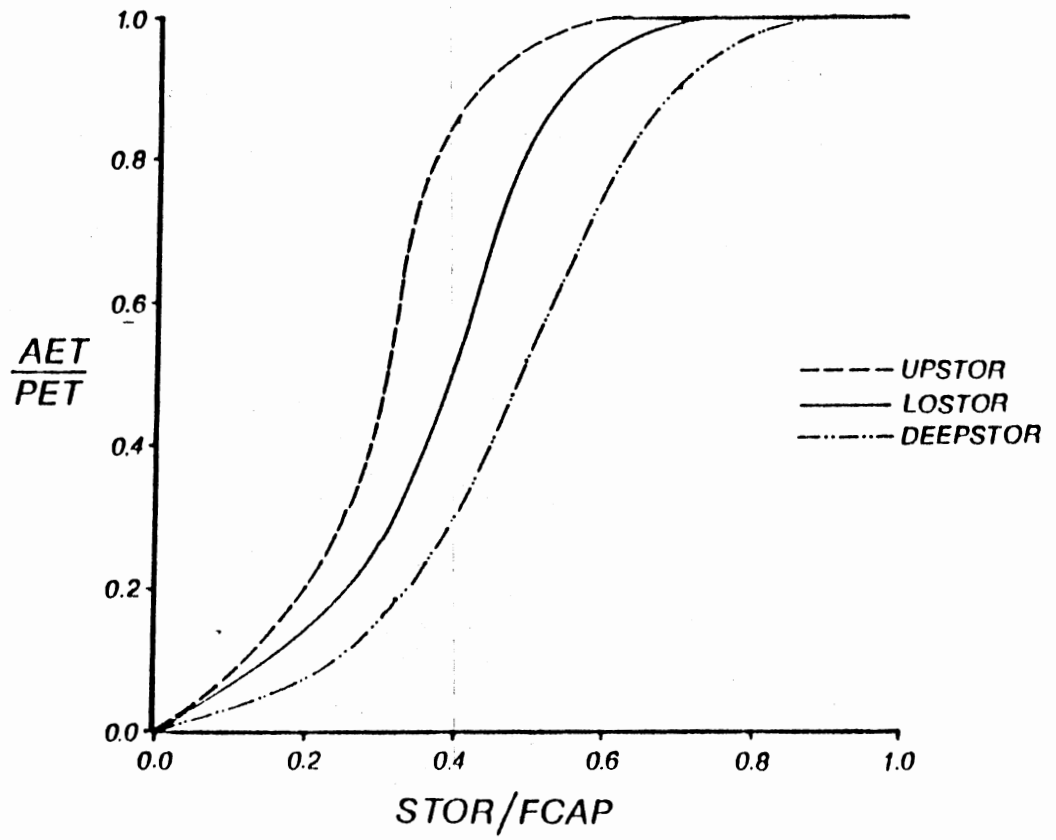


Figure 36. AET/PET Relationships for Soil Storage Tanks

31. During the transition months of November (leaf fall) and April (leaf growth), *CANMAX* was assumed to decrease and increase linearly between the before the dormant and growing seasons respectively.

Litter Layer

As discussed previously, the litter layer is a significant source/sink of chemical constituents. Therefore, the litter layer was included as a separate storage tank (Figure 32). Inflow to the litter storage tank is provided by *TFALL*. Flow, or percolation out of the litter layer (*LPERC*) occurs when the current level of the litter layer storage (*LITSTOR*) exceeds the maximum litter layer storage (*LITMAX*). Water in the litter layer may be lost to evaporation at the lesser of the remaining incremental PET (*IREMPET*) and the available storage (*LITSTOR*).

The maximum litter layer storage (*LITMAX*) was assumed to remain constant throughout the water year. A *LITMAX* of 3.5 mm was estimated from on-site measurements of litter depth and data obtained by Helvey and Patric (1965) and Raison and Khanna (1982). Little data on the litter interception process is available. The litter storage is comparably small, however. Litter interception is probably unimportant to the prediction of streamflow from large precipitation events. On the other hand, litter may represent a significant loss during small storms and in the annual water balance.

Soil Storages

Three soil water storage tanks are used to represent the soils found on Clayton Watershed #3 (Figure 32). The soil is divided into an upper soil tank (*UPSOIL*), a lower soil tank (*LOSOIL*) and a deep soil tank (*DEEPSOIL*). *UPSOIL* simulates the behavior of the A horizon (A1 and E horizons), *LOSOIL* encompasses the B1 and B22t horizons of the soil, and *DEEPSOIL* simulates the behavior of the IIB23t horizon. The division of the soil profile was based on the hydraulic properties of the soils. The division also coincides with the division of the soils between the litter, A and B horizons performed in the preceding field study. Input requirements for describing each soil tank include the total depth, porosity, percent rock, available water capacity, and the water content at the -15 bar wilting point. In the following discussion, a blank line in front of the variable name represents the soil tank name designation (ie: *LOMAX* for the lower soil tank *LOSOIL*). The maximum storage capacity for each tank (*__MAX*) is equal to

$$\text{__MAX} = (\text{__POR} - \text{__WILTP}) \times (\text{__SOILDEP}) \times (1 - \text{__ROCK})$$

where *__POR* is the porosity, *__WILTP* is the wilting point, *__SOILDEP* is the soil depth, and *__ROCK* is the percent rock. All soil property values are in mm/mm. The soil water content at field capacity (*__FCAP*) is given by

$$\text{__FCAP} = \text{__AWC} \times \text{__SOILDEP}$$

where $\text{---}AWC$ is the available water capacity in mm/mm. The soil storage tanks are assumed to be empty at the wilting point.

Upper Soil Storage

Input to the upper soil storage (*UPSOIL*) is provided by percolation from the litter layer (*LPERC*). Outflow from *UPSOIL*, percolation (*UPPERC*), occurs only when the level of storage (*UPSTOR*) exceeds the upper storage field capacity (*UPFCAP*). Water in excess of *UPFCAP* is assumed to percolate from *UPSOIL* in one time increment. No other drainage function is included. Given the fact that the upper horizons contain numerous macropores and are highly porous, the assumption of immediate drainage in excess of field capacity was considered to be valid. The continuity equation for *UPSOIL* for a time increment of simulation is given by

$$UPSTOR_2 = UPSTOR_1 + LPERC - ETLOSS - UPPERC$$

where *ETLOSS* is the loss due to ET, and the subscripts $_1$ and $_2$ represent storage at the beginning and end of the time increment respectively. The order in which the variables appear in the equation above is the same as the order of calculation of the water balance within the *UpperSoilStorage* subroutine. When the lower soil storage is full (*LOSTOR* = *LOMAX*), water in excess of field capacity (*UPGRAV*) in *UPSTOR*

is added to *LOGRAV*, the lower soil tank subsurface flow reservoir.

Lower Soil Storage

Input to *LOSOIL* is provided by percolation from *UPSOIL*. Outflows from *LOSOIL* include evaporative loss (*ETLOSS*), percolation to the deep soil storage (*LOPERC*), and subsurface flow (*LOSSF*). The continuity equation for *LOSOIL* for a time increment may be expressed as

$$LOSTOR_2 = LOSTOR_1 + UPPERC - ETLOSS - LOSSF - LOPERC$$

where *LOSTOR₁* and *LOSTOR₂* are the water contents at the beginning and end of the time increments respectively. The order in which the variables are presented in the equation above is the same as the order of execution of water balance calculations within the *LowerSoilStorage* subroutine.

Subsurface flow is generated from both *LOSOIL* and *DEEPSOIL*. Both soil storage tanks are assumed to behave as linear reservoirs. That is, outflow is a linear function of storage

$$S=KO$$

where *S* is storage, *O* is outflow, and *K* is the outflow constant. The streamflow recession constant, *K_r*, may be estimated from an analysis of hydrograph recession (storage depletion) curves using a procedure described by Linsley, et al. (1975). For precipitation free periods and periods of

low evapotranspiration, the outflow (q_2) from a linear reservoir at a given time period is related to the outflow (q_1) at the beginning of the time period by a recession constant K_r

$$q_2 = q_1 K_r^t$$

Streamflow recession conforming to the equation above plots as a straight line on semilog plot ($\ln Q$ vs. time).

Several storms from Clayton Watershed #3 were plotted as semilog hydrographs to detect whether or not streamflow recession could be described as a linear reservoir. One semilog hydrograph is shown as an example (Figure 37). Observations of other semilogarithmic hydrographs showed a straight line relationship between the natural log of streamflow and time for periods of receding flow. Two distinct slopes, one representing a later delayed flow and one occurring soon after peak streamflow, were apparent during the observations. The two distinct recessions were assumed to be analogous to recession from the *LOSOIL* (rapid release subsurface flow) and *DEEPSOIL* (delayed release subsurface flow) tanks.

The streamflow recession constant is a useful concept, but for model calculations, the storage recession constant is required. All time calculations in the model were performed in days or decimal fractions of days. Recession constants were estimated in days. The daily storage

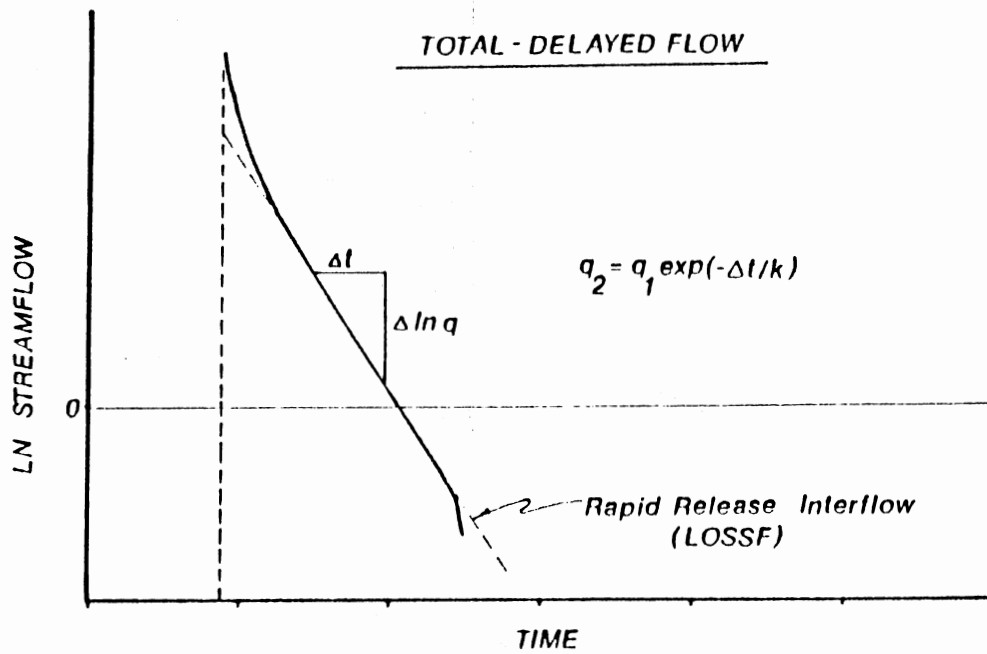
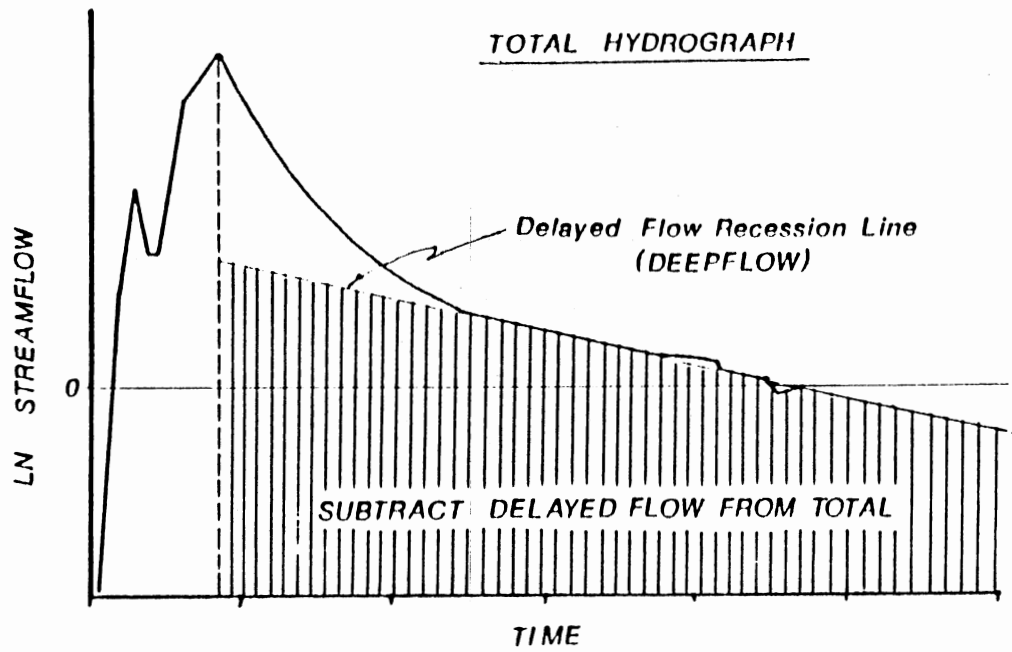


Figure 37. An Example of the Hydrograph Separation Technique Used to Estimate the Soil Tank Storage Release Coefficients

constant (K_{\bullet}) is related to the daily streamflow recession constant by the following expression,

$$K_{\bullet} = -\ln K_r / t$$

where $t = 1$ day. Following the procedures of Linsley, Kohler and Paulus (1975), the delayed flow storage recession constant ($K_{\bullet 1}$) was estimated first. The recession line was extended under the hydrograph to peak flow (Figure 36). Flow due to delayed flow was subtracted from the total hydrograph. The same procedure was repeated on the residual hydrograph in order to calculate the rapid release subsurface flow storage recession constant ($K_{\bullet 2}$). From analysis of five storms, the average values of $K_{\bullet 1}$ and $K_{\bullet 2}$ were found to be 0.6102 and 0.0831 days⁻¹, respectively.

LOSSF and *DEEPSSF* are calculated as a function of *LOGRAV* and *DEEPGRAV*, respectively. The storage above field capacity remaining at the end of the simulation time increment (*REMSTOR*) is given by

$$REMSTOR = \text{__GRAV} \times (K_{\bullet} \text{ DELTAT})$$

where *__GRAV* is the storage above field capacity for the appropriate tank, and *DELTAT* is the simulation time increment. The quantity of subsurface flow released for a simulation time increment, in depth units, is equal to *__GRAV* less *REMSTOR*.

Percolation from *LOSOIL* (*LOPERC*) and deep seepage loss (*DEEPSEEP*) from the deep soil storage tank (*DEEPSOIL*) were

assumed to be equal to the hydraulic conductivity of the soil (HC). A relationship between HC , the saturated hydraulic conductivity (HC_{sat}), and the ratio of the soil water content to the saturated water content (θ/θ_{sat}) was estimated using the procedure described by Campbell (1986). Hydraulic conductivity at a given water content is given by

$$HC = HC_{sat} \times (STOR/MAX)^B$$

where B is a constant determined from soil texture. Percolation is assumed to occur through the entire range of soil water contents for both *LOSOIL* and *DEEPSOIL*. The validity of this procedure depends, among other factors, on how well the constant B may be determined for a particular soil. B is equal to $2b+3$, where $-b$ is the slope of a log-log plot of soil water potential vs. water content obtained from moisture release experiments. Campbell (1986) found that b is mainly a function of the pore size distribution of a soil. Pore size distribution, in turn, is a function of soil texture. Using charts provided in Campbell (1986), B was estimated to be 17 and 25 for *LOSOIL* and *DEEPSOIL*, respectively.

Deep Soil Storage

Input to the deep soil storage, *DEEPSOIL*, is provided by percolation (*LOPERC*) from the lower soil storage tank. Outflow is the sum of transpirational losses (*ETLOSS*), subsurface flow (*DEEPFLOW*), and deep seepage losses (*SEEP*).

Water balance for a simulation time increment in *DEEPSOIL* is equal to

$$\text{DEEPSTOR}_2 = \text{DEEPSTOR}_1 + \text{LOPERC} - \text{ETLOSS} - \text{DEEPFLOW} - \text{SEEP}$$

where *DEEPSTOR1* and *DEEPSTOR2* are the water contents at the beginning and end of the time increment, respectively.

The deep seepage loss term (*SEEP*) is calculated in the same way as *LOPERC*. Direct measurements of deep seepage are not available. However, given the types of soil present and the highly weathered and fractured underlying geologic formations, deep seepage is likely. The assumption is considered to be the best one available, given the present level of knowledge of hydrologic processes on small forested watersheds of the Ouachita Mountains. The seepage loss topic is discussed further in the following chapter.

Quick Release Zone

Shallow subsurface flow (SSF) has previously been shown to contribute significant quantities of flow prior to or near the peak flow rate. The quick release zone (QRZ) was added to the model to conceptually simulate shallow subsurface flow from the steep slopes that surround the stream channels. It was not possible to develop a sound physically based routine for modeling SSF from the data gathered. Therefore, a conceptual approach was taken. The previous field study did show, however, that the area contributing to SSF varied as a function of precipitation.

The data also indicated that the contributing area was a function of soil water content. Since soil water content is determined continuously in the model, it was desired to develop a function that would predict the area contributing to SSF as a function of soil water content.

Field measurements of soil water content were not available. Therefore, the model was used to determine the mean soil water content in *LOSOIL*, expressed as the ratio of the current storage (*LOSTOR*) to the maximum storage (*LOMAX*), for the eight streamflow producing storms (Table 25). *LOSOIL* was assumed to be the horizon that exerted the greatest control on the generation of SSF. The contributing area (CA) in m² for each storm was calculated by multiplying together the contributing slope lengths calculated in the

TABLE 25
ESTIMATED QUICK RELEASE ZONE CONTRIBUTING
AREAS AND SOIL WATER CONTENTS

Storm Date	Contributing Slope Length (m)	AREA (m ²)	Mean LOSTOR (mm)	LOSTOR/ LOMAX
2/11	0.1	220	46	0.58
2/15	0.3	659	51	0.64
2/24	0.1	220	47	0.59
3/1	0.8	1756	60	0.75
3/17	1.8	3951	66	0.83
5/25	0.5	1098	55	0.69
5/28	5.1	11195	78	0.98
6/30	0.4	878	52	0.65

previous chapter (Table 11), the width of the three hillslope segments (5.4865 m), and the watershed scale factor. SSF from the litter layer and the A and B horizons were lumped for the contributing slope length calculation. SSF from the three sources are also lumped in the QRZ subroutine of the model and the analysis below. The contributing area was plotted against *LOSTOR/LOMAX* to observe the shape of the function (Figure 38). Contributing area (*QRZAREA*) appeared to be a logarithmic function of *LOSTOR/LOMAX*. Therefore, the natural log of the contributing area was regressed on *LOSTOR/LOMAX*.

The regression equation obtained was

$$\ln(\text{SSF contributing area}) = 0.075 + 9.764 (\text{LOSTOR/LOMAX}).$$

The regression equation showed that soil moisture in *LOSOIL* explained 96 percent of the variation in the natural log of the *QRZAREA*. The standard error of the estimate was 0.310. The regression equation was highly significant ($F = 126.84$, at a significance level of <0.005). However, the constant of the regression equation was not significantly different than zero in a two-tailed t-test where the test statistic was 0.118 and the significance level was 0.910.

The area of the *QRZ* is calculated for each simulation time increment in the *QRZ* subroutine. Input to the *QRZ* is provided by throughfall (*TFALL*). Quick release SSF (*QRZFLOW*) is calculated using the expression developed above

$$\text{QRZAREA} = \text{EXP}(\text{ZSLOPE} * \text{LOSTOR/LOMAX})$$

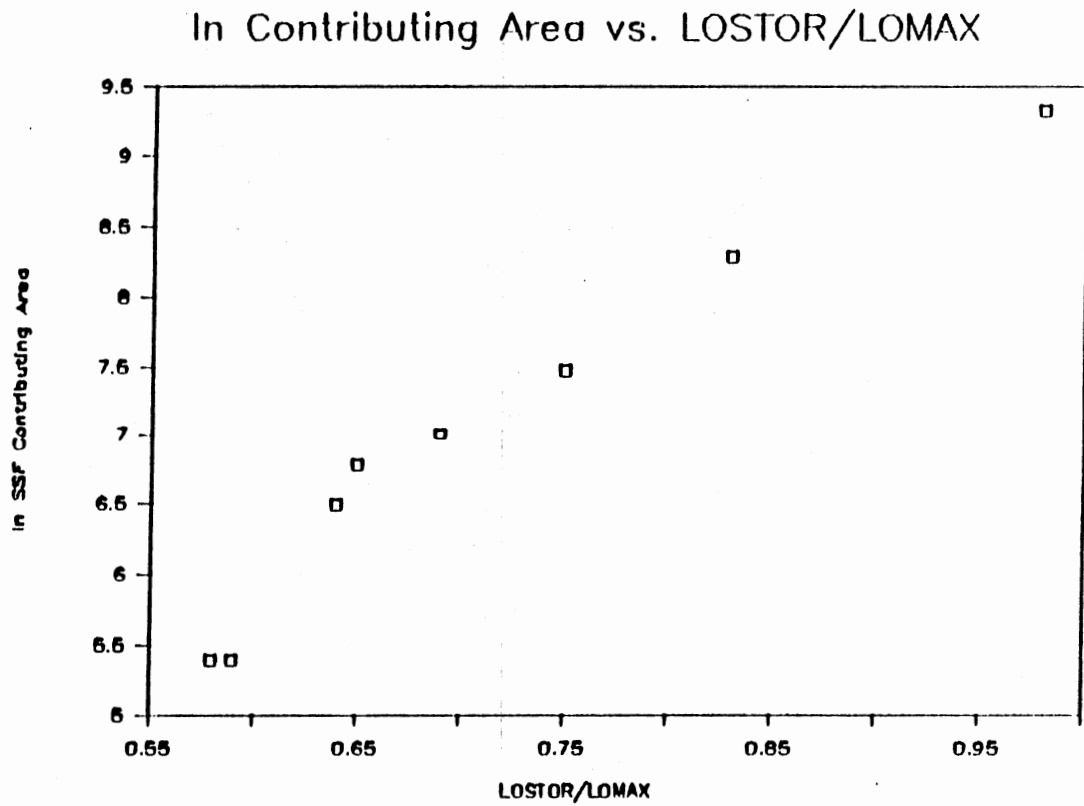


Figure 38. The Relationship Between Soil Water Content in *LOSOIL* (as *LOSTOR/LOMAX*) and the ln of the Estimated SSF Contributing Area

where *QRZAREA* is the contributing area and *ZSLOPE* is the slope of the semi-log regression curve. Quick release SSF (*QRZFLOW*) in liters, for a time increment is equal to

$$QRZFLOW = QRZAREA \times TFALL$$

where *QRZAREA* is in m² and *TFALL* is in mm. All *QRZVOL* produced in a time increment is released to streamflow in the same time increment. The form of the *QRZ* equation is similar to variable source area equations used in the BROOK model (Federer and Lash, 1978) and the USGS-PRMS model (Leavensley, et al., 1983). The variable source area equations in BROOK and PRMS presumably simulate the generation of runoff on saturated zones of the watershed (saturation return flow). The *QRZ* subroutine simulates shallow subsurface flow. The two processes may be described in a similar way mathematically, but are two distinctly different physical processes.

Riparian Zone

The stream draining Clayton Watershed #3 is ephemeral. An early version generated streamflow from channel interception even though the stream channels were, in reality, dry. Apparently, a certain quantity of water must be stored in the near-stream zone area before streamflow can occur. This storage in the riparian zone is defined as the riparian zone storage tank (*RIPSTOR*) (Figure 32). Conceptually, the riparian zone includes the stream channels and the

topographically low alluvial areas that surround parts of the channels (Figure 33). These areas combine to form 4 percent of the watershed area.

RIPSTOR is modeled as a simple tank with a fixed maximum storage (*RIPMAX*). All previously generated flow is routed through *RIPSTOR*. Additional input is provided by throughfall intercepted by the stream channel and litter percolation from the alluvial areas. The outflow from *RIPSTOR* is the predicted streamflow volume (*OUTFLOW*). All water in excess of *RIPMAX* is released as *QFLOW* in the same time increment. Since the riparian zone is vegetated, ET is removed from *RIPSTOR*. The incremental PET remaining after throughfall and litter interception is applied to *RIPSTOR*. AET is equal to the lesser of the remaining incremental PET or the available storage. AET is also a function of the moisture content of *RIPSTOR*. When the ratio of the current storage (*RIPSTOR*) to the maximum storage (*RIPMAX*) is greater than the field capacity of the gravelly soil (0.2), AET is equal to the potential rate. When *RIPSTOR/RIPMAX* is less than the field capacity 0.2, the ration of AET to PET decreases linearly from 1 to zero. The removal of water from storage in *RIPSTOR* by ET allows the storage to dry out between events.

Water balance within *RIPSTOR* is equal to

$$RIPSTOR_2 = RIPSTOR_1 + INFLOW - OUTFLOW - ETLOSS$$

where *INFLOW* is equal to

$$INFLOW = (TFALL \times CHANAREA) + (LPERC \times ALLUVAREA) + GRZVOL + (LOSSF \times LANDAREA) + (DEEPFLOW \times LANDAREA)$$

where *CHANAREA* is the area occupied by stream channels, *ALLUVAREA* is the area occupied by topographically low alluvial areas, *LANDAREA* is the watershed area not occupied by stream channels or alluvial areas. Unlike the other storages, *RIPSTOR* is expressed in volume (liters) units instead of depth units. *OUTFLOW* is converted to a mean discharge (*QFLOW*) for the simulation increment by

$$QFLOW = OUTFLOW / (DELTAT * 86400)$$

where *QFLOW* is in liters, *DELTAT* is in days, and 86400 is the number of seconds in a day.

In lieu of direct measurements of soil depths in the alluvial areas, *RIPMAX* was estimated from streamflow records for events that were preceded by dry conditions. The volume of precipitation (depth x *RIPAREA*), less canopy and litter interception required to initiate streamflow was assumed to equal *RIPMAX*. Estimated values of *RIPMAX* from 4 storm events ranged from 70,000 to 110,000 liters, or 0.9 to 1.4 mm of depth projected over the watershed area. The small quantity of storage is not important during large storms, but is important for predicting small storm events and annual water balance.

Water Chemistry Processes

The modeling objectives for water chemistry originally described were rather broad. It was felt that as a minimum, the model should be representative of the flow paths water takes and the levels of chemical transformation between sources. The watershed model hydrologic processes described above predict total streamflow as the sum of flows generated from different sources. The sources coincide with the sources studied in the field component (except *DEEPSOIL*). The field study provided estimates of the degree of chemical transformation water undergoes as it enters a watershed as precipitation and leaves as streamflow. Therefore, as a first attempt at modeling water chemistry, a simple approach using the hydrologic model and the field data was taken.

Chemical transport from a flow source was assumed to be equal to the long term source mean concentration (mg/l) times the incremental flow (liters) from each source. Long term source mean concentrations were calculated in the previous chapter (Table 15). The total chemical load entering *RIPSTOR* is equal to

$$\begin{aligned} &LANDAREA * [(LOSSF * LOCONC) + (DEEPFLOW * DEEPCONC)] \\ &+ (QRZFLOW * QRZCONC) \end{aligned}$$

The chemical load generated within *RIPSTOR* is equal to

$$(TFALL * CHANAREA * TFALLCONC) + (LPERC * ALUVAREA * LITCONC)$$

The total load entering *RIPSTOR* (*INLOAD*) is equal to the sum of the incoming load and the load generated within. All flow source loads are combined within *RIPSTOR* where complete mixing is assumed to occur. The concentration in the predicted streamflow is assumed to be equal to the mean concentration in *RIPSTOR* for the time increment (*RIPCONC*).

The model is capable of simulating the change in chemical concentrations within storms and predicting daily and annual loads. The mean concentrations of chemical constituents must be entered as input data. Currently, the model is capable of predicting chemical transport for only one constituent at a time.

It is acknowledged that the approach taken to model water chemistry is rather simplistic. The approach would limit the model's application to other watersheds unless chemistry information was available. More detailed and physically based approaches were investigated. However, the data necessary for more detailed approaches, such as initial storages of chemical constituents and rates of biological transformations were not available for watersheds in the region under study. Additionally limitations within the hydrologic component of the model did not justify a more detailed approach to the chemical transport component. It was felt that although simple, the approach taken would help identify future data needs and model improvements required to obtain better predictions.

CHAPTER VII
RESULTS AND DISCUSSION OF
WATERSHED MODELING STUDY

Introduction

The watershed water quality model discussed in the previous chapter was used to simulate streamflow and water chemistry from Clayton Watershed #3 for the 1986 and 1987 water years (10/1 - 9/30). The model was first run using a set of "standard parameters". The standard parameters represent the best estimates, obtained from measurement or available information, of the model parameters. Other runs of the model were made with selected parameter values changed, in order to demonstrate the sensitivity of various parameters.

Modeling With Standard Parameter Set

Standard Parameters

Thirty seven parameters are required as input for the hydrologic component of the model. An additional six parameters are required for each chemical constituent modeled in the chemical transport component. It was desired to see how the model performed using a set of

parameters that represented the "best estimate" of the parameters based on field measurements and available sources of information such as soil surveys. No optimization or calibration was performed. However, the author had to make some assumptions in estimating the parameters. Therefore, some parameter estimates may contain some personal bias.

The standard set of parameters, their expected range in value, and the units of measurement are summarized in Table 26. The input parameters for predicting chemical transport are summarized in Table 27. The expected ranges in values are based on the ranges in values for parameters that were obtained from measurements or as expressed in other sources. The sensitivity analysis performed for selected parameters later in this chapter used different parameter values within the expected ranges.

The total watershed area (*TOTAREA*) was measured from topographic maps developed from detailed surveys of the Clayton Experimental Watersheds. The stream channel area (*CHANAREA*) and the area occupied by topographically low alluvial areas (*ALLUVAREA*) were obtained by field measurement (Table 3).

The soil hydrologic properties were obtained from the Pushmataha County Soil Survey (Bain and Waterson, 1979) supplemented by additional detailed soil mapping performed by USDA Soil Conservation Service soil scientists. Soil depths (*__SOILDEP*) were obtained from the soil surveys and

TABLE 26
STANDARD INPUT PARAMETERS AND THEIR
EXPECTED RANGES IN VALUE

Parameter	Standard Value	Expected Range	Units
<u>Program Control</u>			
MAXINC	15	na	(days)
<u>Geomorphologic Characteristics</u>			
TOTAREA	77100	?	(m ²)
CHANAREA	1635	?	(m ²)
ALLUVAREA	1400	?	(m ²)
<u>Soil Hydrologic Properties</u>			
UPSOILDEP	200	152-254	(mm)
UPPOR	0.45	0.36-0.43	(mm/mm)
UPROCK	0.25	0.10-0.35	(mm/mm)
UPAWC	0.12	0.09-0.19	(mm/mm)
UPWILTP	0.05	0.03-0.08	(mm/mm)
LOSOILDEP	457	360-560	(mm)
LOPOR	0.40	0.40-0.45	(mm/mm)
LOROCK	0.20	0.15-0.25	(mm/mm)
LOAWC	0.13	0.08-0.18	(mm/mm)
LOWILTP	0.18	0.16-0.20	(mm/mm)
DEEPSOILDEP	350	220-420	(mm)
DEEPPOR	0.43	0.40-0.47	(mm/mm)
DEEPROCK	0.05	0.00-0.10	(mm/mm)
DEEPAWC	0.13	0.08-0.19	(mm/mm)
DEEPWILTP	0.27	0.22-0.28	(mm/mm)
HSATLO	350	366-1220	(mm/day)
BLOSOIL	17	?	
HSATDEEP	36	36-122	(mm/day)
BDEEP	25.1	?	
UPSTOR	14	?varies	(mm)
LOSTOR	34	with	(mm)
DEEPSTOR	37	year	(mm)
RIPSTOR	0	run	(mm)

TABLE 26 (continued)

Parameter	Standard Value	Expected Range	Units
<u>Potential Evapotranspiration</u>			
PANCOEFF	1	Pan coefficient for all months	
<u>Vegetative Characteristics</u>			
GROWSTOR	1.8	1.0-3.6	(mm)
DORMSTOR	0.43	0.10-0.6	(mm)
LITMAX	3.5	2.0-7.0	(mm)
UPWEIGHT	0.5	0.4-0.7	must add
LOWEIGHT	0.4	0.3-0.5	up to
DEEPWEIGHT	0.1	0.0-0.2	=1
<u>Subsurface Flow Tank Release Coefficients</u>			
KLO	0.0831	0.06-0.10	(days ⁻¹)
KDEEP	0.6102	0.50-0.70	(days ⁻¹)
<u>Quick Release Zone</u>			
ZSLOPE	9.77	8.40-11.1	
<u>Water Quality</u>			
TFCHEM			(mg/l)
LITCHEM	Concentration varies with the		(mg/l)
UPCHEM	constituent chosen. See		(mg/l)
LOCHEM	Tables 27 for mean concentrations		(mg/l)
DEEPCHEM	1987 and 1986 water years.		(mg/l)
QRZCHEM			(mg/l)

TABLE 27

CHEMICAL TRANSPORT INPUT PARAMETERS

PARAMETER	Mean Concentration of Constituent						
	H+ (mg/l)	NO3-N (mg/l)	DOC (mg/l)	Ca++ (mg/l)	Mg++ (mg/l)	K+ (mg/l)	Na+ (mg/l)
Water Year 1987							
TFCHEM	0.023529	0.28	55	0.65	0.13	2.89	0.2
LITCHEM	0.001851	0.22	314	2.78	1	3.13	0.35
UPCHEM	0.004056	0.24	99	1.39	0.91	1.24	0.87
LOCHEM	0.003311	0.09	50	0.86	0.92	1	1.43
DEEPCHEM	0.001355	0.008	21	0.82	0.78	0.62	1.91
QRZCHEM	0.001995	0.14	230	1.67	0.92	1.79	0.8
Water Year 1986							
TFCHEM	0.023529	0.39		1.1	0.36	0.68	0.26
LITCHEM	0.001851	0.33		2.2	1.3	1.34	0.28
UPCHEM	0.004056	0.22		2.64	1.55	1.16	0.34
LOCHEM	0.003311	0.09		0.86	0.92	1	1.43
DEEPCHEM	0.001355	0.008		0.82	0.78	0.62	1.91
QRZCHEM	0.001995	0.14		1.02	0.79	1.79	0.76

* Mean concentrations not available, 1987 data used

supplemented with measurements taken during the installation of the soil solution and SSF collectors. The wilting point (*__WILTP*) and porosity (*__POR*) estimates were obtained from average values for each soil texture (USDA SCS, 1984). The expected range in soil depth corresponds to data from the soil surveys and field measurements. The percent rock (*__ROCK*) was subtracted from the total soil storage capacity because estimates of soil porosity normally do not include rock in the solid phase. Porosity measurements are performed on homogenous samples of the soil containing only the soil particles themselves. The available water capacities (*__AWC*) and saturated hydraulic conductivities (*__HSAT*) were obtained from soil profile descriptions in the soil survey. All soil hydrologic property values were weighted against area and averaged to obtain estimates that reflect the areal variation in soil type across the watershed. Both the best estimate and the expected range reflect this averaging and the range in characteristics for each soil series as reported in the soil survey. The soil percolation equation constants (*BLOSOIL* and *BDEEP*) were calculated for each of the area weighted average soil textures using graphs and procedures in Campbell (1984).

No measurements of soil moisture were available for the watershed. Therefore, initial values for the soil storage tanks had to be estimated. Antecedent climatic conditions were used as a first attempt at the estimation. Later, the soil storage values predicted for the end of the 1986 water

year were used as the initial storage for the 1987 water year. The same values were used for the initial storages in the 1986 water year. Since streamflow did not exist at the start of either the 1986 or 1987 water year, the riparian storage was assumed to be dry ($RIPSTOR = 0$).

The methods used to estimate the remaining parameters were discussed in the previous chapter. The expected range in values for the vegetative characteristics were estimated from the literature. The expected range of the subsurface flow tank release coefficients were obtained from hydrograph analyses. The range in $ZSLOPE$ was calculated from the standard error of the \ln contributing area vs. $LOSTOR/LOMAX$ regression equation slope coefficient.

The watershed model calculates the soil storage tank properties from the input parameters. Using the standard parameters, the model calculates an average maximum saturated storage of 201 mm (Table 28). The total available water capacity (the sum of field capacity depths) is 129 mm. The total gravity water, or water that is available for subsurface flow release, is 72 mm. The soil storage properties obtained from the model seem reasonable for the soils in the region.

Annual Runoff and Water Balance

The watershed model predicted annual runoff, AET, deep seepage loss, and the change in storage for the 1986 and 1987 water years (Table 29). The model underpredicted the

TABLE 28

SOIL STORAGE PROPERTIES OBTAINED FROM THE
MODEL USING STANDARD PARAMETERS

Storage	Depth	Maximum Storage	Field Capacity	Gravity Water
	(mm)	(mm)	(mm)	(mm)
<i>UPSOIL</i>	200	68	24	44
<i>LOSOIL</i>	457	80	59	21
<i>DEEPSOIL</i>	350	53	45	7
Totals	1007	201	129	72

TABLE 29

PREDICTED ANNUAL WATER BALANCE FROM CLAYTON WATERSHED #3
FOR THE 1986 AND 1987 WATER YEARS

Water Year	Precipi- tation	Actual ET	Runoff	Deep Seepage	Storage Change
	(mm)	(mm)	(mm)	(mm)	(mm)
1987	1266	888	225	150	+10
1986	1752	893	545	318	+1

annual runoff by 9 (-4%) and 35 (-6%) mm for the 1987 and 1986 water years, respectively. Given the potential for error in the estimation of the parameters, the results

for annual flow prediction were considered to be good. No data is available to compare the predicted and actual AET and deep seepage loss. The results obtained seem reasonable, however, given the assumptions made. The effect of changing the ET and seepage parameters on annual water balance is discussed in the next section.

Annual Chemical Loads

The annual loads of 7 constituents were predicted by the model for the 1987 water year. Average source concentrations of dissolved organic carbon (DOC) were not available for the 1986 water year. The predicted chemical loads for the seven constituents were compared to measured loads for both water years (Table 30). Despite underpredicting runoff, the model consistently overpredicted chemical transport for all constituents for both water years.

Two reasons may account for the overpredictions. The model may not be dividing the flow between sources properly. If flow from a more potent source of a particular constituent is overpredicted, the resulting annual load would also be overpredicted. The second reason is the source chemistry means may be too high. The variation about the mean concentrations was large for all of the constituents (Tables 15 and 16). Observations of the data indicated that a few high concentrations increased the mean concentration.

TABLE 30
A COMPARISON OF PREDICTED AND MEASURED
CHEMICAL LOADS

Constituent	Predicted Load (kg)	Measured Load (kg)	Difference (kg)
<u>Water Year 1987</u>			
NO ₃ -N	1.9	0.8	1.1
DOC	1496	-	-
Ca ⁺⁺	18	14	4
Mg ⁺⁺	15	14	1
K ⁺	23	13	10
Na ⁺	22	-	-
H ⁺	0.08	0.02	0.06
<u>Water Year 1986</u>			
NO ₃ -N	5	5	0
Ca ⁺⁺	40	33	7
Mg ⁺⁺	37	26	11
K ⁺	46	28	18
Na ⁺	53	14	39
H ⁺	0.2	0.05	0.15

In a review of soil solution sampling methods. Litaor (1988) found that the type of sampler used can affect the results obtained. The type of sampler used in this study may also have affected the results. Following many storms, the collection buckets from the A and B horizon soil solution samplers were full. As a result, it was not clear when during a storm the samples were taken. More than likely, the samples were collected early in the storm, when greater quantities of the chemical constituents in the soil were available for transport. Mean concentrations of

constituents in SSF tended to be higher than the concentrations in the soil (Tables 15 and 16). The reasons for this result are not clear. Due to the length of pipe and large size of the collection tank, some problems in cleaning the SSF collection system between storms were encountered. However, if contamination was a problem, it would probably have occurred randomly. SSF mean concentrations were consistently higher than the soil solution concentrations.

Daily Runoff

Since the model operates on a daily time scale, predictions of daily runoff volumes were performed (Table 31). The daily runoff table provides information on how well the model performed throughout the water year. The model tended to overpredict daily runoff during periods preceded by dry antecedent conditions early and late in the water year (October - November, July - September). During other periods, the model generally underpredicted daily runoff. The reasons for the discrepancies between predicted and actual runoff are discussed in the next section on individual storm predictions.

Individual Storm Predictions

Streamflow

The watershed model produces continuous simulations of streamflow throughout a water year. An investigation of

predicted streamflow for the 1986 and 1987 water years was performed. The predicted data sets were reviewed completely. The results from four storms (Figures 39,40,41,and 42) are shown here as typical examples of the model's performance. The model's response to precipitation and timing of flow were generally good. However, the model underpredicted stormflow volumes in most cases (Table 32). The model tended to overpredict peak flows by producing large "spikes" of streamflow. The model typically underpredicted streamflow on the recession side of the hydrograph. An analysis of the storm of 5/28/87 shows that following the generation of a rapidly rising peak, the predicted flow dropped well below the actual flow. During recession, predicted flow is generated by the lower and deep soil storage tanks. The volume of water available for flow from the soil tanks is equal to the depth of water in excess of field capacity (__GRAV) times the watershed area less the riparian area (LANDAREA). Assuming that LANDAREA was measured correctly, the low simulated flows are a result of too little water in the __GRAV storages. The size of the __GRAV storages is determined by the difference between the maximum storage (__MAX) and the field capacity (__FCAP). The amount of water in the storage at a given time, however, is determined by a number of inter-related factors such as ET and percolation and storage release rates.

TABLE 31
SIMULATED AND ACTUAL DAILY RUNOFF
WATER YEAR 1987

Month	Day	Actual Runoff (liters)	Simulated Runoff (liters)	Difference Predicted- Actual (liters)
10	1	0	0	0
11	3	0	0	0
11	4	2010410	215610	14200
11	5	6006	24884	18878
11	6	0	0	0
11	9	0	0	0
11	10	23	167197	167174
11	11	782	124926	124144
11	12	0	0	0
11	24	0	0	0
11	25	0	1801	1801
11	26	0	0	0
12	6	0	0	0
12	7	111518	444183	332665
12	8	210054	497937	287883
12	9	173284	199817	26533
12	10	43458	43784	326
12	11	11138	24571	13444
12	12	0	7647	7647
12	13	0	618	618
12	14	0	11469	11469
12	15	0	0	0
12	17	0	0	0
12	18	0	13101	13101
12	19	0	0	0
1	2	0	0	0
1	3	50181	121073	70892
1	4	24347	331	-24016
1	5	3345	33648	30303
1	6	0	0	0
1	7	0	11859	11859
1	8	293	12502	12209
1	9	806285	1061969	255684
1	10	232108	80561	-151547
1	11	118346	38681	-79665
1	12	73763	19979	-53784
1	13	31544	6994	-24550
1	14	14925	50	-14875
1	15	123131	120511	-2650
1	16	287486	337881	50395
1	17	283951	310949	26998
1	18	1310748	1063597	-247151

TABLE 31 (Continued)

Month	Day	Actual Runoff (liters)	Simulated Runoff (liters)	Difference Predicted- Actual (liters)
1	19	356045	83736	-272309
1	20	175088	39195	-135893
1	21	139107	20329	118778
1	22	50127	8670	-41457
1	23	82980	1281	-81699
1	24	49394	9086	-40308
1	25	13168	0	-13168
1	26	9513	0	-9513
1	27	5779	0	-5779
1	28	57	0	-57
1	29	0	0	0
1	31	0	0	0
2	1	30618	0	-30618
2	2	24854	0	-24854
2	3	10003	0	-10003
2	4	1199	0	-1199
2	5	622	0	-622
2	6	3680	0	-3680
2	7	6642	0	-6642
2	8	2573	0	-2573
2	9	0	0	0
2	12	0	0	0
2	13	27411	0	-27411
2	14	35726	0	-35726
2	15	237448	95569	-141879
2	16	136891	57704	-79187
2	17	66326	26446	-39880
2	18	81405	0	-81405
2	19	84401	15698	-68703
2	20	62776	0	-62776
2	21	42950	0	-42950
2	22	21397	4234	-17163
2	23	33183	0	-33183
2	24	139879	113138	-26741
2	25	121407	18824	-102583
2	26	388342	462906	74564
2	27	373995	183485	-190510
2	28	1374806	1382499	7693
3	1	500071	155865	-344206
3	2	154665	44526	-110139
3	3	137596	13167	-124429
3	4	108114	2252	-105862
3	5	63483	13186	-50297
3	6	67166	0	-67166
3	7	30647	0	-30647
3	8	14100	0	-14100
3	9	19029	0	-19029

TABLE 31 (Continued)

Month	Day	Actual Runoff (liters)	Simulated Runoff (liters)	Difference Predicted- Actual (liters)
3	10	4075	0	-4075
3	11	0	0	0
3	16	0	0	0
3	17	1819916	1403371	-416545
3	18	398372	91442	-306930
3	19	184620	31393	-153227
3	20	94769	7177	-87592
3	21	66764	21202	-45562
3	22	42073	0	-42073
3	23	59047	0	-59047
3	24	49058	0	-49058
3	25	36938	0	-36938
3	26	43108	0	-43108
3	27	49769	0	-49769
3	28	28761	0	-28761
3	29	20694	0	-20694
3	30	14071	0	-14071
3	31	5137	0	-5137
4	1	3994	0	-3994
4	2	0	0	0
4	12	0	0	0
4	13	20101	0	-20101
4	14	2487	0	-2487
4	15	0	0	0
5	4	0	0	0
5	5	15	0	-15
5	6	0	0	0
5	19	0	0	0
5	20	20	0	-20
5	21	0	0	0
5	22	9	0	-9
5	23	0	1915	1915
5	24	1	0	-1
5	25	165452	90659	-74793
5	26	2557	0	-2557
5	27	0	0	0
5	28	2553276	2117239	-436037
5	29	1580648	1016693	-563955
5	30	267321	58753	-208568
5	31	271877	48900	-222977
6	1	143661	21237	-122424
6	2	32313	3222	-29091
6	3	1987	0	-1987
6	4	0	0	0
6	18	0	0	0
6	19	113	0	-113
6	20	0	0	0

TABLE 31 (continued)

Month	Day	Actual Runoff (liters)	Simulated Runoff (liters)	Difference Predicted- Actual (liters)
6	21	0	0	0
6	22	0	0	0
6	23	3407	0	-3407
6	24	0	0	0
6	29	0	0	0
6	30	103160	75101	-28059
7	1	0	0	0
7	8	0	0	0
7	9	85230	388856	303626
7	10	0	0	0
9	9	0	0	0
9	10	509	28600	28091
9	11	0	0	0
9	14	0	0	0
9	15	268	468713	468445
9	16	0	551952	551952
9	17	0	0	0
9	18	664929	2881407	2216478
9	19	2822	216964	214142
9	20	0	34803	34803
9	21	0	8971	8971
9	22	0	941	941
9	23	0	0	0
9	27	0	0	0
9	28	29	0	-29
9	29	0	0	0
9	30	0	0	0

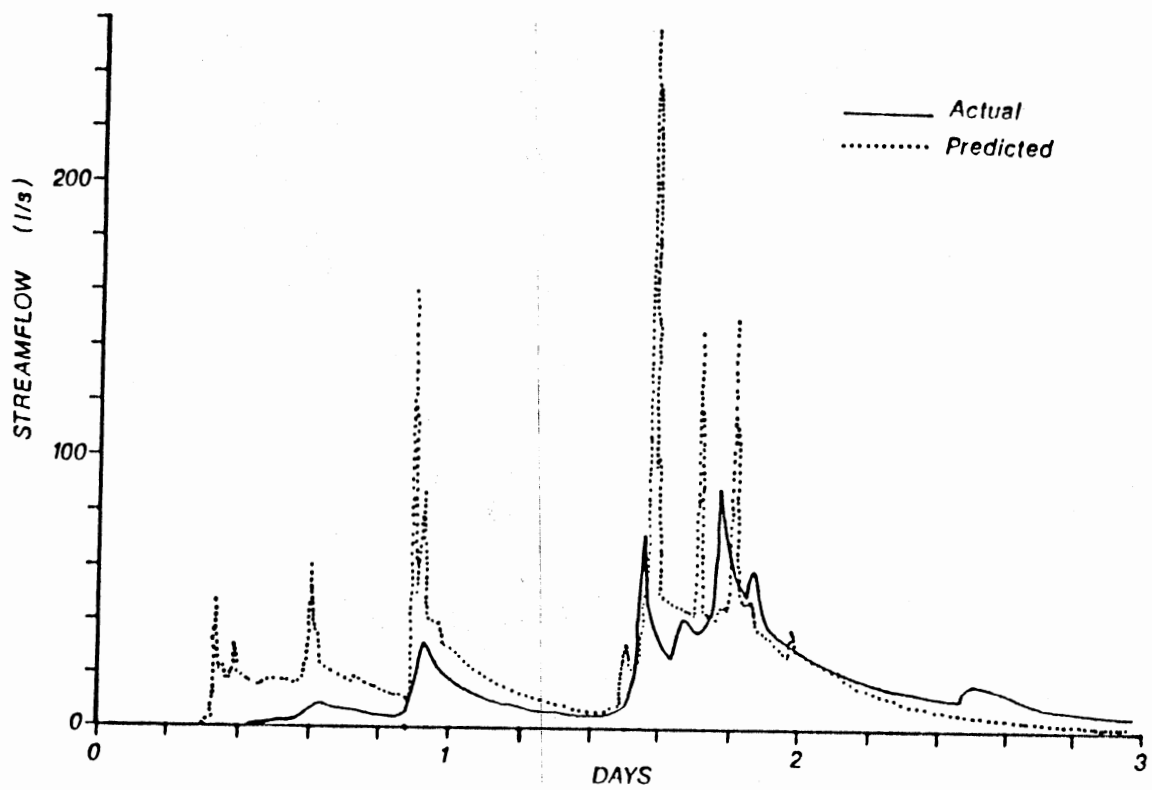


Figure 39. Comparison of Actual and Predicted Streamflows for the Storm of 11/17-11/19/85

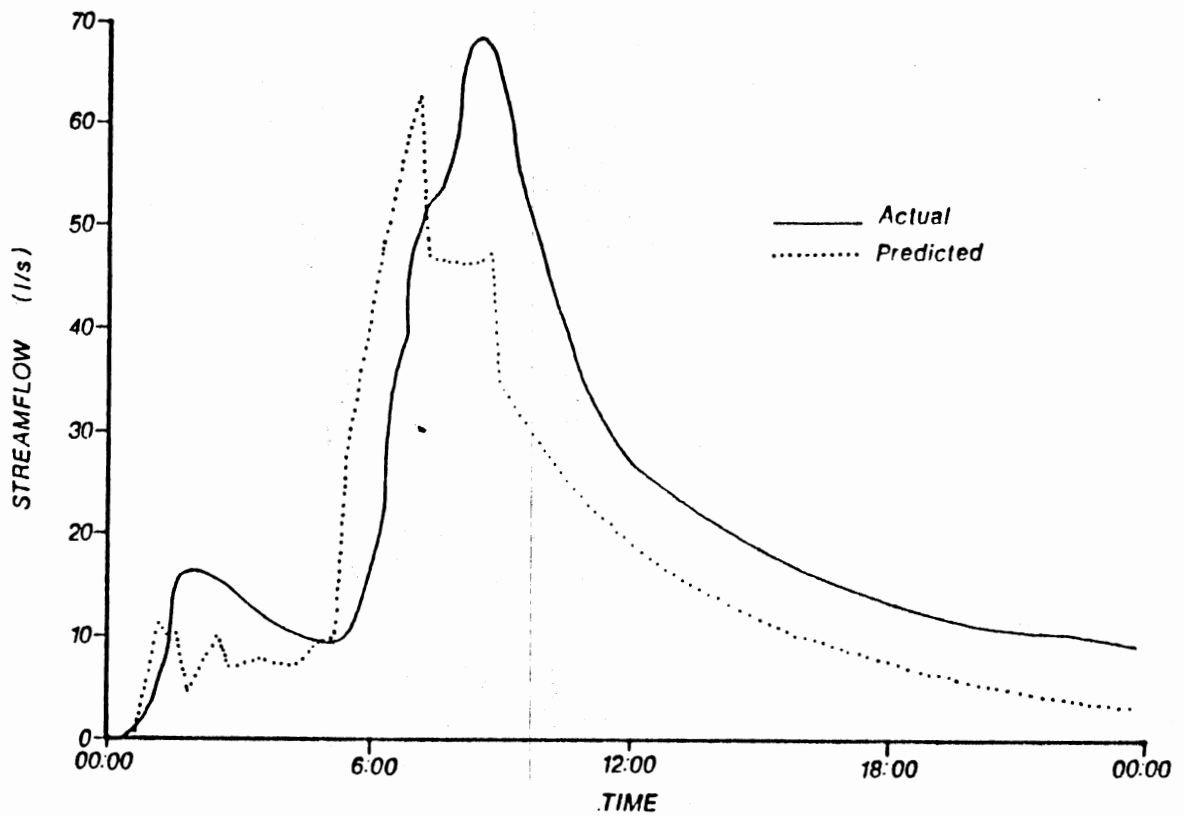


Figure 40. Comparison of Actual and Predicted Streamflows for the Storm of 3/17/87

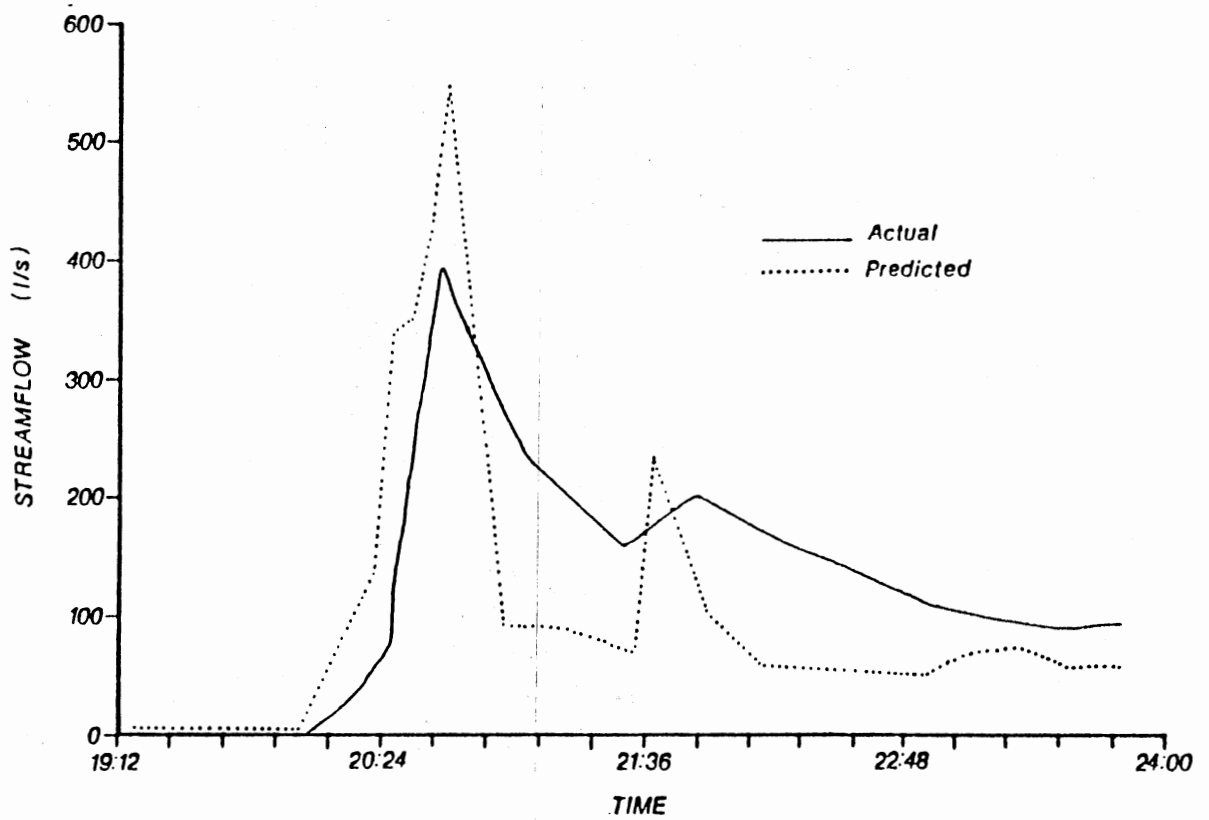


Figure 41. Comparison of Actual and Predicted Streamflows for the Storm of 5/28/87

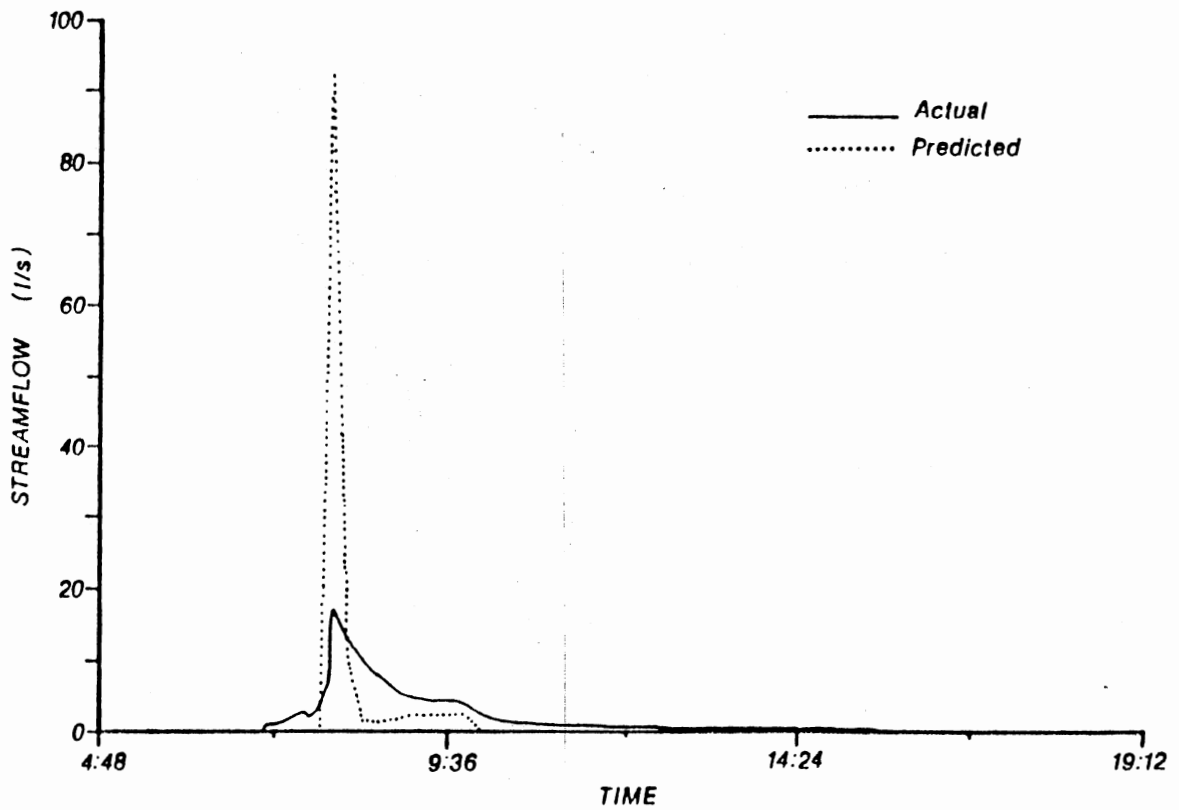


Figure 42. Comparison of Actual and Predicted Streamflows for the Storm of 6/30/87

TABLE 32
COMPARISON OF ACTUAL AND PREDICTED
STORMFLOW VOLUMES AND PEAK FLOW RATES

Storm Date	Actual Volume (1)	Predicted Volume (1)	Actual Peak (1/s)	Predicted Peak (1/s)
11/17/86	3663674	4747956	88	255
3/17/87	1819916	1403371	68	64
3/18/87	398372	91442		
3/19/87	184620	31393		
5/28/87	2553276	2117239	393	547
5/29/87	1580648	1016693		
5/30/87	267321	58753		
6/30/87	103160	75101	17	92

Baseflow following stormflow was generally underpredicted. Simulated baseflow also did not extend as long as did actual baseflow. Too little water in the *DEEPGRAV*, or too rapid of a seepage rate may be the reasons for the underprediction of base flow. The model did, however, generate more simulated flow than actual flow during certain periods. For example, during the months of October and November of water year 1987, the model generated more flow than actual flow. The fall months represent a period of soil moisture storage buildup. The generation of excessive simulated flow may have been due to the soil storages being too small, or the estimate of the initial soil storages being too large.

Chemistry

The watershed model produces output in the form of continuous predictions of streamwater chemistry for the constituent chosen. The predictions for the 1986 and 1987 water years were performed for the constituents listed in the annual chemical load table (Table 30). For all constituents, the predicted annual chemical loads were greater by 107 to 378 percent than the actual loads. A review of the predicted streamflow-chemical concentration files showed that for all constituents, predicted concentrations were generally higher during the early parts of a storm than the actual concentrations. The difference between the predicted and actual concentrations during recession flows and base flows depended on the constituent under study. Due to the large volume of data and similarity of predicted results between constituents, detailed analysis of the model predictions will be limited to two constituents, $\text{NO}_3\text{-N}$ and Ca^{++} . $\text{NO}_3\text{-N}$ was chosen because of its high solubility, mobility and significance as a plant nutrient and a non-point source pollutant. Ca^{++} was chosen as a representative less mobile and reactive cation.

The predicted concentrations of $\text{NO}_3\text{-N}$ were plotted with the actual concentrations and actual streamflow to observe the model's behavior. Actual $\text{NO}_3\text{-N}$ concentrations tend to rise rapidly in the early parts of the storm, and decline to a low baseline level near or soon after peak flow. This

hysteresis of $\text{NO}_3\text{-N}$ concentration has also been observed to occur on Clayton Watershed #1 (Lawrence and Wigington, 1988) and during other storms on Clayton Watershed #3. The model predicts a high concentration of $\text{NO}_3\text{-N}$ at the beginning followed by a gradual decline to a low base level concentration (Figure 43). However, the predicted concentrations are continuously too high by 3 to 5 times throughout the storm. The same trend occurred during predicted storms not illustrated here.

The possible reasons for the overpredictions in $\text{NO}_3\text{-N}$ concentrations are the same as for the overpredictions in the annual $\text{NO}_3\text{-N}$ loads. The model calculates the concentration of $\text{NO}_3\text{-N}$ as a function of flow and a mean concentration. The observed hysteresis effect of the actual concentrations of $\text{NO}_3\text{-N}$ may be the result of potent sources of $\text{NO}_3\text{-N}$ contributing to flow early in a storm. However, $\text{NO}_3\text{-N}$ may also be supply limiting. The supply of available $\text{NO}_3\text{-N}$ in the soil is increased by atmospheric deposition, organic decomposition and mineralization, and decreased by plant uptake, denitrification and leaching (Frere, et al., 1980). It is possible that the pool of available $\text{NO}_3\text{-N}$ in the soils of Clayton Watershed #3 is depleted very rapidly at the beginning of a storm. The change in soil solution $\text{NO}_3\text{-N}$ concentration early in a storm would not be detected by the lumped-sample soil solution collectors used in the field study. The rapid depletion of available $\text{NO}_3\text{-N}$ in combination with the generation of flow from sources

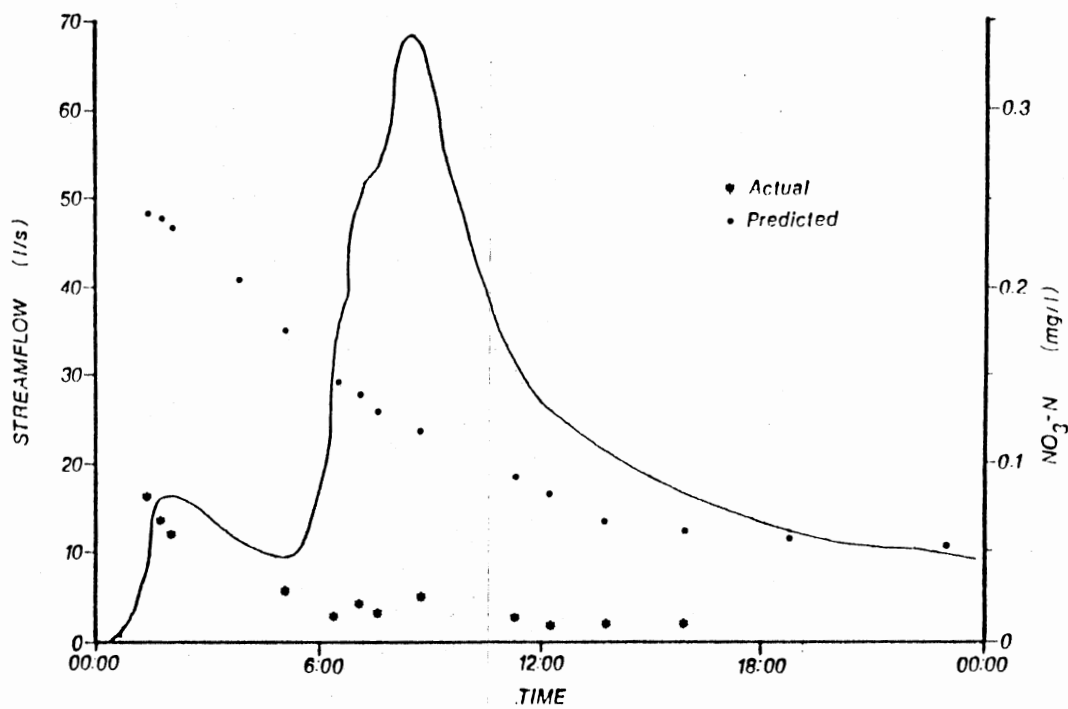


Figure 43. Comparison of Actual and Predicted NO₃-N Concentrations for Storm of 3/17/87

having greater amounts of available $\text{NO}_3\text{-N}$ probably combine to produce the actual hysteresis in $\text{NO}_3\text{-N}$ concentrations.

Another possible reason for the over-prediction of $\text{NO}_3\text{-N}$ concentrations is the manner in which the model mixes flow in the riparian storage tank. Water percolating through the litter in the alluvial soils, a high source of $\text{NO}_3\text{-N}$, is assumed to enter the stream directly and mix with flow from the other sources. In reality, the flow generated in the alluvial zones may penetrate deeper in the soil, undergo chemical transformations, and emerge downslope as streamflow. The deeper mixing may cause a loss of $\text{NO}_3\text{-N}$ and result in an actual concentration that is lower than the assumed concentration. To date, little is known about the chemical processes in the zone immediately around the stream channels.

Calcium and other cations show little fluctuation with streamflow. An investigation of the data file of actual streamflow and chemistry confirmed this observation. A slight decrease in the concentration of calcium (and other cations) is observed prior to peak flow (Figure 44). However, the reductions in concentrations are small, approximately 15 percent or less. Soon after peak flow, the concentrations rise back to a base level concentration that is on the order of 10 percent less than the concentrations that occur initially in the storm. The model predicts the rises and falls in the concentration of calcium reasonably well (Figure 44). However, as with $\text{NO}_3\text{-N}$, the predicted

concentrations are continuously too high. The possible reasons for the over-prediction cited previously also pertain to calcium and the other cations.

Modeling With Different Sets of Parameters

The set of "standard" parameters represented the best estimate or the average value within an expected range of values. From the results obtained from the model, there is good reason to believe that some of the parameter estimates could be improved. No formal mathematical calibration procedure was performed on the model. However, different estimates of certain parameter values were used to observe the sensitivity of the predicted results to the change in parameter values.

After observing the behavior of the model, it became apparent that the set of evaporation pan coefficients and the deep seepage routine were important to the modeling of water balance. These two functions represent the greatest losses of water from the watershed system. They also represent two parts of the model for which the least amount of information could be obtained or measured. As mentioned previously, in lieu of better information, the monthly pan coefficients were held constant at a value equal to one. A set of pan coefficients used in the modeling of a small forested watershed in Kentucky, were obtained from the literature (Leavesly, et al. 1983). The pan coefficients

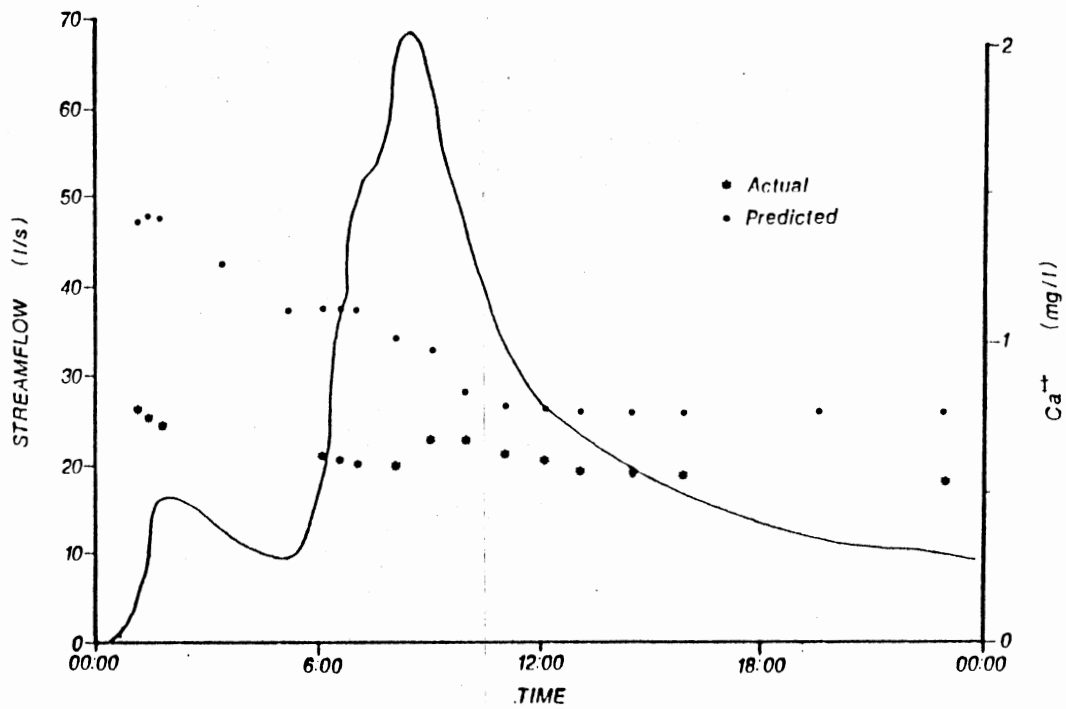


Figure 44. Comparison of Actual and Predicted NO_x-N Concentrations for the Storm of 3/17/87

were 1, 0.9, 0.8, 0.8, 0.9, 1, 1, and 1.2, for the months of October, November, December, January, February, March, April, and May through September, respectively. The new set of pan coefficients were entered into the model and all other parameters were kept at the standard values. The resulting increase in ET reduced annual runoff by 4 percent for both the 1987 and 1986 water years (Table 33). Percolation and soil moisture storage were also reduced. The question may arise as to whether or not there actually is deep seepage loss on Clayton Watershed #3. The assumption that deep seepage loss does occur was based on observations of actual rainfall-runoff data and of the soils and geology at the site. To observe the effect of no deep seepage on the predicted results, the model was run with *DEEPSEEP* set equal to zero, with the new set of pan coefficients, and with all other parameters set at the standard values. As a result of no seepage loss, the predicted runoff was increased by 60 and 50 percent for the 1987 and 1986 water years, respectively. The new predicted annual runoff values are well above the actual values. It is doubtful that increasing the ET pan coefficients further would be realistic, or effective at extracting more water. Therefore, the only reasonable way to account for water balance would be through deep seepage loss. Whether or not the deep seepage function in the model represents the true process remains uncertain.

TABLE 33

SENSITIVITY OF PREDICTED ANNUAL WATER BALANCE TO CHANGES
IN PAN COEFFICIENTS AND THE PERCOLATION FUNCTION

Water Year	Precipitation (mm)	Actual ET (mm)	Runoff (mm)	Deep Seepage (mm)	Storage Change (mm)
<u>Standard Parameters</u>					
1987	1266	888	225	150	+10
1986	1752	893	545	318	+1
<u>New ET Pan Coefficients</u>					
1987	1266	903	216	151	+1
1986	1752	945	523	297	-13
<u>No Percolation and New ET Pan Coefficients</u>					
1987	1266	911	359	0	+1
1986	1752	952	823	0	-10

Since the majority of the incoming precipitation is routed through the soil tanks, it would be reasonable to assume that predicted streamflow would be sensitive to changes in the soil tank parameters. Therefore, the model was run a number of times with different soil tank parameters. The results of all of these tests will not be presented here. However, some general conclusions from the tests can be drawn. Any change in a soil tank parameter that tended to allow flow to be released sooner or faster, increased stormflow and annual runoff. Conversely, any change in a soil tank parameter that tended to increase the

storage below field capacity or allowed flow to be released more slowly, reduced stormflow and annual runoff.

For example if *LOAWC* were reduced, the storage below *LOFCAP* would be reduced. Streamflow would occur sooner, and the pool of water from which ET could extract water would be reduced. Hence, both stormflow and annual flow would be increased. Two values of *LOAWC* (0.10 and 0.15 mm/mm) were used in the model, with all other parameters at the standard values, to observe the effect of the change on predicted flows for the 1987 water year. The values were chosen from within the expected range of the parameter. The reduction of *LOAWC* by 23 percent decreased *LOFCAP* by 22 percent (from 59 to 46 mm) and increased annual runoff by 70 percent (from 225 mm to 381 mm). The increase in *LOAWC* of 13 percent increased *LOFCAP* by 13 percent (from 59 to 69 mm/mm) and decreased annual runoff by 34 percent (from 225 to 148 mm).

The change in *LOAWC* also affected the timing and rate of predicted stormflow (Figure 45). Reducing *LOAWC* to 0.10 changed the predicted peak flow from 62 to 65 l/s and increased recession flows throughout the storm. Increasing *LOAWC* to 0.15 reduced the predicted peak flow from 62 to 50 l/s and reduced predicted streamflow throughout the storm.

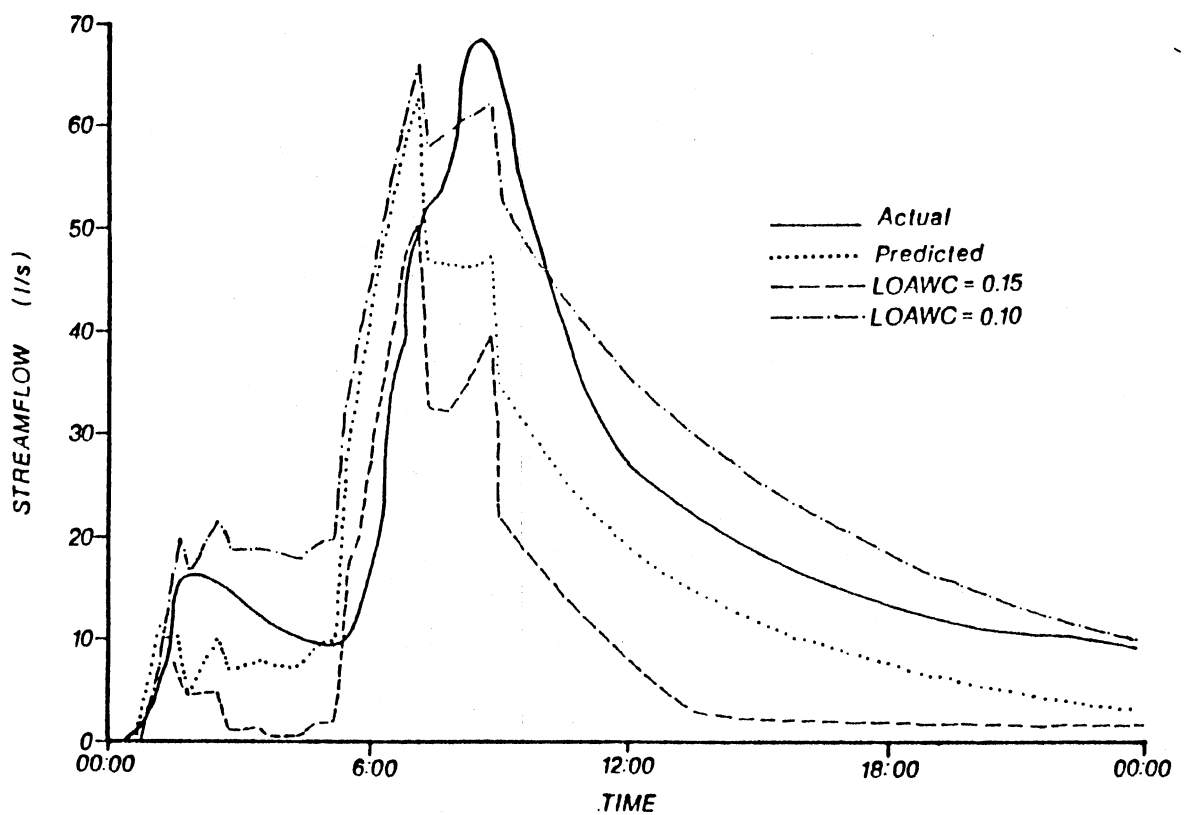


Figure 45. Parameter Sensitivity of *LOAWC* on the Predicted Streamflow of the Storm of 3/17/87

The water chemistry parameter sensitivity was not tested. However, since the predicted load is a function of a mean concentration times predicted flow, any parameter that significantly affects flow would affect the predicted chemical load. The predicted loads and concentrations would also be highly sensitive to changes in the mean concentration estimates.

CHAPTER VIII

CONCLUSIONS

Field Study Conclusions

Shallow subsurface flow (SSF) was found to be a major streamflow generating process on the study watershed. SSF generated up to 48 percent of the total streamflow volume for specific storm periods. The actual quantity of SSF produced was found to be an exponential function of precipitation quantity. The quantity of SSF was also found to be a function of precipitation intensity and duration and the antecedent soil moisture. SSF was generated rapidly and early during storm events, thereby contributing to the generation of peak flow rates. SSF commenced within 15 minutes of the onset of precipitation from even the deepest horizons. The rapid release of SSF suggested that a mechanism such as rapid flow through macropores exists. The area of the watershed contributing to SSF was found to be small and limited to steep slopes surrounding the incised stream channels.

SSF was also found to contribute significantly, from 65 to 200 percent for $\text{NO}_3\text{-N}$, of the total stream chemical load for specific storm periods. The percentage of the total stream load supplied by SSF was a function of the chemical

constituent and the quantity of SSF produced. Since SSF is released rapidly during storm events, chemicals in SSF are also released rapidly and early during storm events. The rapid release of chemicals through SSF helps to explain the early and rapid rise in stream chemical concentrations that have been observed during storm events on the watershed.

Watershed Modeling Conclusions

The watershed hydrology and chemical transport model developed in the study used storage tanks to represent hydrologic processes, similar to the BROOK (Federer and Lash, 1978), Kentucky Daily (Sloan, et al., 1983) and USGS PRMS (Leavely, et al., 1983) watershed models. The model differs from the previously mentioned watershed models in that the storage tanks were assembled in a unique way to represent the conditions found on the study watershed. The division of the watershed into the riparian and quick release zones was based on measurements and observations made during the field component of the study. The riparian zone concept is somewhat site specific, but should hold for small watersheds having incised stream channels and small topographically low alluvial areas surrounding the stream channels. Such conditions are common to small watersheds found in the Ouachita Mountains. The quick release zone functions were obtained from the field measurements of shallow subsurface flow.

The model program was designed for efficient operation and flexibility. The model is capable of simulating individual storm events, daily flows, and the annual water balance. The model is also designed to simulate storm chemical concentrations and daily and annual chemical loads. Although the chemical transport routines are presently very simple, the storage tank concept and model structure allows for the easy future addition of more complex routines. The model could also be used to continuously simulate soil moisture, throughfall, or any component of the hydrologic cycle with minor changes in the output statements. The model structure is flexible in that different subroutines for hydrologic processes may be substituted without affecting the entire model operation.

The majority of the parameters required in the model may be estimated by direct field measurement or obtained from the literature. Streamflow data is required for the estimation of streamflow recession constants. The quick release zone (QRZ) is the most conceptual component of the model. The QRZ parameters were estimated from the field measurements of shallow subsurface flow. In lieu of such information, the QRZ parameters would have to be obtained by calibration. The QRZ flow function is mathematically similar to variable source area functions found in the BROOK, PRMS and Kentucky Daily models. It differs conceptually because it represents a different hydrologic process.

Using a set of parameters that represented the "best" initial estimate that could be made with no calibration, the model provided good predictions of streamflow and water chemistry. The predicted annual runoff for the two water years simulated were within 10 percent of the actual values. The predicted streamflow increased and decreased in response to precipitation in a pattern that generally matched the actual streamflow. As a first attempt at modeling the study watershed, the model performed well.

Suggestions for Future

Field Research

The field study of subsurface flow essentially used a black box approach, inputs and outputs were measured, but processes within the box, or hillslope, were not. A better understanding of the flow generating processes within hillslopes is required to extrapolate the results of limited field studies to other watersheds and to create physically based algorithms that can be used to improve watershed models. A future hillslope hydrologic processes study should include, but not be limited to, the following considerations.

Better measurements of basic soil properties and their range and distribution of values are required. Such an investigation would include the nature and extent of soil macropores. Improved measurements or estimates of soil hydraulic conductivity as affected by macropores such as

those performed by Kneale (1985) and Watson and Luxmoore (1986) would be helpful.

The physics of flow through the hillslope could be better defined with a system of recording piezometers and/or tensiometers and continuous measurement of soil moisture. The additional soil moisture and water tension data, together with better soil physical property measurements and a subsurface flow collection system, would provide a more complete description of the physical factors responsible for generating flow within the soil. The added knowledge could be used to better define the flow paths and flow path length of subsurface flow. An understanding of the physical processes on undisturbed sites would also help in gaining a better understanding of how and to what extent future land use changes may affect streamflow from forested watersheds.

Suggestions for Future

Model Improvements

Measurements of AET from the Clayton Watersheds were not available. ET is a difficult process to measure, yet is necessary to confirm assumptions made in water balance models. Another approach to estimating ET is to account for all other components of the water balance including deep seepage loss. Little is known about the deep seepage process on small watersheds in the Ouachita Mountains. However, given the highly weathered and fractured rock

formations found in the region it is suspected to occur. The actual seepage process would probably be highly spatially variable and difficult to measure. Additional information on the soil hydraulic properties also needs to be gathered. Data from the soil survey and limited measurements were used in the model. No accounting of macropore flow or macroporosity were made. The nature and distribution of such pores could drastically affect the mode of flow in, and the storage capacity of the soil. The range of and distributions of soil property values must be adequately described to obtain useful mean values for lumped parameter models. The same reasoning also holds true for parameters describing chemical transport.

Improved parameter estimates is one method to improve the predictions of the model. Other changes would also be helpful. An ET function that was more closely connected to the vegetative cover would make the model more physically-based. An ET function that uses stand density and leaf area index, such as that used in the BROOK model (Federer and Lash, 1978) could be used. Such an approach links together the ET processes and the vegetative cover, and eliminates the need for relying on questionable pan coefficients. Near stream zone processes, including the riparian area and the quick release SSF zone, need to be made more physically-based so the model could be applied to other watersheds. Improvements in the description of flow within the soil, such as a macropore drainage function, could also be made.

The need for an improved deep seepage loss function has already been mentioned.

The prediction of water chemistry would benefit greatly from improvements in the hydrologic component. However, the water chemistry routines could also be improved. A simple exponential decline in $\text{NO}_3\text{-N}$ concentrations in various storages could improve the prediction of $\text{NO}_3\text{-N}$ concentrations. The storage tank concept of the model is amenable to adding "chemical storage" and transformation routines to each tank. The quantity of each constituent and the transformation of the constituents (ie: denitrification, mineralization, cation exchange) could be accounted for in each storage. Additional parameters would be needed for such an approach, but the modeler would also be freed from using perhaps questionable mean concentration values.

LITERATURE CITED

- Ahuja, L.R. 1986. Characterization and modeling of chemical transfer to runoff. IN: Stewart, B.A., ED. Advances in Soil Science, Vol 4, Springer-Verlag, N.Y., pp 149-188.
- American Public Health Association. 1980. Standard Methods For the Examination of Water and Wastewater, 15th Edition. APHA, Washington D.C. 1134p.
- Anderson, M.G. and T.P. Burt. 1985. Modeling strategies IN: Anderson, M.G. and T.P. Burt, Eds. Hydrological Forecasting. John Wiley & Sons, Chichester, U.K. pp 1-13.
- Atkinson, T.C. 1978. Techniques for measuring subsurface flow on hillslopes. IN: Kirkby, M.J., ed., Hillslope Hydrology. John Wiley, New York. pp. 73-120.
- Bain, Wm. R. and A. Watterson. 1979. Soil survey of Pushmataha County, Oklahoma. USDA Soil Conservation Service, Washington, D.C., 153p.
- Beasley, R.S. 1976. Contribution of subsurface flow from the upper slopes of forested watersheds to channel flow. Soil Sci. America Proc. 40: 955-957.
- Beasley, D.B. and L.F. Huggins. 1982. ANSWERS (Areal nonpoint source watershed environment response simulation) users manual. U.S. EPA-905/9-82-001. U.S. Environmental Protection Agency, Region V.
- Beasley, D.B., L.F. Huggins, and E.J. Monke. 1980. ANSWERS: A model for watershed planning. Transactions of the ASAE 23(4): 938-944.
- Bernier, P.Y. 1985. Variable source areas and storm-flow generation: An update of the concept and simulation effort. Journal of Hydrology 79: 195-213.
- Betson, R.P. and C.V. Ardis. 1978. Implications for modeling surface water hydrology. IN: Kirkby, M.J., Ed., Hillslope Hydrology, John Wiley & Sons, N.Y. pp 295-323.
- Betson, R.P. and J.B. Marius. 1969. Source areas of storm runoff. Water Res. Research. 5(3): 574-582.

- Beven, K.J. and M.J. Kirkby. 1979. A physically based, variable contributing area model of basin hydrology. *Hydrological Sciences Bulletin* 24(1): 43-69.
- Bevin, K. and P. Germann. 1981. Water flow in soil macropores II. A combined flow model. *J. Soil Sci.* 32: 15-29.
- Bevin, K.J. and E.F. Wood. 1983. Catchment geomorphology and the dynamics of runoff contributing areas. *Journal of Hydrology* 65: 139-158.
- Beven, K.J., M.J. Kirkby, N. Schofield, and A.F. Tagg. 1984. Testing a physically-based flood forecasting model (TOPMODEL) for three U.K. catchments. *Journal of Hydrology* 69: 119-143.
- Burges, S.J., 1986. Trends and directions in hydrology. *Water Res. Research* 22(9):1S-5S.
- Campbell, G.S. 1986. Soil Physics With BASIC. Elsevier Science Publishers, N.Y., 150p.
- Campbell, G.S. 1974. A simple method for determining unsaturated conductivity from moisture retention data. *Soil Science* 117(6):311-314.
- Campbell, K.L., M. Yaramanoglu, and F.R. Crow. 1983. The USDAHL hydrologic model. IN: Smolen, M.D., Ed. *Hydrologic and water quality models for agriculture and forestry*. Southern Cooperative Series Bulletin No. 291, pp 19-32.
- Chapman, T.G., P.J. Bliss, and I.C. Smalls. 1982. Water quality considerations in the hydrological cycle. IN: O'Loughlin, E.M. and P. Cullen, Eds., *Prediction in Water Quality, Proceedings of a Symposium on the Prediction of Water Quality*, Australian Academy of Science, Canberra, Nov. 30-Dec.2, 1982, pp 27-68.
- Christophersen, N., H.M. Seip, and R.F. Wright. 1982. A model for streamwater chemistry at Birkenes, Norway. *Water Resources Research* 18(4): 977-996.
- Chow, T.L. 1976. A low-cost tipping bucket flowmeter for overland flow and subsurface stormflow studies. *Can. J. Soil Sci.* 56:197-202.
- Clingenpeel, A.J. 1978. Hydrologic and nutrient relationships on a pine-hardwood forest in southeastern Oklahoma. M.S. Thesis, Oklahoma State University, Department of Forestry, Stillwater, Oklahoma, 97p.

- Cole, D.W. 1968. A system for measuring conductivity, acidity, and rate of water flow in a forest soil. *Water Res. Research* 4: 1127-1136.
- Cosby, B.J., G.M. Hornberger, and J.N. Galloway. 1985. Modeling the effects of acid deposition: Assessment of a lumped parameter model of soil water and streamwater chemistry. *Water Resources Research* 21(1): 51-63.
- Crawford, N.H. and R.K. Linsley. 1966. Digital simulation in hydrology: Stanford Watershed Model IV. Department of Civil Engineering, Stanford University, Stanford, CA. Tech. Rept. No. 39, 210 p.
- De Oliveira Leite, J. 1985. Interflow, overland flow and leaching of natural nutrients on an Alfisol slope of southern Bahai, Brazil. *J. Hydrology* 80: 77-92.
- DeVries, J. and T.L. Chow. 1978. Hydrologic behavior of a forested mountain soil in coastal British Columbia. *Water Resources Research* 14: 935-942.
- Donigian, A.S., Jr. 1981. Water quality modeling in relation to watershed hydrology. IN: Singh, V.P., Ed. *Modeling Components of the Hydrologic Cycle*, Water Resources Publications, Littleton, CO, pp 343-381.
- Donigian, A.C., Jr., D.C. Beyerlein, H.H. Davis, and N.H. Crawford. 1977. Agricultural Runoff Management (ARM) model Version II: Refinement and testing. US EPA, Environmental Research Lab., Athens, Ga., EPA-600/3-77-098, 294p.
- Donigian, A.C., Jr. and N.H. Crawford. 1976a. Modeling pesticides and nutrients on agricultural lands. US EPA, Environmental Research Lab., Athens, Ga., EPA-600/2-76-043, 263p.
- Donigian, A.C., Jr. and N.H. Crawford. 1976b. Modeling nonpoint source pollution from the land surface. US Environmental Protection Agency, EPA-600/3-76-083, 109p.
- Donigian, A.S., Jr. and N.H. Crawford. 1977. Simulation of nutrient loadings in surface runoff with the NPS model. Environmental Research Lab., Athens, GA, EPA-600/3-77-065, 110p.
- Donigian, A.S., Jr., and H.H. Davis. 1978. User's manual for the Agricultural Runoff Management model. Environmental Research Lab. USEPA, Athens, Ga., EPA-600/3-78-080, 163p.

- Dowd, J.F. and W.L. Nutter. 1985. Physical factors in forest hydrology. IN: Blackmon, B.C., ed. Proceedings of Forestry and Water Quality: A Mid-South Symposium, Little Rock Arkansas, May 8-9, 1985, Department of Forest Resources, University of Arkansas, Monticello. pp 10-17.
- Dunne, T. 1978. Field studies of hillslope processes. IN: Kirkby, M.J., ed. Hillslope Hydrology. John Wiley, New York. pp.227-293.
- Dunne, T. and R.D. Black. 1970. An experimental investigation of runoff production in permeable soils. Water Res. Research 6(2): 478-490.
- Dunne, T., T.R. Moore, and C.H. Taylor. 1975. Recognition and prediction of runoff-producing zones in humid regions. Hydrological Sci. Bull. 20: 305-327.
- Ebise, S. 1984. Separation of runoff components by NO_3^- -N loading and estimation of runoff loading by each component. IASH-AISH Publication # 150. pp 393-405.
- Environmental Protection Agency. 1979. Methods for the chemical analysis of water and wastes. EPA 600/4-79-020.
- England, C.B. 1977. Modeling soil water hydrology under a post oak (*Quercus stellata* Wangenh.)-shortleaf pine (*Pinus echinata* Mill.) stand in east Texas. Water Res. Research 13(3): 683-686.
- Federer, C.A. and D. Lash. 1978. Simulated Streamflow Response to possible differences in transpiration among species of hardwood trees. Water Resources Research 14(6): 1089-1097.
- Fleming, G. 1975. Computer simulation techniques in hydrology. Elsevier, N.Y. 333p.
- Ford, D.N. and T.J. McGhee. 1979. A systematic approach to mathematical water quality modeling. IN: Saxton, K.E. and E.R. Perrier, EDS. Proceedings of the Hydrologic Transport Modeling Symposium, Dec 10-11, 1979. ASAE Publication 4-80, ASAE, St. Joseph, Michigan, pp 12-20.
- Freeze, R.A. 1972. Role of subsurface flow in generating surface runoff 2: Upstream source areas. Water Res. Research 8(5): 1272-1283.
- Freeze, R. A. 1978. Mathematical models of hillslope hydrology. IN: Kirkby, M.J., ED. Hillslope Hydrology, John Wiley & Sons, N.Y. pp. 177-225.

- Frere, M.H., C.A. Onstad, and H.N. Holtan. 1975. ACTMO: An agricultural chemical transport model. ARS-H-3, USDA ARS, Washington, D.C., 54p.
- Frere, M.H., J.D. Ross, and L.J. Lane. 1980. Chapter 4: The nutrient submodel. IN: Kneisel, W.G., Ed., CREAMS: Chemicals, runoff, and erosion from agricultural management systems. USDA Conservation Research Report No. 26, pp 65-87.
- Frere, M.H., E.H. Seely, and R.A. Leonard. 1982. Modeling the quality of water from agricultural land. IN: Haan, C.T., H.P. Johnson, and D.L. Brakensiek, EDS, Hydrologic Modeling of Small Watersheds, ASAE Monograph No.5, ASAE, St. Joseph, Michigan, pp 383-405.
- Hartronft, B.C. and C.J. Hayes. Engineering Classification of Geologic Materials, Division 2. Oklahoma Highway Department Research and Development Division, Project 61-01-1, 356p.
- Helvey, J.D. and J.H. Patric. 1965. Canopy and litter interception of rainfall by hardwoods of Eastern United States. Water Res. Research 1(2):193-206.
- Hem, J.D. 1985. Study and interpretation of the chemical characteristics of natural water. USGS Water Supply Paper 1473, 3rd Ed, .
- Hewlett, J.D. and A.R. Hibbert. 1967. Factors affecting the response of small watersheds to precipitation in humid areas. IN: Sopper, Wm.E. and H.W. Lull, eds. International Symposium on Forest Hydrology, Pergamon Press, Oxford. pp. 257-290.
- Hewlett, J.D. and W.L. Nutter. 1970. The varying source area of streamflow from upland basins. IN: Proc. of a Symposium on Interdisciplinary Aspects of Watershed Management at Montana State University, Bozeman, Montana, Aug. 3-6, 1970. ASCE, N.Y. pp. 65-83.
- Holtan, H.N. and N.C. Lopez. 1971. USDAHL-70. Model of watershed hydrology. USDA Technical Bulletin No. 1435.
- Holtan, H.N., G.J. Stiltner, W.H. Henson, and N.C. Lopez. 1975. USDAHL-74 Revised model of watershed hydrology. USDA Tech. Bull. No. 1518.
- Hooper, R.P. and C.A. Shoemaker. 1986. A comparison of chemical and isotopic hydrograph separation. Water Res. Research 22(10): 1444-1454.

- Hornberger, G.M., K.J. Beven, B.J. Cosby, and D.E. Sappington. 1985. Shenandoah Watershed Study: Calibration of a topography-based, variable contributing area hydrological model to a small forested catchment. *Water Resources Research* 21(12): 1841-1850.
- Huggins, L.F. and E.J. Monke. 1968. A mathematical model for simulating the hydrologic response of a watershed. *Water Resources Research* 4(3): 529-539.
- Jackson, W.A., L.E. Assmussen, E.W. Hauser, and A.W. White. 1973. Nitrate in surface and subsurface flow from a small agricultural watershed. *J. Environ. Qual.* 2(4): 480-482.
- James, J.D. and S.J. Burges. 1982. Selection, calibration, and testing of hydrologic models. IN: Haan, C.T., H.P. Johnson, and D.L. Brakensiek, Eds., *Hydrologic Modeling of Small Watersheds*, American Society of Agricultural Engineers Monograph No.5, pp 437-472.
- Jordan, C.F. 1968. A simple, tension free lysimeter. *Soil Science* 105(2): 81-86.
- Kachanoski, R.G. and E. DeJong. 1982. Comparison of the soil water cycle in clear-cut and forested sites. *J. Environ. Qual.* 11(3): 545-549.
- Kimmons, J.P. 1973. Some statistical aspects of sampling throughfall precipitation in nutrient cycling studies in British Columbia coastal forests. *Ecology* 54(5): 1008-1019.
- Kneisel, W.G., ED. 1980. CREAMS: A field scale model for chemicals, runoff, and erosion from agricultural management systems. *USDA Conservation Research Report No. 26.*
- Kneale, W.R. 1985. Observations of the behavior of large cores of soil during drainage, and the calculation of hydraulic conductivity. *J. Soil Sci.* 36: 163-171.
- Kress, M. W. 1988. Chemistry responses of South-Central United States forested watersheds to acid atmospheric deposition. Final Study Report FS-SO-1651-84-4, USFS Southern Forest Experiment Station, Oxford, MS , 44p.
- Lawrence, S.J. and P.J. Wigington. 1987. Oxidized nitrogen in precipitation, throughfall, and streamflow from a forested watershed in Oklahoma. *Water Resources Research* 23(6): 1069-1076.

- Lawrence, S.J. 1985. Oxidized nitrogen and total phosphorus relationships in the hydrology of a mixed pine-hardwood watershed in southeastern Oklahoma, M.S. Thesis, Oklahoma State University, Department of Forestry, Stillwater, Oklahoma, 117p.
- Lawson, E.R. 1967. Throughfall and stemflow in a pine-hardwood stand in the Ouachita Mountains of Arkansas. *Water Res. Research* 3(3): 731-735.
- Leavesley, G.H., R.W. Lichty, B.M. Troutman, and L.G. Saindon. 1983. *Precipitation-Runoff Modeling System: User's Manual*. USGS Water-Resources Investigations Report 83-4238. 207p.
- Leonard, R. E. 1967. Mathematical theory of interception. IN: Sopper, Wm. E. and H.W. Lull, eds. *International Symposium on Forest Hydrology*, Pergamon Press, Oxford, pp 131-136.
- Lewis, Wm. M. and M. C. Grant. 1979. Relationships between stream discharge and yield of dissolved substances from a Colorado mountain watershed. *Soil Science* 128(6): 353-362.
- Likens, G.E., F.H. Bormann, R.S. Pierce, J.S. Eaton, and N.M. Johnson. 1977. *Biogeochemistry of a forested ecosystem*. Springer-Verlag, N.Y. 146p.
- Linsley, R.K., M.A. Kohler, and J.H. Paulus. 1975. Hydrology for Engineers. 2nd Ed. McGraw Hill, N.Y. 482p.
- Litaor, M.I. 1988. Review of soil solution samplers. *Water Resources Research* 24(5):727-733.
- Loague, K.M. and R.A. Freeze. 1985. A comparison of rainfall-runoff modeling techniques on small upland catchments. *Water Resources Research* 21(2): 229-248.
- Miller, E.L. 1984. Sediment yield and storm flow response to clear-cut harvest and site preparation in the Ouachita Mountains. *Water Res. Research* 20(4): 471-475.
- Moore, T.R. 1985. Spectrophotometric determination of dissolved organic carbon in peat waters. *Soil Sci. Soc. of America Journal* 49: 1590-1592.
- Mosley, M.P. 1979. Streamflow generation in a forested watershed, New Zealand. *Water Res. Research* 15(4): 795-806.

- Nix, J.F. 1985. Research needs in evaluating the impact of intensive forest management on water quality IN: Blackmon, B.C. ed. Proceedings of Forestry and Water Quality: A Mid-South Symposium, Little Rock, Arkansas, May 8-9, 1985. Department of Forest Resources, University of Arkansas, Monticello. pp 9.
- Novotny, V. and G. Chesters. 1981. Handbook of Nonpoint Pollution. Van Nostrand Reinhold Co., N.Y., 555p.
- O'Loughlin, E.M. 1986. Saturation regions in catchments and their relations to soil and topographic properties. J. Hydrology 53: 229-246.
- O'Loughlin, E.M. 1981. Water pathways through catchments and their relation to nutrient losses. IN: Proceedings of IUFRO Workshop on Water and Nutrient Simulation Models, Swiss Federal Institute of Forestry Research, Birmensdorf, pp 123-134.
- Pearce, A.J., M.K. Stewart, and M.G. Sklash. 1986. Storm runoff generation in humid headwater catchments 1. Where does the water come from? Water Resources Research 22(8): 1263-1272.
- Pettyjohn, W.A., H. White, and S. Dunn. Water Atlas of Oklahoma. Univ. Center for Water Research, Oklahoma State University, Stillwater, Oklahoma, 72p.
- Pilgrim, D.H., D.D. Huff, and T.D. Steele. 1979. Use of specific conductance and contact time relations for separating flow components in storm runoff. Water Res. Research 15(2): 329-339.
- Pinder, G.F. and J.F. Jones. 1969. Determination of the groundwater component of peak discharge from the chemistry of total runoff. Water Res. Research 5(2): 438-445.
- Raison, R.J. and P.K. Khanna. 1982. Modification of rainwater chemistry by tree canopies and litter layers. IN: O'Loughlin, E.M. and P. Cullen, Proceedings of a Symposium on the Prediction in Water Quality, Australian Academy of Science, Canberra, pp 69-86.
- Reid, J.M., D.A. MacLeod, and M.S. Cresser. 1981. Factors affecting the chemistry of precipitation and river water in an upland catchment. J. Hydrology 50: 129-145.
- Renard, K.G., W.J. Rawls, and M.M. Fogel. 1982. Currently available models. In: Haan, C.T., H.P. Johnson, and D.L. Brakensiek, Eds. Hydrologic Modeling of Small Watersheds, American Society of Agricultural Engineers Monograph No.5, ASAE, St. Joseph, Michigan, pp 507-522.

- Reynolds, 1984. An assessment of the spatial variation in the chemical composition of bulk precipitation within an upland catchment. *Water Res. Research* 20(6): 733-735.
- Richter, D.D. and C. W. Ralston. 1983. Chemical composition and spatial variation of bulk precipitation at a coastal plain watershed in South Carolina. *Water Res. Research* 19(1): 134-140.
- Rochelle, B.P. and P.J. Wigington, Jr. 1986. Surface runoff from Southeastern Oklahoma forested watersheds. *Proc. Oklahoma Academy of Science* 66: 7-13.
- Rogerson, T.L. 1965 Throughfall in Pole sized Loblolly pine as affected by stand density. IN: Sopper, Wm. E. and H.W. Lull, eds. *International Symposium on Forest Hydrology*, Pergamon Press, Oxford. pp.187-190.
- Ross, B.B., V.O. Shanholtz, and D.N. Contractor. 1980. A spatially responsive hydrologic model to predict erosion and sediment transport. *Wat. Resources Research* 16(3): 538-545.
- Sklash, M.G. and R.N. Farvolden. 1979. The role of groundwater in storm runoff. *J. Hydrology* 43: 45-64.
- Sloan, P.G., I.D. Moore, G.B. Coltharp, and J.D. Eigel. 1983. Modeling surface and subsurface stormflow on steeply-sloping forested watersheds. Research Report No. 142, University of Kentucky Water Resources Research Institute, Lexington, Kentucky, 167p.
- Smith, R.E. and J.R. Williams. 1980. Chapter 2: Simulation of surface water hydrology. IN: Kneisel, W.G., Ed. *CREAMS: A field scale model for chemicals, runoff, and erosion from agricultural management systems*. USDA Conservation Research Report No. 26, pp.13-35.
- Smolen, M.D., B.B. Ross, and V.O. Shanholtz. 1983. The Finite Element Storm Hydrograph Model. IN: Smolen, M.D., Ed. *Hydrologic/Water Quality Models for Agriculture and Forestry*. Southern Cooperative Series Bulletin No. 291, June, 1983. pp 60-71.
- Sober, R.F. and M. H. Bates. 1979 The atmospheric contribution of phosphorus to an aquatic system. *Water, Air, and Soil Pollution* 11:63-69.
- Swift, L.W., W.T. Swank, J.B. Mankin, R.J. Luxmoore, and R.A. Goldstein. 1975. Simulation of evapotranspiration and drainage from mature and clear-cut deciduous forests and young pine plantation. *Water Res. Research* 11(5): 667-673.

- Thomas, D.L. and D.B. Beasley. 1986a. A physically-based forest hydrology model I: Development and sensitivity of components. Transactions of ASAE 29(4): 962-972.
- Thomas, D.L. and D.B. Beasley. 1986b. A physically-based forest hydrology model II: Evaluation under natural conditions. Transactions of ASAE 29(4): 973-981.
- Thomas, G.W. and R.E. Phillips. 1979. Consequences of water movement in macropores. J. Environmental Qual. 8(2): 149-152.
- Troendle, C.A. 1985. Chapter 12: Variable source area models. IN: Anderson, M.G. and T.P. Burt, Eds. Hydrological Forecasting, John Wiley & Sons Ltd., Chichester, U.K., pp 347-403.
- Watson, K.W. and R.J. Luxmoore. 1986. Estimating macroporosity in a forest watershed by use of a tension infiltrometer. Soil Sci. Soc. of America Journal 50:578-582.
- Weyman, D.R. 1973. Measurement of the downslope flow of water in a soil. Journal of Hydrology 20: 267-288.
- Weyman, D.R. 1970. Throughflow on hillslopes and its relation to the stream hydrograph. Bull. Int. Assoc. Scientific Hydrology, 15:25-33.
- Whipkey, R.Z. 1965. Subsurface stormflow from forested slopes. Bull. Int. Assoc. Sci. Hydrology 10: 74-85.
- Wooldridge, D.D. and A.G. Larson. 1980. Non-point source pollution in forest streams of the western Olympic Mountains. Project Completion Report OWRT-B-076-WASH, University of Washington, College of Forest Resources, Seattle, Washington, 95p.

APPENDIX A
HYDROLOGIC PROCESSES SUMMARY TABLES

TABLE 34
 HYDROLOGIC PROCESSES DATA FOR
 THE STORM OF 1/15/87

Precipitation Data

Date	Time	Accum. PCP (mm)	Interval PCP (mm)	Intens. (mm/hr)
1/15	5:31	0.0	0.0	0.0
1/15	5:56	1.3	1.3	3.0
1/15	8:22	1.3	0.0	0.0
1/15	8:52	2.5	1.3	2.5
1/15	10:03	2.5	0.0	0.0
1/15	10:43	3.0	0.5	0.8
1/15	11:23	5.6	2.5	3.8
1/15	12:24	8.1	2.5	2.5
1/15	13:04	10.2	2.0	3.0
1/15	14:30	11.2	1.0	0.7
1/15	19:31	11.2	0.0	0.0
1/15	20:46	11.9	0.8	0.6
1/15	21:47	13.5	1.5	1.5
1/15	23:22	15.0	1.5	1.0
1/16	00:00	16.3	1.3	2.0
1/16	01:10	18.8	2.5	2.2
1/16	06:22	18.8	0.0	0.0
1/16	07:12	19.8	1.0	1.2
1/16	13:54	20.3	0.5	0.1
1/17	00:00	21.1	0.8	0.1
1/17	06:42	21.6	0.5	0.1
1/17	08:45	21.6	0.0	0.0
1/17	13:00	21.8	0.3	0.1
1/17	15:31	22.9	1.0	0.4
1/17	16:51	23.9	1.0	0.8
1/17	18:22	23.9	0.0	0.0
1/17	18:52	25.1	1.3	2.5
1/17	20:42	25.9	0.8	0.4
1/17	21:43	28.2	2.3	2.2
1/17	22:43	33.0	4.8	4.8
1/18	00:00	36.6	3.6	2.8
1/18	00:50	36.8	0.3	0.3
1/18	01:50	37.1	0.3	0.3
1/18	02:30	43.9	6.9	10.3
1/18	02:40	45.2	1.3	7.6
1/18	03:41	46.0	0.8	0.7
1/18	05:21	48.0	2.0	1.2

TABLE 34 (Continued)

Date	Time	Accum. PCP (mm)	Interval PCP (mm)	Intens. (mm/hr)
1/18	09:43	49.5	1.5	0.3
1/18	14:44	50.8	1.3	0.3
1/19	00:00	51.3	0.5	0.1

Subsurface Flow Data

Date	Time	Accum Vol. (liters)	Interval Discharge (l/s)*1000
------	------	---------------------------	-------------------------------------

SITE 1: Litter Layer Flow

1/16	10:45	0.4	0.0
1/16	10:50	0.5	0.1
1/16	10:53	0.6	0.3
1/16	10:56	0.6	0.1
1/16	11:15	0.6	0.0
1/16	11:18	0.7	0.2
1/16	11:23	0.7	0.0
1/16	11:29	0.7	0.0
1/16	11:30	0.8	0.2
1/16	11:32	0.8	0.1
1/16	11:34	0.9	0.2
1/16	11:40	1.0	0.2
1/16	11:59	1.1	0.0
1/16	12:14	1.2	0.0
1/16	12:20	1.2	0.0
1/16	12:28	1.2	0.0
1/16	12:38	1.3	0.0
1/16	12:39	1.4	0.7
1/16	12:42	1.4	0.1
1/16	13:11	1.5	0.0
1/16	14:31	1.5	0.0
1/16	20:49	1.5	0.0
1/16	21:00	1.6	0.0
1/16	21:05	1.6	0.1
1/16	21:30	1.7	0.0
1/16	22:00	4.3	0.0
1/16	23:00	6.5	0.0
1/17	00:00	7.3	0.0
1/17	01:16	8.2	0.0
1/17	04:31	8.7	0.0
1/17	07:50	9.0	0.0
1/17	15:18	9.0	0.0

TABLE 34 (Continued)

Date	Time	Accum. Vol. (liters)	Interval Discharge (l/s)*1000
1/17	15:19	9.3	0.2
1/18	00:00	9.3	0.0
1/18	12:00	9.7	0.0
1/18	12:20	9.7	0.0
1/18	15:54	10.6	0.0
1/18	17:50	10.9	0.0
1/18	18:02	11.2	0.0
1/18	19:20	11.3	0.0
1/18	20:24	11.4	0.0
1/18	22:22	12.3	0.0
1/18	22:50	12.7	0.0

All other samplers had no samples
due to faulty equipment

TABLE 35

HYDROLOGIC PROCESSES DATA FOR
THE STORM OF 2/1/87

Precipitation Data

Date	Time	Accum. PCP (mm)	Interval PCP (mm)	Intens. (mm/hr)
2/1	03:20	0.0	0.0	0.0
2/1	04:01	1.3	1.3	1.9
2/1	04:16	2.5	1.3	5.1
2/1	08:52	2.5	0.0	0.0
2/1	09:50	7.1	4.6	4.7
2/1	11:20	11.4	4.3	2.9
2/6	02:09	0.0	0.0	0.0
2/6	03:54	2.0	2.0	1.2
2/6	04:30	3.3	1.3	2.1
2/6	05:00	4.3	1.0	2.0
2/6	10:14	5.1	0.8	0.1

Subsurface Flow Data

Date	Time	Accum. Vol. (liters)	Interval Discharge (l/s)*1000
------	------	----------------------------	-------------------------------------

SITE 1: Litter Layer Flow

2/1	09:46	0.0	0.0
2/1	10:13	0.4	0.3
2/1	10:14	0.5	0.6

TABLE 35 (Continued)

Date	Time	Accum. Vol. (liters)	Interval Discharge (l/s*1000)
------	------	----------------------------	-------------------------------------

SITE 1: A-Horizon Flow

2/1	09:32	0.0	0.0
2/1	09:34	0.4	3.7
2/1	09:38	0.5	0.2
2/1	09:44	0.5	0.1
2/1	10:09	0.6	0.0
2/1	11:43	0.7	0.0
2/1	13:56	0.7	0.0

SITE 1: B-Horizon Flow

1-Feb	nd	0.9	
-------	----	-----	--

SITE 2: Litter Layer Flow

2/1	09:26	0.0	0.0
2/1	09:30	0.5	2.1
2/1	09:34	0.7	0.7
2/1	09:39	0.9	0.8
2/1	09:44	1.1	0.5
2/1	09:50	1.2	0.4
2/1	09:53	1.3	0.5
2/1	09:57	1.5	1.0
2/1	10:00	1.7	1.0
2/1	10:03	2.3	3.4
2/1	10:06	2.9	3.0
2/1	10:16	3.2	0.5
2/1	10:30	5.5	2.8
2/1	10:34	5.9	1.6
2/1	10:35	6.9	15.4
2/1	11:30	7.5	0.2

SITE 2: A and B-Horizon

no data, tanks frozen

TABLE 35 (Continued)

Date	Time	Accum. Vol. (liters)	Interval Discharge (l/s)*1000
<u>SITE 3: Litter Layer Flow</u>			
2/1	09:31	0.0	0.0
2/1	09:45	0.8	1.0
2/1	09:50	0.9	0.2
2/1	10:03	1.3	0.6
2/1	10:28	1.7	0.2
2/1	10:59	4.4	1.4
<u>SITE 3: A and B-Horizon Flow</u>			
no flow			

TABLE 36
 HYDROLOGIC PROCESSES DATA FOR
 THE STORM OF 2/15/87

Date	Time	Accum. PCP (mm)	Interval PCP (mm)	Intens. (mm/hr)
2/15	00:00	0.0	0.0	0.0
2/15	00:05	6.4	6.4	76.2
2/15	1:20	12.7	6.4	5.1
2/15	11:03	13.2	0.5	0.1
2/15	11:43	13.7	0.5	0.8
2/15	14:13	0.0	0.0	0.0
2/15	14:24	5.1	5.1	27.7
2/15	14:44	7.9	2.8	8.4
2/15	16:04	15.5	7.6	5.7
2/15	18:35	17.3	1.8	0.7
2/15	19:35	17.8	0.5	0.5
2/15	22:41	0.0	0.0	0.0
2/16	01:52	1.5	1.5	0.5

Subsurface Flow Data

Date	Time	Accum. Vol. (l)	Interval Discharge (l/s)*1000
------	------	-----------------------	-------------------------------------

SITE 1: Litter Layer Flow

2/15	00:05	0.4	0.0
2/15	00:14	0.4	0.0
2/15	00:37	0.4	0.0
2/15	00:53	0.4	0.0
2/15	00:57	0.5	0.2
2/15	01:01	0.5	0.0
2/15	01:03	0.5	0.3
2/15	01:06	0.6	0.5
2/15	..?..	0.6	
2/15	..?..	0.8	

Table 36 (Continued)

Date	Time	Accum. (Vol.) (liters)	Interval Discharge (l/s*1000)
------	------	------------------------------	-------------------------------------

SITE 1: A-Horizon Flow

2/15	00:07	0.0	0.0
2/15	00:34	0.6	0.4
2/15	01:05	0.7	0.1
2/15	01:25	0.8	0.1
2/15	01:50	0.8	0.0
2/15	02:22	0.8	0.0
2/15	03:11	0.8	0.0
2/15	14:51	0.9	0.0
2/15	14:59	0.9	0.1
2/15	15:15	1.0	0.1
2/15	15:28	1.0	0.1
2/15	16:44	1.1	0.0
2/15	18:00	1.3	0.0

SITE 1: B-Horizon Flow

2/15	15:40	0.4	0.0
2/15	16:10	0.8	0.2
2/15	16:36	1.1	0.2
2/15	16:50	1.2	0.1
2/15	17:04	1.3	0.1
2/15	17:44	1.5	0.1
2/15	18:17	1.6	0.0
2/15	18:53	1.7	0.0
2/15	19:33	1.7	0.0

SITE 2: Litter Layer Flow

2/15	00:24	0.4	0.0
2/15	00:26	0.4	0.1
2/15	00:28	0.5	0.4
2/15	00:30	0.5	0.2
2/15	00:32	0.6	1.1
2/15	00:33	0.7	1.7
2/15	00:37	1.0	1.0
2/15	00:40	1.1	0.8
2/15	00:42	1.2	0.7

Table 36 (Continued)

Date	Time	Accum. (Vol.) (liters)	Interval Discharge (l/s*1000)
2/15	00:50	1.4	0.4
2/15	00:52	1.4	0.4
2/15	00:57	1.5	0.2
2/15	01:04	1.6	0.2
2/15	01:11	1.6	0.1
2/15	01:17	1.7	0.1
2/15	01:28	1.9	0.3
2/15	01:55	2.6	0.5
2/15	02:08	2.9	0.3
2/15	02:38	3.2	0.2
2/15	03:00	3.2	0.1
2/15	05:12	3.5	0.0
2/15	10:05	3.9	0.0
2/15	10:50	3.9	0.0
2/15	11:00	4.0	0.1
2/15	11:15	4.2	0.2
2/15	11:20	4.2	0.3
2/15	11:23	4.3	0.4
2/15	11:25	4.5	1.3
2/15	11:26	4.6	2.6
2/15	11:27	5.0	6.4
2/15	14:14	5.1	0.0
2/15	14:20	6.0	2.6
2/15	14:21	6.0	0.0
2/15	14:25	6.4	1.6
2/15	14:27	6.6	1.9
2/15	14:31	6.9	1.3
2/15	14:37	7.2	0.9
2/15	14:41	7.4	0.6
2/15	15:13	7.5	0.1
2/15	15:32	7.7	0.1
2/15	15:33	8.0	5.1
2/15	15:50	8.1	0.1
2/15	15:54	8.2	0.3
2/15	15:56	8.3	1.3
2/15	15:58	8.5	1.3
2/15	16:51	8.6	0.0
2/15	16:53	9.0	3.2

Table 36 (Continued)

Date	Time	Accum. (Vol.) (liters)	Interval Discharge (l/s * 1000)
<u>SITE 2: A-Horizon Flow</u>			
2/15	14:55	0.4	0.0
2/15	14:59	1.1	2.7
2/15	15:06	6.4	12.7
2/15	15:15	7.9	2.9
2/15	15:45	9.9	1.1
2/15	15:55	10.7	1.3
2/15	16:05	11.8	1.9
2/15	16:26	13.4	1.2
2/15	16:45	15.0	1.4
2/15	17:15	17.3	1.3
2/15	17:55	20.4	1.3
2/15	18:15	25.1	3.9
2/15	18:51	25.9	0.4
2/15	22:15	26.3	0.0
<u>SITE 2: B-Horizon Flow</u>			
2/15	15:06	0.4	0.0
2/15	15:10	0.4	0.1
2/15	16:36	0.5	0.0
2/15	17:58	0.5	0.0
2/15	23:10	0.6	0.0
<u>SITE 3: Litter Layer Flow</u>			
2/15	00:02	0.4	0.0
2/15	00:07	0.9	1.7
2/15	00:09	0.9	0.1
2/15	00:10	1.3	5.6
2/15	00:15	1.7	1.5
2/15	00:18	2.4	3.7
2/15	00:30	4.4	2.8
2/15	00:37	5.0	1.6
2/15	00:42	5.7	2.2
2/15	00:46	5.8	0.6
2/15	00:53	6.0	0.5
2/15	01:15	6.4	0.3

Table 36 (Continued)

Date	Time	Accum (Vol.) (liters)	Interval Discharge (l/s*1000)
2/15	14:46	6.4	0.0
2/15	14:51	7.7	4.4
2/15	15:01	8.4	1.1
2/15	15:08	8.7	0.8
2/15	15:47	8.8	0.0
2/15	16:18	9.7	0.5
2/15	16:27	9.7	0.0
2/15	17:16	9.9	0.1
2/15	17:30	10.4	0.6
2/15	18:44	10.6	0.0

SITE 3: A-Horizon flow

2/15	17:02	0.4	0.0
2/15	18:00	0.5	0.0
2/15	19:10	0.6	0.0
2/15	21:21	0.6	0.0
2/16	00:00	0.6	0.0

SITE 3: B-Horizon Flow

no flow

TABLE 37

HYDROLOGIC PROCESSES DATA FOR
THE STORM OF 2/24/87

Precipitation Data

Date	Time	Accum. PCP (mm)	Interval PCP (mm)	Intens. (mm/hr)
2/24	02:30	0.0	0.0	0.0
2/24	03:30	3.0	3.0	3.0
2/24	04:20	7.1	4.1	4.9
2/24	05:55	9.1	2.0	1.3
2/24	06:55	9.7	0.5	0.5
2/24	07:50	11.9	2.3	2.5
2/24	09:05	12.7	0.8	0.6
2/24	10:30	13.2	0.5	0.4

Subsurface Flow Data

Site 1: Litter Layer and B-Horizon tanks dry
Total volume in A-Horizon tank = 0.54 liters

Date	Time	Accum. Vol (l)	Interval Discharge (l/s)*1000
------	------	----------------------	-------------------------------------

SITE 2: Litter Layer Flow

2/24	02:31	1.0	0.0
2/24	02:52	1.9	0.7
2/24	02:57	2.3	1.5
2/24	02:59	2.4	0.2
2/24	03:00	2.4	0.4
2/24	03:02	2.4	0.1
2/24	03:11	2.8	0.8
2/24	03:14	2.8	0.1
2/24	03:31	2.9	0.0

TABLE 37 (Continued)

Date	Time	Accum. Vol. (liters)	Interval Discharge (l/s*1000)
2/24	03:56	2.9	0.0
2/24	04:31	2.9	0.0
2/24	05:36	2.9	0.0
<u>SITE 2: A-Horizon Flow</u>			
2/24	06:25	0.4	0.0
2/24	07:06	0.4	0.0
2/24	08:33	0.6	0.0
2/24	08:56	0.6	0.0
2/24	10:00	0.6	0.0
<u>SITE 2: B-Horizon Flow</u>			
no flow			
<u>SITE 3: Litter Layer Flow</u>			
2/24	02:32	1.0	0.0
2/24	02:50	1.8	0.8
2/24	03:08	2.2	0.3
2/24	03:43	2.5	0.2
<u>SITE 3: A-Horizon Flow</u>			
2/24	08:43	0.4	0.0
2/24	09:42	0.6	0.1
2/24	10:40	0.6	0.0
2/24	11:28	0.7	0.0
2/24	13:00	0.7	0.0
<u>SITE 3: B-Horizon Flow</u>			
no flow			

TABLE 38
 HYDROLOGIC PROCESSES DATA FOR
 THE STORM OF 2/28/87

Precipitation Data

Date	Time	Accum. PCP (mm)	Interval PCP (mm)	Intens. (mm/hr)
2/26	02:25	0.0	0.0	0.0
2/26	03:15	0.1	0.1	0.1
2/26	05:40	0.1	0.1	0.0
2/26	07:00	0.2	0.1	0.1
2/26	08:15	0.2	0.0	0.0
2/26	08:40	0.2	0.0	0.0
2/26	10:20	0.4	0.2	0.1
2/26	12:10	0.5	0.1	0.1
2/26	12:29	0.5	0.0	0.1
2/26	13:45	0.5	0.0	0.0
2/26	15:49	0.6	0.0	0.0
2/26	16:54	0.6	0.1	0.1
2/27	00:30	0.7	0.0	0.0
2/27	10:00	0.0	0.0	0.0
2/27	13:09	0.0	0.0	0.0
2/27	14:19	0.1	0.1	0.0
2/27	17:09	0.0	0.0	0.0
2/27	17:39	0.1	0.1	0.3
2/28	01:24	0.0	0.0	0.0
2/28	01:49	0.5	0.5	1.3
2/28	02:10	0.7	0.2	0.4
2/28	03:00	0.8	0.1	0.1
2/28	05:20	0.0	0.0	0.0
2/28	05:45	0.0	0.0	0.1
2/28	07:14	0.0	0.0	0.0
2/28	07:40	0.2	0.1	0.3
2/28	10:40	0.2	0.0	0.0
2/28	12:49	0.3	0.1	0.1
2/28	16:20	0.4	0.1	0.0
2/28	18:50	0.5	0.1	0.0

TABLE 38 (Continued)

Subsurface Flow Data

Date	Time	Accum. Vol. (1)	Interval Discharge (1/s)*1000
------	------	-----------------------	-------------------------------------

SITE 1: Litter Layer Flow

2/28	01:36	1.4	0.0
2/28	01:37	1.9	8.4
2/28	01:40	2.0	0.5
2/28	01:41	2.0	0.4
2/28	01:53	2.6	0.8
2/28	01:55	2.6	0.5
2/28	02:00	2.6	0.0
2/28	02:05	3.0	1.4
2/28	02:07	3.1	0.3
2/28	02:10	3.1	0.1
2/28	02:15	3.1	0.1
2/28	04:27	4.2	0.1
2/28	04:30	4.2	0.2
2/28	04:55	4.3	0.0
2/28	05:05	4.3	0.0
2/28	05:13	4.3	0.0
2/28	05:14	4.4	1.2
2/28	08:26	4.5	0.0
2/28	09:18	4.6	0.0

SITE 1: A-Horizon Flow

2/28	02:33	0.4	0.0
2/28	03:01	0.5	0.1
2/28	04:00	0.6	0.0
2/28	08:30	0.7	0.0
2/28	12:00	0.8	0.0
2/28	13:10	0.9	0.0
2/28	17:29	1.0	0.0
2/28	18:40	1.1	0.0

TABLE 3B (Continued)

Date	Time	Accum. (Vol.) (liters)	Interval Discharge (l/s*1000)
<u>SITE 1: B-Horizon Flow</u>			
2/28	02:10	0.4	0.0
2/28	02:31	0.5	0.1
2/28	02:39	0.6	0.1
2/28	02:54	0.6	0.1
2/28	03:05	0.7	0.1
<u>SITE 2: Litter Layer Flow</u>			
2/26	08:50	1.4	0.0
2/26	08:56	1.4	0.0
2/26	09:03	1.7	0.7
2/26	09:05	1.7	0.1
2/26	09:18	2.1	0.5
2/26	09:21	2.1	0.3
2/26	09:22	2.2	0.4
2/26	09:24	2.5	2.9
2/26	09:30	2.5	0.1
2/26	09:35	2.8	0.9
2/26	09:51	3.1	0.3
2/26	10:00	3.4	0.5
2/26	11:23	4.2	0.2
2/26	14:15	4.4	0.0
2/26	16:30	4.5	0.0
2/26	18:55	4.6	0.0
2/26	21:50	4.7	0.0
2/27	01:00	4.8	0.0
2/27	17:00	4.8	0.0
2/27	17:17	4.9	0.0
2/27	17:21	7.0	8.8
2/27	17:30	7.2	0.4
2/27	17:44	7.5	0.3
2/27	17:55	7.5	0.1
2/27	21:40	7.6	0.0
2/28	1:32	7.8	0.0
2/28	01:33	8.0	3.8
2/28	01:34	9.1	19.2
2/28	01:35	9.5	5.1
2/28	01:37	9.5	0.0
2/28	01:38	9.6	2.6

TABLE 38 (Continued)

Date	Time	Accum. (Vol.) (liters)	Interval Discharge (l/s*1000)
2/28	01:40	9.9	2.6
2/28	01:44	10.1	1.0
2/28	01:46	10.4	1.9
2/28	01:53	10.6	0.6
2/28	02:00	10.8	0.4
2/28	02:10	11.0	0.4
2/28	02:12	11.1	0.6
2/28	02:28	11.2	0.2
2/28	02:30	11.4	1.3
2/28	03:00	11.6	0.1
2/28	03:18	11.6	0.0
2/28	03:22	11.8	0.6
2/28	03:45	11.9	0.1
2/28	06:49	12.1	0.0
2/28	06:56	12.2	0.2
2/28	06:58	12.5	2.6
2/28	09:07	12.5	0.0
2/28	10:18	12.7	0.0
2/28	10:25	12.8	0.4
2/28	10:40	13.0	0.2
2/28	14:54	13.0	0.0
2/28	15:03	13.1	0.2
2/28	15:07	13.8	2.6

SITE 2: A-Horizon

No Data

SITE 2: B-Horizon Flow

2/28	01:48	0.4	0.0
2/28	02:05	2.3	1.9
2/28	02:15	6.9	7.7
2/28	02:35	10.7	3.1
2/28	02:52	14.7	3.9
2/28	03:06	17.7	3.6
2/28	03:30	21.4	2.6
2/28	04:00	24.2	1.5
2/28	04:12	25.1	1.3
2/28	04:30	26.0	0.9

TABLE 38 (Continued)

Date	Time	Accum. (Vol.) (liters)	Interval Discharge (l/s*1000)
2/28	05:25	27.9	0.6
2/28	08:00	29.2	0.2
2/28	08:40	29.7	0.2
2/28	11:57	30.6	0.1
2/28	13:36	30.9	0.1
2/28	16:30	31.5	0.1

SITE 3: Litter Layer Flow

2/26	09:00	0.4	0.0
2/26	09:15	0.7	0.4
2/26	09:24	0.8	0.2
2/26	09:35	0.9	0.1
2/26	10:23	1.4	0.2
2/26	10:24	1.6	3.1
2/26	11:45	1.7	0.0
2/26	15:51	1.7	0.0
2/26	16:20	2.4	0.4
2/26	17:30	2.7	0.1
2/27	15:09	2.7	0.0
2/27	15:12	3.4	3.7
2/27	16:00	4.4	0.4
2/28	01:33	4.4	0.0
2/28	01:35	5.0	5.6
2/28	01:37	6.0	8.3
2/28	01:41	7.0	4.2
2/28	01:52	7.7	1.0
2/28	02:07	8.0	0.4
2/28	03:01	9.0	0.3
2/28	06:36	9.0	0.0
2/28	07:21	9.7	0.3
2/28	08:00	10.0	0.1

SITE 3: A-Horizon Flow

2/26	11:30	0.0	0.0
2/26	13:30	0.8	0.1
2/26	14:00	0.9	0.0
2/26	16:28	0.9	0.0
2/26	16:56	1.0	0.1

TABLE 38 (Continued)

Date	Time	Accum. (Vol.) (liters)	Interval Discharge (l/s*1000)
2/26	17:43	1.1	0.1
2/26	18:11	1.2	0.0
2/26	20:10	1.3	0.0
2/26	22:16	1.4	0.0
2/27	00:00	1.5	0.0
2/28	04:30	1.5	0.0
2/28	11:50	7.3	0.2
2/28	11:56	8.1	2.2
2/28	12:00	8.5	1.7
2/28	19:00	9.7	0.1

SITE 3: B-Horizon Flow

2/28	02:08	0.4	0.0
2/28	02:55	1.0	0.2
2/28	03:14	1.2	0.2
2/28	03:50	1.4	0.1
2/28	04:30	1.6	0.1
2/28	06:30	3.3	0.2
2/28	08:35	5.7	0.3
2/28	11:00	11.4	0.6
2/28	12:00	12.7	0.4
2/28	12:47	14.8	0.8
2/28	14:27	17.3	0.4
2/28	17:55	20.7	0.3
2/28	20:49	24.2	0.3
3/1	02:30	28.4	0.0
3/1	03:00	28.7	0.2
3/1	14:30	31.0	0.1

TABLE 39
 HYDROLOGIC PROCESSES DATA FOR
 THE STORM OF 3/17/87

Precipitation Data

Date	Time	Accum. Depth (mm)	Interval PCP (mm)	Intens. (mm/hr)
3/16	21:50	0.0	0.0	0.0
3/16	22:19	0.5	9.5	19.7
3/16	22:30	12.7	3.2	17.3
3/16	23:30	14.6	1.9	1.9
3/17	00:00	16.5	0.6	1.3
3/17	00:51	24.8	8.3	9.7
3/17	01:11	31.8	7.0	21.0
3/17	01:36	35.6	3.8	9.1
3/17	02:32	39.4	3.8	4.1
3/17	03:32	40.6	1.3	1.3
3/17	04:28	41.3	0.6	0.7
3/17	05:13	42.5	1.3	1.7
3/17	07:05	61.0	18.4	9.9
3/17	08:45	69.9	8.9	5.3

Subsurface Flow Data

SITE 1: Litter Layer Flow

Date	Time	Accum. Vol. (liters)	Interval Discharge (l/sx1000)
3/17	04:15	1.0	0.0
3/17	04:40	1.7	0.5
3/17	04:48	1.8	0.1
3/17	05:00	1.9	0.2
3/17	05:12	2.1	0.3
3/17	05:18	2.2	0.3
3/17	05:21	2.3	0.2
3/17	05:30	2.3	0.1
3/17	05:31	2.4	0.7
3/17	05:32	2.5	1.7

TABLE 39 (Continued)

Date	Time	Accum. Vol. (liters)	Interval Discharge (l/s*1000)
3/17	05:57	2.6	0.0
3/17	06:00	2.6	0.0
3/17	06:06	5.6	8.3
3/17	06:07	5.7	2.7
3/17	06:08	5.9	3.0
3/17	06:09	6.1	2.8
3/17	06:10	7.2	19.3
3/17	06:11	10.5	54.3
3/17	06:12	11.5	16.7
3/17	06:13	12.9	23.5
3/17	06:14	13.5	10.0
3/17	06:16	15.9	20.1
3/17	06:17	17.1	20.0
3/17	06:22	18.1	3.4
3/17	06:25	19.3	6.4
3/17	06:30	21.6	7.7

SITE 1: A-Horizon Flow

3/17	01:21	0.0	0.0
3/17	01:40	0.5	0.4
3/17	02:00	0.6	0.1
3/17	02:30	0.7	0.0
3/17	04:00	0.7	0.0
3/17	04:25	0.8	0.1
3/17	05:00	1.0	0.1
3/17	05:40	1.2	0.1
3/17	06:07	1.4	0.1
3/17	06:40	1.6	0.1
3/17	07:16	2.5	0.4
3/17	07:40	3.3	0.6
3/17	08:09	4.1	0.5

SITE 1: B-Horizon Flow

3/17	01:14	0.0	0.0
3/17	01:42	0.5	0.3
3/17	02:04	0.6	0.1
3/17	02:24	0.6	0.0
3/17	04:20	0.7	0.0

TABLE 39 (Continued)

Date	Time	Accum. Vol. (liters)	Interval Discharge (l/s*1000)
3/17	05:06	0.7	0.0
3/17	05:18	0.8	0.1
3/17	06:03	1.6	0.3
3/17	06:12	1.7	0.2
3/17	07:00	2.1	0.1
3/17	07:04	3.1	4.3
3/17	07:06	4.5	11.6
3/17	07:08	8.0	29.0
3/17	07:12	12.2	17.5
3/17	07:16	21.0	36.7
3/17	07:23	30.8	23.3
3/17	07:31	45.2	30.1
3/17	07:34	50.1	27.3
3/17	07:38	58.3	34.2
3/17	07:42	64.1	23.9
3/17	07:49	72.3	19.5
3/17	07:53	76.4	17.1
3/17	07:58	79.7	10.9
3/17	08:01	81.3	9.1
3/17	08:07	82.9	4.6
3/17	08:10	83.8	4.6
3/17	08:16	84.6	2.3
3/17	08:41	85.4	0.5
3/17	09:50	86.2	0.2

SITE 2: Litter Layer Flow

3/16	23:21	1.0	0.0
3/16	23:23	1.8	7.0
3/16	23:25	2.0	1.0
3/16	23:30	2.1	0.3
3/16	23:35	2.4	1.2
3/17	00:00	3.5	0.7
3/17	00:15	3.5	0.0
3/17	00:25	3.6	0.1
3/17	00:35	3.6	0.1
3/17	00:41	3.7	0.1
3/17	00:52	3.7	0.1
3/17	00:59	3.8	0.1
3/17	01:17	4.1	0.3
3/17	01:30	4.4	0.3
3/17	01:39	4.6	0.5

TABLE 39 (Continued)

Date	Time	Accum. Vol. (liters)	Interval Discharge (l/s*1000)
3/17	01:45	4.9	0.7
3/17	01:48	4.9	0.2
3/17	01:49	5.0	0.7
3/17	01:50	5.2	3.2
3/17	01:52	5.2	0.0
3/17	01:54	5.4	2.0
3/17	01:58	5.5	0.2
3/17	02:00	5.6	1.3
3/17	02:15	6.2	0.6
3/17	03:15	6.7	0.1
3/17	04:30	7.0	0.1
3/17	04:40	7.2	0.3
3/17	06:10	7.2	0.0
3/17	07:00	34.3	9.0

Clock stopped, final volume=34.3 l

SITE 2: A-Horizon Flow

3/17	00:09	0.0	0.0
3/17	00:12	1.4	7.9
3/17	00:13	1.6	3.2
3/17	00:17	6.4	19.9
3/17	00:26	7.9	2.9
3/17	01:05	13.4	2.3
3/17	01:51	18.9	2.0
3/17	01:56	18.9	0.0
3/17	02:12	20.4	1.6
3/17	02:50	22.0	0.7
3/17	04:43	22.4	0.1
3/17	05:03	22.8	0.3
3/17	05:12	23.5	1.3
3/17	05:16	24.3	3.3
3/17	05:21	25.9	5.3
3/17	05:26	27.4	5.0
3/17	05:35	32.1	8.7
3/17	05:41	36.8	13.1
3/17	05:48	46.2	22.4
3/17	05:54	56.3	28.1
3/17	05:59	65.7	31.3
3/17	06:01	73.5	65.0

TABLE 39 (Continued)

Date	Time	Accum. Vol. (liters)	Interval Discharge (l/s*1000)
3/17	06:03	77.4	32.5
3/17	06:06	84.4	38.9
3/17	06:07	86.7	38.3

Tank overflowed, final projected
volume = 340 liters

Site 2: B-Horizon Flow

3/17	02:12	0.0	0.0
3/17	02:18	0.8	2.1
3/17	02:29	1.1	0.6
3/17	02:36	1.4	0.7
3/17	02:46	1.5	0.1
3/17	04:39	1.5	0.0
3/17	04:48	1.7	0.4
3/17	05:00	4.2	3.4
3/17	05:18	7.9	3.4
3/17	05:27	8.5	1.1
3/17	05:34	9.1	1.5
3/17	06:09	22.3	6.3
3/17	07:02	42.6	6.4
3/17	07:32	52.8	5.7
3/17	08:10	61.1	3.6
3/17	08:32	64.8	2.8
3/17	09:02	68.5	2.1
3/17	09:30	71.2	1.6
3/17	09:44	72.2	1.2
3/17	10:20	73.6	0.6
3/17	10:36	74.0	0.4
3/17	11:10	74.9	0.4
3/17	12:59	75.4	0.1

SITE 3: Litter Layer Flow

3/16	23:09	0.0	0.0
3/16	23:12	0.9	4.8
3/16	23:13	1.3	7.8
3/16	23:15	1.4	0.7
3/16	23:27	1.6	0.3

TABLE 39 (Continued)

Date	Time	Accum. Vol. (liters)	Interval Discharge (l/s*1000)
3/16	23:30	1.7	0.2
3/16	23:46	1.7	0.1
3/17	00:00	2.0	0.4
3/17	00:25	2.0	0.0
3/17	00:58	3.7	0.8
3/17	01:02	4.4	2.8
3/17	01:11	4.7	0.6
3/17	01:15	5.0	1.4
3/17	01:52	7.0	0.9
3/17	01:56	8.4	5.6
3/17	02:22	9.0	0.4
3/17	03:30	11.5	0.6
3/17	06:00	11.5	0.0
3/17	06:26	12.4	0.6
3/17	06:38	13.3	1.3
3/17	06:52	14.1	1.0
3/17	07:04	15.0	1.3
3/17	07:36	17.7	1.4
3/17	08:05	20.4	1.6
3/17	08:25	21.3	0.7
3/17	08:57	23.0	0.9
3/17	09:15	23.9	0.8
3/17	09:38	24.8	0.7
3/17	10:00	25.3	0.4

SITE 3: A-Horizon Flow

3/17	03:00	0.0	0.0
3/17	03:20	0.5	0.4
3/17	03:44	0.6	0.1
3/17	04:20	0.7	0.0
3/17	04:48	0.7	0.0
3/17	05:30	0.8	0.0
3/17	07:00	0.9	0.0
3/17	07:42	1.0	0.0
3/17	08:08	8.1	4.6
3/17	08:09	8.9	13.3
3/17	08:20	9.7	1.2
3/17	08:40	10.5	0.7
3/17	09:00	11.4	0.7
3/17	10:10	15.6	1.0

TABLE 39 (Continued)

Date	Time	Accum. Vol. (liters)	Interval Discharge (l/s*1000)
3/17	10:30	16.4	0.7
3/17	11:10	17.3	0.4

SITE 3: B-Horizon Flow

No Flow

TABLE 40
 HYDROLOGIC PROCESSES DATA FOR
 THE STORM OF 3/23/87

Precipitation Data

Date	Time	Accum. PCP (mm)	Interval PCP (mm)	Intens. (mm/hr)
3/23	08:12	0	0.0	0.0
3/23	08:33	2.5	2.5	7.3
3/23	09:03	3.8	1.3	2.5
3/23	09:33	5.6	1.8	3.6
3/23	09:53	5.8	0.3	0.8
3/23	10:18	8.4	2.5	6.1
3/23	12:24	10.2	1.8	0.8

No subsurface flow

TABLE 41

HYDROLOGIC PROCESSES DATA FOR
THE STORM OF 3/26/87

Precipitation Data

Date	Time	Accum. PCP (mm)	Interval PCP (mm)	Intens. (mm/hr)
3/26	08:40	0.0	0.0	0.0
3/26	09:14	1.3	1.3	2.2
3/26	09:29	2.5	1.3	5.1
3/26	10:19	7.1	4.6	5.5
3/26	10:34	7.6	0.5	2.0
3/28	12:49	0.0	0.0	0.0
3/28	13:29	1.3	1.3	1.9
3/28	14:40	1.3	0.0	0.0
3/28	16:24	1.8	0.5	0.3
3/28	17:54	3.3	1.5	1.0
3/28	20:29	3.8	0.5	0.2
3/30	09:30	0.0	0.0	0.0
3/30	10:34	1.3	1.3	1.2

No Subsurface Flow Occurred

TABLE 42
 HYDROLOGIC PROCESSES DATA FOR
 THE STORM OF 4/13/87

Precipitation Data

Date	Time	Accum. PCP (mm)	Interval PCP (mm)	Intens. (mm/hr)
4/13	05:20	0.0	0.0	0.0
4/13	05:40	9.7	9.7	29.0
4/13	06:05	10.2	0.5	1.2
4/13	06:56	10.4	0.3	0.3
4/13	08:01	11.4	1.0	0.9
4/13	08:16	11.9	0.5	2.0
4/13	10:46	0.0	0.0	0.0
4/13	11:06	1.5	1.5	4.6
4/13	11:41	1.5	0.0	0.0
4/13	12:01	2.5	1.0	3.0
4/13	12:11	0.0	0.0	0.0
4/13	12:51	3.8	3.8	5.7

No Subsurface Flow Occurred

TABLE 43

HYDROLOGIC PROCESSES DATA FOR
THE STORM OF 5/4/87

Precipitation Data

Date	Time	Accum. PCP (mm)	Interval PCP (mm)	Intens. (mm/hr)
5/3	07:39	0.0	0.0	0.0
5/3	07:59	1.3	1.3	3.8
5/3	08:19	9.1	7.9	23.6
5/3	11:09	10.2	1.0	0.4
5/3	23:20	0.0	0.0	0.0
5/4	00:45	0.5	0.5	0.4
5/4	01:00	4.3	3.8	15.2
5/4	01:10	5.6	1.3	7.6
5/4	02:00	7.6	2.0	2.4
5/4	04:00	10.7	3.0	1.5
5/4	06:00	9.4	0.0	0.0
5/4	08:00	12.7	3.3	1.6

No Subsurface Flow Occurred

TABLE 44
 HYDROLOGIC PROCESSES DATA FOR
 THE STORM OF 5/16/87

Precipitation Data

Date	Time	Accum. PCP (mm)	Interval PCP (mm)	Intens. (mm/hr)
5/16	15:51	0.0	0.0	0.0
5/16	16:31	1.3	1.3	1.9
5/16	17:36	0.0	0.0	0.0
5/16	17:56	0.8	0.8	2.3
5/16	00:20	0.0	0.0	0.0
5/16	00:40	7.1	7.1	21.3
5/16	00:50	10.2	3.0	18.3
5/16	01:00	10.4	0.2	1.5
5/16	01:10	17.8	7.4	44.2
5/16	01:20	18.5	0.8	4.6
5/16	01:25	21.6	3.0	36.6
5/16	11:04	0.0	0.0	0.0
5/16	11:09	1.3	1.3	15.2
5/16	12:04	2.0	0.8	0.8

No Subsurface Flow Occurred

TABLE 45

HYDROLOGIC PROCESSES DATA FOR
THE STORM OF 5/21/87

Precipitation Data

Date	Time	Accum. PCP (mm)	Interval PCP (mm)	Intens. (mm/hr)
5/22	07:23	0.0	0.0	0.0
5/22	07:37	7.1	7.1	30.5
5/22	08:13	7.6	0.5	0.8
5/22	08:23	9.9	2.3	13.7
5/22	08:33	10.2	0.2	1.5
5/22	08:38	20.3	10.2	121.9
5/22	08:53	21.6	1.3	5.1
5/23	14:15	0.0	0.0	0.0
5/23	14:20	4.8	4.8	57.9
5/23	14:46	4.8	0.0	0.0
5/23	14:51	5.1	0.2	3.0
5/23	16:01	0.0	0.0	0.0
5/23	16:31	4.6	4.6	9.1
5/23	18:22	10.2	5.6	3.0

No Subsurface Flow Occurred

TABLE 46

HYDROLOGIC PROCESSES DATA FOR
THE STORM OF 5/25/87

Precipitation Data

Date	Time	Accum. PCP (mm)	Interval PCP (mm)	Intens. (mm/hr)
5/25	06:20	0.0	0.0	0.0
5/25	06:30	6.4	6.4	38.1
5/25	07:50	6.9	0.5	0.4
5/25	08:10	12.7	5.8	17.5
5/25	08:20	20.6	7.9	47.2
5/25	08:55	30.5	9.9	17.0
5/25	09:15	31.8	1.3	3.8
5/25	09:50	32.3	0.5	0.9
5/25	10:35	35.6	3.3	4.4
5/25	11:00	36.1	0.5	1.2
5/25	12:40	36.8	0.8	0.5

SITE 1: Litter Layer Flow

Date	Time	Accum. Vol. (l)	Interval Discharge (l/s*1000)
5/25	06:42	1.4	0.0
5/25	06:44	1.9	3.6
5/25	06:48	1.9	0.1
5/25	07:02	2.1	0.3
5/25	07:17	2.6	0.5
5/25	08:04	2.8	0.9
5/25	08:07	2.8	0.2
5/25	08:08	3.0	2.7
5/25	08:12	3.1	0.2
5/25	08:20	3.9	1.8
5/25	08:24	5.3	5.6
5/25	08:31	6.4	2.7
5/25	08:44	8.5	2.7
5/25	08:50	8.6	0.3
5/25	10:10	9.1	0.1
5/25	10:20	9.5	0.7

TABLE 46 (Continued)

Date	Time	Accum. Vol. (liters)	Interval Discharge (l/s*1000)
5/25	10:40	9.6	0.1
5/25	12:20	10.1	0.1
<u>SITE 1: A-Horizon Flow</u>			
5/25	08:30	0.4	0.0
5/25	08:36	0.5	0.2
5/25	08:46	0.7	0.3
5/25	08:52	0.8	0.2
5/25	09:01	1.0	0.4
5/25	09:06	1.0	0.3
5/25	09:12	1.1	0.2
5/25	09:20	1.2	0.2
5/25	10:00	1.3	0.0
5/25	10:10	1.4	0.2
5/25	10:23	1.5	0.1
5/25	10:40	1.7	0.2
5/25	10:53	2.5	1.0
5/25	12:20	3.3	0.2
<u>SITE 1: B-Horizon Flow</u>			
5/25	08:28	0.4	0.0
5/25	08:31	1.0	3.1
5/25	08:35	1.6	2.7
5/25	08:41	1.7	0.2
5/25	08:50	2.4	1.3
5/25	09:02	3.1	1.0
5/25	09:20	3.8	0.6
5/25	10:20	4.5	0.2
5/25	11:10	5.2	0.2
5/25	12:04	5.5	0.1
5/25	13:00	5.9	0.1
<u>SITE 2: Litter Layer Flow</u>			
5/24	16:00	1.4	0.0
5/24	16:06	1.6	0.6

TABLE 46 (Continued)

Date	Time	Accum. Vol. (liters)	Interval Discharge (l/s*1000)
5/24	16:08	1.7	0.4
5/24	16:14	1.7	0.2
5/24	16:28	2.3	0.7
5/24	16:29	2.3	0.7
5/24	17:58	2.9	0.1
5/24	19:14	3.3	0.7
5/24	20:34	3.4	0.1
5/25	00:15	3.5	0.3
5/25	06:47	3.9	2.2
5/25	06:50	4.0	0.1
5/25	06:51	4.0	0.8
5/25	07:12	4.1	0.5
5/25	07:30	4.2	0.2
5/25	07:32	4.4	1.3
5/25	08:08	4.7	0.1
5/25	08:12	6.2	6.4
5/25	08:14	7.2	7.8
5/25	08:16	8.1	7.7
5/25	08:19	9.3	6.8
5/25	08:24	10.2	3.1
5/25	08:26	11.0	6.4
5/25	08:28	11.5	3.8
5/25	08:30	12.3	6.9
5/25	08:32	13.5	9.9
5/25	08:37	14.8	4.3
5/25	08:42	15.6	2.7
5/25	08:48	16.0	1.1
5/25	08:52	16.6	2.5
5/25	09:00	17.0	0.8
5/25	09:08	17.4	0.8
5/25	09:20	17.8	0.6
5/25	09:37	17.9	0.1
5/25	10:00	18.0	0.1
5/25	10:20	18.7	0.6
5/25	10:34	19.5	1.0
5/25	10:54	19.9	0.3
5/25	11:06	20.1	0.3
5/25	11:20	20.2	0.1

TABLE 46 (Continued)

Date	Time	Accum. Vol. (liters)	Interval Discharge (l/s*1000)
<u>SITE 2: A-Horizon Flow</u>			
5/25	08:20	0.6	0.0
5/25	08:22	1.4	6.9
5/25	08:26	1.7	1.2
5/25	08:28	3.3	13.0
5/25	08:32	7.9	19.5
5/25	08:35	11.1	17.6
5/25	08:37	12.6	12.5
5/25	08:43	15.7	8.6
5/25	08:48	17.3	5.3
5/25	08:52	18.9	6.7
5/25	08:58	20.4	4.2
5/25	09:05	22.0	3.8
5/25	09:10	22.8	2.7
5/25	09:20	23.5	1.2
5/25	09:30	24.3	1.3
5/25	10:19	25.1	0.3
5/25	11:10	25.9	0.3
5/25	12:18	26.7	0.2
5/25	14:00	27.4	0.1
<u>SITE 2: B-Horizon Flow</u>			
5/25	08:13	0.4	0.0
5/25	08:28	0.5	0.1
5/25	08:39	0.6	0.2
5/25	09:06	0.7	0.1
5/25	09:20	0.7	0.1
5/25	10:30	0.8	0.1
5/25	11:00	0.9	0.1
Total volume, not timed: 9.9			
<u>SITE 3: Litter Layer Flow</u>			
5/25	no times	17.8	
<u>SITE 3: A-Horizon Flow</u>			
no flow			
<u>SITE 3: B-Horizon Flow</u>			
no flow			

TABLE 47

HYDROLOGIC PROCESSES DATA FOR
THE STORM OF 5/28/87

Precipitation Data

Date	Time	Accum. PCP (mm)	Interval PCP (mm)	Intens. (mm/hr)
5/28	02:53	0.0	0.0	0.0
5/28	03:00	3.2	3.2	27.2
5/28	03:43	5.1	1.9	2.7
5/28	03:53	9.5	4.4	26.7
5/28	04:14	11.4	1.9	5.4
5/28	04:24	20.3	8.9	53.3
5/28	04:35	21.6	1.3	6.9
5/28	04:50	22.9	1.3	5.1
5/28	05:09	24.1	1.3	4.0
5/28	05:46	25.4	1.3	2.1
5/28	06:06	27.9	2.5	7.6
5/28	07:27	30.0	2.0	1.5
5/28	08:18	30.5	0.5	0.6
5/28	08:49	31.8	1.3	2.5
5/28	10:41	33.5	1.8	1.0
5/28	11:52	36.8	3.3	2.8
5/28	12:23	39.4	2.5	4.9
5/28	12:53	42.7	3.3	6.6
5/28	13:45	43.2	0.5	0.6
5/28	20:31	0.0	0.0	0.0
5/28	20:52	14.7	14.7	42.1
5/28	20:57	20.8	6.1	73.2
5/28	21:02	26.2	5.3	64.0
5/28	21:07	32.5	6.4	76.2
5/28	21:12	41.1	8.6	103.6
5/28	21:43	44.5	3.3	6.4
5/28	22:03	44.5	0.0	0.0
5/28	22:08	47.8	3.3	39.6
5/28	22:23	50.8	3.0	12.2
5/28	22:54	52.1	1.3	2.5
5/28	23:24	52.1	0.0	0.0
5/28	23:50	54.9	2.8	6.4
5/29	00:30	57.2	2.3	3.4
5/29	01:21	57.2	0.0	0.0
5/29	01:56	57.9	0.8	1.3
5/29	02:52	58.4	0.5	0.5

TABLE 47 (Continued)

Subsurface Flow Data

Date	Time	Accum. Vol (1)	Interval Discharge (1/s*1000)
<u>SITE 1: Litter Layer Flow</u>			
5/28	03:30	1.4	0.0
5/28	03:44	1.4	0.0
5/28	03:49	1.7	0.9
5/28	03:54	1.7	0.1
5/28	03:57	1.9	0.8
5/28	04:00	2.2	1.8
5/28	04:01	2.2	0.8
5/28	04:04	2.4	1.2
5/28	04:11	2.5	0.0
5/28	04:26	2.7	0.3
5/28	04:38	3.0	0.3
5/28	04:48	3.0	0.0
5/28	05:02	3.0	0.0
5/28	05:20	3.1	0.0
5/28	05:32	3.1	0.0
5/28	05:47	3.6	0.5
5/28	06:08	3.7	0.1
5/28	06:20	3.9	0.2
5/28	06:40	3.9	0.0
5/28	11:16	3.9	0.0
5/28	11:17	4.0	0.3
5/28	11:22	4.0	0.1
5/28	11:36	4.0	0.0
5/28	11:44	4.0	0.1
5/28	11:52	4.1	0.1
5/28	12:00	4.1	0.0
5/28	12:12	4.1	0.0
5/28	12:26	4.1	0.0
5/28	12:28	4.2	0.2
5/28	12:40	4.2	0.1
5/28	12:52	4.3	0.1
5/28	13:06	4.3	0.0
5/28	13:48	4.3	0.0
5/28	20:03	4.3	0.0
5/28	20:08	6.6	7.6
5/28	20:12	8.5	8.1
5/28	20:14	9.3	6.7
5/28	20:16	9.7	3.3
5/28	20:17	10.5	13.5

TABLE 47 (Continued)

Date	Time	Accum. Vol. (liters)	Interval Discharge (l/s*1000)
5/28	20:18	15.8	87.7
5/28	20:19	35.8	333.3
5/28	20:24	55.9	67.0
5/28	20:26	76.1	168.3
5/28	20:30	96.0	82.9
5/28	20:32	116.1	167.5
5/28	20:36	136.2	83.7
5/28	20:39	156.2	111.1
5/28	20:41	176.3	167.5
5/28	20:42	196.4	335.0
5/28	20:46	216.4	83.3
5/28	20:48	231.9	129.2
5/28	21:40	232.7	0.3

SITE 1: A-Horizon Flow

5/28	20:32	0.4	0.0
5/28	20:40	0.6	0.4
5/28	21:00	0.7	0.1
5/28	21:19	0.7	0.0
5/28	22:24	0.8	0.0
5/28	22:33	2.5	3.2
5/28	22:36	3.7	6.7
5/28	22:40	4.5	3.3
5/28	22:45	4.9	1.3
5/29	00:25	5.3	0.1

SITE 1: B-Horizon Flow

5/28	04:24	0.4	0.0
5/28	04:50	1.1	0.4
5/28	05:11	1.4	0.3
5/28	05:20	1.5	0.2
5/28	05:44	1.6	0.1
5/28	06:06	1.7	0.1
5/28	06:40	2.4	0.3
5/28	08:02	3.1	0.1
5/28	09:10	3.1	0.0
5/28	11:20	3.8	0.1
5/28	12:00	4.1	0.1

TABLE 47 (Continued)

Date	Time	Accum. Vol. (liters)	Interval Discharge (l/s*1000)
5/28	12:10	4.5	0.6
5/28	12:50	5.2	0.3
5/28	13:31	5.9	0.3
5/28	20:11	5.9	0.0
5/28	20:14	6.6	3.9
5/28	20:15	7.3	11.6
5/28	20:17	14.1	57.0
5/28	20:18	20.0	98.0
5/28	20:20	28.8	73.5
5/28	20:21	35.3	109.0
5/28	20:24	45.2	54.7
5/28	20:26	50.1	41.0
5/28	20:27	55.0	82.0
5/28	20:28	60.0	82.1
5/28	20:30	66.5	54.7
5/28	20:31	69.8	54.7
5/28	20:32	74.7	82.1
5/28	20:33	82.9	136.7
5/28	20:34	92.0	150.4
5/28	20:35	99.3	123.1
5/28	20:36	105.9	109.5
5/28	20:37	110.8	82.0
5/28	20:38	119.0	136.7
5/28	20:39	125.6	109.5
5/28	20:40	135.4	164.0
5/28	20:41	142.0	109.5
5/28	20:42	151.9	164.0
5/28	20:43	156.8	82.2
5/28	20:44	163.3	109.3
5/28	20:45	168.3	82.0
5/28	20:46	173.2	82.2
5/28	20:47	178.1	82.0
5/28	20:48	181.4	54.7
5/28	20:50	189.6	68.4
5/28	20:51	194.5	82.0
5/28	20:52	197.8	54.7
5/28	20:54	206.0	68.4
5/28	20:56	215.0	75.2
5/28	20:57	220.8	95.8
5/28	20:58	224.1	54.7
5/28	21:00	232.3	68.3
5/28	21:01	238.8	109.5

TABLE 47 (Continued)

Date	Time	Accum. Vol. (liters)	Interval Discharge (l/s*1000)
<u>SITE 2: Litter Layer Flow</u>			
5/28	02:58	1.4	0.0
5/28	03:00	1.4	0.2
5/28	03:04	2.1	2.8
5/28	03:06	2.2	1.0
5/28	03:11	2.2	0.1
5/28	03:30	2.9	0.6
5/28	03:32	3.1	1.6
5/28	03:33	3.3	3.8
5/28	03:34	3.5	3.0
5/28	03:35	3.7	3.2
5/28	03:39	4.8	4.6
5/28	03:40	4.9	2.6
5/28	03:41	5.1	2.6
5/28	03:47	5.2	0.3
5/28	03:52	5.3	0.5
5/28	03:57	5.6	0.9
5/28	03:59	6.1	3.9
5/28	04:01	6.8	6.4
5/28	04:03	7.2	2.6
5/28	04:06	7.5	2.0
5/28	04:08	8.3	6.4
5/28	04:11	8.8	2.6
5/28	04:14	9.5	4.3
5/28	04:16	10.0	4.3
5/28	04:19	10.2	0.9
5/28	04:23	10.3	0.6
5/28	04:39	10.9	0.5
5/28	04:46	11.4	1.3
5/28	05:22	12.4	0.4
5/28	05:30	12.7	0.8
5/28	05:37	13.1	0.7
5/28	05:40	13.2	0.9
5/28	05:41	13.5	5.1
5/28	05:48	13.9	0.9
5/28	05:52	14.2	1.3
5/28	06:00	14.5	0.6
5/28	06:02	14.6	1.3
5/28	09:28	15.3	0.1
5/28	09:56	16.1	0.5
5/28	10:16	16.4	0.2
5/28	10:40	16.8	0.3

TABLE 47 (Continued)

Date	Time	Accum. Vol. (liters)	Interval Discharge (l/s*1000)
5/28	10:52	17.0	0.3
5/28	11:08	17.4	0.4
5/28	11:20	17.8	0.6
5/28	11:24	18.2	1.7
5/28	11:36	18.7	0.6
5/28	11:48	19.1	0.6
5/28	11:49	19.5	6.8
5/28	11:52	19.9	2.3
5/28	12:06	20.3	0.5
5/28	12:22	20.7	0.4
5/28	12:32	21.1	0.7
5/28	12:40	21.5	0.9
5/28	12:48	21.7	0.4
5/28	12:57	21.9	0.4
5/28	13:36	22.3	0.2
5/28	20:12	22.3	0.0
5/28	20:13	24.4	34.2
5/28	20:14	26.2	29.6
5/28	20:16	28.9	22.5
5/28	20:18	37.0	67.4
5/28	20:20	48.2	93.6
5/28	20:22	59.7	95.5
5/28	20:24	102.2	354.1
5/28	20:25	144.9	711.7
5/28	20:26	187.4	708.7
5/28	20:28	229.9	354.3
5/28	20:29	236.4	108.8
5/28	20:32	250.3	77.1

Tank overflowed.

Inflow stopped at 23:20, the same time
the rain stopped.

SITE 2: A-Horizon Flow

5/28	04:13	1.4	0.0
5/28	04:20	1.6	0.4
5/28	04:40	1.7	0.1
5/28	05:19	11.7	4.3
5/28	05:50	12.5	0.4
5/28	06:10	13.3	0.6
5/28	06:30	13.7	0.3
5/28	07:10	14.0	0.2

TABLE 47 (Continued)

Date	Time	Accum. Vol. (liters)	Interval Discharge (l/s*1000)
5/28	11:30	14.8	0.0
5/28	12:09	15.6	0.3
5/28	12:30	16.4	0.6
5/28	12:42	17.2	1.1
5/28	12:50	17.9	1.6
5/28	13:00	19.5	2.6
5/28	13:06	20.3	2.2
5/28	13:11	20.7	1.3
5/28	13:28	23.4	2.7
5/28	13:40	25.0	2.2
5/28	13:54	26.5	1.9
5/28	14:00	27.3	2.2
5/28	14:16	28.1	0.8
5/28	15:00	28.9	0.3
5/28	20:12	29.6	0.0
5/28	20:14	30.4	6.5
5/28	20:16	40.6	84.5
5/28	20:17	48.4	130.0
5/28	20:18	62.4	234.0
5/28	20:19	78.8	273.0
5/28	20:20	90.5	195.0
5/28	20:21	101.4	182.0
5/28	20:22	113.1	195.0
5/28	20:23	124.8	195.0
5/28	20:24	136.5	195.0
5/28	20:25	148.2	195.0
5/28	20:26	158.3	169.0
5/28	20:27	168.5	169.0
5/28	20:28	179.4	182.0
5/28	20:29	190.3	182.0
5/28	20:30	202.8	208.0
5/28	20:31	218.4	260.0
5/28	20:32	233.2	247.0

Tank overflowed, final volume was projected.

SITE 2: B-Horizon Flow

5/28	03:42	0.9	0.0
5/28	03:56	1.0	0.1
5/28	04:30	1.1	0.0

TABLE 47 (Continued)

Date	Time	Accum. Vol. (liters)	Interval Discharge (l/s*1000)
5/28	05:06	1.1	0.0
5/28	05:26	1.4	0.2
5/28	05:44	1.6	0.2
5/28	05:46	1.7	0.8
5/28	07:14	2.9	0.2
5/28	09:00	3.5	0.1
5/28	12:40	4.2	0.0
5/28	13:08	4.8	0.4
5/28	13:48	6.0	0.5
5/28	14:13	6.6	0.4
5/28	14:40	7.2	0.4
5/28	20:00	7.2	0.0
5/28	20:29	7.5	0.2
5/28	20:36	16.7	21.8
5/28	20:44	22.3	11.7
5/28	21:00	37.1	15.4
5/28	21:12	47.4	14.4
5/28	21:22	55.4	13.3
5/28	21:34	64.2	12.2
5/28	21:46	73.0	12.2
5/28	21:56	81.8	14.7
5/28	22:00	85.0	13.3
5/28	22:14	95.4	12.4
5/28	22:20	100.2	13.3
5/28	22:30	107.4	12.0
5/28	22:40	113.8	10.7
5/28	22:50	120.2	10.7
5/28	22:54	121.8	6.7
5/28	23:08	129.0	8.6
5/28	23:14	132.2	8.9
5/28	23:57	153.8	8.4
5/29	00:08	158.6	7.3
5/29	00:15	161.8	7.6
5/29	00:22	165.0	7.6
5/29	00:34	169.8	6.7
5/29	00:56	177.8	6.1
5/29	01:05	180.2	4.4
5/29	01:12	181.8	3.8
5/29	01:36	186.6	3.3
5/29	01:43	188.2	3.8
5/29	02:00	190.6	2.4
5/29	02:38	194.6	1.8
5/29	03:00	197.0	1.8
5/29	03:30	197.8	0.4

TABLE 47 (Continued)

Date	Time	Accum. Vol. (liters)	Interval Discharge (l/s*1000)
5/29	04:14	199.4	0.6
5/29	05:00	200.2	0.3
5/29	07:30	201.0	0.1

SITE 3: Litter Layer Flow

5/28	03:45	0.4	0.0
5/28	03:47	1.1	6.2
5/28	03:48	1.3	3.1
5/28	03:53	1.4	0.3
5/28	04:12	1.5	0.1
5/28	04:20	1.7	0.4
5/28	04:28	3.7	4.2
5/28	04:52	4.4	0.5
5/28	05:31	5.0	0.3
5/28	06:08	6.4	0.6
5/28	06:32	6.7	0.2
5/28	11:00	7.0	0.0
5/28	11:40	7.7	0.3
5/28	12:50	9.0	0.3
5/28	13:20	9.7	0.4
5/28	20:22	9.7	0.0
5/28	20:36	22.5	15.3
5/28	20:38	23.4	6.9
5/28	20:42	24.2	3.5
5/28	20:53	29.2	7.6
5/28	21:04	30.0	1.3
5/28	21:45	30.9	0.3
5/28	21:53	31.7	1.7
5/28	22:08	32.5	0.9
5/28	22:40	33.4	0.4
5/28	23:40	34.2	0.2
5/29	00:00	35.0	0.7
5/29	01:36	35.9	0.1

SITE 3: A-Horizon Flow

5/28	08:40	0.4	0.0
5/28	10:00	0.5	0.0
5/28	11:50	0.6	0.0

TABLE 47 (Continued)

Date	Time	Accum. Vol. (liters)	Interval Discharge (l/s*1000)
5/28	13:30	0.7	0.0
5/28	17:00	0.8	0.0
5/28	20:12	0.8	0.0
5/28	20:14	0.9	0.8
5/28	20:15	1.6	12.4
5/28	20:16	10.5	148.9
5/28	20:18	16.4	49.1
5/28	20:21	19.8	18.7
5/28	20:23	20.6	7.0
5/28	20:33	36.6	26.7
5/28	20:37	49.3	52.6
5/28	20:40	56.9	42.1
5/28	20:43	61.9	28.1
5/28	20:48	68.6	22.5
5/28	20:50	70.3	14.0
5/28	20:53	72.0	9.4
5/28	20:57	73.7	7.0
5/28	21:05	76.2	5.3
5/28	21:12	77.1	2.0
5/28	21:30	78.8	1.6
5/28	21:36	79.6	2.3
5/28	21:40	80.4	3.5
5/28	21:54	87.2	8.0
5/28	22:00	89.7	7.0
5/28	22:10	92.2	4.2
5/28	22:20	93.9	2.8
5/28	22:30	94.8	1.4
5/28	22:50	96.4	1.4
5/28	23:00	96.9	0.7
5/28	23:02	97.3	3.5
5/28	23:50	101.5	1.5
5/29	00:10	103.2	1.4
5/29	00:40	104.9	0.9
5/29	00:54	105.7	1.0
5/29	01:50	107.4	0.5
5/29	02:50	108.2	0.2
5/29	04:30	109.1	0.1

SITE 3: B-Horizon Flow

5/28	20:19	0.4	0.0
5/28	20:22	11.4	61.1

TABLE 47 (Continued)

Date	Time	Accum. Vol. (liters)	Interval Discharge (l/s*1000)
5/28	20:24	26.7	127.7
5/28	20:26	36.9	85.1
5/28	20:27	47.1	170.2
5/28	20:30	55.7	47.3
5/28	20:34	69.3	56.7
5/28	20:35	77.8	141.8
5/28	20:42	120.3	101.3
5/28	20:50	162.9	88.7
5/28	21:01	205.4	64.5
5/28	21:08	214.0	20.3
5/28	21:11	218.2	23.6
5/28	21:15	222.5	17.7
5/28	21:24	231.0	15.8
5/28	21:37	239.5	10.9
5/28	21:50	247.1	9.8

Tank overflowed, inflow stopped at 2300.

TABLE 48
 HYDROLOGIC PROCESSES DATA FOR
 THE STORM OF 5/31/87

Precipitation Data

Date	Time	Accum. PCP (mm)	Interval PCP (mm)	Intens. (mm/hr)
31-May	08:45	0.0	0.0	0.0
31-May	09:10	0.8	0.8	1.8
31-May	09:55	0.8	0.0	1.0
31-May	10:20	2.0	1.3	4.9
31-May	10:41	8.9	6.9	25.4
31-May	15:33	10.2	1.3	2.1

Subsurface Flow Data

Date	Time	Accum. Vol. (liters)	Interval Discharge (l/s)*1000
------	------	----------------------------	-------------------------------------

SITE 1: Litter Layer Flow

30-May	10:55	1.4	0.0
30-May	11:02	1.4	0.0
30-May	12:40	1.4	0.0
31-May	16:44	1.4	0.0
31-May	16:50	2.2	2.3
31-May	16:52	2.9	5.5

Site 1 A-Horizon Flow

No Flow Occurred

TABLE 48 (Continued)

Date	Time	Accum. Vol. (liters)	Interval Discharge (l/s*1000)
<u>SITE 1: B-Horizon Flow</u>			
29-May	09:50	0.4	0.0
29-May	10:31	0.5	0.0
29-May	11:10	0.6	0.0
29-May	12:30	0.9	0.1
29-May	15:00	1.1	0.0
29-May	17:00	1.3	0.0
29-May	19:00	1.3	0.0
31-May	11:44	1.3	0.0
31-May	14:00	1.4	0.0
31-May	17:28	1.5	0.0
<u>SITE 2: Litter Layer Flow</u>			
30-May	12:44	1.4	0.0
30-May	13:02	1.4	0.0
30-May	13:07	1.4	0.0
30-May	13:08	1.7	3.7
30-May	13:12	1.7	0.1
30-May	13:20	1.9	0.5
30-May	13:24	2.0	0.3
30-May	13:43	2.3	0.3
30-May	14:04	2.3	0.0
30-May	14:10	2.4	0.1
30-May	14:28	2.4	0.0
30-May	14:37	2.4	0.1
30-May	15:00	2.5	0.0
30-May	16:00	2.6	0.0
30-May	17:00	2.6	0.0
30-May	18:00	2.7	0.0
30-May	19:00	2.7	0.0
30-May	20:00	2.7	0.0
30-May	21:20	2.8	0.0
31-May	04:00	2.8	0.0
31-May	09:20	2.8	0.0
31-May	10:00	2.9	0.0
31-May	10:36	2.9	0.0
31-May	10:38	2.9	0.2
31-May	10:44	2.9	0.0
31-May	10:48	3.0	0.4

TABLE 48 (Continued)

Date	Time	Accum. Vol. (liters)	Interval Discharge (l/s*1000)
31-May	10:50	3.1	0.5
31-May	10:56	3.1	0.0
31-May	11:00	4.0	3.9
31-May	11:01	5.0	16.7
31-May	11:03	6.0	8.3
31-May	11:05	6.4	3.2
31-May	11:12	7.0	1.5
31-May	11:20	7.1	0.2
31-May	11:37	7.2	0.2
31-May	12:10	8.0	0.4

SITE 2: A-Horizon Flow

29-May	20:40	0.4	0.0
30-May	14:48	1.2	0.0
30-May	14:55	1.3	0.1
30-May	14:57	1.4	1.3
30-May	18:20	1.5	0.0
31-May	11:00	1.5	0.0
31-May	11:04	1.6	0.6
31-May	11:08	1.7	0.4
31-May	11:14	12.1	28.9
31-May	11:30	13.7	1.6
31-May	11:48	14.4	0.7
31-May	12:30	14.8	0.2
31-May	13:30	15.2	0.1
31-May	16:00	15.6	0.0

SITE 2: B-Horizon Flow

31-May	11:18	0.4	0.0
31-May	11:25	0.5	0.2
31-May	11:30	0.7	0.8
31-May	11:41	1.1	0.6
31-May	11:43	1.7	5.2
31-May	12:30	2.6	0.3
31-May	12:50	2.8	0.1
31-May	16:00	3.2	0.0

TABLE 4B (Continued)

Date	Time	Accum. Vol. (liters)	Interval Discharge (l/s*1000)
<u>SITE 3: Litter Layer Flow</u>			
31-May	10:46	1.4	0.0
31-May	10:48	2.3	7.4
31-May	10:52	2.6	1.2
31-May	11:06	4.3	2.0
<u>SITE 3: A-Horizon Flow</u>			
No Flow Occurred			
<u>Site 3: B-Horizon Flow</u>			
31-May	11:37	9.8	0.0
31-May	11:41	10.1	1.2
31-May	11:58	10.6	0.4
31-May	12:37	11.4	0.4
31-May	14:18	12.6	0.2
31-May	18:27	13.5	0.1

TABLE 49

HYDROLOGIC PROCESSES DATA FOR
THE STORM OF 6/19/87

Precipitation Data

Date	Time	Accum. PCP (mm)	Interval PCP (mm)	Intens. (mm/hr)
6/19	15:17	0.0	0.0	0.0
6/19	15:22	6.4	6.4	76.2
6/19	15:27	7.1	0.8	9.1
6/19	15:57	12.2	5.1	10.2
6/19	17:17	12.7	0.5	0.4
6/19	18:32	15.2	2.5	2.0
6/20	01:05	16.3	1.0	0.2
6/20	01:40	16.8	0.5	0.9
6/20	01:45	21.6	4.8	57.9
6/20	02:05	22.1	0.5	1.5
6/23	04:16	0.0	0.0	0.0
6/23	04:36	12.7	12.7	38.1
6/23	05:01	25.4	12.7	30.5
6/23	05:06	27.2	1.8	21.3
6/23	05:42	27.9	0.8	1.3

No Subsurface Flow Occurred

TABLE 50
 HYDROLOGIC PROCESSES DATA FOR
 THE STORM OF 6/30/87

Precipitation Data

Date	Time	Accum. PCP (mm)	Interval PCP (mm)	Intens. (mm/hr)
6/30	04:51	0.0	0.0	0.0
6/30	05:01	2.3	2.3	13.7
6/30	05:06	2.8	0.5	6.1
6/30	05:27	12.4	9.7	27.6
6/30	07:22	13.2	0.8	0.4
6/30	07:32	21.1	7.9	47.2
6/30	07:40	21.6	0.5	3.8
6/30	07:50	31.8	10.2	61.0
6/30	08:00	50.8	19.1	114.3
6/30	08:13	53.3	2.5	11.7
6/30	08:53	54.6	1.3	1.9
6/30	09:50	57.2	2.5	2.7

SITE 1: Litter Layer Flow

Date	Time	Accum. Vol. (l)	Interval Discharge (l/s)*1000
------	------	-----------------------	-------------------------------------

SITE 1: Litter Layer Flow

6/30	no times	41	
------	----------	----	--

SITE 1: A-Horizon Flow

6/30	08:10	0.4	0.0
6/30	08:14	0.5	0.6
6/30	08:46	1.0	0.2
6/30	09:22	1.3	0.2
6/30	09:40	1.4	0.1
6/30	10:36	1.5	0.0

TABLE 50 (Continued)

Date	Time	Accum. Vol. (liters)	Interval Discharge (l/s*1000)
6/30	11:20	2.9	0.4
6/30	11:50	5.3	1.3
6/30	12:00	5.5	0.4
6/30	12:10	5.7	0.3
6/30	12:54	6.1	0.2

SITE 1: B-Horizon Flow

6/30	07:52	0.4	0.0
6/30	07:54	1.0	4.6
6/30	07:56	1.6	5.4
6/30	08:00	1.7	0.2
6/30	08:06	1.7	0.1
6/30	08:18	2.7	1.4
6/30	08:32	3.4	0.8
6/30	09:26	4.2	0.2

SITE 2: Litter Layer Flow

6/30	05:29	1.4	0.0
6/30	05:37	1.7	0.6
6/30	05:41	1.7	0.1
6/30	05:45	1.9	0.9
6/30	05:47	2.0	0.7
6/30	05:52	2.0	0.1
6/30	05:53	2.1	0.5
6/30	06:01	2.3	0.5
6/30	06:07	2.3	0.1
6/30	06:21	2.4	0.0
6/30	06:25	2.4	0.2
6/30	07:05	2.5	0.0
6/30	07:07	2.5	0.5
6/30	07:29	2.5	0.0
6/30	07:35	2.5	0.1
6/30	07:37	2.6	0.6
6/30	07:41	3.2	2.5
6/30	07:45	3.3	0.3
6/30	07:49	3.6	1.4
6/30	07:51	4.2	5.1
6/30	07:54	10.2	33.3

TABLE 50 (Continued)

Date	Time	Accum. Vol. (liters)	Interval Discharge (l/s*1000)
6/30	07:57	13.2	16.3
6/30	07:59	14.0	6.8
6/30	08:01	14.4	3.4
6/30	08:05	15.0	2.5
6/30	08:09	15.2	0.9
6/30	08:14	15.6	1.4
6/30	08:18	16.0	1.7
6/30	08:33	16.4	0.5
6/30	08:41	16.6	0.4
6/30	08:56	16.8	0.2

Site 2: A-Horizon Flow

6/30	05:24	0.6	0.0
6/30	05:28	1.2	2.7
6/30	06:00	1.3	0.0
6/30	07:00	1.3	0.0
6/30	07:38	1.3	0.0
6/30	07:43	1.6	0.9
6/30	07:51	11.7	21.0
6/30	07:53	15.6	32.5
6/30	07:54	23.4	130.3
6/30	07:55	31.2	130.0
6/30	07:58	39.0	43.2
6/30	08:00	43.7	39.0
6/30	08:03	46.8	17.3
6/30	08:08	52.3	18.2
6/30	08:13	54.6	7.8
6/30	08:27	62.4	9.3
6/30	08:38	65.9	5.3
6/30	09:00	68.6	2.1
6/30	09:30	70.2	0.9
6/30	10:30	71.0	0.2
6/30	11:30	71.4	0.1
6/30	12:30	71.8	0.1
6/30	15:30	72.2	0.0

TABLE 50 (Continued)

Date	Time	Accum. Vol. (liters)	Interval Discharge (l/s*1000)
<u>SITE 2: B-Horizon Flow</u>			
6/30	07:53	0.4	0.0
6/30	07:54	1.0	9.3
6/30	07:55	2.9	32.8
6/30	07:56	3.9	15.3
6/30	07:58	5.4	12.8
6/30	08:00	6.3	7.8
6/30	08:06	7.9	4.2
6/30	08:16	9.1	2.1
6/30	08:26	10.7	2.7
6/30	08:41	11.7	1.1
6/30	09:10	12.7	0.6
6/30	10:06	13.2	0.1
<u>SITE 3: Litter Later Flow</u>			
6/30	05:20	1.4	0.0
6/30	05:28	2.2	1.8
6/30	07:46	2.2	0.0
6/30	07:50	2.5	1.1
6/30	07:56	2.7	0.5
6/30	08:14	3.0	0.3
6/30	08:24	3.7	1.1
6/30	08:56	4.4	0.3
6/30	09:26	4.7	0.2
<u>SITE 3: A-Horizon Flow</u>			
no flow			
<u>SITE 3: B-Horizon Flow</u>			
6/30	08:53	0.4	0.0
6/30	09:10	0.6	0.2
6/30	09:30	0.7	0.1
6/30	10:10	0.9	0.1

TABLE 50 (Continued)

Date	Time	Accum. Vol. (liters)	Interval Discharge (l/s*1000)
6/30	10:43	1.0	0.0
6/30	11:23	1.1	0.0
6/30	11:52	1.1	0.0
6/30	12:10	1.2	0.0
6/30	12:44	1.3	0.0
6/30	14:30	1.3	0.0
6/30	15:21	1.3	0.0
6/30	15:30	1.5	0.3
6/30	15:40	1.5	0.0
6/30	18:30	1.6	0.0

APPENDIX B

SOURCE CHEMISTRY SUMMARIES BY STORM

TABLE 51

WATERSHED PROCESSES CHEMISTRY DATA
FOR THE STORM OF 1/15/87

Lab#	Sample Type	pH	Cond. (umhos)	NO3-N (mg/l)	DOC (mg/l)	Ca (mg/l)	Mg (mg/l)	K (mg/l)	Na (mg/l)
1	1 TF1	4.26	36.3	0.583	22	0.59	0.13	0.57	0.14
2	1 TF2	4.34	31.6	0.630	10	0.44	0.06	0.32	0.07
3	1 TF3	4.16	37.5	0.673	6	0.37	0.02	0.12	0.07
4	1 TF4	4.20	42.2	0.504	0	0.15	0.00	0.02	0.02
5	1 SP1A	5.29	43.3	0.220	45	2.19	1.06	1.25	1.19
6	1 SP1B	5.52	29.3	0.000	46	1.63	1.39	1.18	1.47
7	1 SP2B	5.72	30.5	0.050	13	1.34	1.34	0.97	1.65
8	1 SP3L	5.55	32.8	0.152	261	2.91	0.99	2.13	0.24
9	1 SP3A	5.31	34.0	0.510	119	2.90	1.05	1.55	0.60
10	1 SP3B	5.08	27.0	0.000	15	1.04	1.01	0.87	0.99
11	1 TL	5.16	84.4	0.127	215	10.19	1.05	4.40	1.78
12	2 TF1	4.30	31.1	0.599	2	0.27	0.00	0.08	0.07
13	2 TF2	4.24	32.2	0.536	13	0.41	0.06	0.37	0.03
14	2 TK3	4.25	28.7	0.524	1	0.23	0.00	0.04	0.02
15	2 TF4	4.30	28.7	0.547	11	0.53	0.07	0.49	0.07
16	2 SP1L	5.74	22.3	0.193	97	1.43	0.47	4.02	0.07
17	2 SP1A	5.38	36.3						
18	2 SP1B	5.03	29.3	0.013	64	1.58	1.20	1.30	1.26
19	2 SP2L	5.62	25.8	0.107	179	1.27	0.56	4.07	0.44
20	2 SP2A	5.08	49.2	1.341	62	1.36	1.84	1.18	2.72
21	2 SP2B	5.03	55.1	0.013	32	1.47	2.17	0.58	3.87
22	2 TA	5.15	29.9	0.062	105	1.88	1.07	1.17	0.90
23	3 TF1	4.38	36.3	0.777	23	0.89	0.19	1.81	0.16
24	3 TF2	4.31	30.5	0.627	13	0.64	0.18	0.50	0.19

TABLE 51 (Continued)

Lab#	Sample Type	pH	Cond. (umhos)	NO3-N (mg/l)	DOC (mg/l)	Ca (mg/l)	Mg (mg/l)	K (mg/l)	Na (mg/l)
25	3 TF3	4.22	32.8	0.561	12	0.63	0.17	0.32	0.13
26	3 TF4	4.08	4.3	0.849	16	0.60	0.12	0.59	0.10
27	3 SP3B	5.31	19.9	0.000	1	0.45	0.80	0.59	1.55
28	3 STR	5.30	27.0	0.000	6	0.84	0.83	0.52	1.81

TABLE 52
 WATERSHED PROCESSES CHEMISTRY DATA
 FOR THE STORM OF 2/11/87

Lab#	Sample Type	pH	Cond. (umhos)	NO3-N (mg/l)	DOC (mg/l)	Ca (mg/l)	Mg (mg/l)	K (mg/l)	Na (mg/l)
30	1 TF1	4.75	29.3	0.73	19	1.42	0.3	0.51	0.58
31	1 TF2	4.8	24.6	0.766	16	1.51	0.27	0.44	0.47
32	1 TF3	4.44	31.6	0.837	22	1.21	0.21	0.26	0.53
33	1 TF4	4.47	22.1			0.61	0.14	0.12	0.42
34	1 SP3L	5.28	30.8			2.48	0.81	1.92	0.4
35									
36	2 TF1	4.57	23.3			0.61	0.11	0.12	0.33
37	2 TF2	4.62	27.9			1.31	0.32	0.45	0.44
38	2 TF3	4.45	27.3			0.7	0.11	0.12	0.34
39	2 TF4	4.62	24.4			0.87	0.17	0.43	0.35
40	2 SP1L	6.04	37.8			2.58	0.97	3.66	0.37
41	2 T-L	6.08	50.6			4.85	1.22	4.09	0.45
42	3 TF1	4.22	80.2			3.79	0.72	2.66	0.96
43	3 TF2	4.25	52			2.27	0.53	1.04	0.7
44	3 TF3	5.14	29.7			1.88	0.42	0.7	0.38
45	3 TF4	4.08	68.6			2.05	0.36	0.96	0.87
46	3 SP2B	5.6	23.3			1.03	0.72	0.73	1.05
47	3 SP3B	5.55	21			0.36	0.65	0.52	1.25
48	3 TL	5.94	62.8			4.95	1.15	4.2	0.68

TABLE 53
 WATERSHED PROCESSES CHEMISTRY DATA
 FOR THE STORM OF 2/16/87

Lab#	Sample Type	pH	Cond. (umhos)	NO3-N (mg/l)	DOC (mg/l)	Ca (mg/l)	Mg (mg/l)	K (mg/l)	Na (mg/l)
49	1 TF1	6.2	16.3			1.8	0.18	0.34	0.26
50	1 TF2	5.92	16.3			1.64	0.17	0.41	0.26
51	1 TF3	5.5	14.5			1.49	0.1	0.17	0.31
52	1 TF4	5.92	11			1.28	0.04	0.1	0.24
53	1 SP1A	5.24	34.9			2.15	1.16	1.3	0.98
54	1 SP1B	5.6	29.1			1.23	0.98	0.94	1.11
55	1 SP2B	5.93	27.9			0.93	0.98	0.89	1.34
56	1 SP3L	5.75	27.9			2.76	0.82	1.97	0.28
57	1 SP3A	5.68	34.3			2.66	1.05	1.72	0.53
58	1 SP3B	5.68	25.6			0.86	0.83	0.82	0.95
59	2 TF1	6.13	11			1.19	0.06	0.09	0.22
60	2 TF2	6.12	12.8			1.45	0.13	0.2	0.2
61	2 TF3	6.23	11.6			1.25	0.05	0.09	0.21
62	2 TF4	6.09	16			1.57	0.13	0.34	0.25
63	2 SP1L	5.89	23.4		158	1.81	0.63	2.48	0.25
64	2 SP1B	5.46	16.3			1.26	0.85	1.13	0.99
65	2 SP2L	5.72	33.4		216	2.59	0.88	3.53	0.4
66	2 SP2A	4.92	43.4		51	0.96	1.47	0.53	2.42
67	2 SP2B	5.24	45.7		37	1.23	1.62	0.56	2.91
68	2 SP3A	6.3	25.8			2.38	0.75	0.42	0.91
69	2 SP3B	5.3	45.7		23	1	1.67	0.33	3.33
70	2 TL	5.77	45.7		313	2.92	0.85	2.81	0.44
71	2 TA	5.55	29.3		129	1.94	0.98	0.95	0.85
72	2 TB	6.76	99.6		286	15.4	2.4	1.87	1.99
73	2 STR	6.45	29.9		25	1.12	0.92	0.47	2.39

TABLE 53 (Continued)

Lab#	Sample Type	pH	Cond. (umhos)	NO3-N (mg/l)	DOC (mg/l)	Ca (mg/l)	Mg (mg/l)	K (mg/l)	Na (mg/l)
74	3 TF1	5.36	26.4		52	2.04	0.31	1.17	0.49
75	3 TF2	5.4	17.6	0.694	22	1.51	0.22	0.44	0.32
76	3 TF3	5.83	15.2		28	1.53	0.24	0.37	0.3
77	3 TF4	5.19	18.8		33	1.49	0.18	0.39	0.31
78	3 SP1L	5.89	30.5	0.121	265	2.54	0.86	2.73	0.39
79	3 SP1A	5.57	22.8	0.086	41	0.94	0.73	1.13	0.53
80	3 SP3B	5.43	32.8	0	27	0.64	0.95	0.74	0.79
81	3 SP2L	5.89	28.1		277	2.3	0.77	3.08	0.4
82	3 SP2A	6.11	29.9		140	2.05	1	1.36	0.82
83	3 SP3A	5.97	21.1		10	0.42	0.75	0.55	1.33
84	3 SP3B	5.4	21.1		7	0.24	0.76	0.54	1.37
85	3 TL	5.4	49.2	0.981	313	4.27	1.1	4.31	0.58
86	3 TA	5.7	14.1	0.306	23	1.48	0.16	0.56	0.2
87	3 STR	5.83	25.8	0.031	23	0.74	0.78	0.56	1.81

TABLE 54
 WATERSHED PROCESSES CHEMISTRY DATA
 FOR THE STORM OF 2/21/87

Lab#	Sample Type	pH	Cond. (umhos)	NO3-N (mg/l)	DOC (mg/l)	Ca (mg/l)	Mg (mg/l)	K (mg/l)	Na (mg/l)
100	1 TF1	4.43	42.2	1.379	24	2.37	0.35	0.45	0.43
101	1 TF2	4.41	37.5	1.332	20	2.01	0.25	0.33	0.26
102	1 TF3	4.16	44.5	1.375	24	1.57	0.17	0.23	0.33
103	1 TF4	4.26	36	1.035	18	1.18	0.07	0.19	0.18
104	1 SP1B	5.9	27	0.023	18	0.81	0.96	0.62	1.57
105	2 TF1	4.21	39.5	1.127	13	1.3	0.08	0.12	0.17
106	2 TF2	4.21	45.3	1.297	24	1.91	0.3	0.29	0.17
107	2 TF3	4.18	41	1.109	13	1.25	0.08	0.09	0.18
108	2 TF4	4.15	49.2	0.707	22	1.91	0.25	0.32	0.21
109	2 SP3B	5.73	51.5	0.011	18	0.84	1.74	0.31	4.07
110	3 TF1	4.1	61.6	1.275	25	2.83	0.41	1.36	0.32
111	3 TF2	4.18	42.2	1.223	18	1.74	0.25	0.35	0.24
112	3 TF3	4.32	38.7	1.137	21	1.81	0.29	0.53	0.19
113	3 TF4	3.95	68	1.745	26	2.41	0.35	0.87	0.33
114	3 SP3B	5.93	18.8	0.009	10	0.26	0.69	0.51	1.47
115	3 STR	6.11	28.7	0.013	14	0.75	0.81	0.57	2.21
116	3 STR	5.62	27.3	0.012	13	0.63	0.8	0.57	2.19

TABLE 55

WATERSHED PROCESSES CHEMISTRY DATA
FOR THE STORM OF 2/24/87

Lab#	Sample Type	pH	Cond. (umhos)	NO3-N (mg/l)	DOC (mg/l)	Ca (mg/l)	Mg (mg/l)	K (mg/l)	Na (mg/l)
117	1 TF1	5	9.4	0.111	18	0.6	0.07	0.2	0.19
118	1 TF2	4.99	8.2	0.119	18	0.45	0.04	0.09	0.27
119	1 TF3	4.86	9.4	0.169	11	0.25	0	0.02	0.08
120	1 TF4	5.04	5.9	0.091	10	0.22	0	0	0.03
121	1 SP1B	5.23	27	0.006	11	0.69	1	0.52	1.71
122	1 SP2B	5.4	29.3	0.086	11	0.8	1.09	0.63	1.75
123	1 SP3B	5.62	23.3	0.015	15	0.63	0.82	0.82	1.08
124	2 TF1	5.05	0.64	0.094	7	0.09	0	0.04	0.01
125	2 TF2	4.89	0.99	0.2	18	0.27	0.05	0.12	0.06
126	2 TF3	4.83	0.76	0.124	10	0.07	0	0.03	0.02
127	2 TF4	4.87	0.81	0.124	13	0.22	0	0.2	0.03
128	2 SP1L	5.75	29.1	0.25	188	2.26	0.76	3.2	0.34
129	2 SP1B	4.78	26.7	0.034	59	1.02	0.87	1.09	1.15
130	2 SP2B	5.29	51.2	0.03	27	1.04	1.72	0.55	3.86
131	2 SP3B	5.12	49.4	0.016	18	0.72	1.64	0.29	3.98
135	2 STR	6.16	30.8	0.016	20	0.8	0.89	0.56	2.85
136	3 TF3	4.29	43.4	1.455	46	1.8	0.31	1.17	0.25
137	3 TF2	4.29	32.6	0.851	48	1.06	0.25	0.55	0.16
138	3 TF3	5.22	11.6	0.18	22	0.33	0.05	0.24	0.03
139	3 TF4	4.24	54.6	1.241	54	1.05	0.17	0.74	0.14
140	3 SP1A	5.3	23.3	0.057	33	0.76	0.77	1.07	0.64
141	3 SPB3	5.23	20	0.022	8	0.18	0.72	0.55	1.34
142	3 STR	5.63	26.4	0.043	22	0.76	0.69	0.57	1.9
143	3 TL	5.66	46.9	1.087	253	4.36	0.89	3.56	1.4
144	3 TR	5.74	17.6	0.448	38	1.53	0.17	0.83	0.19

TABLE 56

WATERSHED PROCESSES CHEMISTRY DATA
FOR THE STORM OF 2/28/87

Lab#	Sample Type	pH	Cond. (umhos)	NO3-N (mg/l)	DOC (mg/l)	Ca (mg/l)	Mg (mg/l)	K (mg/l)	Na (mg/l)
148	1 TF1	4.93	9.73	0.141	27	0.25	0	0.2	0.09
149	1 TF2	4.96	7.44	0.155	27	0.23	0	0.2	0.09
150	1 TF3	4.78	8.02	0.158	14	0.09	0	0.03	0.05
151	1 TF4	4.75	8.02	0.144	12	0.09	0	0.05	0.12
152	1 SP1A	5.9	28.6	0.065	69	1.2	0.97	1.02	1.29
153	1 SP1B	6.01	28.6	0.015	47	1.05	0.98	0.8	1.61
154	1 SP1B	6.1	26.3	0.011	26	0.7	0.96	0.69	1.64
155	1 SP2B	6.13	28.6	0.079	28	0.73	0.98	0.7	1.45
156	1 SP3L	5.29	28.6	0.127	468	2.32	0.77	1.93	0.23
157	1 SP3A	5.54	29.8	0.778	258	2.16	0.87	1.6	0.61
158	1 SP3B	5.94	24.1	0.009	33	0.89	0.81	0.85	1.09
159	1 TL	6.9	36.1	0.074	42	1.71	0.21	3.46	2.74
160	1 TA	5.74	6.87	0.126	26	0.52	0.03	0.23	0.12
161	1 TB	6.27	35.5	0.146	171	3.14	1.03	1.46	0.94
166	2 TF1	4.85	8.01	0.146	11	0.07	0	0.04	0.1
167	2 TF2	4.85	8.01	0.133	24	0.15	0	0.12	0.09
168	2 TF3	4.73	8.01	0.144	11	0.17	0.05	0.06	0.06
169	2 TF4	4.83	9.16	0.149	23	0.28	0.06	0.27	0.1
170	2 SP1L	6.28	17.2	0.038	197	1.52	0.43	2.35	0.16
171	2 SP1A	5.21	34.4	0.137	137	2.13	0.86	1.29	1.12
172	2 SP2B	5.5	26.9	0.026	112	1.37	0.84	1.1	1.02
173	2 SP2L	5.66	25.2	0.194	285	2.33	0.68	2.74	0.32
174	2 SP2A	4.99	40.1	0.033	69	1.08	1.26	0.76	2.42
175	2 SP2B	5.86	47.5	0.034	49	1.24	1.54	0.59	3.15
176	2 SP3A	5.18	24.1	0.03	146	1.21	0.87	0.53	1.23

TABLE 56 (Continued)

Lab#	Sample Type	pH	Cond. (umhos)	NO3-N (mg/l)	DOC (mg/l)	Ca (mg/l)	Mg (mg/l)	K (mg/l)	Na (mg/l)
177	2 SP3B	5.88	46.9	0.019	32	1.08	1.46	0.41	3.45
178	2 TL	5.87	22.9	0.094	365	2.31	0.65	2.19	0.36
179	2 TA	5.68	26.3	0.047	141	1.81	0.8	0.98	0.75
180	2 TB	6.22	26.3	0.019	170	2.41	0.79	0.93	0.68
192	2 STR	6.64	28.1	0.011	25	0.91	0.73	0.55	1.69
193	3 TF1	4.72	13.2	0.102	43	0.43	0.05	0.86	0.11
194	3 TF2	4.67	9.7	0.119	23	0.28	0.03	0.22	0.07
195	3 TF3	4.86	8.6	0.119	31	0.5	0.09	0.28	0.06
196	3 TF4	4.52	12.1	0.068	34	0.25	0.01	0.31	0.04
197	3 SP1L	5.51	19.5	0.032	33	0.83	0.57	0.72	0.72
198	3 SP1A	5.06	19.5	0.016	58	0.58	0.58	0.82	0.49
199	3 SP1B	5.31	18.3	0.016	13	0.45	0.57	0.55	0.77
200	3 SP2L	6.1	26.3	0.088	343	2.52	0.62	2.9	0.44
201	3 SP2A	5.31	21.8	0.015	44	1.12	0.62	0.73	0.63
202	3 SP2B	5.44	21.4	0.015	16	0.81	0.57	0.7	0.82
203	3 SP3A	5.37	21.8	0.034	74	0.96	0.69	0.79	0.66
204	3 SP3B	5.38	20	0.013	13	0.36	0.58	0.58	1.08
205	3 SP3B	5.33	19.5	0.013	8	0.34	0.6	0.56	1.19
206	3 TL	5.36	36.1	0.158	440	3.21	0.7	3.43	0.31
207	3 TS	5.44	18.3	0.417	60	1.64	0.16	1	0.17
208	3 TB	5.52	28.1	0.013	144	1.89	0.81	1.24	0.75
209	3 STR	5.8	22.3	0.008	22	0.71	0.54	0.58	1.36

TABLE 57
 WATERSHED PROCESSES CHEMISTRY DATA
 FOR THE STORM OF 3/17/87

Lab#	Sample Type	pH	Cond. (umhos)	NO3-N (mg/l)	DOC (mg/l)	Ca (mg/l)	Mg (mg/l)	K (mg/l)	Na (mg/l)
217	1 TL1	5.58	27.9	0.08	181	2.27	0.54	2.4	0.75
218	1 TA1	5.82	1	0.16	22	0.53	0.09	0.45	0.19
219	1 TB	5.62	29.6	0.12	171	1.51	0.71	1.34	0.57
220	1 TF1	5.43	0.81	0.22	13	0.24	0.05	0.1	0.07
221	1 TF2	5.31	0.64	0.16	7	0.2	0.02	0.08	0.08
222	1 TF3	5.23	0.58	0.15	3	0.21	0	0	0.04
223	1 TF4	5.36	0.47	0.1	2	0.03	0	0	0.03
224	1 SP1L	5.71	29.6	0.005	153	1.74	0.67	1.83	0.74
225	1 SP1A	5.77	36	0.23	126	2.18	0.85	1.55	0.94
226	1 SP1B	5.52	29.1	0.06	96	1.41	0.82	1.27	1.08
227	1 SP2A	5.62	26.7	0.44	104	1	0.69	1.2	0.52
228	1 SP2B	5.61	27.9	0.29	81	1.12	0.87	1.2	0.99
229	1 SP3L	5.71	25.6	0.14	317	2.27	0.76	1.58	0.63
230	1 SP3A	5.65	32	1.26	171	2.4	0.93	1.61	0.53
231	1 SP3B	5.24	23.3	0.05	49	0.73	0.64	0.9	0.82
243	2 TL	5.42	22.1	11.98	123	1.17	0.56	1.23	0.6
244	2 TA	5.47	21	0.02	118	1.15	0.6	1.19	0.79
245	2 TB	5.47	22.1	0.03	133	1.2	0.68	1.04	0.75
246	2 STR	5.96	27.9	0.01	22	0.75	0.73	0.59	2.17
247	2 TF1	5.74	0.47	0.1	214	0.03	0	0	0.03
248	2 TF2	5.33	0.81	0.2	11	0.38	0.06	0.14	0.15
249	2 TF3	5.37	0.47	0.1	3	0.1	0	0.04	0.09
250	2 TF4	5.3	0.58	0.1	7	0.09	0	0.1	0.06
251	2 SP1L	6.08	21.5	0.07	146	1.69	0.51	2.88	0.17
252	2 SP1A	5.29	26.7	0.12	115	1.4	0.7	1.23	1.03

TABLE 57 (Continued)

Lab#	Sample Type	pH	Cond. (umhos)	NO3-N (mg/l)	DOC (mg/l)	Ca (mg/l)	Mg (mg/l)	K (mg/l)	Na (mg/l)
253	2 SP1B	5.47	24.4	0.08	104	0.97	0.55	1.08	1.06
254	2 SP2L	5.72	23.2	0.08	192	1.14	0.37	3.04	0.31
255	2 SP2A	5.34	34.9	0.05	83	0.92	0.86	1.02	1.75
256	2 SP2B	5.47	32.6	0.18	76	0.97	0.99	0.78	2.07
257	2 SP3L	5.6	22.1	0.18	200	1.69	0.54	2.06	0.34
258	2 SP3A	5.27	26.2	0.04	139	1.17	0.81	0.82	1.13
259	2 SP3B	5.2	31.4	0.14	79	0.85	0.96	0.54	1.93
282	3 TL	5.87	46.8	1.606	265	3.59	0.84	4.13	0.57
283	3 TA	6.42	36.4	0.063	161	3.64	0.97	2.84	0.67
284	3 TB	5.68	31.6	0.123	182	2.13	1.06	2.1	0.91
285	3 TF1	4.72	18.9	0.51	56	0.87	0.13	0.97	0.27
286	3 TF2	4.74	18.2	0.74	47	0.87	0.12	0.6	0.27
287	3 TF3	5.52	8.5	0.272	33	0.53	0.1	0.36	0.15
288	3 TF4	4.4	26.1	0.904	76	0.92	0.12	0.62	0.26
289	3 SP1L	6.42	20.7	0.07	59	1.02	0.62	1.23	0.69
290	3 SP1A	5.44	17	0.048	51	0.5	0.55	0.95	0.52
291	3 SP1B	5.77	17.3	0.059	26	0.41	0.61	0.67	0.84
292	3 SP2L	6.11	20.2	0.257	173	1.53	0.47	2.68	0.23
293	3 SP2A	5.75	13.9	0.008	70	1.07	0.62	0.82	0.71
294	3 SP2B	5.61	20	0.027	28	0.6	0.65	0.72	0.97
295	3 SP3L	5.12	22.2	0.011	184	1.36	0.57	1.54	0.38
296	3 SP3A	5.13	20.6	0.016	11	0.87	0.72	0.98	0.52
297	3 SP3L	5.72	18.9	0.043		0.2	0.69	0.58	1.26

TABLE 58
WATERSHED PROCESSES CHEMISTRY DATA
FOR THE STORM OF 3/23/87

Lab#	Sample Type	pH	Cond. (umhos)	NO3-N (mg/l)	DOC (mg/l)	Ca (mg/l)	Mg (mg/l)	K (mg/l)	Na (mg/l)
298	1 TF1	5.13	17.2	0.411	46	1.28	0.24	0.59	0.33
300	1 TF3	4.65	18.9	0.553	16	0.89	0.11	0.3	0.29
301	1 TF4	4.67	4.67	0.389	11	0.66	0.07	0.21	0.23
302	1 SP1B	5.53	5.53	0.026	20	0.69	0.93	0.69	1.45
303	1 SP2A	5.56	5.56	0.394		1.32	0.06	1.47	0.74
304	1 SP3B	5.52	5.52	0.026	35	0.62	0.05	0.99	0.87
305	2 TL	6.01	6.01	0.166	311	2.68	0.92	2.57	0.91
306	2 TA	5.59	5.59	0.047	145	1.53	0.76	1.48	0.83
307	2 STR	6.29	6.29	0.013	22	0.9	0.82	0.63	2.3
308	2 TF1	4.72	4.72	0.263	13	0.71	0.08	0.19	0.25
309	2 TF2	4.75	4.75	0.461	32	0.94	0.17	0.32	0.25
310	2 TF3	4.64	4.64	0.333	12	0.55	0.06	0.18	0.22
311	2 TF4	5.23	5.23	0.074	23	0.63	0.1	0.33	0.2
312	2 SP2B	5.31	5.31	0.02	33	1.06	1.36	0.56	3.2
313	2 SP3B	5.14	5.14	0	25	0.76	1.43	0.43	3.58
317	3 TF1	4.49	4.49	1.444	69	2.1	0.34	1.62	0.46
318	3 TF2	4.51	4.51	0.709	40	1.04	0.19	0.65	0.34
319	3 TF3	4.81	4.81	0.503	35	0.86	0.19	0.55	0.24
320	3 TF4	4.31	4.31	0.965	69	1.12	0.2	0.79	0.31
321	3 SP2P	5.64	5.64	0.009	17	0.67	0.67	0.77	0.94
322	3 SP3A	5.8	18.3	0.02	20	0.23	0.66	0.62	1.3
323	3 SP3B	5.66	20	0.006	12	0.17	0.66	0.6	1.37
324	3 STR	5.91	26.1	0.015	16	0.72	0.77	0.69	1.9

TABLE 59
 WATERSHED PROCESSES CHEMISTRY DATA
 FOR THE STORM OF 3/26/87

Lab#	Sample Type	pH	Cond. (umhos)	NO3-N (mg/l)	DOC (mg/l)	Ca (mg/l)	Mg (mg/l)	K (mg/l)	Na (mg/l)
325	BP	5.62	13.1	0.481	12	1.01	0.04	0.13	0.24
326	1 TF1	5.35	18.8	0.589	46	1.63	0.13	0.33	0.32
327	1 SP18	6.41	23	0.008	23	0.6	1.02	0.57	0.22
328	1 TF3	5.2	24.4	0.949	27	1.95	0.18	0.35	0.39
329	1 TF4	5.13	14.3	0.525	23	1.06	0.08	0.1	0.19
330	2 TL	9.29	209.1	0.107	229	5.56	0.67	11	6.23
333	2 TF1	5.09	16.8	0.293	26	0.99	0.09	0.15	0.18
334	2 TF2	5.38	15.1	0.218	42	1.37	0.15	0.23	0.23
335	2 TF3	5.07	15	0.263	20	1.06	0.08	0.07	0.2
336	2 TF4	5.06	16.6	0.235	35	1.46	0.15	0.24	0.25
337	2 SP38	5.89	45.5	0.013	25	0.69	0.16	0.33	4
338	3 TF1	4.96	23	0.419	54	1.49	1.62	1.17	0.24
339	3 TF2	4.74	18	0.267	30	1.06	0.25	0.26	0.23
340	3 TF3	4.99	18.4	0.295	33	1.36	0.13	0.31	0.23
341	3 TF4	4.66	21.8	0.371	39	1.15	0.18	0.35	0.21
342	3 STR	6.3	27.3	0.011	22	0.82	0.14	0.64	2.16

TABLE 60
 WATERSHED PROCESSES CHEMISTRY DATA
 FOR THE STORM OF 4/13/87

Lab#	Site	Type	pH	Cond. (umhos)	NO3-N (mg/l)	DOC (mg/l)	Ca (mg/l)	Mg (mg/l)	K (mg/l)	Na (mg/l)
400		BP	5.83	17.9			1.47	0.05	0.05	0.08
401	1	TL	7.09	242			7.04	0.51		
402	1	TR	6.44	36.9			3.82	0.47	1.37	0.29
406	1	TF1	5.77	28.8			2.89	0.59	1.94	0.15
407	1	TF3	5.4	19.6			1.32	0.13	0.42	0.06
408	1	TF4	5.09	16.7			0.94	0.1	0.3	0.04
409	1	SP3L	5.95	31.2			2.8	1.04	1.46	0.07
410	1	SP3A					2.72	1.53	2.44	0.45
411	2	TL	5.54	39.8			3.33	1.35	3.06	0.34
412	2	TF1	5.28	13.8			0.81	0.09	0.2	0.05
413	2	TF2	5.3	21.9			1.97	0.31	1.25	0.09
414	2	TF3	4.98	17.3			0.67	0.06	0.23	0.01
415	2	TF4	5.32	15.6			1.06	0.2	0.78	0.13
416	2	SP1L	6.01	53.1			5.06	1.77	6.99	0.09
417	2	SP1B	5.72	24.8			0.05	0.35	1.2	0.89
418	2	SP2L	5.48	29.4			1.11	0.9	3.78	0.47
419	2	SP3L	5.63	43.8			3.31	1.64	2.98	0.14
420	2	SP3B	5.82	44.4			0	0.6	0.32	3.01
422	3	TL	5.75	62.9			4.98	1.29	4.82	0.46
423	3	TF1	4.44	63.5			4.72	0.67	2.28	0.46
424	3	TF2	4.72	27.1			1.81	0.29	0.64	0.3
425	3	TF3	5.38	24.8			2.27	0.45	1.25	0.28
426	3	TF4	4.44	45			2.58	0.36	1.07	0.3
427	3	SP1L	5.7	43.8			4.3	1.5	3.19	0.33
428	3	SP1A	5.32	21.9			0.86	0.88	1.11	0.59
429	3	SP2L	5.99	31.2			2.56	0.76	3	0.24
432	3	STR	5.7	30			1	0.91	0.67	2.14

TABLE 61
WATERSHED PROCESSES CHEMISTRY DATA
FOR THE STORM OF 5/4/87

Lab#	Sample Type	pH	Cond. (umhos)	NO3-N (mg/l)	DOC (mg/l)	Ca (mg/l)	Mg (mg/l)	K (mg/l)	Na (mg/l)
433	3 TL	6.78	387	0.041	1126	16.4	3.3	22	5.7
434	3 TF1	6.07	62.3	0.048	268	3.74	0.95	12.04	1.13
435	3 TF1	5.71	51.9	0.312	333	2.73	0.83	8.82	0.89
436	3 TF3	5.26	36.9	0.048	641	2.12	0.77	5.08	0.88
437	3 TF4	4.24	66.9	0.369	268	3.05	0.73	3.5	1.03
438	3 SP1L	6.33	73.8	0.625	711	8.95	2.56	6.18	1.11
439	3 SP2L	5.94	34.6	0.228	253	0.89	0.29	1.25	0.19
440	1 TL	7.02	113	0.04	4	5.06	1.04	17.38	4.32
441	1 TB	7.14	114	0.057	4	5.16	1.07	17.96	4.19
442	1 TA	5.84	47.2	0.483	376	4.19	0.88	3.83	0.7
446	1 TF1	5.4	68.1	0.2072	1600	4.09	1.57	12.58	0.67
447	1 TF2	5.04	65.8	0.249	770	3.65	1.19	5.16	0.65
448	1 TF3	5.31	23.1	0.074	279	1.41	0.48	2.41	0.4
449	1 TF4	5.4	15.6	0.032	72	0.83	0.23	1.25	0.36
450	1 SP3L	6.4	47.9	0.654	374	3.85	1.32	3.01	0.34
451	2 TL	6.61	116	0.053	964	14.1	2.96	11.82	2.02
452	2 TF1	5.46	17.3	0.036	128	0.97	0.28	1.55	0.41
453	2 TF2	5.26	45.6	0.132	900	3.6	1.18	4.8	0.68
454	2 TF3	6.01	18.5	0.058	82	0.89	0.29	4.83	0.42
455	2 TF4	5.14	36.3	0.09	755	1.94	0.84	11	0.5
456	2 SP1L	6.22	98.1	0.88	924	9.09	3.22	15.92	0.53
457	2 SP2L	6.19	34.6	0.993	403	9.21	2.82	14.31	0.7
458	2 SP3L	5.87	70.4	0.6	712	3.26	3.12	4.39	0.27
459	2 SP3A	7.25	57.7	0.028	47	3.26	0.3	0.16	0.27
460	2 SP3B	5.82	45.2	0.027	13				
472	BP	4.62	23.1	0.805	12	1.1	0.18	0.68	0.29

TABLE 62
WATERSHED PROCESSES CHEMISTRY DATA
FOR THE STORM OF 5/19/87

Lab#	Sample Type	pH	Cond. (umhos)	NO3-N (mg/l)	DOC (mg/l)	Ca (mg/l)	Mg (mg/l)	K (mg/l)	Na (mg/l)
473	3 TL	5.7	65.9	0.595	471	2.56	0.74		0.41
474	3 TA	6.89	93.8	0.177	282	6.38	1.54		1.42
475	3 TF1	4.68	29.5	0.45	121	1.04	0.22	2.79	0.28
476	3 TF2	4.38	32.4	0.347	233	0.96	0.34	1.92	0.27
477	3 TF3	4.63	29.5	0.289	440	1.16	0.37	2.68	0.25
478	3 TF4	4.38	36	0.364	205	0.75	0.16	1.15	0.22
479	3 SP1L	5.9	35	0.336	435	3.23	1.09	3.74	0.24
480	3 SP1B	4.96	21.6	0.152	54	0.66	0.85	1.28	0.77
481	1 TF1	4.39	29	0.124	356	1.25	0.36	1.5	0.19
482	1 TF2	4.34	30.1	0.219	299	1.2	0.31	1.4	0.22
483	1 TF3	4.47	23.9	0.258	130	0.44	0.12	0.59	0.16
484	1 TF4	4.43	21	0.119	53	0.31	0.05	0.34	0.4
485	2 TF1	4.45	22.2	0.205	71	0.29	0.06	0.41	0.49
486	2 TF2	4.42	31.8	0.236	272	1.3	0.43	1.28	0.76
487	2 TF3	4.51	19.9	0.219	30	0.33	0.08	0.33	0.64
488	2 TF4	4.33	35.3	0.159	359	1	0.38	1.5	0.21
490	1 TL	7.05	105	0.177	667	7.08	1.28	2.51	
497	1 SP2L	6.01	42	0.419	475	3.67	1.06	3.32	1.03
498	2 TL	5.81	38.6	0.38	597	2.69	0.97	2.88	1.27
499	2 TA	5.85	41.5	0.408	389	3.2	1.46	3.48	1.37
505	2 SP1L	5.51	59.6	0.585	793	4.21	1.35	8.6	0.22
506	2 SP3L	5.18	44.1	0.342	589	2.55	1.15	4.21	0.25
507	2 SP3L	5.68	34.7	0.321	263	2.87	1.13	2.24	0.18

TABLE 63

WATERSHED PROCESSES CHEMISTRY DATA
FOR THE STORM OF 5/22/87

Lab#	Sample Type	pH	Cond. (umhos)	NO3-N (mg/l)	DOC (mg/l)	Ca (mg/l)	Mg (mg/l)	K (mg/l)	Na (mg/l)
508	BP	5.1	13.8	0.358	8.2	0.08	0	0.18	0.18
509	3 TL	5.72	52.9	0.28	506	3.68	0.95	1.12	0.35
510	3 TA	7.15	111.4	0.047	254	6.49	1.44	1.43	1.36
511	3 TF1	4.7	25.4	0.347	28.4	0.72	0.15	2.21	0.24
512	3 TF2	4.62	19.9	0.285	76.9	0.26	0.11	0.48	0.14
513	3 TF3	4.62	21.51	0.309	37.2	0.58	0.2	0.94	0.19
514	3 TF4	4.48	23.2	0.352	83.8	0.42	0.09	0.65	0.16
515	3 SP1L	6.04	41.9	0.24	501	4.71	1.37	3.52	0.27
516	3 SP1A	4.88	43	1.953	37.2	1.7	1.67	2.07	0.65
517	3 SP1B	5.3	21	0.039	48.5	0.5	0.77	1.19	0.74
518	3 SP2A	6.15	37.5	0.206	195	3.28	1.21	2.07	0.77
519	3 SP2B	5.84	17.1	0.024	23.3	0.58	0.58	0.78	0.93
520	1 TL	7.26	73	0.121	319	4.5	0.81	0.82	1.86
521	1 TA	6.86	110	0.992	328	20.4	0.96	2.88	1.08
522	1 TF1	4.52	25.4	0.264	138	0.76	0.18	0.81	0.16
523	1 TF2	4.36	28.7	0.332	127	0.57	0	0.68	0.18
524	1 TF3	4.51	18.8	0.28	58.6	0.18	0.04	0.22	0.16
525	1 TF4	4.84	13.2	0.28	25.9	0.17	0.02	0.12	0.08
526	1 SP1L	5.63	0	0.21	274	2.45	0.65	2.21	0.25
527	1 SP3L	5.77	37.5	0.17	440	3.72	1.16	2.42	0.17
534	2 TL	5.73	27	0.309	312	2.18	0.76	1.88	0.18
535	2 TA	6.4	41.9	0.039	248	3.3	1.22	2.11	0.78
536	2 TB	7.5	108	0.79	128	24	1.77	1.59	1.04
537	2 TF1	4.67	16.5	0.236	48.5	0.18	0.01	0.18	0.12
538	2 TF2	4.5	23.6	0.304	106	0.64	0.19	0.59	0.17
539	2 TF3	4.95	11.37	0.267	12	0.02	0	0.07	0.1
540	2 TF4	4.33	32.5	0.308	156	0.65	0.2	0.96	0.24

TABLE 63 (Continued)

Lab#	Sample Type	pH	Cond. (umhos)	NO3-N (mg/l)	DOC (mg/l)	Ca (mg/l)	Mg (mg/l)	K (mg/l)	Na (mg/l)
541	2 SP1L	5.95	42.5	0.082	707	3.78	1.11	0.81	0.26
542	2 SP1B	6.18	29.1	0.234	49.2	1.35	0.92	1.42	1.14
543	2 SP2L	5.4	30.2	0.098	378	1.85	0.85	3.25	0.37
544	2 SP3L	5.61	33.6	0.151	377	3.51	1.25	1.87	0.25
545	2 SP3A	7.19	58.8						

TABLE 64
 WATERSHED PROCESSES CHEMISTRY DATA
 FOR THE STORM OF 5/25/87

Lab#	Sample Type	pH	Cond. (umhos)	NO3-N (mg/l)	DOC (mg/l)	Ca (mg/l)	Mg (mg/l)	K (mg/l)	Na (mg/l)
547	1 TL	7.19	66.6	0.204	425	5.42	0.94	0.89	2.09
548	1 TA	6.67	64.9	0.542	187	10.13	0.13	1.63	0.61
549	1 TB	6.98	108.6	0.723	502	3.38	0.48	0.81	1.59
550	1 TF1	4.49	23.5	0.173	88	0.59	0.15	0.59	0.18
551	1 TF2	4.3	30.2	0.221	81	0.39	0.1	0.45	0.21
552	1 TF3	4.33	23.5	0.237	20	0.11	0.04	0.07	0.12
553	1 TF4	4.38	21.3	0.233	8	0.08	0.03	0.04	0.09
554	1 SP1A	6.22	32.5	0.344	112	2.15	0.98	1.4	0.85
555	1 SP1B	5.72	33.6	0.073	156	2.36	1.18	1.66	0.98
556	1 SP2B	6.05	31.3	1.121	26	1.19	1.26	1.28	1.28
557	1 SP3L	5.87	41.4	0.094	472	5.02	1.62	2.38	0.34
558	1 SP3A	6.09	81.7	5.693	149	7.74	3	3.19	0.52
559	1 SP3B	6.15	20.2	0.05	30	0.74	0.77	1.15	0.85
560	2 TL	5.26	24.3	0.216	272	1.96	0.8	1.65	0.18
561	2 TA	5.43	30.7	0.121	233	1.89	1.16	1.39	0.58
562	2 TB	6.98	109	1.767	171	17.4	1.97	2.48	1.12
563	2 TF1	4.32	24.4	0.243	35	0.16	0.08	0.13	0.12
564	2 TF2	4.4	27.3	0.209	108	0.68	0.24	0.68	0.12
565	2 TF3	4.4	20.5	0.204	10	0.06	0.03	0.05	0.12
566	2 TF4	4.2	35.2	0.224	129	0.46	0.13	0.91	0.11
567	2 STR	6.12	35.8	0.025	81	1.34	1.21	0.99	2.41
568	2 SP1L	5.93	39.8	0.085	348	3.85	1.2	6.1	0.13
569	2 SP1B	6	31.8	0.128	109	1.52	1.05	1.8	1.27
570	2 SP2L	5.26	39.2	0.095	568	2.55	1.19	4.37	0.34
571	2 SP2B	5.51	31.8	0.073	69	0.91	1.1	0.75	1.96

TABLE 64 (Continued)

Lab#	Sample Type	pH	Cond. (umhos)	NO3-N (mg/l)	DOC (mg/l)	Ca (mg/l)	Mg (mg/l)	K (mg/l)	Na (mg/l)
572	2 SP3L	5.58	34.1	0.083	525	4.08	1.58	1.92	0.27
573	2 SP3A	6.66	40.9	0.033	36	4.55	0.99	0.62	0.93
574	2 SP3B	5.55	35.2	0.041	69	0.74	1.36	0.51	2.43
575	3 TL	5.7	36.9	0.102	420	3.04	0.82	6.2	0.26
576	3 TF1	4.65	18.2	0.136	57	0.4	0.14	1.38	0.13
577	3 TF2	4.37	23.9	0.172	66	0.34	0.14	0.38	0.06
578	3 TF3	4.42	23.9	0.18	68	0.42	0.16	0.66	0.1
579	3 TF4	4.36	24.4	0.212	54	0.22	0.09	0.54	0.1
580	3 SP1L	6.19	36.4	0.134	400	4.82	1.42	2.9	0.16
581	3 SP1A	5.48	25.6	0.333	95	0.82	1.02	1.7	0.44
582	3 SP1B	5.21	23.9	0.054	84	0.52	0.97	1.82	0.46
583	3 SP2A	5.73	34.1	0.069	224	3.16	1.5	2.39	0.68
584	3 SP2B	6.14	21.6	0.062	34	0.86	0.81	1.18	0.97
585	3 SP3A	5.83	28.4	0.85	50	0.96	1.35	1.79	0.85
586	3 STR	6.04	25	0.028	106	0.56	0.69	1.11	1.57

TABLE 65

WATERSHED PROCESSES CHEMISTRY DATA
FOR THE STORM OF 5/28/87

Lab#	Sample Type	pH	Cond. (umhos)	NO3-N (mg/l)	DOC (mg/l)	Ca (mg/l)	Mg (mg/l)	K (mg/l)	Na (mg/l)
700	BP	4.72	28.4	0.151	0	0.01	0.03	0.06	0.2
701	1 TL	5.62	34.1	0.044	244	2.11	0.73	1.8	0.36
702	1 TA	6.82	39.8	0.105	193	4.63	0.69	2.58	0.58
703	1 TB	5.62	38.6	0.071	219	1.67	0.82	1.61	0.39
704	1 TF1	4.82	13.1	0.139	42	0.36	0.11	0.38	0.22
705	1 TF2	4.62	16.5	0.163	49	0.23	0.07	0.35	0.25
706	1 TF3	4.67	12.5	0.167	16	0.05	0.04	0.07	0.23
707	1 TF4	4.77	11.4	0.166	8	0.02	0.02	0.06	0.23
708	1 SP1A	5.71	5.71	0.073	129	1.42	0.9	1.53	0.74
709	1 SP1B	5.78	30.7	0.298	63	1.43	1.05	1.28	1.09
710	1 SP2L	6.06	25.6	0.38	205	2.1	0.87	2.3	0.44
711	1 SP2A	5.32	22.7	0.339	152	1.29	0.77	1.58	0.35
712	1 SP2B	5.39	26.1	0.647	130	1.48	1.02	1.73	0.54
713	1 SP3L	5.76	23.9	0.046	267	2.31	0.92	2.07	0.24
714	1 SP3A	5.7	20.4	0.211	128	1.47	0.78	1.14	0.31
715	1 SP3B	5.7	21.6	0.028	146	0.85	0.83	1.22	0.51
716	1 SP2B	5.35	23.9	0.761	73	1.11	1.11	1.45	0.76
725	2 TL	5.44	21.6	0.036	182	1.51	0.69	1.25	0.47
726	2 TA	5.21	22.7	0.032	161	1.43	0.75	1.2	0.57
727	2 TB	5.27	22.7	0.035	175	1.46	0.79	1.22	0.48
728	2 STR	6.14	23.9	0.028	64	1	0.87	0.83	1.17
729	2 TF1	4.7	13.1	0.151	19	0.08	0.04	0.11	0.2
730	2 TF2	4.71	14.2	0.157	40	0.32	0.09	0.29	0.25
731	2 TF3	4.82	10.8	0.161	6	0.1	0.04	0.08	0.25
732	2 TF4	4.53	18.2	0.138	61	0.24	0.08	0.38	0.27
733	2 SP1L	6.02	21	0.083	293	1.66	0.49	3.18	0.2
734	2 SP1A	5.45	27.3	0.126	145	1.66	0.9	1.41	0.73

TABLE 65 (Continued)

Lab#	Sample Type	pH	Cond. (umhos)	NO3-N (mg/l)	DOC (mg/l)	Ca (mg/l)	Mg (mg/l)	K (mg/l)	Na (mg/l)
735	2 SP1B	6.21	39.8	0.064	308	2.49	0.75	5.7	0.97
736	2 SP2L	5.21	24.4	0.051	226	1.65	0.7	1.72	0.54
737	2 SP2A	4.98	31.8	0	119	1.1	0.92	1.1	1.33
738	2 SP2B	5.25	34.4	0.013	56	0.92	1.03	0.65	2.1
739	2 SPL3	5.54	25.8	0.026	283	2.42	0.83	1.85	0.42
740	2 SPA3	5.67	29.8	0.072	115	1.3	1.07	0.86	1.31
741	2 SP3B	5.98	33.2	0.093	68	1.07	1.14	0.85	1.78
742	2 SP2A	5.02	34.3	0	68	0.82	1.03	0.76	1.55
743	2 SP3B	5.32	33.8	0.015	71	1.06	1.11	0.8	1.54
770	3 TL	6.29	48.7	0.144	404	3.49	0.78	6.3	0.78
771	3 TA	6.49	46.9	0.012	288	4.27	0.94	3.5	0.51
772	3 TB	5.87	32.1	0.016	236	2.36	0.7	2.86	0.48
773	3 TF1	5.03	12.6	0.11	43	0.27	0.08	1.33	0.53
774	3 TF2	4.87	12	0.128	29	0.09	0.04	0.18	0.19
775	3 TF3	4.99	12.1	0.111	45	0.26	0.09	0.38	0.2
776	3 TF4	4.76	14.3	0.144	31	0.13	0.05	0.28	0.25
777	3 SP1L	6.22	23.5	0.214	142	1.64	0.72	1.46	0.42
778	3 SP1A	5.27	19.5	0.048	159	1.09	0.69	1.33	0.28
779	3 SP1B	5.39	18.3	0.018	56	0.47	0.6	1.05	0.55
780	3 SP2L	6.07	21.8	0.013	150	1.64	0.52	1.48	0.46
781	3 SP2A	5.61	21.2	0.008	71	1.14	0.68	0.97	0.57
782	3 SP2B	5.57	17.8	0.048	83	0.76	0.55	1.15	0.5
783	3 SP3L	5.47	22.9	0.009	192	1.75	0.67	1.8	0.33
784	3 SP3A	5.93	24	0.162	129	0.94	0.71	1.49	0.66
785	3 SP3B	5.44	20.6	0.376	31	0.25	0.74	0.83	0.92
786	3 SP3B	5.86	19.5	0.107	18	0.2	0.68	0.78	0.91
787	3 STR	6.1	22.9	0	72	0.87	0.68	0.87	1.02

TABLE 66

WATERSHED PROCESSES CHEMISTRY DATA
FOR THE STORM OF 5/31/87

Lab#	Sample Type	pH	Cond. (umhos)	NO3-N (mg/l)	DOC (mg/l)	Ca (mg/l)	Mg (mg/l)	K (mg/l)	Na (mg/l)
904	1 TF1	4.8	19.5	0.104	64	0.96	0.17	0.63	0.21
905	1 TF2	4.42	27.5	0.265	56	0.68	0.14	0.54	0.21
906	1 TF3	4.45	20.6	0.11	16	0.13	0.04	0.13	0.19
907	1 TF4	4.35	25.2	0.297	0	0.09	0.02	0.08	0.2
909	1 SP1A	5.72	23.5	0.043	92	1.18	0.75	1.54	0.6
910	1 SP1B	5.81	26.3	0.075	75	1.36	0.8	1.47	0.79
911	1 SP2A	6.25	28.6	0.362	49	1.46	0.98	1.47	0.76
912	1 SP2B	6.04	28.6	0.457	43	1.26	1.03	1.35	0.83
913	1 SP3B	5.83	23.5	0.035	32	0.91	0.81	1.3	0.64
914	1 TL	7.37	65.3	0.137	231	4.01	0.84	6.1	1.81
915	1 TA	7.15	42.9	0.208	233	5.36	0.62	2.92	0.53
916	1 TB	6.81	29.8	0.1	228	1.89	0.83	2.57	0.57
920	BP	4.2	36.1	0.348	0	0.17	0.06	0.18	0.4
921	2 TF1	4.35	26.3	0.273	6	0.05	0.01	0.12	0.2
922	2 TF2	4.37	29.8	0.282	49	0.54	0.12	0.53	0.2
923	2 TF3	4.37	26.3	0.29	0	0.08	0.02	0.1	0.18
924	2 TF4	4.48	24	0.187	39	0.35	0.1	0.57	0.19
925	2 SP1L	6.57	34.9	0.263	309	2.66	0.79	3.89	0.22
926	2 SP1B	6.39	26.3	0.035	87	1.09	0.62	2.09	0.92
927	2 SP2L	5.89	34.4		234	1.42	0.62	2.28	0.65
928	2 SP2A	5.11	34.4	0.026	63	0.82	1.01	0.73	1.64
929	2 SP2B	5.29	36.1	0.028	52	0.94	1.14	0.57	1.98
930	2 SP3L	5.88	27.5	0.212	227	2.44	0.95	1.56	0.54
931	2 SP3A	5.67	33.2	0.047	95	1.53	1.21	0.98	1.23
932	2 SP3B	6.04	34.4	0.031	48	1.1	1.25	0.74	2.07
933	2 TL	5.96	27.5	0.202	285	2.48	1.01	1.59	0.42
934	2 TA	5.47	26.3	0.056	154	1.61	0.86	1.29	0.71

TABLE 66 (Continued)

Lab#	Sample Type	pH	Cond. (umhos)	NO3-N (mg/l)	DOC (mg/l)	Ca (mg/l)	Mg (mg/l)	K (mg/l)	Na (mg/l)
935	2 TB	5.86	25.2	0.085	147	1.82	0.98	1.19	0.65
939	3 TF1	4.9	19.6	0.121	50	0.49	0.13	1.08	0.25
940	3 TF2	4.64	19.6	0.056	52	0.49	0.18	0.72	0.23
941	3 TF3	4.64	20.8	0.12	64	0.7	0.23	0.75	0.21
942	3 TF4	4.48	23.7	0.125	49	0.45	0.12	0.76	0.23
943	3 SP1L	6.57	30.7		348		0.96		
944	3 SP1A	5.31	23.6	0.135	69	0.93	0.8	1.31	0.51
945	3 SP1B	5.46	19.6	0	22	0.38	0.9	0.78	0.91
946	3 SP2A	5.85	23.6	0.024	69	1.28	0.83	0.98	0.78
947	3 SP2B	5.72	21.9	0.03	20	0.82	0.69	0.96	0.93
948	3 TL	6.9	50.8	0.04	362	2.81	0.69		1.52
950	3 TB	6.32	30.6	0	170	1.91	0.91	2.32	0.73

TABLE 67
 WATERSHED PROCESSES CHEMISTRY DATA
 FOR THE STORM OF 6/30/87

Lab#	Sample Type	pH	Cond. (umhos)	NO3-N (mg/l)	DOC (mg/l)	Ca (mg/l)	Mg (mg/l)	K (mg/l)	Na (mg/l)
1015	BP		13.7	0.163	0	0.12	0.01	0.04	0.11
1016	3 TF1	4.84	17.2	0.145	68	0.62	0.08	1.61	0.13
1017	3 TF2	4.59	15.5	0.171	42	0.42	0.11	0.36	0.08
1018	3 TF3	4.62	17.8	0.262	72	0.6	0.17	1.16	0.1
1019	3 TF4	4.22	25.2	0.368	74	0.54	0.13	0.79	0.11
1020	3 SP1L	6.07	25.2	0.376	182	2.73	0.87	1.3	0.13
1021	3 SP1A	4.92	21.2	0.157	99	0.72	0.68	1.27	0.38
1022	3 SP1B	5.06	22.9	0.146	81	0.54	0.65	2.19	0.43
1023	3 SP2L	6.68	31.4		137				
1024	3 SP2A	6.13	26.3	0.049	136	1.76	0.92	1.76	0.61
1025	3 SP2B	5.94	18.9	0.007	42	0.65	0.61	1.18	0.88
1026	3 SP3A	5.62	24.1	0.126	93	0.6	0.74	1.56	0.57
1027	3 SP3B	5.84	16	0.174	95	0.35	0.25	1.44	0.77
1028	3 TL	6.91	79	0.306	686	7.77	1.38	14.8	2.46
1029	3 TA	7.23	83	0.357	241	3.62	0.97	8.12	0.96
1030	3 TB	6.1	37.2	0.458	216	1.33	0.56	7.54	1.52
1036	1 TL	7.78	200.4	0.017	443	4.2	1.06	42.5	6.4
1037	1 TA	7.52	109.9	0.042	222	3.84	0.6	9.4	1.02
1038	1 TB	6.33	36.6	0.466	318	2.75	0.9	5.4	0.22
1039	1 TF1	4.88	16	0.038	79	0.73	0.16	0.9	0.17
1040	1 TF2	4.86	15.5	0.04	73	0.69	0.12	0.75	0.15
1041	1 TF3	4.65	13.7	0.105	24	0.18	0.02	0.18	0.13
1042	1 TF4	4.49	17.8	0.192	8	0.09	0	0.05	0.08
1043	1 SP1L								
1044	1 SP1A	6.08	22.9	0.185	91	1.55	0.68	1.42	0.58
1045	1 SP1B	5.73	25.6	0.053	96	1.36	0.82	1.66	0.68
1046	1 SP2L	5.95	24.6	0.186	200	1.95	0.71	2.24	0.24

TABLE 67 (Continued)

Lab#	Sample Type	pH	Cond. (umhos)	NO3-N (mg/l)	DOC (mg/l)	Ca (mg/l)	Mg (mg/l)	K (mg/l)	Na (mg/l)
1047	1 SP2B	5.57	30.9	0.703	29	0.79	1.01	1.85	1.17
1048	1 SP3L	6.03	17.2	0.178	166	1.58	0.61	1.06	0.17
1049	1 SP3A	6.18	18.3	0.162	102	1.36	0.61	1.46	0.25
1050	1 SP3B	5.7	18.3	0.023	73	0.5	0.56	1.42	0.73
1065	2 TL	6.17	28.6	0.208	272	2.3	0.87	2.82	0.35
1066	2 TA	5.28	22.3	0.068	163	1.39	0.74	1.39	0.39
1067	2 TB	5.53	23.5	0.14	151	1.66	0.87	1.5	0.42
1072	2 TF2	4.73	21.8	0.292	79	0.72	0.24	1.16	0.14
1073	2 TF3	4.62	13.2	0.076	9	0.08	0.03	0.08	0.08
1074	2 TF4	4.95	13.7	0.035	68	0.43	0.13	1.64	0.12
1076	1 SP1B	5.71	26.3	0.097	86	1.17	0.81	2.65	1.14
1077	2 SP2L	5.68	17.2	0.093	159	1.09	0.53	2.28	0.17
1078	2 SP2A	5.16	20	0.035	103	0.63	0.57	1.42	0.86
1079	2 SP3L	6.02	24	0.233	178	2.17	0.91	1.9	0.2
1080	2 SP3A	5.43	20.6	0.05	76	1.03	0.72	0.86	0.8
1081	2 SP3B	5.53	22.3	0.239	71	0.55	0.73	0.87	1.54

APPENDIX C

SUMMARY OF THROUGHFALL DATA

TABLE 68

SUMMARY OF THROUGHFALL DATA

Data is lumped and arranged sequentially

Storm Date	Gross PCPN (mm)	Throughfall (mm)
1/16	45.7	43.7
1/16	45.7	43.9
1/16	45.7	47.5
1/16	45.7	43.7
1/16	45.7	47.5
1/16	45.7	44.5
2/12	21.6	21.3
2/12	21.6	19.1
2/12	21.6	18.3
2/12	21.6	20.6
2/12	21.6	20.1
2/12	21.6	19.3
2/12	21.6	19.1
2/12	21.6	20.3
2/12	21.6	16.3
2/12	21.6	19.8
2/16	31.8	29.2
2/16	31.8	29.0
2/16	31.8	29.0
2/16	31.8	29.5
2/16	31.8	29.7
2/16	31.8	33.8
2/16	31.8	30.5
2/16	31.8	32.5
2/16	31.8	31.8
2/16	31.8	35.8
2/21	6.4	5.8
2/21	6.4	6.1
2/21	6.4	5.8
2/21	6.4	5.8
2/21	6.4	5.8
2/21	6.4	6.4
2/21	6.4	6.4
2/21	6.4	6.6
2/21	6.4	6.6
2/21	6.4	6.4
2/21	6.4	6.9
2/21	6.4	7.4
2/24	14.0	14.0
2/24	14.0	13.5

TABLE 68 (Continued)

Storm Date	Gross PCPN (mm)	Throughfall (mm)
2/24	14.0	13.7
2/24	14.0	14.2
2/24	14.0	13.0
2/24	14.0	13.5
2/24	14.0	14.7
2/24	14.0	14.5
2/24	14.0	13.7
2/24	14.0	5.6
2/24	14.0	14.2
2/24	14.0	14.0
3/1	53.6	45.7
3/1	53.6	49.0
3/1	53.6	47.2
3/1	53.6	49.5
3/1	53.6	52.1
3/1	53.6	51.8
3/1	53.6	51.3
3/1	53.6	44.2
3/1	53.6	53.3
3/1	53.6	41.4
3/1	53.6	51.6
3/1	53.6	49.5
3/17	62.2	53.3
3/17	62.2	57.4
3/17	62.2	59.9
3/17	62.2	58.7
3/17	62.2	63.5
3/17	62.2	63.8
3/17	62.2	65.0
3/17	62.2	64.5
3/17	62.2	65.5
3/17	62.2	63.0
3/17	62.2	63.2
3/17	62.2	64.8
3/25	10.2	7.1
3/25	10.2	7.4
3/25	10.2	11.9
3/25	10.2	10.9
3/25	10.2	8.9
3/25	10.2	11.9
3/25	10.2	11.4
3/25	10.2	7.4
3/25	10.2	8.6
3/25	10.2	11.9
3/25	10.2	11.7

TABLE 68 (Continued)

Storm Date	Gross PCPN (mm)	Throughfall (mm)
4/1	11.9	10.2
4/1	11.9	10.2
4/1	11.9	10.4
4/1	11.9	10.9
4/1	11.9	12.7
4/1	11.9	13.0
4/1	11.9	10.2
4/1	11.9	12.7
4/1	11.9	10.9
4/1	11.9	11.9
4/1	11.9	13.0
4/13	19.6	17.8
4/13	19.6	16.5
4/13	19.6	17.5
4/13	19.6	18.0
4/13	19.6	21.1
4/13	19.6	21.8
4/13	19.6	22.9
4/13	19.6	21.6
4/13	19.6	15.7
4/13	19.6	18.8
4/13	19.6	16.5
4/13	19.6	17.3
4/30	20.3	15.0
4/30	20.3	16.0
4/30	20.3	16.3
4/30	20.3	14.5
4/30	20.3	17.8
4/30	20.3	16.5
4/30	20.3	17.3
4/30	20.3	17.0
4/30	20.3	12.4
4/30	20.3	14.2
4/30	20.3	12.7
4/30	20.3	14.5
5/24	36.8	33.0
5/24	36.8	24.1
5/24	36.8	21.8
5/24	36.8	22.6
5/24	36.8	24.9
5/24	36.8	27.9
5/24	36.8	34.8
5/24	36.8	26.7
5/24	36.8	32.3
5/24	36.8	38.9

TABLE 68 (Continued)

Storm Date	Gross PCPN (mm)	Throughfall (mm)
5/24	36.8	34.5
5/24	36.8	33.8
5/25	36.8	45.2
5/25	36.8	30.5
5/25	36.8	29.2
5/25	36.8	31.2
5/25	36.8	35.8
5/25	36.8	34.0
5/25	36.8	37.6
5/25	36.8	25.4
5/25	36.8	36.1
5/25	36.8	35.8
5/25	36.8	35.1
5/25	36.8	31.8
5/28	102.4	92.5
5/28	102.4	85.9
5/28	102.4	71.9
5/28	102.4	90.9
5/28	102.4	100.6
5/28	102.4	96.3
5/28	102.4	98.3
5/28	102.4	75.4
5/28	102.4	97.0
5/28	102.4	114.6
5/28	102.4	99.1
5/28	102.4	86.4
6/2	1.3	0.8
6/2	1.3	1.0
6/2	1.3	1.5
6/2	1.3	1.0
6/2	1.3	0.8
6/2	1.3	0.8
6/2	1.3	2.0
6/2	1.3	0.8
6/2	1.3	1.0
6/2	1.3	1.5
6/2	1.3	0.8
6/2	1.3	0.5
6/9	20.8	17.0
6/9	20.8	17.5
6/9	20.8	14.0
6/9	20.8	16.5
6/9	20.8	14.5
6/9	20.8	16.0
6/9	20.8	12.2
6/9	20.8	12.2

TABLE 68 (Continued)

Storm Date	Gross PCPN (mm)	Throughfall (mm)
6/9	20.8	27.4
6/9	20.8	19.6
6/9	20.8	22.6
6/9	20.8	16.5
6/23	49.8	46.0
6/23	49.8	40.1
6/23	49.8	32.3
6/23	49.8	38.9
6/23	49.8	44.5
6/23	49.8	46.7
6/23	49.8	52.3
6/23	49.8	42.2
6/23	49.8	43.9
6/23	49.8	55.6
6/23	49.8	37.6
6/23	49.8	44.7
6/30	59.7	64.0
6/30	59.7	49.5
6/30	59.7	49.3
6/30	59.7	73.9
6/30	59.7	62.2
6/30	59.7	64.3
6/30	59.7	52.8
6/30	59.7	49.3
6/30	59.7	62.2
6/30	59.7	50.8
6/30	59.7	48.0

APPENDIX D

WATERSHED MODEL PROGRAM

FIGURE 46

WATERSHED MODEL PROGRAM

'PROGRAM WSCHM3 8-18-88

'WATERSHED WATERQUALITY MODEL 3rd ATTEMPT

'Model uses simple weighting factors to calculate chemical loads in the stream.

'Uses Model 37 as a base

'*****WRITES OUTPUT TO A FILE*****

'Input program control variables:

MAXINC = .010417 'Maximum storm simulation time increment

'Input geomorphologic parameters:

'All areas are given in square meters

TOTAREA = 77100 'Total watershed area
CHANAREA = 1635 'Stream channel area
ALUVAREA = 1400 'Alluvial and flood plain area
RIPAREA = CHANAREA + ALUVAREA 'Area of riparian zone

'Input soil hydrologic parameters:

FIGURE 46 (Continued)

UPSOILDEP = 200	'Upper soil storage soil depth (mm)
LOSOILDEP = 457	'Lower soil storage soil depth (mm)
DEEPSOILDEP = 350	
UPPOR = .45	'Upper soil storage porosity
LOPOR = .4	'Lower soil storage porosity
DEEPPOR = .43	'Deep soil delayed response storage porosity
UPROCK = .25	'Upper soil storage rock content
LOROCK = .2	'Lower soil storage rock content
DEEPROCK = .05	'Deep soil delayed response storage rock content
UPANC = .12	'Upper soil storage available water capacity (mm/mm)
LOANC = .13	'Lower soil storage available water capacity (mm/mm)
RIPANC = .07	'Riparian gravels available water content
DEEPANC = .13	'Deep soil delayed response storage available water content (mm/mm)
UPWILTP = 0.05	'Upper soil storage wilting point (mm/mm)
LOWILTP = .18	'Lower soil storage wilting point (mm/mm)
DEEPWILT = .27	'Deep soil delayed response storage wilting point (mm/mm)
HSATLO = 350	'Losoil saturated hydraulic conductivity (mm/day)
HSATDEEP = 36	'Deepsoil saturated hydraulic conductivity (mm/day)
BLOSOIL = 17	'Losoil percolation constant
BDEEP = 25.1	'Deepsoil percolation constant

'Subsurface low release coefficients

KLO = .0831	'Days, Losoil storage release constant
KDEEP = .6102	'Days, Deep soil storage release constant

FIGURE 46 (Continued)

'Input vegetative parameters:

GROWSTOR = 1.8 'Maximum canopy storage during the growing season (mm)
DORMSTOR = .43 'Maximum canopy storage during the dormant season (mm)
LITMAX = 3.5 'Maximum litter layer storage (mm)

'Input soil evapotranspiration weighting factors:

UPWEIGHT = .5
LOWEIGHT = .4
DEEPWEIGHT = .1

'Calculate soil water variables:

UPMAX = (UPPOR - UPWILT) * UPSOILDEP * (1 - UPROCK) 'Upper soil maximum storage
UPFCAP = UPANC * UPSOILDEP 'Upper soil storage field capacity
UPANC = UPFCAP
LOMAX = (LOPOR - LOWILT) * LOSOILDEP * (1 - LOROCK) 'Lower soil maximum storage
LOFCAP = LOANC * LOSOILDEP 'Lower soil storage field capacity
LOANC = LOFCAP
DEEPMAX = (DEEPPOR - DEEPWILT) * DEEPSOILDEP * (1 - DEEPROCK) 'Deep soil maximum storage (mm)
DEEPFCAP = DEEPANC * DEEPSOILDEP 'Deep soil delayed flow storage field capacity (mm)
DEEPANC = DEEPFCAP

'PRINT OUT SOIL WATER PARAMETERS

LPRINT USING "USOILDEP = ### UPMAX = ###.## UPFCAP = ###.##"; USOILDEP, UPMAX, UPFCAP
LPRINT

FIGURE 46 (Continued)

```
LPRINT USING "LOSOILDEP = ### LOMAX = ###.## LOFCAP = ###.##"; LOSOILDEP, LOMAX, LOFCAP
```

```
LPRINT
```

```
LPRINT USING "DESOILDEP = ### DEEPX = ###.## DEFCAP = ###.##"; DEEPSOILDEP, DEEPMAX, DEEPCAP
```

```
LPRINT
```

```
'Calculate the total soil profile available water capacity:
```

```
AVAIL = UPFCAP + LOFCAP + DEEPCAP
```

```
LPRINT USING "TOTAL SOIL PROFILE AVAILABLE WATER CAPACITY = #####.##"; AVAIL
```

```
LPRINT
```

```
-----  
'INPUT NAME OF DATA FILE
```

```
INPUT "ENTER NAME OF DATA INPUT FILE"; DATIN$
```

```
OPEN "I", #1, DATIN$
```

```
'INPUT NAME OF OUTPUT FILE:
```

```
INPUT "ENTER NAME OF DATA OUTPUT FILE"; DATOUT$
```

```
OPEN "O", #2, DATOUT$
```

```
-----  
'INPUT WATER QUALITY PARAMETERS FOR ONE CONSTITUENT
```

```
'Input the name of the constituent to be modeled
```

```
INPUT "ENTER NAME OF THE CONSTITUENT TO BE ANALYZED"; CHEMNAME$
```

```
'Input the mean chemical concentrations in the order specified
```

```
INPUT "MEAN TFALL,LITTER,UPSOIL,LOSOIL,DEEPSOIL,GRZ CONCENTRATIONS"; TFALLCONC, LITCONC, UPCONC, LOCONC, DEEPCONC, GRZCONC
```

FIGURE 46 (Continued)

'Initialize soil water storages :

UPSTOR = 14

LOSTOR = 34

DEEPSTOR = 37

RIPSTOR = 0

'Extend characters per line on the printout and use compressed mode

LPRINT CHR\$(27); CHR\$(15); 'Compressed print

WIDTH LPRINT 140 'Increase page width

'LOOP THAT CONTROLS DAILY INCREMENTAL CALCULATIONS

50 DO UNTIL ENDDAY = 999

J = J + 1

I = 0

TOTALPCP = TOTALPCP + DAYPCP

TOTALFLOW = TOTALFLOW + DAYFLOW

TOTALFLOW2 = TOTALFLOW2 + DAYFLOW2

TOTALSEEP = TOTALSEEP + DAYSEEP

TOTALET = TOTALET + (SUMET * (73595 / 77100)) + (SUMET3 / 77100)

TOTALCHEM = TOTALCHEM + DAYCHEM

'RESET DAILY ACCUMULATOR VARIABLES

SUMET = 0

SUMET3 = 0

IPET = 0

IPET3 = 0

ISUM = 0

ISUM3 = 0

FIGURE 46 (Continued)

```

DAYPCP = 0
DAYTFALL = 0
DAYFEET = 0
DAYFLOW = 0
DAYFLOW2 = 0
DAYSEEP = 0
DAYCHEM = 0
'LOOP THAT CONTROLS WITHIN DAY INCREMENTAL CALCULATIONS
DO UNTIL ENDDAY = 999

    MONTH1 = MONTH
    BEGCALDAY = ENDCALDAY
    BEGDAY = ENDDAY
    BEGTIME = ENDTIME
    PCP1 = PCP
    TEMP1 = TEMP
    PANET1 = PANET
    SOILTEMP1 = SOILTEMP

    INPUT #1, MONTH, ENDCALDAY, ENDDAY, ENDTIME, PCP, TEMP, PANET, SOILTEMP
    IF ENDDAY = 999 THEN GOTO 150
    IF BEGDAY = 1 THEN GOTO 100
    IPCP = PCP - PCP1
    IF PCP1 > 0 AND PCP = 0 THEN IPCP = 0
    DELTAT = (ENDDAY + ENDTIME) - (BEGDAY + BEGTIME)
    GOSUB PanCoefficients
    -----
    'Based on the time increment and existence/non-existence of streamflow,
    'choose the time increment of simulation:
    DAY = BEGDAY
    'Condition 1: Present time increment suitable
    IF DELTAT < MAXINC THEN GOSUB NoTimeSplit

```

100

FIGURE 46 (Continued)

```

'Condition 2: Deltat > maximum allowable time increment
IF DELTAT > MAXINC AND DELTAT < 1 THEN
  IF IPCC = 0 THEN
    IF STREAMFLOW = 0 THEN
      GOSUB NoTimeSplit      'No store
    ELSE
      GOSUB TimeSplit2      'No pcp, but flow exists (recession)
    END IF
  ELSE
    GOSUB TimeSplit2      'Store occurring
  END IF
END IF

'Condition 3: Daily time increment, flow present:
IF DELTAT = 1 AND STREAMFLOW > 0 THEN GOSUB TimeSplit1
'Condition 4: Daily time increment, no flow:
IF DELTAT = 1 AND STREAMFLOW = 0 THEN GOSUB NoTimeSplit
-----

'Leave day loop if new day is reached:
IF ENDDAY > BEGDAY THEN GOTO 50

```

LOOP

LOOP

```

150 LPRINT
LPRINT USING " TOTAL ANNUAL PRECIPITATION = #####.## "; TOTALPCP
LPRINT
LPRINT USING " TOTAL ANNUAL ACTUAL EVAPOTRANSPIRATION = #####.##"; TOTALET
LPRINT

```

FIGURE 46 (Continued)

```
LPRINT USING " TOTAL ANNUAL FLOW VOLUME IN LITERS = *****"; TOTALFLOW
LPRINT
LPRINT USING " TOTAL ANNUAL DEEP SEEPAGE LOSS = *****"; TOTALSEEP
LPRINT
TOTALCHEM = TOTALCHEM / 1000000
LPRINT USING " TOTAL ANNUAL TRANSPORT OF \      \ = *****"; CHEMNAME$, TOTALCHEM
LPRINT
LPRINT ACCUMPCP, ACCUMTFALL, ACCUMET, ACCUMSEEP, UPSTOR, LOSTOR, DEEPSTOR, RIPSTOR
LPRINT
LPRINT ACCUMET3
LPRINT
LPRINT ACCUMCHEM
LPRINT
CLOSE #1
```

200
END

TIME CONTROL SUBROUTINES

NoTimeSplit:

'Subroutine for daily time increments with no streamflow occurring
'OR: Present time increment is acceptable

'Set time variables:

DAY = ENDDAY
CDAY = ENDCALDAY
TIME = ENDTIME

FIGURE 46 (Continued)

'Calculate incremental evapotranspiration:
'The maximum incremental ET demand is the same for each zone.

IPET = DAYPET * DELTAT

GOSUB Throughfall
GOSUB LitterLayer
GOSUB UpperSoilStorage
GOSUB LowerSoilStorage
GOSUB DeepSoil
GOSUB Riparian
GOSUB PrintOut

'Add results to daily accumulators:

DAYPCP = DAYPCP + IPCP
DAYTFALL = DAYTFALL + TFALL
DAYFLOW = DAYFLOW + STREAMFLOW
ACCUMPCP = ACCUMPCP + IPCP
DAYSEEP = DAYSEEP + SEEP
DAYCHEM = DAYCHEM + QCHEMLOAD

RETURN

FIGURE 46 (Continued)

TimeSplit1:

'Subroutine for daily time increments when flow is present
'One hour time increments are used.

'Set time variables:

TIMEINC = 1 / 24
DELTAT = DELTAT / 24
DAY = BEGDAY
CDAY = BEGCALDAY

'Loop and branch to hydrologic processes subroutines:

FOR K = 1 TO 24

'Calculate the incremental evapotranspiration:

IPET = DAYPET * DELTAT

TIME = BEGTIME + (K * DELTAT)

IF TIME >= 1 THEN

TIME = 0

DAY = ENDDAY

CDAY = ENDCALDAY

END IF

'Input variables are now all correct, run data through all simulation subroutines

FIGURE 46 (Continued)

```
GOSUB Throughfall
GOSUB LitterLayer
GOSUB UpperSoilStorage
GOSUB LowerSoilStorage
GOSUB DeepSoil
GOSUB Riparian
GOSUB PrintOut      'Writes and/or prints incremental results
```

```
'Add results to daily accumulators:
DAYPCP = DAYPCP + IPCP
DAYTFALL = DAYTFALL + TFALL
DAYFLOW = DAYFLOW + STREAMFLOW
ACCUMPCP = ACCUMPCP + IPCP
DAYSEEP = DAYSEEP + SEEP
DAYCHEM = DAYCHEM + QCHEMLOAD
```

```
      NEXT K
RETURN
```

```
TimeSplit2:
```

```
'Subroutine for splitting large time increments during storflow
'Divide time increment into smaller increments of designated maximum size:
```


FIGURE 46 (Continued)

```
NM = DELTAT / MAXINC
INCNUM = CINT(NM)      'The number of whole increments
IPCP = IPCP / INCNUM
DELTAT = DELTAT / INCNUM
DAY = BEGDAY
CDAY = BEGSCALDAY

'Loop and branch to hydrologic processes subroutines:

FOR K = 1 TO INCNUM

    'Calculate the maximum incremental evapotranspiration:
    _____

    IPET = DAYPET * DELTAT

    -----

    'Calculate the day and time of next incremental step:
    TIME = BEGTIME + (K * DELTAT)
    IF K = INCNUM AND ENDDAY > BEGDAY THEN TIME = 0: DAY = ENDDAY: CDAY = ENDCALDAY

    'Input variables are now correct, run data through all simulation subroutines:

    GOSUB Throughfall
    GOSUB LitterLayer
    GOSUB UpperSoilStorage
    GOSUB LowerSoilStorage
    GOSUB DeepSoil
    GOSUB Riparian
    GOSUB PrintOut      'Writes and/or prints incremental results
```

FIGURE 46 (Continued)

'Add results to daily accumulators:

```
DAYPCP = DAYPCP + IPCP
DAYTFALL = DAYTFALL + TFALL
DAYFLOW = DAYFLOW + STREAMFLOW
ACCUMPCP = ACCUMPCP + IPCP
DAYSEEP = DAYSEEP + SEEP
DAYCHEM = DAYCHEM + QCHEMLOAD
```

NEXT K

RETURN

POTENTIAL EVAPOTRANSPIRATION PAN COEFFICIENTS

PanCoefficients:

'Subroutine to choose proper monthly evaporation pan coefficient

```
IF BEGDAY >= 1 AND BEGDAY <= 31 THEN PANCOEFF = 1
IF BEGDAY >= 32 AND BEGDAY <= 61 THEN PANCOEFF = 1
IF BEGDAY >= 62 AND BEGDAY <= 92 THEN PANCOEFF = 1
IF BEGDAY >= 93 AND BEGDAY <= 123 THEN PANCOEFF = 1
IF BEGDAY >= 124 AND BEGDAY <= 151 THEN PANCOEFF = 1
IF BEGDAY >= 152 AND BEGDAY <= 182 THEN PANCOEFF = 1
IF BEGDAY >= 183 AND BEGDAY <= 212 THEN PANCOEFF = 1
IF BEGDAY >= 213 AND BEGDAY <= 273 THEN PANCOEFF = 1
IF BEGDAY >= 274 AND BEGDAY <= 304 THEN PANCOEFF = 1
IF BEGDAY >= 305 AND BEGDAY <= 335 THEN PANCOEFF = 1
IF BEGDAY >= 336 AND BEGDAY <= 366 THEN PANCOEFF = 1
DAYPET = PANET1 * PANCOEFF
```

RETURN

FIGURE 46 (Continued)

 SEASONAL TRANSPIRATION FACTORS

SeaTranspire:

'Subroutine to calculate a seasonal transpiration factor
 'Transpiration factor for the growing season is assumed to be 1
 'The transpiration factor for the dormant season is assumed to be equal
 'to the reduction in leaf area index over the watershed area.

IF BEGDAY >= 1 AND BEGDAY <= 31 THEN SEATRANS = 1 'Growing season
 IF BEGDAY >= 32 AND BEGDAY <= 61 THEN SEATRANS = 1 - (BEGDAY - 32) * .0283 'Transitional period
 IF BEGDAY >= 62 AND BEGDAY <= 182 THEN SEATRANS = .15 'Dormant season
 IF BEGDAY >= 183 AND BEGDAY <= 212 THEN SEATRANS = .15 + (BEGDAY - 183) * .0283 'Transitional period
 IF BEGDAY >= 213 AND BEGDAY <= 366 THEN SEATRANS = 1 'Growing season

RETURN

 THROUGHFALL

Throughfall:

'Subroutine calculates throughfall for a time increment
 'Calculate seasonal maximum canopy storage
 GROWSTOR = 1.8 'Growing season maximum canopy storage (mm)
 DORMSTOR = .43 'Dormant season maximum canopy storage (mm)
 'CANMAX = Maximum canopy storage (mm)
 IF BEGDAY >= 1 AND BEGDAY <= 31 THEN CANMAX = GROWSTOR
 IF BEGDAY >= 32 AND BEGDAY <= 61 THEN CANMAX = GROWSTOR - .0472 * (BEGDAY - 32)
 IF BEGDAY >= 62 AND BEGDAY <= 182 THEN CANMAX = DORMSTOR
 IF BEGDAY >= 183 AND BEGDAY <= 212 THEN CANMAX = DORMSTOR + .0472 * (BEGDAY - 182)
 IF BEGDAY >= 213 AND BEGDAY <= 366 THEN CANMAX = GROWSTOR

FIGURE 46 (Continued)

```
'CANSTOR = Current canopy storage
'DEFICIT = Canopy storage deficit

DEFECIT = CANMAX - CANSTOR
CANSTOR1 = CANSTOR 'At the beginning of a storm
TOTALCAN = CANSTOR + IPCP 'Total temporary storage for chemical mixing
IF DEFECIT > 0 AND IPCP <= DEFECIT THEN TFALL = 0: CANSTOR = CANSTOR + IPCP
IF DEFECIT > 0 AND IPCP > DEFECIT THEN TFALL = IPCP - DEFECIT: CANSTOR = CANMAX
IF DEFECIT = 0 THEN TFALL = IPCP: CANSTOR = CANMAX
ACCUMTFALL = ACCUMTFALL + TFALL

'Calculate the average throughfall chemistry:

TFCHEM = TFALL * TFALLCONC

'Calculate evaporation loss from canopy
'IPET = the maximum incremental PET demand

'Condition 1: Canopy storage not limiting; ET available
IF CANSTOR >= IPET THEN ETLOSS = IPET
'Condition 2: Canopy storage limiting; ET available
IF CANSTOR < IPET THEN ETLOSS = CANSTOR
'Condition 3: No ET available
IF IPET = 0 THEN ETLOSS = 0
CANSTOR = CANSTOR - ETLOSS
CANLOSS = ETLOSS
SUMET = SUMET + ETLOSS
ACCUMET = ACCUMET + ETLOSS
ACCUMET3 = ACCUMET3 + ETLOSS
```

FIGURE 46 (Continued)

'Enter canopy chemistry subroutine:

'Calculate the remaining incremental PET demands:

IREMPET = IPET - ETLOSS

RETURN

' LITTER LAYER

LitterLayer:

'Subroutine for calculating litter layer storage and release

'LITMAX = Maximum litter layer storage (mm)

'LITSTOR = Current litter layer storage

'LITDEF = Litter layer storage deficit

'LPERC=Percolation outflow from litter layer

LITMAX = 3.5 mm Average value for eastern hardwoods

LITDEF = LITMAX - LITSTOR

LITSTOR1 = LITSTOR 'LITSTOR1 = variable for testing subroutine

IF LITDEF > 0 AND TFALL <= LITDEF THEN LPERC = 0: LITSTOR = LITSTOR + TFALL

IF LITDEF > 0 AND TFALL > LITDEF THEN LPERC = TFALL - LITDEF: LITSTOR = LITMAX

IF LITDEF = 0 THEN LPERC = TFALL

'Calculate evaporation loss from litter layer at potential rate.

'IREMPET is the maximum remaining incremental PET

FIGURE 46 (Continued)

```
'Condition 1: Litter storage not limiting; ET available
IF LITSTOR >= IREMPET THEN ETLOSS = IREMPET
'Condition 2: Litter storage limiting; ET available
IF LITSTOR < IREMPET THEN ETLOSS = LITSTOR
'Condition 3: No ET available
IF IREMPET = 0 THEN ETLOSS = 0
LITSTOR = LITSTOR - ETLOSS
SUMET = SUMET + ETLOSS
ACCUMET3 = ACCUMET3 + ETLOSS
LITLOSS = ETLOSS
TOTALLIT2 = LITSTOR      'ET-Corrected storage for chemical transport calculations

'Calculate the remaining incremental PET demands:

IREMPET = IREMPET - ETLOSS

'Calculate the average chemical properties of litter percolation:

LITCHEM = LPERC * LITCONC
ETLOSS = ETLOSS * (1 - QRZAREA / TOTAREA)
ACCUMET = ACCUMET + ETLOSS 'Corrects accum et for qrz area
RETURN

UpperSoilStorage:
'Subroutine for performing water and chemical balance for the upper
'soil zone (A1,A2, and upper B-Horizons).
'UPSTOR = the current storage
UPWILT = 0      'Storage is assumed to be empty at the wilting point
'Input to the upper soil zone is percolation from the litter layer.
```

FIGURE 46 (Continued)

```
UPSTOR1 = UPSTOR 'Test variable for checking subroutine operation.
UPSTOR = UPSTOR + LPERC
TOTALUP = UPSTOR 'Storage used for chemical mixing
```

```
'Calculate ET loss from the upper soil zone:
'The remaining incremental PET demand is applied to the entire soil profile.
'The quantity of PET demand applied to each storage is determined by the
'soil evapotranspiration weighting factors upweight, lowweight, and deepweight.
'The sum of the weighting factors must equal 1.
```

```
UPPET = IREMPET * UPWEIGHT
LOPET = IREMPET * LOWEIGHT
DEEPPET = IREMPET * DEEPWEIGHT
```

```
'Actual ET loss is a function of soil moisture and available PET demand.
```

```
'Soil Moisture Condition 1: > wilting point
```

```
'Calculate maximum AET for existing soil moisture conditions:
IF UPSTOR / UPANC > .4 THEN AET = UPPET
IF UPSTOR / UPANC <= .4 AND UPSTOR / UPANC > .2 THEN AET = UPPET * (.8 + (UPSTOR / UPANC - .2))
IF UPSTOR / UPANC <= .2 AND UPSTOR / UPANC > .1 THEN AET = UPPET * (.2 + 6 * (UPSTOR / UPANC - .1))
IF UPSTOR / UPANC <= .1 THEN AET = UPPET * 2 * (UPSTOR / UPANC)
```

```
'Condition 1a: Moisture limiting
IF UPSTOR >= AET THEN ETLOSS = AET
```

FIGURE 46 (Continued)

```
'Condition 1b: Moisture limiting
IF UPSTOR < AET THEN ETLOSS = UPSTOR

'Soil Moisture Condition 2: Upstor < wilting point
IF UPSTOR <= UPWILT THEN ETLOSS = 0

'For all soil moisture conditions, if IPET =0:
IF UPPET = 0 THEN ETLOSS = 0

'Update amount of daily PET demand used
SUMET = SUMET + ETLOSS

'Update upper zone storage:
UPSTOR = UPSTOR - ETLOSS
UPLOSS = ETLOSS
TOTALUP2 = UPSTOR

'Calculate quantity of percolation from the upper zone:
'UPGRAV = available gravity water

UPGRAV = UPSTOR - UPFCAP
IF UPSTOR <= UPFCAP THEN UPGRAV = 0
UPPERC = UPGRAV

'Check to see if LOSTOR is filled to LOMAX:
LODEFECIT = LOMAX - LOSTOR      'Lower soil storage deficit
IF UPPERC > LODEFECIT THEN UPPERC = LODEFECIT

'Adjust upper storage for losses:
UPSTOR = UPSTOR - UPPERC

'Calculate the average chemical properties of Upsoil percolation:
```


FIGURE 46 (Continued)

UPCHEM = UPPERC * UPCONC

ETLOSS = ETLOSS * (1 - QRZAREA / TOTAREA)

ACCUMET = ACCUMET + ETLOSS

RETURN

LowerSoilStorage:

'Subroutine for performing water and chemical balance for the lower

'LOSTOR = the current lower zone storage

'LOAW = the current plant available water

LOWILT = 0 'Storage is assumed to be empty at the wilting point.

'Input to the lower soil zone is percolation from the upper soil zone:

LOSTOR = LOSTOR + UPPERC

LOSTOR1 = LOSTOR 'Variable for checking subroutine operation.

TESTSTOR = LOSTOR

'Calculate ET loss from the lower soil zone:

'ET is removed from the lower soil zone by transpiration only.

'Calculate the seasonal transpiration factor, SEATRANS:

GOSUB SeaTranspire

LOPET = LOPET * SEATRANS

'Actual ET loss is a function of soil moisture and available PET demand

'Soil Moisture Condition 1: LOSTOR > wilting point

'Calculate maximum AET for the existing soil moisture conditions:

FIGURE 46 (Continued)

```
IF LOSTOR / LOANC <= 1 AND LOSTOR / LOANC > .6 THEN AET = LOPET
IF LOSTOR / LOANC <= .6 AND LOSTOR / LOANC > .4 THEN AET = LOPET * (.8 + (LOSTOR / LOANC - .4))
IF LOSTOR / LOANC <= .4 AND LOSTOR / LOANC > .2 THEN AET = LOPET * (.2 + 3 * (LOSTOR / LOANC - .2))
IF LOSTOR / LOANC <= .2 THEN AET = LOPET * (LOSTOR / LOANC)
```

```
'Condition 1a: Moisture not limiting:
```

```
IF LOSTOR >= AET THEN ETLOSS = AET
```

```
'Condition 1b: Moisture limiting:
```

```
IF LOSTOR < AET THEN ETLOSS = LOSTOR
```

```
'Soil Moisture Condition 2: Upstor <= wilting point
```

```
IF LOSTOR <= LOWILT THEN ETLOSS = 0
```

```
'For all soil moisture conditions, if PET = 0:
```

```
IF LOPET = 0 THEN ETLOSS = 0
```

```
'Update amount of daily PET demand used:
```

```
SUMET = SUMET + ETLOSS
```

```
'Update lower soil zone storage:
```

```
LOSTOR = LOSTOR - ETLOSS
```

```
'Calculate the quantity of subsurface flow from the lower soil zone:
```

```
'Include the upper soil zone gravity water if the lower zone is full:
```

```
'LOSSF = lower zone subsurface flow
```

```
'LOGRAV= Gravity water storage available for percolation or SSF
```

```
LOGRAV = LOSTOR - LOFCAP
```

FIGURE 46 (Continued)

```
IF LOSTOR <= LOFCAP THEN LOGRAV = 0
TOTALGRAV = LOGRAV
IF TESTSTOR >= LOMAX THEN TOTALGRAV = LOGRAV + UPGRAV

TOTALGRAV1 = TOTALGRAV
'Storage remaining at end of time increment after SSF release
REMSTOR = TOTALGRAV * (KLO ^ DELTAT)
'Lo soil SSF volume released equals the difference between storage at
'the beginning of the time increment and the remaining storage:
LOSSF = TOTALGRAV - REMSTOR
IF TOTALGRAV <= 0 THEN LOSSF = 0
TOTALGRAV = TOTALGRAV - LOSSF
IF UPGRAV >= LOSSF THEN UPSTOR = UPSTOR - LOSSF
IF UPGRAV < LOSSF THEN LOSTOR = LOSTOR - (LOSSF - UPGRAV); UPSTOR = UPSTOR - UPGRAV

'Calculate quantity of percolation from the lower soil zone.
'Percolation occurs at an exponential function of soil moisture content above field capacity:
'Percolation is controlled by the ability of the clay layer below to transmit water
'Percolation takes place above and below field capacity

LOPERC = (HSATLO * (LOSTOR / LOMAX) ^ BLOSOIL) * DELTAT

IF LOSTOR <= LOPERC THEN LOPERC = LOSTOR

'Check to see if the DEEPSOIL storage is filled:

DEEPDEFECIT = DEEPMAX - DEEPSTOR      'Deep storage deficit
IF LOPERC > DEEPDEFECIT THEN LOPERC = DEEPDEFECIT
```

FIGURE 46 (Continued)

'Account for losses from lower soil zone storage:

LOSTOR = LOSTOR - LOPERC

'Calculate the average chemical properties of subsurface flow:

LSSFCEM = LOSSF * LOCONC

ETLOSS = ETLOSS * (1 - QRZAREA / TOTAREA)

ACCUMET = ACCUMET + ETLOSS

GOSUB QRZ

RETURN

QRZ:

'Subroutine for calculating the flow contribution of steep slopes
'surrounding the stream channels. The size of the QRZ area is a function
'of the current storage in the LoSoil storage.

QRZAREA = EXP(9.7 * (LOSTOR / LOMAX))

IF TFALL = 0 THEN QRZAREA = 0 'IF NO RAIN, NO FLOW FROM QRZ AREA!!!!

QRZVOL = TFALL * QRZAREA

QRZFLOW = QRZVOL / (DELTAT * 86400) 'Flow in liters per second

FIGURE 46 (Continued)

'Calculate the average chemical composition of the Quick Release Flow

QRZCHEM = QRZVOL * QRZCONC

RETURN

DeepSoil:

'Subroutine for performing water and chemical balance for the
'deep soil delayed response storage.

'DEEPSTOR = the current level of storage

'DEEPFLOW = delayed flow to the stream

'Input to the deep soil storage is LOPERC

'SEEP = accounts for any possible deep seepage losses

DEEPSTOR1 = DEEPSTOR

DEEPSTOR = DEEPSTOR + LOPERC

'Calculate ET loss from the deep soil storage:

'ET is removed from the deep soil zone by transpiration only.

'Calculate the seasonal transpiration factor, SEATRANS

GOSUB SeaTranspire

DEEPPET = DEEPPET * SEATRANS 'Allotted PET adjusted for seasonal transpiration

'Actual ET loss is a function of existing soil moisture and PET demand:

FIGURE 46 (Continued)

```
'Calculate the maximum AET for the existing soil moisture conditions:
IF DEEPSTOR / DEEPAWC > .9 THEN AET = DEEPPET
IF DEEPSTOR / DEEPAWC <= .9 AND DEEPSTOR / DEEPAWC > .6 THEN AET = DEEPPET * (.7 + (DEEPSTOR / DEEPAWC - .6))
IF DEEPSTOR / DEEPAWC <= .6 AND DEEPSTOR / DEEPAWC > .3 THEN AET = DEEPPET * (.2 * (1.667 * (DEEPSTOR / DEEPAWC - .3)))
IF DEEPSTOR / DEEPAWC <= .3 THEN AET = DEEPPET * .6667 * DEEPSTOR / DEEPAWC

'Condition 1: DEEPSTOR not limiting, PET demand available
IF DEEPSTOR >= AET THEN ETLOSS = AET
'Condition 2: DEEPSTOR limiting, PET demand available
IF DEEPSTOR < AET THEN ETLOSS = DEEPSTOR
'Condition 3: No PET demand available
IF DEEPPET = 0 THEN ETLOSS = 0

'Update portion of daily demand met:
SUMET = SUMET + ETLOSS
'Update quantity of deep soil storage:
DEEPSTOR = DEEPSTOR - ETLOSS

'Calculate the quantity of delayed flow released:
DEEPGRAV= storage of water in excess of field capacity, or gravity water

DEEPGRAV = DEEPSTOR - DEEPPCAP

'Calculate quantity of gravity water remaining at the end of a time increment:

REMDEEPSTOR = DEEPGRAV * (KDEEP ^ DELTAT)

'Delayed flow release to streamflow is equal to the storage at the beginning
of the time increment minus the remaining storage:
```

FIGURE 46 (Continued)

```
DEEPFLOW = DEEPGRAV - REMDEEPSTOR
IF DEEPGRAV <= 0 THEN DEEPFLOW = 0
DEEPGRAV = DEEPGRAV - DEEPFLOW
DEEPSTOR = DEEPSTOR - DEEPFLOW
```

'Calculate quantity of deep soil storage lost to deep seepage:

```
SEEP = (HSATDEEP * (DEEPSTOR / DEEPMAX) ^ BDEEP) * DELTAT
IF DEEPSTOR <= SEEP THEN SEEP = DEEPSTOR
```

'Update deep soil storage to account for losses:
DEEPSTOR = DEEPSTOR - SEEP

'Calculate the chemical composition of the deepflow:

```
DEEPCHEM = DEEPFLOW * DEEPCONC
```

```
ETLOSS = ETLOSS * (1 - QRZAREA / TOTAREA)
ACCUMET = ACCUMET + ETLOSS
SEEP = SEEP * (1 - QRZAREA / TOTAREA) * (LANDAREA / TOTAREA)
ACCUMSEEP = ACCUMSEEP + SEEP
```

RETURN

Riparian:

'Subroutine calculates contributions to streamflow from channel interception
'and interception by low-lying alluvial terraces.

FIGURE 46 (Continued)

```

LANDAREA = TOTAREA - CHANAREA - ALUVAREA - QRZAREA
RIPAREA = CHANAREA + ALUVAREA
RIPMAX = 90000      'Storage of riparian gravels in liters

'Riparian gravel storage must be satisfied before streamflow can occur
'Input to the riparian gravel storage is assumed to be the sum of the flows
'from channel side slopes, subsurface flow, groundwater, and throughfall falling
'directly on the channel area and alluvial area.

'RIPSTOR = the current storage
INFLOW = (TFALL * CHANAREA) + (LPERC * ALUVAREA) + (QRZVOL) + (LOSSF * LANDAREA) + (DEEPFLOW * LANDAREA)
.
'Calculate the mean chemical composition of the total streamflow:
RIPCHEM = RIPCONC * RIPSTOR
INCHEM = (TFALL * CHANAREA * TFALLCONC) + (LPERC * ALUVAREA * LITCONC) + (QRZVOL * QRZCONC) + (LOSSF * LANDAREA * LOCONC) + (DEEP
FLOW * LANDAREA * DEEPCONC)
COMBICHEMLOAD = RIPCHEM + INCHEM      'COMBICHEMLOAD = combined load of RIPSTOR and inflow
RIPSTOR = RIPSTOR + INFLOW
.
'Assuming complete mixing, the streamflow chemical concentrations are:
.
IF RIPSTOR > 0 THEN QCHEMCONC = COMBICHEMLOAD / RIPSTOR      'Conc. in ug/l
IF RIPSTOR = 0 THEN QCHEMCONC = 0
.

RIPDEF = RIPMAX - RIPSTOR      'Riparian zone storage deficit
IF RIPDEF >= 0 THEN OUTFLOW = 0
IF RIPDEF < 0 THEN OUTFLOW = RIPSTOR - RIPMAX
STREAMFLOW = OUTFLOW

```


FIGURE 46 (Continued)

'The incremental chemical load is:

QCHEMLOAD = STREAMFLOW * QCHEMCONC

RIPCONC = QCHEMCONC

ACCUMCHEM = ACCUMCHEM + QCHEMLOAD

'Update storage for losses:

RIPSTOR = RIPSTOR - OUTFLOW

RIPSTOR2 = RIPSTOR

'Actual ET loss is a function of available ET and soil moisture

'By definition, the riparian gravels are at field capacity at RIPMAX

IRIPPET = IREMPET * RIPAREA

IF RIPSTOR / RIPMAX > .2 THEN AET = IRIPPET

IF RIPSTOR / RIPMAX <= .2 THEN AET = IRIPPET * 5 * (RIPSTOR / RIPMAX)

'Soil Moisture Condition 1: Moisture not limiting:

IF RIPSTOR >= AET THEN ETLOSS = AET

'Soil Moisture Condition 2: Moisture limiting:

IF RIPSTOR < AET THEN ETLOSS = RIPSTOR

'Soil Moisture Condition 3: Storage empty:

IF RIPSTOR = 0 THEN ETLOSS = 0

'For all soil moisture conditions:

IF IRIPPET = 0 THEN ETLOSS = 0

FIGURE 46 (Continued)

'Update the amount of the daily PET demand used:

SUMET3 = SUMET3 + ETLOSS

ACCUMET3 = ACCUMET3 + (ETLOSS / 77100)

RIPLOSS = ETLOSS 'Test variable

'Update riparian zone storage:

RIPSTOR = RIPSTOR - ETLOSS

QFLOW = OUTFLOW / (DELTAT * 86400)

RETURN

' OUTPUT CONTROL SUBROUTINE

PrintOut:

'Subroutine for routing incremental results to printer and/or file output

ACCUMVOL = ACCUMVOL + STREAMFLOW

SSFLOW = LOSSF

DDFLOW = DEEPFLOW

WRITE #2, MONTH, CDAY, TIME, QFLOW, ACCUMVOL, QCHEMCONC

RETURN

VITA

Donald J. Turton

Candidate for the Degree of

Doctor of Philosophy

Thesis: MEASUREMENT AND MODELING OF WATER QUALITY FROM A
SMALL FORESTED WATERSHED IN SOUTHEASTERN OKLAHOMA

Major Field: Agricultural Engineering

Biographical:

Personal Data: Born in Buffalo, New York, August 15,
1951, the son of Thomas J. and Geraldine Turton.

Education: Graduated from Hamburg Senior High School,
Hamburg, New York, in June, 1969; received the
Bachelor of Science Degree in Resources Management
from SUNY College of Environmental Sciences and
Forestry at Syracuse in May, 1977; received
the Master of Science degree in Forest Hydrology
from University of Washington at Seattle in May,
1982, completed requirements for the Doctor of
Philosophy degree at Oklahoma State University in
May, 1989.

Professional Experience: Soil Conservationist, USDA
Soil Conservation Service, Warsaw, N.Y., May 1976
to August, 1976. Soil Conservationist, USDA Soil
Conservation Service, Brattleboro, Vermont, May
1977 to May 1979. Research Assistant in Forest
Hydrology, University of Washington College of
Forest Resources, Seattle, Washington, June 1979
to January, 1981. Consulting Forest Hydrologist,
D. Wooldridge Forest Hydrology Consulting,
Cashmere, Washington, January 1981 to December
1981. Research Hydrologist, Oklahoma State
University Department of Forestry Forest Watershed
Lab, Stillwater, Oklahoma, May, 1982 to August,
1985. Research Fellow, USDA National Needs
Fellowship in Agricultural Engineering, Oklahoma
State University Department of Agricultural
Engineering, Stillwater, Oklahoma, September, 1985
to August, 1988.